INVESTIGATING THE MECHANISMS OF DRUG RESISTANCE IN GASTRO-INTESTINAL CANCERS

Georgia Spain

The Institute of Cancer Research, University of London

Supervisor: Dr Marco Gerlinger

A thesis submitted for the degree of
Doctor of Philosophy,
University of London

September 2019

Declaration

This thesis was completed under the supervision of Dr Marco Gerlinger and the work described here was carried out at Translational Oncogenomics Lab, Division of Molecular Pathology, The Institute of Cancer Research, 237 Fulham Road, SW3 6JB.

I, Georgia Heather Spain, confirm that the work presented in this thesis is my own. Where others have made contributions or information has been derived from other sources, this has been clearly referenced and acknowledged.

Signed: Georgia Spain
September 2019

Acknowledgements

First and foremost I would like to thank my supervisor, Dr Marco Gerlinger, not only for the opportunity to undertake my PhD in his lab, but for the ongoing support, advice and encouragement. It has been a very exciting yet challenging 4 years, and I am very grateful for having such a positive and supportive supervisor.

I would also like to thank all the members of my lab, both past and present for all their help and guidance over the past 4 years. Without the bioinformatics help of Dr Andy Woolston, much of this work would not be possible. In particular, I would like to say a massive thank you to both Beatrice Griffiths and Dr Louise Barber. Both have helped me not only to develop my lab skills, but have also provided endless advice and mentorship throughout my PhD. It has been a joy getting to know both of you.

To all those at the ICR who have given their time, advice or reagents over the past 4 years, thank you also. The ICR has been a wonderful institute and community in which to study and work.

Above all, I would like to thank my family. The hard work that has gone into this thesis is a testament to the unconditional support and love provided to me by my parents, Alexander, Kath and Cameron. Particularly in these last few months, I could not have done it without their love and encouragement.

Abstract

Despite many effective therapies for gastro-intestinal (GI) cancers, both primary and acquired mechanisms of resistance commonly occur. The subclonal complexity of intra-tumoural heterogeneity in these cancers further complicates our understanding of drivers of resistance. Using DNA and RNA sequencing data from patients, this thesis functionally validates putative novel drivers of resistance in GI cancers and tests potential new therapeutic regimens that may overcome the complex heterogeneous resistance landscape.

In gastro-oesophageal adenocarcinoma, the novel use of the pan-RAF inhibitor CCT196969 in this cancer type has shown successful growth inhibition of cell lines with a wide range of Mitogen Activated Protein Kinase (MAPK) pathway activating aberrations that are seen in patients. Pan-RAF inhibition successfully constrained growth better than current in-use downstream MEK or ERK inhibitors, thus indicating pan-RAF as a putative novel therapeutic option for gastric cancer patients.

In colorectal cancer (CRC) cell lines, non-canonical *BRAF* and *KRAS* mutations and loss-of-function *NF1* have been successfully modelled and validated as drivers of MAPK reactivation in response to the anti-EGFR therapy, cetuximab. Furthermore the use of cancer-associated fibroblast conditioned medium has been shown to induce resistance to cetuximab therapy in CRC cell lines as well as elucidation of the individual growth factors contributing to the resistance phenotype. Using biopsies from metastatic colorectal cancer patients, a living biobank of chemotherapy naïve and resistant patient derived organoids (PDOs) has been established. Drug sensitivity assays have been developed to investigate the resistance of the spheroid lines to chemotherapeutics and RNA sequencing of PDOs treated with 5FU has begun to elucidate pathways involved in 5FU chemoresistance.

Publications

Some of the work presented in this thesis has been published;

Woolston, A*., Khan, K*., **Spain, G***., Barber, L. J.*, Griffiths, B., Gonzalez-Exposito, R., Hornsteiner, L., Punta, M., Patil, Y., Newey, A.*, et al.* (2019). **Genomic and Transcriptomic Determinants of Therapy Resistance and Immune Landscape Evolution during Anti-EGFR Treatment in Colorectal Cancer**. Cancer Cell *36*, 35-50.e39.

* Co-first authors.

Table of Contents

List of Figures

List of Tables

Abbreviations

ATCC	American Type Culture Collection
ATP	Adenosine tri-phosphate
BL	Baseline
BSA	Bovine serum albumin
CAF	Cancer-associated fibroblast
CMS	Consensus molecular subtypes
CRC	Colorectal Cancer
CRISPR	Clustered regularly interspaced palindromic repeats
CTB	CellTitre Blue
CTG	CellTitre Glo
DAPI	4',6-diamidino-2-phenylindole
DMSO	Dimethyl sulfoxide
DNA	Deoxyribonucleic acid
DTT	Dithriothreitol
ECL	Enhanced Chemiluminescence
EDTA	Ethylenediaminetetraacetic acid
EGFR	Epidermal growth factor receptor
E_{max}	Maximal Inhibition
EMT	Epithelial-mesenchymal transition
FACS	Fluoresence-activated cell sorting
FBS	Foetal bovine serum
FDR	False discovery rate
FGF	Fibroblast growth factor
FGFR	Fibroblast growth factor receptor
FITC	Fluorescein isothiocyanate
FOrMAT	Feasibility of Molecular Approach to Treatment
GCTS	Glycine Citrate Tween Sodium chloride
GDP	Guanosine diphosphate
GFP	Green fluorescent protein
GI	Gastro-intestinal
GOA	Gastro-oesophageal adenocarcinoma
GSEA	Gene Set Enrichment Analysis
GTP	Guanosine triphosphate
HGF	Hepatocyte growth factor

HRP	Horseradish Peroxidase
IC_{50}	Inhibitory concentration 50
ITH	Intratumour heterogeneity
MCP	Microenvironment cell populations
MEK	MAPK/ERK kinase
MSI	Microsatellite Instable
NaF	Sodium fluoride
NES	Normalised enrichment score
NF1	Neurofibromin 1
PBS	Phosphate buffered saline
PD	Progressive disease
PDO	Patient derived organoid
PDX	Patient derived xenograft
pERK	Phosphorylated ERK
PROSPECT-C	A Prospective Translational Study Investigating Molecular Predictors of Resistance and Response to Cetuximab or Panitumimab in Metastatic Colorectal Cancer
PROSPECT-R	A Prospective Translational Study Investigating Molecular Predictors of Resistance and Response to Regorafenib in RAS mutant Metastatic Colorectal Cancer
qRT-PCR	Quantitative reverse transcriptase polymerase chain reaction
RNA	Ribonucleic acid
SD	Standard deviation
SDS-PAGE	Sodium dodecyl sulphate-polyacrylamide gel electrophoresis
SEM	Standard error of mean
SL	Stem-like
TA	Transit-amplifying
TBS	Tris buffered saline
TGF	Transforming growth factor
TME	Tumour microenvironment

Chapter 1: Introduction

1.1. The Hallmarks of Cancer

Tumourigenesis is the multistage process through which normal cells in the body undergo the transformational changes that eventually allow them to become a malignant cancer. In Hanahan and Weinberg's 2000 seminal paper "The Hallmarks of Cancer", they described six key characteristics that normal cells need to acquire in order to become neoplastic and ultimately malignant (Hanahan and Weinberg, 2000). When undergoing tumourigenesis, normal cells acquire resistance to cell death, have sustained proliferative signalling, evade growth-suppressing signals, activate invasion and metastasis, enable replicative immortality and induce angiogenesis. These changes can occur through both genetic and non-genetic mechanisms in the cell. In 2011 these hallmarks were updated to include genetic instability and mutation, deregulating cellular energetics, tumour-promoting inflammation and avoiding immune destruction, with the latter two further highlighting an important role of the tumour microenvironment in cancer development and progression (Hanahan and Weinberg, 2011).

1.1.1. The Genetic Basis of Cancer

Many of the hallmarks of cancer are established by genetic alterations, including mutations but also structural variants and copy number changes, of more or less tumour type specific driver genes (Vogelstein et al., 2013). These include so-called oncogenes that usually gain functions through genetic alterations and tumour suppressor genes, which are inactivated in cancers. As the human genome is diploid, harbouring two copies of most genes, tumour suppressor gene inactivation often occurs through two genetic hits affecting both copies.

In addition to the key role of somatic genetic alteration for carcinogenesis, Peter Nowell proposed back in 1976 that somatic genetic changes are likely to continue to be acquired by cancers during progression and drug treatment and that this leads to evolutionary adaptation (Nowell, 1976). Extensive recent work over the last ten years has substantiated this concept of cancer as an evolving entity (Gerlinger et al., 2014; Gerlinger et al., 2012; Swanton, 2012; Yates and Campbell, 2012). Instead of the classic view of cancer as a monoclonal disease, malignant tumours are now hence recognized to consist of many subclones, each harbouring mutations that were acquired during cancer progression. Many of these heterogeneous mutations are likely passenger mutations providing little functional or fitness advantage for tumourigenesis or cancer progression. However, there is strong evidence that some subclonal mutations are driver mutations that confer a selective advantage to individual subclones (Gerlinger et al., 2014; Gerlinger et al., 2012; Kandoth et al., 2013; Lawrence et al., 2014; Von Loga et al., 2019) and these allow the tumour to adapt and survive through Darwinian evolution.

1.1.2. Non-genetic basis of cancer

The transformation of a normal cell into a cancer is not only dependent on genetic aberrations in tumour cells. Many genes involved in cancer development or progression are deregulated through altered gene expression, for example as a consequence of promoter hypermethylation that leads to gene silencing. This shows the importance of not only studying DNA but also gene regulation and activity for example through RNA sequencing. Furthermore, the tumour microenvironment (TME) and particularly the stromal cells within the TME, such as cancer-associated fibroblasts and infiltrating immune cells, are increasingly recognised for their critical contribution to at least seven of the hallmarks of cancer (Hanahan and Coussens, 2012) and also for an important role in not only determining prognosis but also treatment sensitivity in many cancer types (Honkanen et al., 2019; Mariathasan et al., 2018). Malignant cells are both influenced by and able to influence or even corrupt the non-malignant

cells that surround them in the TME. The concept of microenvironmental involvement was first postulated by Stephen Paget in 1889 with his “seed and soil” theory for the emergence of metastasis (Paget, 1889). Furthermore, cancer cell plasticity, which allows cells to access different cell states, is another factor that contributes to carcinogenesis and tumour progression. A process termed ‘Epithelial to Mesenchymal Transition’ (EMT), whereby cells switch from an epithelial state to a more mesenchymal state, is a well characterised mechanism for tumour initiation, progression and invasion (Hay and Zuk, 1995; Nieto et al., 2016). This transition is mediated by the activation of transcription factors such as SNAIL, TWIST and ZEB, epigenetics and post-translational regulators. This is a plastic and also a reversible process. Neoplastic cells become more invasive, migratory and importantly more stem-like as a consequence of EMT (Polyak and Weinberg, 2009; Tam and Weinberg, 2013). These examples illustrate that cancer initiation and progression are usually the consequence of underlying genetic and non-genetic alterations in tumour cells, that are however complemented and influenced by the microenvironment. These complex interactions contribute to different outcomes of different cancers but also enable spatial and temporal variability within tumours.

1.1.3. Personalised medicine and drug resistance

The concept termed “personalised medicine” or “precision medicine” tailors drug treatments to individual patients, often according to the genomic profile of their tumour (Ciardiello et al., 2014). Part of the concept of personalised oncology is stratified oncology, the grouping of patients by molecular characteristics. Therapies that target treatment to cancer cells through exploiting distinct molecular abnormalities of the cancer cell versus a normal cell, such as the overexpression of a receptor in a signalling pathway (Piccart-Gebhart, 2005) or mutation of a particular gene (Chapman et al., 2011; Maemondo et al., 2010) were developed and given to subgroups of patients that were identified to benefit. The presence of said molecular abnormalities is known as a predictive biomarker for response or benefit. In contrast, the

treatment decision in giving broad-spectrum chemotherapeutics is traditionally based on the cancer type and stage rather than molecular characteristics. Stratifying patients and tailoring treatments has not only increased clinical efficacy but it also saves over-treating patients who would not benefit based on their molecular profile and thus reduces unnecessary toxicities and costs.

However despite personalised medicine approaches, resistance to the therapies used to treat cancers is inevitable, and occurs in over 90% of metastatic cancers (Longley and Johnston, 2005) . There are a multitude of drug resistance mechanisms and how they interact to result in a resistant tumour is not fully understood. Drug resistance is commonly categorized as being either primary or acquired. Primary or intrinsic drug resistance mechanisms pre-exist in a tumour population prior to treatment and subsequently result in a tumour showing no response to a treatment and thus tumour progression is clinically observed. Tumours with acquired resistance however, initially either respond to the treatment resulting in tumour shrinkage or a prolonged period of stable disease is observed, before eventual tumour progression. In addition to acquiring mechanisms of resistance to the drug used, acquired resistance can result in cross-resistance to drugs with similar mechanisms of action also known as multi-drug resistance (MDR) (Longley and Johnston, 2005).

Drug resistance mechanisms can also be broadly categorised into pharmacokinetic, tumour-cell specific or tumour microenvironment mechanisms (Agarwal and Kaye, 2003). Pharmacokinetic mechanisms impact the delivery and metabolism of the drug. Pharmacokinetic variables, such as tumour vascularity, conversion of prodrug to active metabolic and renal or hepatic drug clearance differ between patients, thus resulting in drug resistance in some patient populations.

Tumour-cell specific mechanisms affect drug uptake through reduced influx or increased efflux, alter drug responses due to changes in the molecular target, and can impact programmed cell death **Figure 1.1** (Gottesman et al., 2002;

Gottesman et al., 2009; Holohan et al., 2013). Drug efflux pumps such as members of the ATP- binding cassette (ABC) transporter family of transmembrane proteins; multi-drug resistance protein 1 (MDR1), MDR-associated protein 1 (MRP1 or ABCC1) and breast cancer resistance protein (BRCP1 or ABCG2), have been extensively studied and implicated in chemoresistance to broad spectrum of therapeutics including taxanes, topoisomerase inhibitors and anti-metabolites (Nooter et al., 1997; Triller et al., 2006; Zalcberg et al., 2000). These drug efflux pumps are often overexpressed in cancers, and expression of MDR1 has even been previously shown to increase in lung cancer cells in response to doxorubicin (Abolhoda et al., 1999). Use of efflux pump inhibitors however has not translated well clinically (Robey et al., 2018). Alteration of drug targets can occur via mutation or changes in gene expression. This is a particularly relevant mechanism to tolerate targeted therapies. Therapies that target signalling kinases such as Epidermal growth factor receptor (EGFR) can be circumvented by mutations that constitutively activating downstream signalling kinases e.g. *KRAS* (Douillard et al., 2013; Karapetis et al., 2008). Such mutations can be pre-existing or acquired throughout the course of treatment.

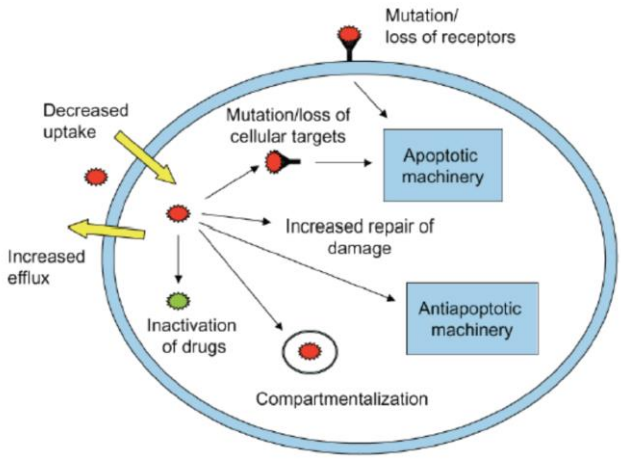

Figure 1.1 Tumour-cell specific mechanisms of drug resistance

Summary diagram of some of the mechanisms of drug resistance within a tumour cell. Decreased uptake and increased efflux are amongst some of the major mechanisms preventing drug efficacy. Image taken from (Gottesman et al., 2009)

Extrinsic cell factors such as intratumour heterogeneity, discussed further in 1.1.4., and the tumour microenvironment (TME) further play a role in contributing to drug resistance. Cytokines and growth factors, such as hepatocyte growth factor (HGF) present in the TME, help mediate tumour growth and survival (Straussman et al., 2012).

Furthermore, a role for cancer stem cells (CSCs) has been increasingly investigated in relation to drug resistance. CSCs are a subpopulation of tumour initiating cells that have stem-like properties (Singh and Settleman, 2010). CSCs can be identified and isolated by epithelial cell markers such as CD133, CD24/CD44 and ALDH1 (Al-Hajj et al., 2003; O'Brien et al., 2007), however these markers are not exclusive to CSCs. The cancer stem cell hypothesis postulates that only these cells are capable of propagating the tumour. Cancer stem cells share many features with normal stem cells including relative quiescence, expression of ABC transporters, resistance to apoptosis through increased expression of pro-survival proteins such as BCL-2 and BCL-XL (Todaro et al., 2007) and active DNA-repair mechanisms. As with normal stem cells these properties accumulate to produce an inherently drug resistance population (Clevers, 2006; Clevers, 2011; Zhou et al., 2009). Moreover it has been shown that a resistance phenotype in CSCs is not static and is reversibly governed by epigenetic modifications (Sharma et al., 2010). Subpopulations of resistant cells that survive treatment, proliferate and their progeny are capable of either reverting back to chemosensitivity when drug exposure is removed or continue to establish and maintain a more stable drug resistant population in the presence of continued drug exposure.

1.1.4. Intratumour heterogeneity and drug resistance

Intratumour heterogeneity (ITH) and the ability of cancers to evolve helps in part to explain the inescapable emergence of drug resistance in tumours.

Multiple driver aberrations are often found in tumours (Gerlinger et al., 2014) and thus if the intended target of the targeted therapies is not expressed in all cells then subpopulations of the tumour will evade the drug's anti-cancer effect. ITH as a result of genetic instability leads to multiple subclones in a tumour in which some cells can harbour resistance mechanisms. These subclones may remain insignificant until treatment induced selection pressure results in rapid outgrowth and thus tumour relapse ensues (Gerlinger and Swanton, 2010). It is therefore described that resistance is a fait accompli (Diaz et al., 2012). Resistance is often defined as being primary when a tumour does not show any response to treatment and progresses or as acquired, when a response or at least a prolonged period of stable disease is followed by progression, usually after at least several months. Genetic alterations such as mutations and amplifications are well-characterised as inducing resistance to targeted therapies through a host of different mechanisms; by preventing drug binding (Montagut et al., 2012), constitutively activating the targeted signalling pathway (Banck and Grothey, 2009; Corcoran et al., 2012) or even activating alternative signalling pathways (Terai et al., 2013; Ware et al., 2013). Resistance not only emerges due to genetic aberrations. Epigenetic mechanisms altering gene expression and stochastic phenotype switches that can persist for many generations have both been shown to contribute to resistance (Jänne et al., 2009; Sharma et al., 2010).

Finally, several studies that investigated either circulating tumour DNA (ctDNA) or multiple biopsies taken from different tumour areas from patients that had acquired resistance to targeted drugs showed that multiple genetic resistance drivers evolved in parallel in different subclones (Bettegowda et al., 2014; Liegl et al., 2008; Shah et al., 2002; Shi et al., 2014). Such polyclonal resistance demonstrates the potency of cancer evolutionary adaptation in circumventing therapeutic selection pressures.

1.2. Gastro-Oesophageal Adenocarcinoma

Gastro-oesophageal adenocarcinoma (GOA) is the fourth most common cancer type worldwide and is a highly aggressive form of cancer (Ferro et al., 2014; Jemal et al., 2011). Encouragingly, in the last few decades there has been a downward trend in incidence (Carcas, 2014). There is a strong geographical bias in incidence and diagnosis, with nearly three-quarters of all gastric cancer cases reported in Asia (Carcas, 2014). Gastro-oesophageal adenocarcinoma (GOA) can be classified anatomically into gastric adenocarcinomas (GA), a highly heterogeneous tumour type, gastro-oesophageal junction cancers and oesophageal cancers. GA can be further categorised into 4 molecular subgroups; Epstein-Barr Virus positive (EBV), microsatellite unstable (MSI), chromosomally unstable (CIN) and genomically stable GOAs (Network, 2014). Almost all GAs are of the CIN subtype. CIN tumours also dominate in the stomach and at the gastro-oesophageal junction (~50% of cases) whereas MSI, EBV+ and genomically stable subtypes are less common. Importantly, CIN subtype GAs can harbour high-level amplifications encompassing receptor tyrosine kinases such as *ERBB2, EGFR, MET* or *FGFR2* or the *KRAS* gene or other genes encoding for members of the mitogen activated protein kinase pathway (MAPK pathway), which transmits signals from these receptor tyrosine kinases (Campbell et al., 2008; Secrier et al., 2016; TCGA, 2012).

1.2.1. Treatment of GOA

The only curative therapeutic option for GOA is surgical resection. Perioperative chemotherapy is given for locally advanced disease, with either fluroropyrimidine based or platinum based treatments administered (Cunningham et al., 2006; Ychou et al., 2011). Metastatic GOAs have a very poor prognosis with median survival of 12 months when treated with combination chemotherapeutics (Cunningham et al., 2008). Approximately one-fifth of GOAs are HER2/ERBB2 positive. HER2/ERBB2 is a receptor tyrosine kinases belonging to the Epidermal Growth Factor Receptor (EGFR) family and co-targeting of

HER2 with the monoclonal antibody trastuzumab during 1st line chemotherapy (Van Cutsem et al., 2007) has led to survival advantages in metastatic HER2 positive GOAs . HER2 positivity is thus used to inform therapeutic patient stratification and therapeutic decisions. Targeted therapies are only routinely used in HER2 –positive cases. Trastuzumab, an anti-HER2 monoclonal antibody has been approved for first-line use in combination with chemotherapeutics in advanced GOA (Bang et al., 2010), increasing median survival to 13.8 months versus 11.1 months in chemotherapy alone treatment groups. More recently, anti-angiogenic treatment with ramucirumab (Fuchs et al., 2014) and immunotherapy with immune-checkpoint inhibitors (Janjigian et al., 2018) have been shown to have modest activity and response rates (<5% and <15% for ramucirumab and immunotherapy, respectively) in these tumours. Nevertheless, survival remains very poor in metastatic GOAs and novel therapies are a major clinical need.

1.3. Colorectal cancer

Colorectal cancer (CRC) is the 3rd most common cause of cancer mortality, with deaths from CRC accounting for 10% of all cancer deaths (World Health Organisation). Fearon and Vogelstein (1990) described the so-called adenoma to carcinoma sequence of CRC development to occur through the sequential acquisition of genetic events such as *APC*, *KRAS* and *TP53* mutations over many years (**Figure 1.1**). Fearon and Vogelstein describe that the accumulation of alterations of each of these genes is most relevant for tumorigenesis, but not necessarily the specific order of acquisition (Fearon and Vogelstein, 1990). Further mutations were then suggested to subsequently enable metastasis, however they have not been defined in the same way as for early cancer progression (Jones et al., 2008; Vanharanta and Massagué, 2013). Instead of metastatic-specific genes being found, genomic sequencing efforts have in fact revealed that genes associated with metastasis are also those commonly altered in primary cancers (Gerlinger et al., 2012; Vanharanta and Massagué, 2013) and metastases are clones that have evolved and survived under therapy-

induced and microenvironmental pressures (Diaz et al., 2012; Hanahan and Coussens, 2012). Metastasis is the result of both selection pressures and stochastic events (Vanharanta and Massagué, 2013).

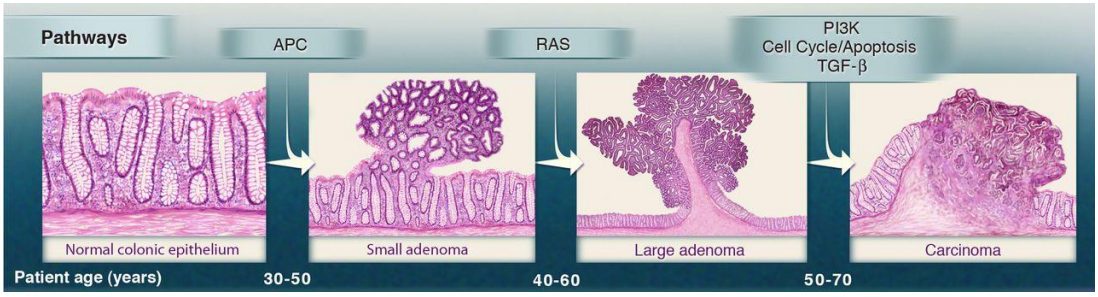

Figure 1.2 Progression of CRC

The key mutations and stages of CRC carcinogenesis as detailed by Fearon and Vogelstein. Image taken from (Vogelstein et al., 2013).

1.3.1. CRC Subtyping

Until recently, CRC was classified into chromosomally unstable (CIN), microsatellite unstable (MSI) and CpG-island methylator phenotype (CIMP) tumours. CIN tumours are the most common type of CRC, accounting for >85% of cases. MSI cancers account for ~15% of early stage CRCs. Their frequency is much lower in metastatic tumours as they have a relatively good prognosis in comparison to CIN CRCs (Walther et al., 2009). MSI CRCs are characterized by inactivation of genes in the DNA mismatch repair pathway such as MutL homolog 1 (MLH1) or MutS homolog 2 (MSH2) through either mutation or hypermethylation. This leads to genetic instability characterized by a hypermutator phenotype that predominantly alters dinucleotide repeats in the genome which are also called microsatellites (Boland et al., 1998).

With the advent of personalised cancer medicine, the use of gene expression profiling has become more commonly used to aid the identification of classification groups and this led to several new classification systems for CRC

subtyping (Guinney et al., 2015; Sadanandam et al., 2013). The CRC subtyping consortium (CRCSC) subsequently started a comprehensive effort to combine these transcriptomic classifications into one reliable and reproducible subtyping system. Prior to the CRCSC analysis, all groups had identified both an MSI-high subtype and a mesenchymal-rich subtype however little consistency emerged when it came to the remaining subtypes (Guinney et al., 2015). The efforts by the CRCSC led to the definition of four Consensus Molecular Subtypes (CMS); CMS1 (MSI Immune Subtype), CMS2 (Canonical Subtype), CMS3 (Metabolic Subtype) and CMS4 (Mesenchymal Subtype). CMS4 is associated with more advanced disease stages of colorectal cancer and worse overall survival rates compared to the other 3 subtypes. Importantly, one of the classification systems that preceded the CMS system (Sadanandam et al., 2013) had identified what they called the Transit-Amplifying like (TA) subtype that is most similar to the CMS2 subtype in the new classification. The TA subtype was predictive of response to cetuximab therapy with 54% of metastatic CRCs assigned to the TA responding compared to only 23% of the stem-like subtype. This demonstrated that transcriptomic subtypes may be a useful tool to predict treatment responses for patient stratification approaches. Notably, neither the CRC-assigner subtypes nor the CMS subtypes showed a specific association with distinct driver mutations and it is likely that subtype identity reflects the cells from which the tumour originated from in different CRCs but also reflects microenvironmental composition and abundance.

1.3.2. Treatment of Colorectal cancer

Standard of care for metastatic colorectal cancer is treatment with fluoropyrimidines (5-fluorouracil, 5FU) in combination with either the topoisomerase-I inhibitor irinotecan (FOLFIRI) or the platinum drug oxaliplatin (FOLFOX). The combination of irinotecan or oxaliplatin to the well-established regimen of 5FU (Cunningham et al., 1998; Rutman et al., 1954) increased response rates to 40-50% versus 10-15% with 5FU monotherapy (Douillard et al., 2000; Giacchetti et al., 2000). 5FU is an antimetabolite that inhibits

biosynthetic processes through inhibition of the enzyme thymidylate synthase (Longley et al., 2003; Rutman et al., 1954). Irinotecan, a derivative of camptothecin, acts through interactions with topoisomerase-I and preventing the repair of double strand DNA breaks (Liu et al., 2000). Oxaliplatin is a platinum drug related to cisplatin and carboplatin, although it has a different mechanism of action. It is a DNA binding drug capable of forming guanine-guanine or guanine-adenine adducts and thus disrupt DNA replication and transcription (Martinez-Balibrea et al., 2015; Raymond et al., 2002).

Targeted anti-EGFR monoclonal antibodies such as cetuximab and panitumimab have been approved in first-line treatment for *KRAS* and *NRAS* wildtype metastatic CRC in combination with either FOLFOX or FOLFIRI regimen (Bokemeyer et al., 2011; Cunningham et al., 2004; Douillard et al., 2013; Heinemann et al., 2014; Jonker et al., 2007; Van Cutsem et al., 2011; Van Cutsem et al., 2009b; Van Cutsem et al., 2007) EGFR-targeted antibodies can alternatively be used in *RAS* wildtype metastatic CRCs that failed chemotherapy, either together with irinotecan or as single agent. Further active drugs in CRC include anti-angiogenics which can also be combined with chemotherapy (Heinemann et al., 2014), regorafenib (Grothey et al., 2013), or single agent chemotherapy with TAS-102 in the third line setting (Grothey et al., 2013; Mayer et al., 2015). However clinical benefit of each of these agents is rather modest. Overall, RAS status is routinely used to stratify patients to treatment with anti-EGFR therapies either in combination with chemotherapy or as single agents. Despite stratification, many patients do not benefit from cetuximab or panitumimab treatment and biomarkers have so far not been identified for the other treatment modalities mentioned above

1.4. MAPK signalling pathway

Mitogen-activated protein kinases (MAPK) form critical signalling networks within the cell. They transmit signals from extracellular mitogens to initiate key cellular responses such proliferation, growth, apoptosis. Three families of MAPK

signalling have been characterised; MAPK/ERK, c-JUN-N- terminal kinase/stress-activated protein kinase (JNK/SAPK) and p38 kinase (Zhang and Liu, 2002). The classical MAPK/ERK signalling pathway (subsequently referred to as the MAPK pathway) is fundamental for cell proliferation and growth. It is deregulated in up to one-third of all cancers (Cox et al., 2014; Dhillon et al., 2007; Samatar and Poulikakos, 2014) and is frequently targeted by therapeutics.

1.4.1. MAPK pathway signalling cascade

In normal cells the cascade can be initiated by the binding of ligands to receptor tyrosine kinases (RTKs). RAS proteins are recruited to the intracellular SH2 binding domain of RTKs through the binding of adaptor proteins GRB2 and SOS (**Figure 1.2**). SOS removes GDP from RAS, to which it is bound in the inactive RAS state. This allows for the binding of GTP and subsequent activation of RAS. The ratio of RAS-GDP to RAS-GTP is tightly regulated, both positively and negatively, by Guanine nucleotide Exchange Factors (GEFs) such as SOS and GTPase Activating Proteins (GAPs) such as NF1. HRAS, KRAS and NRAS are the most extensively studied RAS proteins due to their known roles as proto-oncogenes. These three RAS family members are mutated in 20% of all human tumours, 9.8% of GOAs and 52.2% of CRCs (Cox et al., 2014; Downward, 2009).

Once activated, RAS binds the N-terminal RAS binding domain (RBD) of RAF. This induces conformational change and stimulates its serine/threonine kinase activity thus initiating the phosphorylation cascade (Kolch, 2000; Morrison and Cutler Jr, 1997). There are three main isoforms of RAF; ARAF, BRAF and CRAF, all of which are activated by RAS although through different regulatory mechanisms. ARAF and CRAF require the binding of Src as well as a RAS protein for activation, whereas Src binding is not necessary for BRAF activation (Marais et al., 1997). Furthermore BRAF has greater basal kinase activity than the other two isoforms (Wan et al., 2004). Similarly to RAS, RAF is mutated in 15% of all cancers. BRAF in particular is mutated in ~10% of CRCs but RAF proteins are almost never mutated in GOA (Davies et al., 2002; Oliveira et al., 2003).

Following activation, RAF is recruited to the plasma membrane, where it phosphorylates MEK1/2 (also known as MAP2K1) at serine 217 and 221 (Zheng and Guan, 1994). MEK1/2 subsequently dual phosphorylates ERK1 and 2 at the sites threonine 202/tyrosine 204 and threonine185/tyrosine187 respectively. Phosphorylation at both sites is required for ERK activation (Ferrell and Bhatt, 1997). Once ERK is phosphorylated, it translocates to the nucleus where it regulates the transcription of many key factors that contribute to cell growth and proliferation, including MYC (Chuang and Ng, 1994), Cyclin D1 (Weber et al., 1997) and ternary complex factors (TCFs). It can also indirectly regulate transcription through the 90kDA Ribosomal S6 Kinases (RSKs) and mitogen- and stress-activated stress kinases (MSKs) (Deak et al., 1998). ERK also has a number of cytosolic downstream targets, including the MAPK-interacting kinase (MNK1), a kinase crucially involved in translation efficiency. ERK's downstream effectors critically culminate to give an overall increase in cellular proliferation and growth.

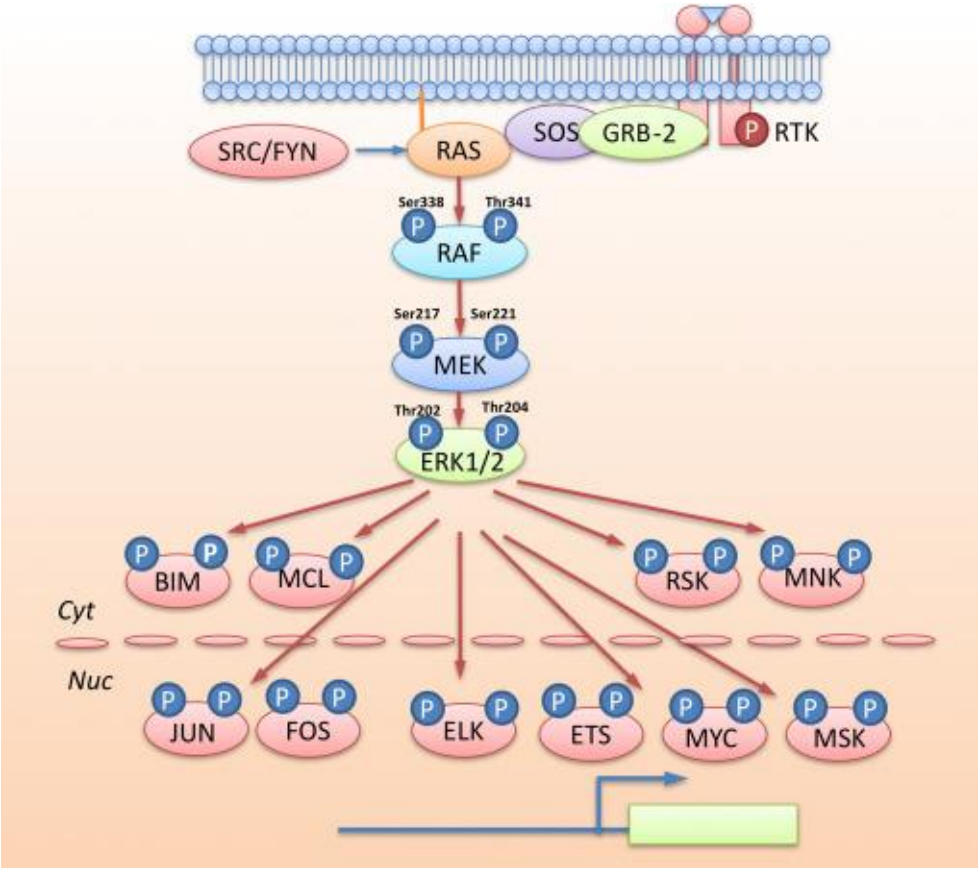

Figure 1.3 The MAPK Signalling pathway

Ligand binding at the cell membrane by RTKs induces a phosphorylation cascade through RAS, RAF, MEK and ERK. ERK then regulates the transcription of many downstream factors. Image taken from (Liu et al., 2018).

1.4.2. EGFR Receptor Tyrosine Kinase

The Epidermal Growth Factor Receptor (EGFR) is a receptor tyrosine kinase upstream of the MAPK pathway. It was recognised as one of the first oncogenic drivers in epithelial cancers (Downward et al., 1984) and is constitutively active in a number of human malignancies (Salomon et al., 1995). Following ligand binding, conformational changes occur that allow two EGFR molecules to dimerise as a homodimer. EGFR is bound by one of its six ligands; epidermal growth factor (EGF), transforming growth factor alpha (TGFa), amphiregulin (AREG) and epiregulin (EREG), heparin-binding growth factor (HB-EGF) and betacellulin (BTC). Ligand binding results in autophosphorylation of the EGFR intracellular domain and activation of the MAPK pathway but also of other signalling pathways such as the PI3K-Akt pathway.

1.4.3. Targeting EGFR signalling with monoclonal antibodies

Sustained proliferative signalling is one of the hallmarks of cancer. Many epithelial cancers are characterised by functional activation of growth factors and EGFR receptors (Ciardiello and Tortora, 2008). Furthermore upregulated expression of the receptor is observed in up to 80% of cases of colorectal cancer (Cunningham et al., 2004; Salomon et al., 1995). Thus targeted therapies have been developed to dampen this signalling pathway. Chimeric IgG anti-EGFR antibodies are competitive antagonists and bind the extracellular part of the receptor thus inhibiting ligand binding through promoting receptor internalisation and preventing subsequent signal transduction (Mendelsohn et al., 2015)

1.4.4. Known Resistance mechanisms to anti-EGFR monoclonal antibodies

Despite improvements in overall survival and progression free survival following cetuximab treatment in early clinical trials, resistance developed in virtually all cases (Karapetis et al., 2008). Tumours with genetic aberrations in signalling nodes further downstream of the EGFR target are able to constitutively activate the MAPK signalling pathway in a ligand-independent manner. Common primary resistance mechanisms to anti-EGFR therapies in colorectal cancer include mutations of exon 2 (codons 12 and 13) in *KRAS* (Douillard et al., 2013; Karapetis et al., 2008). *KRAS* mutations found in 30-45% of mCRC patients, significantly associated with non-responder groups to cetuximab (Lievre et al., 2006; Moroni et al., 2005), with combined datasets revealing that in the presence of a *KRAS* mutation there is a 91.3% chance of no response to cetuximab (Lievre et al., 2006; Moroni et al., 2005). Patients with codon 12 mutations (G12V, G12C, G12V) have a significantly worse response rate to cetuximab than G13D mutations (Mao et al., 2013). However it is not only codon 12 and 13 mutations that predict negative response. Retrospective analysis of early clinical trials showed mutations in *KRAS* exon 3 and 4, in addition to *NRAS* exons 2,3 and 4 were also informative for response (Van Cutsem et al., 2016). Therefore testing for *KRAS* and *NRAS* mutational status prior to administration of anti-EGFR antibodies was introduced in the clinic (Schmoll et al., 2012). Despite the routine use of stratification for KRAS, NRAS wildtype CRCs, primary resistance still occurs. Retrospective clinical studies have suggested that mutations in additional *KRAS* and *NRAS* codons, *BRAF*, and *PIK3CA* (Allegra et al., 2016; Amado et al., 2008; Bokemeyer et al., 2012; Douillard et al., 2013; Loupakis et al., 2009; Sartore-Bianchi et al., 2009; Tejpar et al., 2016) and activation of *ERBB2, MET* and *FGFR1* (Bertotti et al., 2015) are all further drivers of primary resistance to anti-EGFR therapies, however there is insufficient clinical validation to recommend their use as additional biomarkers for stratification.

EGFR mutations are not associated with primary resistance in CRC and have only been reported in cases of acquired resistance. S492R mutations have been described (Montagut et al., 2012) to induce resistance specifically to cetuximab as the amino acid change affects the binding epitope of EGFR, preventing cetuximab binding. This mutation has never previously been described in untreated CRC and is thought to exclusively be the result of selective pressure (Misale et al., 2015). More commonly found are acquired mutations in *KRAS* and *NRAS* that occur in 50-80% of patients (Arena et al., 2015; Bettegowda et al., 2014; Diaz et al., 2012; Misale et al., 2012). Non-mutually exclusive mutations in both *KRAS* and *EGFR* have been found in ctDNA, indicating heterogeneous acquired resistance mechanisms arise (Morelli et al., 2013). Furthermore amplifications in *ERBB2* and *MET* also result in acquired cetuximab resistance (Bardelli et al., 2013; Yonesaka et al., 2011). Thus in addition to primary resistance, which is currently stratified for in the clinic, there are evidently many mechanisms of acquired resistance at play, and parallels can be seen in primary and acquired resistance such the emergence of KRAS mutations following exposure to cetuximab.

1.5. Outline of subsequent chapters and PhD Aims

The aim of my PhD Thesis is to investigate new targeted therapies in GOA and investigate mechanisms of drug resistance in CRCs to the anti-EGFR antibody cetuximab in *RAS* wildtype patients, and to combination chemotherapies. The first results chapter (Chapter 3) describes the first use of a pan-RAF inhibitor in GOA, providing a novel targeted therapeutic option that is effective in a multitude in MAPK-aberrant GOAs. Chapters 4 and 5 focus on mechanisms of both primary and acquired resistance to the anti-EGFR therapy cetuximab in metastatic CRC. Here, novel genetic and transcriptomic driver mechanisms of resistance are described and validated. In the final results chapter (Chapter 6), I established patient-derived organoids models from patients with chemotherapy

refractory CRCs as novel model systems to interrogate the molecular mechanisms of resistance to chemotherapy.

Chapter 2: Materials and Methods

2.1. Materials

2.1.1. Drugs

Drug	Target	Manufacturer
5FU	Thymidylate Synthase	Sigma
AMG-337	c-MET	SelleckChem
BGJ398	FGFR	SelleckChem
Cetuximab	EGFR	MerckKG
CCT196969	Pan-RAF	Basilea
Staurosporine	Non-selective protein kinase	Abcam
SCH772984	ERK	SelleckChem
SN38	Topoisomerase I	Sigma
Trametinib	MEK	Cambridge Bioscience
Blasticidin Hydrochloride	Antibiotic	Sigma
Puromycin	Antibiotic	

Table 2.1 Drugs

2.1.2. Antibodies

Antibody	Manufacturer	Catalogue No	Dilution
p42/44 ERK	Cell Signalling Technologies	9101	1:1000
ERK	Cell Signalling Technologies	9102	1:1000
p-EGFR	Cell Signalling Technologies	2236	1:1000
EGFR	Cell Signalling Technologies	2232	1:1000
NF1	Cell Signalling Technologies	14623	1:1000
Cas9	Cell Signalling Technologies	14697	1:1000
Beta Tubulin-HRP	Abcam	ab21058	1:5000
GAPDH	Abcam	ab9482	1:5000
ERK	Santa Cruz Technologies	Sc-514302	1:1000

Table 2.2 Antibodies

2.1.3. DNA Constructs

Construct	Source	Catalogue No
R777-E053-Hs.EGFR	Addgene	70377
R777-E015-Hs.BRAF	Addgene	70299
pDONOR223_BRAF_p.D594H	Addgene	82816
KRAS(NM_004985)Human Tagged ORF Clone	Origene	RC201958
pENTRA1A	Invitrogen	A10462
pLX304	Addgene	25890
pLENTI-CMV-Puro-DEST	Addgene	17477

psPAX2	Addgene	12260
pMD2.G	Addgene	12259
lentiCas9-Blast	Addgene	52962
pLentiguide-Puro	Addgene	52963
pLV-GFP	Addgene	25999

Table 2.3 DNA constructs

2.1.4. siRNA oligonucleotides

siRNA	Sequence	Manufacturer
siNF1-3	CAACAAAGCUAAUCCUUAA	siGENOME Dharmacon
siNF1-4	CACCGAGUCUUACAUUUAA	siGENOME Dharmacon
Non-Targeting Pool 2	/	siGENOME Dharmacon
siGAPDH	/	siGENOME Dharmacon

Table 2.4 siRNA Oligonucleotides

2.1.5. Real-time quantitative polymerase chain reaction (RTqPCR) primers

Name	Identifier	Manufacturer
NF1	Hs01035108_m1	Thermo Fisher Scientific
GAPDH	Hs02758991_g1	Thermo Fisher Scientific

Table 2.5 Real-time quantitative polymerase chain reaction (RTqPCR) primers

2.1.6. QuikChange Custom Primers

Variant	QuikChange primer ID	Primer sequence
EGFR-D278N	EGFR_QCh_D278N_F	cctcggggttcacattcatctggtacgtggt
	EGFR_QCh_D278N_R	accacgtaccagatgaatgtgaaccccgagg
FGFR3-P148L	FGFR3_QCh_P418L_F	cctgtcgcttgagcaggaagcgggagatc
	FGFR3_QCh_P418L_R	gatctcccgcttcctgctcaagcgacagg
BRAF-D594N	BRAF_QCh_D594N_F	tcactgtagctagaccaaaattacctatttttactgtgaggtc
	BRAF_QCh_D594N_R	gacctcacagtaaaaataggtaattttggtctagctacagtga
BRAF-D594F	BRAF_QCh_D594F_F	gatttcactgtagctagaccaaaaaaacctatttttactgtgaggtcttca
	BRAF_QCh_D594F_R	tgaagacctcacagtaaaaataggttttttttggtctagctacagtgaaatc
KRAS-STOP	KRAS_MUTSTOP_F	gagcggccgcgtacgctacataattacacactttgtctttg
	KRAS_MUTSTOP_R	caaagacaaagtgtgtaattatgtagcgtacgcggccgctc
KRAS-A18D	KRAS_QCh_A18D_F	tagctgtatcgtcaagtcactcttgcctacgcc
	KRAS_QCh_A18D_R	ggcgtaggcaagagtgacttgacgatacagcta
KRAS-L19F	KRAS_QCh_L19F_F	attagctgtatcgtaaaggcactcttgcctacgc
	KRAS_QCh_L19F_R	gcgtaggcaagagtgcctttacgatacagctaat

Table 2.6 Quikchange Custom Primers

2.1.7. Sanger Sequencing Primers

Gene sequenced	Gene-specific Sanger sequencing primer ID	Primer sequence
EGFR	EGFR-seqF1	AGGTGGCTGGTTATGTCCTC
EGFR	EGFR-seqF2	CAAATTCCGAGACGAAGCCA
EGFR	EGFR-seqF3	CCTCCATGCCTTTGAGAACC
EGFR	EGFR-seqF4	TGTGCCCACTACATTGACGG
EGFR	EGFR-seqF5	GCAACATCTCCGAAAGCCAA
EGFR	EGFR-seqF6	TATGACGGAATCCCTGCCAG
EGFR	EGFR-seqF7	GGACAGCATAGACGACACCT
EGFR	EFGR-seqRmut	CGTAGCATTTATGGAGAGTGAGT
BRAF	BRAF_D594_chk_F	AGATATTGCACGACAGACTGC
BRAF	BRAF_D594_chk_R	TCTGATGACTTCTGGTGCCA
BRAF	BRAF_seq1	TGTTTCTAGCTCTGCATCAATGG
BRAF	BRAF_seq2	TGACCAACTTGATTTGCTGTTTG
BRAF	BRAF_seq3	ACACTTGGTAGACGGGACTC
BRAF	BRAF_seq4	GGGTCCCATCAGTTTGAACAG

Table 2.7 Gene specific Sanger primers

Gene(s) sequenced	Vector-specific Sanger sequencing primer ID	Primer sequence
BRAF and EGFR 5' end	M13(-21)F	TGTAAAACGACGGCCAGT
BRAF 3' end	M13R	CAGGAAACAGCTATGACC
KRAS	pENTR-F	CTACAAACTCTTCCTGTTAGTTAG
KRAS	pENTR-R	ATGGCTCATAACACCCCTTG

Table 2.8 Vector specific Sanger primers

Primer ID	Primer sequence (with M13F/R tails)
NF1_C08_check-F	TGTAAAACGACGGCCAGTGAGCCTGCACTCCACAGACC
NF1_C08_check-R	CAGGAAACAGCTATGACCCCCAGGTCACTCATCCCCATTT
NF1_C09_check-F	TGTAAAACGACGGCCAGTAGTTGCAAATATATGTCTTCCACCCTT
NF1_C09_check-R	CAGGAAACAGCTATGACCGCTTCAGTGTCAGGGTTCCA
NF1_D09_check-F	TGTAAAACGACGGCCAGTGGGAAACTGGCTGAGCACATA
NF1_D09_check-R	CAGGAAACAGCTATGACCTCGTTTACAAAACACAGACTGGAACT
NF1_D08_check-Flong	TGTAAAACGACGGCCAGTAAAGATTCCAATGAAGTCTACACGTT
NF1_D08_check-Rlong	CAGGAAACAGCTATGACCACTGCATTTTAAACTTGCTCCCAAT
M13(-21)F	TGTAAAACGACGGCCAGT
M13R	CAGGAAACAGCTATGACC

Table 2.9 NF1 Sanger Primers

2.1.8. Commercial Assays

Commercial Assays	
All Prep DNA/RNA Micro Kit	Qiagen
Bioanalyzer High Sensitivity DNA	Agilent
CellTiter-Blue	Promega
CellTiter-Glo	Promega
esiCRISPR kit	Eupheria Biotech
Human Cytokine Array C5	RayBiotech
Lipofectamine 2000	Thermo Fisher Scientific
Mix2Seq	Eurofins
Mouse Cell Depletion Kit	Miltenyi Biotec
NEBNext® Ultra™ Directional RNA Library Prep Kit	New England Biolabs
QIAamp DNA Blood Mini Kit (50)	Qiagen
QIAmp Circulating Nucleic Acid Kit	Qiagen
QuantSeq 3' mRNA-Seq Library Preparation Kit for Illumina (FWD)	Lexogen
Qubit dsDNA Broad Range Assay Kit	Thermo Fisher Scientific
Qubit RNA High Sensitivity Kit	Thermo Fisher Scientific
Quickstart Bradford Protein Assay	BioRad
QuikChange Lightning	Agilent
RNeasy Mini Kit	Qiagen
siGenome	Dharmacon
SureSelectXT Human All Exon v5 Kit	Agilent
TransIT-LT1	Mirus
Tumour Dissociation Kit	Miltenyi Biotech

Table 2.10 Commerical Assays

2.1.9. Reagents

Reagent	Manufacturer
0.05% Trypsin with 0.02% Versene	In house
1-Thioglycerol	Sigma
100 % reduced Growth Factor matrigel	Corning
4-12% NuPAGE Bis-Tris Gels	Invitrogen
Acetic Acid	Fisher
Advanced:F12 DMEM	Invitrogen
BSA fraction V	Sigma
Crystal Violet	Sigma
DAPI	Sigma
DMEM	Sigma
DMEM:F12	Sigma
DMSO	Sigma
DTT	Sigma
ECL Prime	GE Healthcare
EDTA	In-house
EDTA-free Protease Inhibitor	Roche
EnGEN CAas9 NLS	New England Biolabs
Foetal Bovine Serum (FBS)	Invitrogen
Full range Rainbow Marker	GE Healthcare
Glutamax	Invitrogen
Hydrocortisone	Thermo Fisher Scientific

Insulin	Thermo Fisher Scientific
Insulin-Transferrin-Selenium (ITS)	Thermo Fisher Scientific
Lipofectamine™ CRISPRMAX Cas9 Plus	Invitrogen
Lipofectamine™ RNAiMAX	Thermo Fisher Scientific
Methanol	VWR
Milk powder	Marvel
MOPS Running buffer	Invitrogen
NaCL	In-house
NaF	
Nitrocellulose membrane	GE Healthcare
Nuclease-free water	
NuPAGE LDS Sample Buffer	Invitrogen
OptiMEM	Invitrogen
Pen/Strep	In-house
PFA	Sigma
Phosphatase Inhibitor Cocktail II	Sigma
PVDF membrane	Millipore
Q5® High-Fidelity 2X Master Mix	New England Biolabs
RPMI1640	Invitrogen
siRNA buffer	Dharmacon
Sodium Azide	Sigma
Transfer buffer	In-house
Tris pH 7.6	In-house
Trypan Blue	Invitrogen
Tryple Express	Sigma
Ultra-filtered (UF) water	In house

Table 2.11: Reagents

2.2. Patient Samples

2.2.1. Gastro-oesophageal adenocarcinoma Cohort

Archival formalin fixed and paraffin embedded (FFPE) specimens were selected by the pathologist at Semmelweis University (AMS) from ten treatment naïve GOAs. These had been surgically resected as part of routine clinical management. The study was approved by the Institutional Ethics Board at Semmelweis University (Biomarker Studies in Gastrointestinal Tumours, including primary tumours and consecutive distant metastases, approval number IKEB #207/2011). The requirement for consent was waived by the Board as only leftover tissues from routine procedures were used and all samples had been anonymised. Sample location (tumour centre, lateral and deep invasive front and lymph node or omental metastases) was microscopically confirmed separately by two pathologists, Dr von Loga and Dr Wotherspoon.

2.2.2. PROSPECT-C

PROSPECT-C is a Phase II clinical trial (clinical trials.gov number NCT02994888) investigating molecular biomarkers of response or resistance to anti-epidermal growth factor receptor (anti-EGFR) monoclonal antibodies in chemo-refractory *KRAS* WT metastatic colorectal cancer. Patients over the age of 18 and with a World Health Organisation performance status of 0-2 were eligible if;

- All conventional chemotherapeutic options (5-fluorouracil, oxaliplatin and irinotecan) had been exhausted, or patients were intolerant or showed contraindications to irinotecan/oxaliplatin therapy.
- They had metastatic colorectal cancer amenable to biopsy and repeated measurements with computed tomography (CT) scanning.

Written informed consent was obtained from all patients. The study was carried out in accordance with the Declaration of Helsinki and approved by the national UK ethics committee (UK Research Ethics Committee approval: 12/LO/0914). All patients were required to have mandatory image guided core biopsies of metastases at pre-treatment (BL) and at the time of RECIST-defined progressive disease (PD). Cetuximab was provided by the Cancer Drug Fund and patients were given single-agent dose at 500 mg/m^2 administered every other week until progression or intolerable side effects. The primary endpoint of the study was the identification of biomarkers in DNA and RNA for primary and acquired resistance to cetuximab therapy. The study recruited 30 patients who had BL and PD biopsies available for genetic analyses. 24 sample pairs had sufficient DNA yield for sequencing and analyzable tumour content. Progression, partial response and stable disease were determined according to RECISTv1.1 criteria. Progression free survival (PFS) was measured from start of treatment date until progression date or death due to any cause. Overall survival (OS) was measured from the start of treatment date until date of death due to any cause. PFS and OS were estimated in patients with no event at the final follow-up. The cohort

was grouped into primary progressors defined by PD on or before the first scheduled per protocol CT scan (range 9-16 weeks post start of treatment) and patients with prolonged clinical benefit who remained progression free at the first scan.

2.2.3. PROSPECT-R

The PROSPECT-R trial (clinical trials.gov number NCT03010722) is an exploratory clinical trial investigating molecular biomarkers of response or resistance to multi-kinase inhibitor regorafenib in *RAS* mutant chemorefractory metastatic colorectal cancer. Patients over the age of 18 and with a World Health Organisation performance status of 0-1 were eligible if;

- All conventional treatment options including fluorouracil, irinotecan, oxaliplatin and at least one anti-VEGF therapeutic (where available) had been exhausted.
- They had metastatic tumour amenable to biopsy and repeat measurements with Dynamic Contrast-Enhanced DCE-MRI.

All patients gave written consent and the study was approved by a research ethics committee and National institutional review boards (Medicines and Healthcare products Regulatory Agency: 15983/0249/001–0001). Mandatory biopsies of metastases were taken at pre-treatment (BL), at 2 months (if response or stable disease), and at time of progression (PD).

2.2.4. FOrMAT

The Feasibility of a Molecular Characterisation Approach to Treatment (FOrMAT) trial (clinical trials.gov number NCT02112357) was a prospective study that aimed to investigate the feasibility of molecular profiling in malignant gastro-intestinal (GI) cancers in routine clinical practice. Patients with the following cancer types were eligible;

- Locally advanced or metastatic oesophagogastric (OGA)

- Pancreatic
- Biliary tract
- Colorectal

The study collected FFPE archival samples from the primary tumour, non-bony metastasis or biopsiable site of disease and a total of 71 advanced OGA patients were recruited. All patients gave written consent and the study was approved by the UK National Ethics Committee (approval 434 number: 13/LO/1274RM).

2.3. Mammalian Cell culture

2.3.1. Cell Line Culture

Cell lines were obtained from and cultured under the conditions stated in Table 2.12.

Cell Line	Cell Type	Source	Culture conditions
MKN45	Gastric adenocarcinoma	ATCC	RPMI1640, 10% Foetal Bovine Serum, 1% Glutamax, 1% Penicillin/Streptomycin, 5% $C0_2$, 37°C
SKGT4	Oesophagus adenocarcinoma	ATCC	RPMI1640, 10% Foetal Bovine Serum, 1% Glutamax, 1% Penicillin/Streptomycin, 5% $C0_2$, 37°C
NCI-N87	Liver metastasis from stomach	ATCC	RPMI1640, 10% Foetal Bovine Serum, 1% Glutamax, 1% Penicillin/Streptomycin, 5% $C0_2$, 37°C
MKN74	Gastric adenocarcinoma	Japanese Cell Bank	RPMI1640, 10% Foetal Bovine Serum, 1% Glutamax, 1% Penicillin/Streptomycin, 5% $C0_2$, 37°C
KATOIII	Gastric carcinoma	Gift from N.Turner (ICR)	RPMI1640, 10% Foetal Bovine Serum, 1% Glutamax, 1% Penicillin/Streptomycin, 5% $C0_2$, 37°C
OCUM-2M	Gastric adenocarcinoma	Gift from N.Turner (ICR)	DMEM, 10% Foetal Bovine Serum, 1% Glutamax, 1% Penicillin/Streptomycin, 5% $C0_2$, 37°C
FG-51	Gastric carcinoma	Gift from N.Turner (ICR)	RPMI1640, 10% Foetal Bovine Serum, 1% Glutamax, 1% Penicillin/Streptomycin, 5% $C0_2$, 37°C
DiFi	Colorectal carcinoma	Gift from N. Valeri (ICR)	RPMI1640, 5% Foetal Bovine Serum, 1% Glutamax, 1% Penicillin/Streptomycin, 5% $C0_2$, 37°C

LIM1215	Colorectal carcinoma	Gift from N.Valeri (ICR)	RPMI1640, 10% Foetal Bovine Serum, 1% Glutamax, 1% Penicillin/Streptomycin, 0.000066% Insulin, 0.0000606% Hydrocortisone, 0.000001% 1-Thioglycerol, 5% $C0_2$, 37°C
RC-11	Rectal cancer associated fibroblasts	Gift from F.Calvo (ICR) and D.Vignjevic (Institut Curie, Paris)	DMEM, 10% Foetal Bovine Serum, 1% Glutamax, 1% Penicillin/Streptomycin, 10% ITS-A, 10% $C0_2$, 37°C
HEK293T	Embryonic renal	ATCC	DMEM, 10% Foetal Bovine Serum, 1% Glutamax, 1% Penicillin/Streptomycin, 5% $C0_2$, 37°C
NIH-3T3	Mouse fibroblasts	Gift from P.Huang (ICR)	DMEM, 10% Foetal Bovine Serum, 1% Glutamax, 1% Penicillin/Streptomycin, 5% $C0_2$, 37°C
SKCO-1	Colorectal adenocarcinoma	ATCC	DMEM, 10% Foetal Bovine Serum, 1% Glutamax, 1% Penicillin/Streptomycin, 5% $C0_2$, 37°C
T84	Colorectal carcinoma	ATCC	DMEM:F12, 10% Foetal Bovine Serum, 1% Glutamax, 1% Penicillin/Streptomycin, 5% $C0_2$, 37°C
NCI-H508	Colorectal adenocarcinoma	ATCC	RPMI1640, 10% Foetal Bovine Serum, 1% Glutamax, 1% Penicillin/Streptomycin, 5% $C0_2$, 37°C
HCA-46	Colorectal adenocarcinoma	ATCC	DMEM, 10% Foetal Bovine Serum, 1% Glutamax, 1% Penicillin/Streptomycin, 5% $C0_2$, 37°C
U20S	Osteosarcoma	ATCC	M^{c}Coys, 10% Foetal Bovine Serum, 1% Glutamax, 1% Penicillin/Streptomycin, 5% $C0_2$, 37°C

Table 2.12: Cell Lines

To split cells, medium was aspirated, cells were washed with PBS and then incubated with 0.05% Trypsin in 0.02% Versene until cells detached. Fresh medium was added to neutralise the trypsin and cells were spun for 5 minutes at 300 xg. Cells were counted using the Countess and then plated at appropriate densities for continued culture or for experiments.

For long-term storage, cells were trypsinised and spun down as previously described. Cell pellets were then resuspended in freezing medium (FBS with

10% DMSO) and aliquoted into cryofreeze vials. Vials were frozen down in polystyrene containers to slow the freezing and stored short-term at -80°C before being transferred to liquid nitrogen for long term freezing.

2.3.2. Conditioned medium

Cells were seeded at a confluency of ~70-80%. After 2-3 days, medium was changed and 75% of the normal volume for a stock flask was added. After ~72 hr medium was taken off, filtered and used immediately in conditioned medium experiments. CAF conditioned medium was frozen at -80°C for use in the cytokine array.

2.3.3. Culturing Patient-Derived Organoids (PDOs)

Organoid cultures were established from metastatic colorectal cancer biopsies from patients enrolled in PROSPECT-C (CCR3770), PROSPECT-R (CCR4164) and FORMAT (CCR3994) clinical trials.

Direct Cultures

Core biopsies were cut into several <1mm^3 pieces, one small piece was snap frozen in liquid nitrogen and stored at -80 °C for future genomic analyses, and the rest was plated in a 24-well plate 100% reduced growth factor matrigel. The matrigel was left to set at 37°C and then covered with supplemented advanced DMEM:F12 medium, herein referred to as Adv DMEM:F12 medium (Table 2.13: Advanced DMEM:F12 supplements). To passage, the matrigel was mechanically disrupted with a pipette tip, suspended in PBS and centrifuged at 300xg for 5min. TrypLE Express was added (~500 µL per well) and cultures were incubated for exactly 20 minutes at 37 °C. TrypLE Express was neutralised with 10% FBS DMEM:F12 medium and cultures were spun again at 300xg for 5 minutes. The cell pellet was resuspended in matrigel, replated, left to set at 37°C and then covered with Adv DMEM:F12 medium.

Indirect cultures

A piece of the core biopsy (~25%) was given to the Tumour Profiling Unit to be implanted into immunodeficient nude mice. The resulting tumour from the PDX model was dissociated into a single cell suspension using a tumour dissociation kit and then depleted of mouse cells using immunomagnetic beads. The resulting cells were then embedded in matrigel, left to set at 37^{o}C and covered in Adv DMEM:F12.

Component	Supplier	Final concentration
Glutamax	Invitrogen	X1
Pen/strep	Invitrogen	X1
B27	Invitrogen	X1
N2	Invitrogen	X1
HEPES	Invitrogen	10mM
NAC	Sigma	1mM
Nicotinamide	Sigma	10mM
EGF	Merck	50ng/ml
SB202190	Sigma	10um
PGE2	R&D systems	10nM
Gastrin	Sigma	10nM
A-83-01	R&D systems	500nM
R-Spondin	Peprotech	1ug/ml
Noggin	Peprotech	100ng/ml
FGF10	Peprotech	100ng/ml
Wnt3a	R&D systems	100ng/ml
Y27632	Sigma	10uM

Table 2.13: Advanced DMEM:F12 supplements

2.4. Drug sensitivity assays

2.4.1. Adherent cell lines

Cells were plated in 96-well Optilux plates at an appropriate density in 50 µL medium, to ensure exponential growth throughout the experiment; 10,000 cells for gastric cell lines, 5,000 cells for DiFi and 2,500 cells for LIM1215 per well. Cells were not seeded in the outer wells, which were instead filled with 100 µL of PBS to prevent adverse readings due to excess evaporation. After 24 hr, cells were treated with 2X drug in 50 µL. For each experiment a reference plate was seeded alongside the experimental plates. To measure cell viability, 20 µL CellTiter Blue (CTB) was added 24 hr after seeding and fluorescence read on the Cytation3 (BioTek Instruments Inc.) at 590 nM following 1-2 hr incubation. After 3-5 days the experimental plates were also read on the Cytation3 following 1-2 hr incubation with CTB at 37^{o}C. 6 replicates were plated per dose unless otherwise stated. Data were then analysed by subtracting the mean value for the reference plate at Day 0 of treatment, and normalised to the mean value for growth in control buffer only wells (DMSO or GCTS (Glycine Citrate Tween Sodium Chloride), the buffer for cetuximab), whereby a value of 1 indicated full growth and a value of 0 indicated no growth from seeding. Data were plotted in Graphpad Prism versions 6-8. Non-linear regressions were plotted using the log inhibitor vs response (three parameters) function on GraphPad. IC_{50}s were then subsequently determined.

2.4.2. PDO lines

PDOs were passaged as previously described. The method was adapted for manual pipetting and a 96-well format. Briefly, PDOs were disrupted as previously described and one dense 12-well was re-seeded in a 6-well plate in 10 µL drops of matrigel. This was left for ~5 days until organoids had grown. 96-well plates were coated with 25 µL of matrigel and spun at 180 xg for 1 minute to ensure even coating of the wells. The plates were then incubated for 20 mins

at 37°C. The organoids in matrigel droplets were then manually dislodged using a pipette tip and spun down in the Adv DMEM:F12 medium for 2 minutes at 300 xg. The pellet was then resuspended in Adv DMEM:F12 medium supplemented with 2% matrigel. 100 µL was pipetted into each well, and the outside wells were filled with PBS to reduce the effects of evaporation. A reference plate was seeded in addition to each experimental plate. At 24 hr, 50 µL medium was added to the reference plate to bring the total volume up to 150 µL. 30 µL of Cell-Titer Glo (CTG) was added according to manufacturers instructions. The plate was left at room temperature for 30 mins before luminescence was read on a Cytation3 plate reader at 560 nm. Each experimental plate was treated for 6 days with the relevant concentration of drug according to the plate design. Staurosporine at a final concentration of 1 µM was used as a control for effective cell death. After 6 days, 30 µL of CTG was added and read as above. The average of the reference plate was used to confirm growth in the assay. 3 replicates were plated per dose level. Data analysis was performed according to the Sanger protocol (Francies et al., 2016). Mean values for DMSO treated and medium-only treated and the respective fold change was calculated. Fold change between DMSO treated and medium-only had to fall between 0.8-1.2 for the plate to be accepted for analysis. Mean values for staurosporine treated wells were subtracted from the raw data and the growth was calculated relative to DMSO-treated control. Non-linear regressions were fitted as described in section 2.4.1. IC_{50}s were then calculated using GraphPad. E_{max} was manually calculated by subtracting the percentage of growth from 100 and plotted in GraphPad.

2.4.3. Co-Culture

CAFs and GFP-labelled tumour cells were seeded together in either a 2:1 or 5:1 ratio in 96-well plates. After 24 hr, drug treatment was added. Plates were read using the ImageXpress Micro Confocal Microscope to assess quantity of GFP in each well. For each well 25 images (5x5) were acquired in the FITC channel using 10X Plan Apo Lambda magnification. Images were then analysed using the

MetaXpress software. A custom analysis pipeline was built to account for the fact that the fibroblasts were very autofluorescent in the FITC channel. An adaptive threshold that identifies objects based on size and signal intensity was set to exclude fibroblasts based on their size. Thresholds for inclusion were a minimum width of 5.4 µm and maximum width of 20.82 µm with intensity above local background set to 145 arbitrary units. A further filter mask was then applied which excludes objects based on measurement values. This was set to exclude based on total area and was set to a MaxFilter of 400 arbitrary units. Cell counts were given by the software as an average per image in the well. Data were plotted using GraphPad Prism.

2.5. Protein Analysis

2.5.1. Cell Lysis

Cells were lysed with NP-40 buffer; 50 mM Tris pH7.6, 250 mM NaCl, 5mM EDTA, 10 mM NaF, 1X Phosphatase Inhibitor Cocktail II, 1% Igepal CA-63, made up to 10 mL with UF water. One COMPLETE ULTRA EDTA-free Protease inhibitor tablet was added to 10 mL. Cells were washed with ice-cold PBS and then ice-cold lysis buffer was added (1 mL per 10^7 cells/100 mm dish/150 cm^2 flask; 0.5 mL per $5x10^6$ cells/60 mm dish/75 cm^2 flask). Lysates were incubated on ice for 30 mins and vortexed every 10 mins. Lysates were centrifuged for 10 minutes at 13,000 rpm at 4^oC. Lysate supernatant was then transferred to a fresh eppendorf tube and lysates stored at -80^oC.

2.5.2. Protein quantification

The protein concentration of lysates was quantified using BioRad Quick Start Bradford Protein Assay. A standard curve was produced using the BSA standard set provided (0.125, 0.25, 0.5, 0.75, 1, 1.5, 2 mg/mL). 5 µL of standards and 5 µL of sample were added in triplicate and 250 µL of Bradford reagent added. This was incubated for 5 minutes at room temperature before absorbance was read

on the Cytation3 at 595 nM. Protein concentration of the lysates was then determined based on the equation of the standard curve. Samples were then made up containing 1X sample buffer (4X NuPAGE LDS Sample buffer + 1M DTT), protein (10-30 µg) and made up to a final volume with nuclease free water. A pre-stained molecular weight marker was also diluted in 1X sample buffer and water. Lysates and marker were heated to 70^{o}C for 10 minutes prior to loading on gels.

2.5.3. SDS PAGE separation

Proteins were resolved by SDS PAGE (sodium dodecyl sulphate polyacrylamide gel electrophoresis). Lysates were run on 4-12% NuPAGE Bis-Tris gradient gels (Invitrogen) in running buffer; 0.05% 20X MOPS running buffer in ultra-filtered (UF) water). Gels were run at 120V for 1.5-2 hr until the proteins had reached the bottom of the gel in the Invitrogen XCell II Blot module system.

2.5.4. Western Blotting

Protein was then transferred from the gel to either nitrocellulose or PVDF (polyvinylidene fluoridine) membrane. PVDF membranes were activated in 100% methanol prior to blotting. Transfer was carried out in transfer buffer; 192 mM glycine, 25 mM Tris and 200 mM methanol in UF water, at 30V for 3 hr or overnight at 4^{o}C for larger (>200 kDa proteins). Cold UF water was used to surround the blot module system and prevent overheating.

2.5.5. Detection of Protein

Membranes were blocked with 3% BSA, 0.01% Sodium Azide in TBST (0.01% Tween20 in TBS) for 1 hr at room temperature. Primary antibody was incubated overnight at 4^{o}C at a dilution of 1:1000 in blocking buffer. Membranes were then washed 3x for 5 minutes in 5% milk in TBST and 2x for 5 minutes in TBST.

Membranes were incubated with secondary antibody diluted 1:2000 in 5% milk for 2 hr at room temperature. Membranes were then washed again as described.

2.5.6. Enhanced Chemiluminescence

Protein bands were visualised using the ECL Prime detection reagents. Equivolumes of Detection reagent A and B were mixed, and membranes were incubated with the mixture for 3 minutes. Membranes were then blotted onto filter paper to remove excess reagent and placed between sheets of laser transparency film. Excess liquid was removed and membranes were imaged using the Azure Biosystems c300 Gel Imaging System.

2.6. In Vivo Experiments

All animal experiments were carried out under UK Home Office Project licences 70/7413 and P6AB1448A (held by Professor Clare Isacke), license PPL-70/7635 (held by Caroline Springer) and license PD498FF8D) (held by Amanda Swain), Establishment License, X702B0E74 70/2902. Work was carried out by David Vicente, the Tumour Profiling Unit (TPU) and Filipa Lopes or members of the Biological Services Unit (BSU) at Institute of Cancer Research, Chelsea and were approved by the Animal Welfare and Ethical Review Body at The Institute of Cancer Research. All animals were housed in groups of 5 mice in individually ventilated cages (IVC). Mice were monitored on a daily basis by staff from the ICR Biological Service Unit for signs of ill health, and bedding, food and water were replenished twice weekly. Tumours were measured twice weekly by digital calipers, and bodyweight was also recorded.

2.6.1. GOA xenografts

Nude mice at 6 weeks of age (Charles River Laboratories) were injected subcutaneously with cancer cells and tumours were grown to ~100 mm3, size

matched, then mice were randomised and allocated into either the control or treated group. Each group consisted of 8 mice. The animals were treated by oral gavage once daily with vehicle (5% DMSO/water) or CCT196969 at a dose of 20 mg/kg. Data were calculated relative to the first weight and tumour measure recorded on the first day of treatment.

2.6.2. CRC xenografts

Six to eight week-old CD1 nudes were purchased from Charles River. Mice were injected subcutaneously with $2x10^6$ cells in 200 µL ($4x10^6$ in matrigel for co-culture experiments). Mice were randomised into treatment groups and dosed with 1 mg/mL cetuximab via intraperitoneal injection. Tumour and bodyweight measurements were uploaded to Lab Tracks portal and tumour volume was calculated. Data were plotted using GraphPad Prism 8. Mice were sacrificed at the end of the dosing period and tumours were fixed in 4% paraformaldehyde (PFA) for 24 hr at room temperature before being transferred in PBS. Tumours were then submitted to the Histopathology Department at the Institute of Cancer Research for paraffin embedding and staining with Haematoxylin and Eosin (H&E) and alpha smooth muscle actin (α-SMA).

2.6.3. Patient derived xenografts (PDXs)

Very small fragments available from PROSPECT-C and PROSPECT-R core biopsies were first grafted subcutaneously or under the kidney capsule of CD1 nude mice by the Tumour Profiling Unit at the Institute of Cancer Research. Mice were culled once tumors had grown and tumors were removed and dissociated in a gentle MAX Octo dissociator using the Human Tumour Dissociation Kit.

2.7. Cytokine Array

The Human Cytokine Array C5 from Raybiotech was used to semi-quantify 80 human cytokines. The manufacturer's protocol was followed. Medium was collected prior to the experiment and stored at -80^{o}C. The array was blocked with 2mL of provided Blocking Buffer for 30 minutes at room temperature. 1 mL of thawed, undiluted medium from each culture condition was placed on an array and incubated overnight at 4^{o}C. Each array was washed three times with 2 mL of Wash Buffer I for 5 minutes at room temperature, followed by three washes with 2 mL of Wash Buffer II under the same conditions. 1 mL of Biotinylated Antibody Cocktail was pipetted onto each array and incubated for 2 hr at room temperature. The previously described wash steps were then repeated. The arrays were incubated with HRP-Streptavidin for 2 hr at room temperature, and wash steps repeated for a third time. Signal was then read by incubating with Detection Buffers C and D on the Azure Biosystems c300 Gel Imaging System. Images were quantified using Image J. The signal was inverted and the density of each spot measured. Background was subtracted by subtracting the average density value for the negative control spots. Values were then normalised to positive spots as the amount of Biotinylated antibody printed per positive control spot is consistent from array to array. Signal fold expression was then calculated according to the below equation and plotted using GraphPad Prism 8.

$$Normalised\ Signal\ for\ Spot\ X = Normalised\ signal\ for\ Spot\ "X"\ on\ ref\ array \times \frac{mean\ signal\ density\ for\ positive\ spots\ on\ ref\ array}{mean\ signal\ density\ for\ positive\ spots\ on\ test\ array}$$

2.8. siRNA transfections

In a 6-well plate, reverse transfections were carried out as follows. siRNA oligonucleotides were resuspended in 1X siRNA buffer to a final concentration of 20 µM. 3 µL of 20 µM siRNA in 497 µL of OPTI-MEM serum-free medium and

3 µL RNAiMAX transfection reagent in 497 µL of OPTI-MEM were incubated for 5 minutes each at room temperature and then combined and incubated for 20 mins at room temperature. $5x10^5$ cells in 1 mL medium were plated and 1 mL of transfection mix added dropwise on top to a final concentration of 30 nM siRNA per well. For 96-well experiments, 0.15 µL of 20µM siRNA and 0.15 µL of RNAiMAX were added to 9.85 µL of OPTI-MEM and a total of 20 µL of combined transfection mix was added to each well. Cells were incubated with siRNA for 48 hr before further downstream experiments.

2.9. Real-time quantitative polymerase chain reaction (RTqPCR)

mRNA was extracted according to the Qiagen RNeasy Plus protocol. RNA was eluted into 30 µL of RNase-free water and quantified using the Qubit RNA broad range kit. 1 µg RNA was converted to cDNA using the SuperScript II Reverse Transcriptase protocol. Quantitative PCR reactions were set up using 2 µL of cDNA, 1 µL of Taqman Gene Expression Assay probe, 10 µL of Taqman Universal Master Mix II with UNG and 7 µL of water per reaction. Relative quantification was performed on QuantStudio6-Flex sequence detection and all reactions were performed in triplicate. Data were normalised according to the endogenous control GAPDH and analysed using the delta-delta CT method.

2.10. DNA constructs and site-directed mutagenesis

The Gateway Entry clones R777-E053-Hs.EGFR, R777-E015-Hs.BRAF (Addgene #70337 and #70299 respectively) were a gift from Dominic Esposito. Entry clone pDONR223_BRAF_p. D594H (Addgene #82816) was a gift from Jesse Boehm, Matthew Meyerson and David Root. RC201958 KRAS TrueORF gold clone was purchased from Origene and subcloned into the Gateway entry vector pENTR1A (Invitrogen) using BamH1/EcoRV double digest. Site directed mutagenesis to

generate EGFR p.G322S, EGFR p.D278N, BRAF p.D594F, BRAF p.D594N, KRAS STOP (to remove the c-terminal tag), KRAS p.A18D, KRAS p.L19F and KRAS p.G12V was performed by Louise Barber at the Institute of Cancer Research using QuikChange Lightning site-directed mutagenesis (Agilent Technologies) and custom designed primers. Full-length sequences were then assessed by Sanger sequencing performed by Eurofins Genomics. LR Gateway recombination (Invitrogen) was then used to generate destination vectors using the expression constucts pLX304 (Addgene #25890, a gift from David root), pLENTI-CMV-Puro-DEST (Addgene #17452, a gift from Eric Campeau and Paul Kaufman) and pLENTIGuide-PURO (Addgene #52963, a gift from Feng Zhang). pLX304-LacZ (a gift from Steven Whittaker) and pLENTI-CMV-Puro-LUC (a gift from Eric Campeau and Paul Kaufman) were used as control vectors. Plasmid DNA was purified by Qiagen Maxiprep, according to the manufacturer's protocol and quantified using a Nanodrop UV Visible Spectrophotometer.

2.11. Lentiviral production

2.11.1. pLX304 and pLV-GFP transfection

The transfection mixture made up of 54 µL TransIT-LT1 transfection reagent and 90 µL OptiMEM was incubated at room temperature for 5 minutes. This was then added to the DNA mixture consisting of 9 µg plasmid DNA, 9 µg psPAX2 packaging plasmid and 0.9 µg pMD2.G envelope plasmid, made up to a total volume of 225 µL in OptiMEM and incubated for 30 minutes at room temperature. psPAX2 and pMD2.G were a gift from Didier Trono (Addgene #12260 and #12259 respectively). On the day prior to transfection $2x10^6$ HEK293T cells were seeded. The transfection mix was then added dropwise onto HEK293T cells. Within 15 hr of transfection the medium was changed. Virus was harvested 24 hr and 48 hr post medium change and either used fresh or stored at -80^{o}C.

2.11.2. pLENTI-CMV-Puro-DEST and pLENTIGuide transfection

The transfection mixture made up of 54 µL TransIT-LT1 transfection reagent and 90 µL OptiMEM was incubated at room temperature for 5 minutes. This was then added to the DNA mixture consisting of 10 µg plasmid DNA, 7.5 µg psPAX2 packaging plasmid and 1.5 µg pMD2.G envelope plasmid, made up to a total volume of 225 µL in OptiMEM and incubated for 30 minutes at room temperature. psPAX2 and pMD2.G were a gift from Didier Trono (Addgene #12260 and #12259 respectively. On the day prior to transfection $2x10^6$ HEK293T cells were seeded. The transfection mix was then added dropwise onto HEK293T cells. Within 15 hr of transfection the medium was changed. Virus was harvested 24 hr and 48 hr post medium change and either used fresh or stored at -80^oC.

2.11.3. Lentiviral transduction

Cells were seeded at a confluency of ~80% one day prior to viral infection. 1 mL of viral supernatant was added onto a 6-well plate with 8 µg/mL Polybrene to aid transduction efficiency. Medium was changed after 24 hr to Blasticidin-containing medium (5 µg/mL) for pLX304/pLV-GFP constructs or Puromycin-containing medium (5 µg/mL) for pLENTI constructs to select positively transduced cells. A non-transduced control well was seeded alongside and cells were kept under selection until complete cell death in the control well was observed.

2.12. CRISPR gene knockouts

2.12.1. Eupheria ribonucleoprotein-complex delivery system

Ribonuceloprotein (RNP) complex delivery system CRISPR was carried out as follows. The gRNA was diluted to a working solution of 3 µM in nuclease free water. For a single 24-well reaction the RNP complexes were made up as follows; 3 µL of sgRNA was mixed with 3 µL of EnGen Cas9 NLS, 3.6 µL Cas9 Plus and made up to 75 µL in Optimem, and incubated for 10 minutes at room temperature. The liposome complexes master mix was made up by adding 75 µL of RNP with 7.2 µL CRISPRmax transfection reagent and made up to 75 µL per sample. Cells were counted and diluted to a concentration of $2x10^6$ cells per mL. Cells were then reverse transfected with 75 µL of RNP/liposome complex and incubated for 48 hr before analysis by FACS.

2.12.2. Fluoresence-Activated Cell Analysis

U2OS cells treated with EnGen Cas9 with or without an eGFP guide RNA for FACS analysis of GFP intensity were harvested, pelleted by centrifugation and fixed with 4% PFA for 30 mins at room temperature. PBS was added, cells were pelleted again and resuspended in PBS at a concentration of 1-$2x10^6$/mL. 4',6-Diamidino-2-Phenylindole, Dihydrochloride (DAPI) stain was added to all samples at a concentration of 5 µM for live/dead exclusion. Samples were run on BS LSRII and gating set up according to standard FACS protocols and the percentage of GFP positive cells was quantified.

2.12.3. Lentiviral CRISPR

LIM1215 cells were transduced with Cas9 viral particles (a gift from Feifei Song, Stephen Pettitt and Chris Lord, derived from lentiCas9-Blast (Addgene # 52962, a gift from Feng Zhang)) in the presence of Polybrene (8 µg/mL) and selected with 5 µg/mL Blasticidin to create constitutively expressing Cas9 lines. To produce lentiviral guide RNAs targeting NF1, HEK293T cells were transfected with pLentiguide-NF1#C08, pLentiguide-NF1#C09, pLentiguide-NF1#D08, pLentiguide-NF1#D09 (a gift from Stephen Pettitt and Chris Lord, customized

from pLentiguide-Puro (Addgene #52963, a gift from Feng Zhang)) in combination with packaging plasmids psPAX and pMD2.G. LIM1215-Cas9 cells were transduced with the resultant viral gRNA supernatants in the presence of Polybrene (8 µg/mL) and selected for with puromycin (5 µg/mL).

2.13. Sanger sequencing to confirm NF1 gene disruption or successful site directed mutagenesis

Cells were trypsinised and pelleted for DNA extraction. DNA was extracted using the Qiagen DNeasy Blood and Tissue Extraction kit, according to manufacturer's protocol. Custom designed primers with M13 tails were made up to 100 µM concentration with nuclease-free water. The PCR reaction was set up with 20 ng DNA and 1.25 µL 10 µM each forward and reverse primer and made up to 12.5 µL with water. Equivolume of NEB Q5 2x Mastermix was added. Annealing temperature was determined using the NEB Tm online calculator tool. PCR was then run according to the thermocycling conditions of the Q5 High fidelity DNA Polymerase protocol. Following PCR amplification, products were cleaned up using the QiaQuick PCR amplification kit according to manufacturer's protocol, and final product was eluted in 30 µL nuclease-free water. DNA concentration was quantified using the Qubit dsDNA High Sensitivity protocol. Purified DNA was then added to pre-ordered Mix2Seq tubes at a concentration of 1ng/µL in 15 µL with 2 µL of either M13 forward or reverse primer and submitted to Eurofins Genomics for sequencing. Sanger sequencing traces were received back from Eurofins for analysis.

2.14. RNA sequencing

Three independent RNA sequencing experiments were carried out, including cell lines, $PDO_{naïve}$ and PDO res untreated and $PDO_{naïve}$ and PDOres treated with 5 µM 5FU. Cell lines were seeded in 12-well dishes 48 hr prior to RNA extraction. PDOs were split into 24 well dishes from a relatively dense stock 12-

well and left to grow for 2-3 days. Plates were checked visually to ensure relatively equal seeding across all experimental wells. Plates were medium changed with drug-containing medium (or DMSO-treated for control wells) and 5 µM 5FU was left on for 48 hr. PDOs were harvested as normal and pelleted. RNA was extracted according to the Qiagen RNEasy Plus protocol. RNA was eluted into 30 µL of RNase-free water and quantified using the Qubit RNA broad range kit. Samples where the concentration was less than 50 ng/µL were concentrated by speedvac for 10-20 mins at room temperature. Samples were then processed for RNA sequencing according to the Lexogen QuantSeq 3' mRNA-Seq Library for Illumina preparation protocol – briefly 250 ng of RNA in 5 µL was used as input, optimal cycles of PCR was determined by qPCR before final libraries were quantified by Qubit and Bioanalyzer DNA High Sensitivity kits. Equimolar pools were sequenced by the Tumour Profiling Unit (TPU) on an Illumina HiSeq500 in Rapid 100-bp single-end mode with dual indexing; generating a median 6.9M reads per sample. Sequencing data were then analysed using the FWD Human (GRCh38) Lexogen QuantSeq 2.2.3 and Lexogen DE 1.3.0 pipelines on the Bluebee cloud platform. DEseq values were filtered to exclude any genes with a fold change <±1.5 (±0.585 on a Log2 scale) and to include only genes with a adjusted p value of <0.1.

2.15. Pathway Enrichment Analysis

To identify pathways enriched in PDO_{res} compared to $PDO_{naïve}$, normalised read counts generated by Bluebee software were used as input into Broad Institute Gene Set Enrichment Analysis (GSEAv4.0.1) tool (Subramanian et al., 2005). Genes for which values across all samples=0 were excluded, and normalised read counts were filtered to only include those from protein coding genes. GSEA parameters were as following for all runs: Number of permutations=1000, collapse data set to gene symbols = false and permutation type=gene set. Enrichment results were viewed in html format. Gene sets are automatically ranked Normalised Enrichment Score (NES) and those that had a false discovery

rate (FDR) of <0.25 were manually reviewed. Gene sets that related to specific cancer types other than colorectal cancer were excluded.

To identify molecular pathways that were deregulated in PDO_{res} compared to $PDO_{naïve}$ in the absence of drug treatment, we applied Gene Set Enrichment Analysis (GSEA v4.0.1) using default parameters to normalized expression data from $PDO_{naïve}$ and PDO_{res}. To further identify molecular pathways that were significantly deregulated in $PDO_{naïve}$ compared to PDOres during 5FU treatment, genes that were significantly over- or under expressed by at least 2 fold in $PDO_{naïve}$ vs PDO_{res} when either untreated or treated with 5 µM 5FU for 48 hr were identified. For this, differential expression analyses were performed on the Bluebee cloud platform as recommended by the manufacturer of the Lexogen 3' RNA-sequencing using False Discovery Rate multiple testing correction with a q-value below 0.1 considered to be significant. Significantly differentially expressed genes from both conditions were then analysed by overlapping with curated molecular signatures separately for over and under expressed genes using the investigate signature function in the Molecular Signature database V7.0 (http://software.broadinstitute.org/gsea/msigdb/annotate.jsp). Gene sets that showed inconsistent results based on significant overexpression and downregulation within an experiment and gene sets overlapping with 5 or fewer genes were removed. Gene sets that were overexpressed in PDO_{res} with and without 5FU treatment and those under expressed in PDO_{res} with and without treatment were also removed as these were consistently deregulated in the presence and absence of 5FU treatment but not specifically enriched during 5FU treatment.

2.16. Statistics

Statistical tests were performed using GraphPad Prism and Microsoft Excel. Signficance was assessed by paired student's t-test unless otherwise stated. All error bars represent standard deviation unless otherwise stated. All

experiments were carried out in at least technical triplicate. 3 biological repeats were performed per experiment. One representative repeat is shown throughout unless stated otherwise.

2.17. Acknowledgments

The following people are credited for their work presented in this thesis. Dr Andrew Woolston performed all bioinformatics analyses including exome sequencing analyses. Dr Louise Barber performed all RNA library preparations for lexogen sequencing, and carried out the site-directed mutagenesis. Beatrice Griffiths established PDO culturing methods within my host lab. *In vivo* experiments in Chapter 3 were performed by Filipa Lopes and *in vivo* experiments in Chapter 4 were performed by David Vicente. *In vivo* work for the establishment of patient-derived xenografts (PDX) from biopsy material was performed by members of the Tumour Profiling Unit (TPU) at the Institute of Cancer Research (ICR). Tumour embedding and immunohistochemistry was performed by the Breast Cancer Now Histopathology unit and were analysed by a histopathologist registrar, Dr Ben Challoner. Dr Marta Gomez-Martinez performed some western blots. Lisa Hornsteiner assisted with some of the drug sensitivity assays and western blot experiments.

Chapter 3: Investigating downstream MAPK pathway inhibitors in Gastro-Oesophageal Adenocarcinomas

3.1. Introduction

In gastric and gastro-oesophageal junction adenocarcinomas (GOA) there is unmet clinical need for better therapeutic options. Despite overall survival rates almost tripling in the last 40 years (Cancer Research UK), survival of metastatic disease remains low (5%). Treatment options for metastatic disease are limited to chemotherapies, anti-angiogenics (Fuchs et al., 2014), HER2 targeted therapy (Van Cutsem et al., 2009a) and more recently immunotherapies but response rates and duration are short for all modalities. Only the anti-ERBB2 antibody trastuzumab is administered based on the presence of *ERBB2* overexpression or amplification (Bang et al., 2010).

MAPK pathway activation through amplifications of receptor tyrosine kinases (RTKs), in particular *ERBB2, FGFR, EGFR and MET*, are common, as are the amplifications of *KRAS*. However, a clinical trial found that treatment success with FGFR inhibitors was limited to a small fraction of patients whose tumours harboured clonal *FGFR2* amplifications whereas the majority of tumours with *FGFR* amplifications were found to harbour subclonal amplifications and those progressed rapidly (Pearson et al., 2016). Genetic intratumour heterogeneity is common in GOAs and heterogeneous amplification of druggable RTKs including *MET*, *EGFR* and *FGFR* has been described (Lordick et al., 2013; Pearson et al., 2016; Waddell et al., 2013). In addition, my host lab analysed eight primary GOA tumours and matched lymph node metastases by multi-region DNA sequencing and identified clonal amplifications of receptor tyrosine kinases or MAPK pathway genes; *ERBB2* in six cases and *KRAS* and *NRAS* in one case each. In addition, half of tumours analysed (4/8) harboured subclonal amplifications of RTK genes or downstream genes in the MAPK pathway (**Figure 3.1**). A significant

enrichment of subclonal RTK or MAPK pathway aberrations was observed in the lymph node metastases when compared to the primary tumours. This shows that ITH continues to evolve in metastatic sites, complicating the detection of such aberrations as many metastatic sites are difficult to access. These and other data (Silva et al., 2016) show that oncogenic aberrations of different RTKs and/or of the MAPK pathway often co-exist in the same patient. This suggests that in many tumours, only a subclonal fraction of the cancer cell population may be sensitive to a drug targeting a single one of these aberrations. Resistance is likely to occur inevitably and rapidly through subclonal mutations and amplification of the MAPK pathway that are not controlled by a single target therapy and this likely explains why recent trials of EGFR- and MET-inhibitors failed (Cunningham et al., 2015; Dutton et al., 2014).

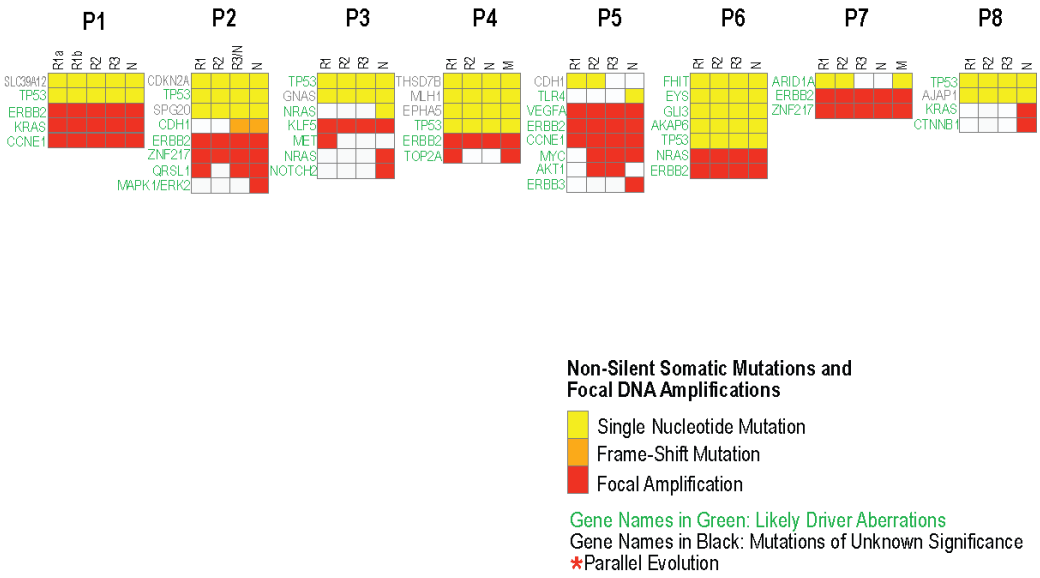

Figure 3.1 Driver gene aberrations found in 8 surgically removed GOAs that were analysed by my host lab by multi-region sequencing of an 81-gene panel.

Genes with likely driver aberrations are shown in green and the heatmap shows the presence (yellow: mutation, red: amplification) or absence (white box) of an aberrations across the different primary tumour regions (labelled R1, R2, R3), nodal metastases (labelled N) or distant metastasis (labelled M). Aberrations detected in RTKs or the genes of the MAPK pathway were: P1: clonal ERBB2 and KRAS amplifications, P2: clonal ERBB2 amplification and subclonal ERK2 amplification, P3: Subclonal NRAS mutation, subclonal MET and NRAS amplifications, P4: clonal ERBB2 amplification, P4: clonal ERBB2 and VEGFA amplifications and subclonal ERBB3 amplification, P6: Clonal NRAS amplification, P7: clonal ERBB2 amplification, P8: subclonal KRAS amplification.

Strategies that directly target MAPK pathway members have been investigated in colorectal cancers and melanomas, however there are key differences between tumour types. Potent and selective BRAF inhibitors (vemurafenib and dabrafenib) are used in BRAF mutant melanomas with very high initial response rates, although most tumours will acquire resistance within 6-7 months (Chapman, 2013; Long et al., 2014; Paterson et al., 2013). Acquired resistance to the BRAF inhibitors occurs predominantly through genetic alterations resulting in the reactivation of the MAPK pathway. This has been reported through a host of different genetic mechanisms including *NRAS* and *MAP2K1* mutations, amplifications and overexpression of pathway genes (Long et al., 2014; Whittaker et al., 2015). There is an interesting paradox in targeting the MAPK pathway with BRAF inhibitors, whereby they inhibit signalling in BRAF mutant melanomas yet activate the pathway in NRAS mutant melanomas (Girotti et al., 2015). Furthermore, despite the promise in BRAF mutant melanoma, efficacy in BRAF mutant CRC is poor, with response rates at less than 5% (Corcoran et al., 2012; Kopetz et al., 2015; Whittaker et al., 2015). Primary resistance in BRAF mutant CRC is mediated through feedback loops that rapidly reactivate EGFR (Prahallad et al., 2012). Feedback loops such as this preclude the use of single agent BRAF inhibitors in CRC. The success of BRAF inhibitors has thus been hampered by problems with resistance and paradoxical activation.

Newly developed pan-RAF inhibitors hit all three isoforms of RAF (ARAF, BRAF and CRAF) as well as the Src family kinases (SFK) and thus achieve a more effective blockade of the MAPK pathway. They are described as paradox-breakers as they have been shown to successfully block proliferation in both BRAF and NRAS mutant melanoma (Girotti et al., 2015). In light of the intra- and inter-tumour heterogeneity of genetic aberrations of RTKs and of MAPK pathway members such as *KRAS* in GOA, inhibitors of the distal MAPK pathway, and particularly pan-RAF inhibitors, may offer novel treatment options for these heterogeneous tumours.

3.2. Prevalence of RTK and MAPK pathway aberrations in GOA

Multiple subclonal and truncal mutations were observed in genes involved in canonical MAPK signalling (*ERBB2, EGFR, MET, KRAS, NRAS* and *ERK)*, in our patient cohort. As this is a small case series, I furthermore interrogated the prevalence of driver aberrations in receptor tyrosine kinases and in members of the MAPK pathway in 773 samples of oesophageal and stomach adenocarcinoma in The Cancer Genome Atlas (TCGA) database and the Dana-Farber Cancer Institute (DFCI) database to assess what percentage of patients have likely activating aberrations in this pathway and may hence benefit form a treatment approach that targets the MAPK pathway downstream of most of these aberrations. RTKs were altered in 36% of samples across the two datasets (*EGFR*=10%, *ERBB2*=16%, *MET*=5% and *FGFR2*=5%). The majority of aberrations reported, particularly in *EGFR* and *ERBB2*, were amplifications as were observed in our patient cohort. This is important as many of the point mutations in these genes are likely passenger mutations and only the amplifications may be functionally relevant. The frequency of alteration in the MAPK pathway itself was 28.3%. In particular *KRAS* was aberrant in 12% of cases. Thus it can be concluded that the aberrant MAPK genes detected in the eight patient cohort previously described are representative of the genotypic diversity observed in oesophageal and stomach cancers. Aberrations of MEK (*MAP2K1*) and ERK (*MAPK1*) were rare (1.7% and 2.1% respectively), thus strengthening the rationale for targeting at RAF, MEK or ERK. Overall this analysis has justified the potential value in investigating MAPK pathway inhibitors in GOA.

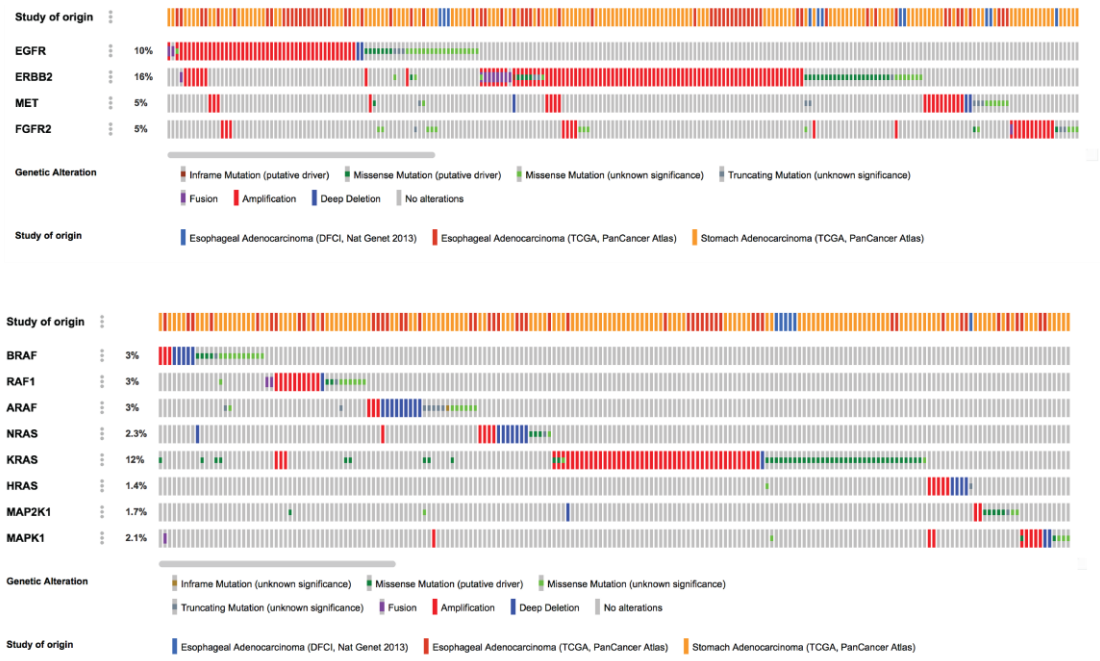

Figure 3.2 Prevalence of RTK and MAPK pathway gene aberrations in GOA.

Screenshots from cBIOPortal accessed on 15/09/2019 show the prevalence of RTK and MAPK pathway aberrations in the DFCI esophageal adenocarcinoma, TCGA esophageal adenocarcinoma and TCGA GOA cohorts (total number of samples = 773) datasets. Coloured legends indicate type of alteration.

3.3. Selection of Cell Line Panel

I next identified GOA cell lines from the literature and databases that should represent the aberrations of RTKs and the MAPK pathway that showed intratumour heterogeneity in our own data and published work. I was able to source GOA cell lines that harboured *NRAS*, *KRAS*, *MET* or *FGFR2* amplifications. I furthermore included an *ERBB2* amplified cell line to assess if downstream MAPK pathway targeting would also be effective in such tumours and a GOA cell line without any known RTK or MAPK pathway amplifications or mutations (FLO-1).

Cell Line	Origin	MAPK or RTK aberration
FLO1	Oesophageal adenocarcinoma	Wildtype
SKGT4	Oesophageal adenocarcinoma	*KRAS* Mutant
MKN45	Gastric adenocarcinoma, poorly differentiated	*MET* Amplification
NCI N87	Gastric carcinoma derived from liver metastasis	*ERBB2* Amplification
MKN74	Gastric carcinoma derived from liver metastasis	*NRAS* Amplification
KATOIII	Scirrhous gastric carcinoma	*FGFR2* Amplification

Table 3.1 GOA Cell Line Panel

3.4. MEK and ERK inhibition in GOA cell lines

MEK inhibitors have been clinically approved for the treatment of BRAF-mutant melanomas in combination with BRAF inhibitors (Flaherty et al., 2012; Long et al., 2015) and ERK inhibitors have been promising in early clinical trial evaluation (Jha et al., 2016; Sullivan et al., 2018). Thus, I chose a MEK inhibitor

(trametinib) and an ERK inhibitor (SCH772984) in addition to the pan-RAF inhibitor for further investigation.

The five GOA cell lines with RTK/MAPK aberrations (SKGT4, KATOIII, MKN45, MKN74 and NCI N87) were first assayed for sensitivity to the ERK inhibitor, respectively (**Figure 3.3**). IC_{50}s ranged from 0.66 μM in *KRAS* mutant SKGT4 to 5.94 μM in *ERBB2*-amplified NCI N87. Whilst all cell lines responded to ERK inhibition, *NRAS* and *ERBB2* amplified lines showed considerable residual growth even at the highest dose of 10 μM (42% residual growth compared to untreated cells in both).

A

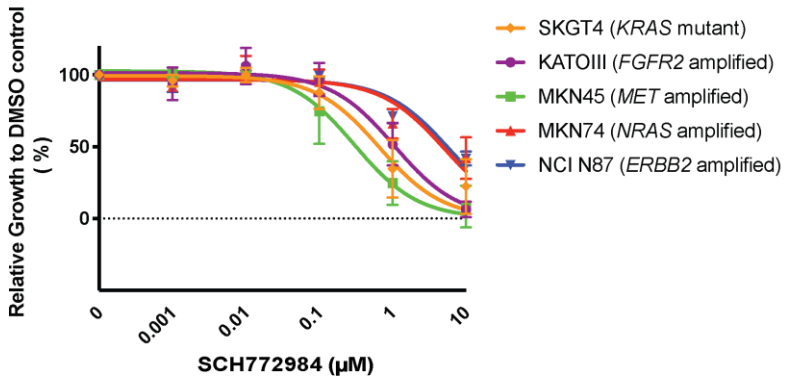

B

Cell Line	IC50 μM	Residual Growth %
SKGT4	0.66	22
KATOIII	1.05	6
MKN45	0.30	8
MKN74	5.17	42
NCI N87	5.94	42

Figure 3.3 ERK inhibition in GOA cell lines.

(A) 5 day growth assay of GOA cell lines treated with 0.001-10 μM) SCH772984. Cell viability was measured by CellTitre-Blue. Signal at Day 0 was subtracted and data were normalised such that 100%= untreated growth and 0%=seeding density. Non-linear regression log response v three parameters curves were fitted by Graphpad Prism. Graphs indicate average of three repeats. Error bars indicate SEM of three biological repeats. (B) Table detailing IC_{50} values and residual growth. IC_{50}s were calculated by Graphpad Prism, and residual growth was calculated manually.

Next, I treated all cell lines with trametinib, a reversible allosteric inhibitor of MEK1 and MEK2 (**Figure 3.4**). All cell lines, regardless of their specific genetic aberration, showed inhibition of growth with the MEK inhibitor. However even at the highest dose of 10 μM, residual growth was observed across the panel (range: 16-64%). IC_{50} values ranged from 0.05 μM in the *MET*-amplified cell line to 1.28 μM in the *ERBB2* amplified line. IC_{50}s were then compared to the published IC_{50}s for trametinib in the Genomics of Drug Sensitivity in Cancer database (Yang et al., 2012). No published data were available for the MKN74

cell line and the remaining IC_{50}s determined in my experiments for the other four cell lines correlated strongly with the published data (r=0.996), supporting the validity of these results.

A

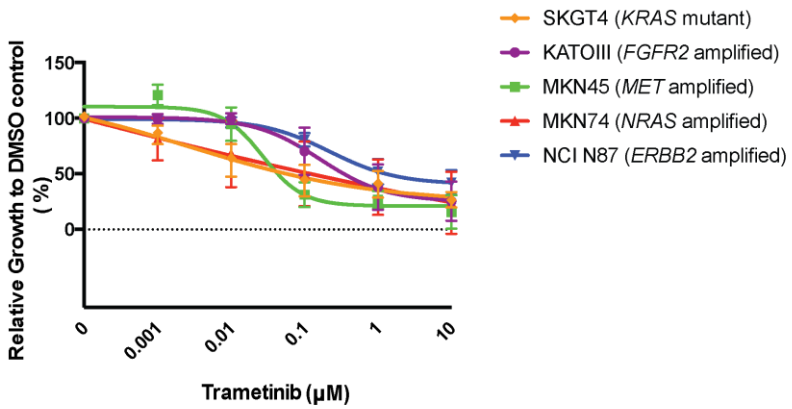

B

Cell Line	IC50 µM	Residual Growth %	GDSC IC50
SKGT4	0.05	27	0.02
KATOIII	0.34	26	0.41
MKN45	0.04	16	0.04
MKN74	0.12	24	
NCI N87	1.28	64	2.39

Figure 3.4 MEK inhibition in GOA cell lines.

(A) 5 day growth assay of GOA cell lines treated with 0.001-10 µM) Trametinib. Cell viability was measured by CellTitre-Blue. Signal at Day 0 was subtracted and data were normalised such that 100%= untreated growth and 0%=seeding density. Non-linear regression log response v three parameters curves were fitted by Graphpad Prism. Graphs indicate average of three repeats. Error bars indicate SEM of three biological repeats. (B) Table detailing IC_{50} values and residual growth. IC_{50}s were calculated by Graphpad Prism, and residual growth was calculated manually.IC_{50}s calculated by the Genomics of Drug Sensitivity in Cancer (GDSC) project are indicated as a reference.

Thus, all cell lines responded to some degree in response to ERK and MEK inhibition and no specific aberration in the MAPK pathway was associated with a high level of resistance. However, considerable residual growth was seen in many cell lines with both inhibitors, even when they were used at high doses of 10 μM.

3.5. Investigating the use of pan-RAF inhibitors in GOA

3.5.1. Pan-RAF inhibition in GOA cell lines

As inhibition of the MAPK pathway with MEK or ERK inhibitors resulted in residual growth in our panel of cell lines, I next wanted to investigate whether novel "paradox-breaking" pan-RAF inhibitors would show higher activity (Girotti et al., 2015). These inhibitors have shown promise in BRAF mutant melanoma and in colorectal cancer cell lines but they have not previously been investigated in the GOA cell lines. Through collaboration with Prof. Springer (ICR, currently: CRUK Manchester Research Institute) I obtained 3 novel pan-RAF inhibitor compounds for an initial sensitivity analysis. MKN45, SKGT4 and NCI N87 were selected as MKN45 and SKGT4 were consistently the most sensitive to MEK or ERK inhibition, with NCI N87 consistently the least sensitive.

Growth was inhibited in all three cell lines when treated with each of the three compounds, thus confirming activity of these inhibitors in MAPK-mutant or amplified gastric cell lines (**Figure 3.5**). Despite higher IC_{50}s of Compound A and D compared to Compound C, Compound A was selected for further investigation as it is the published compound (CCT196969) and has been further developed for clinical use (Girotti et al., 2015).

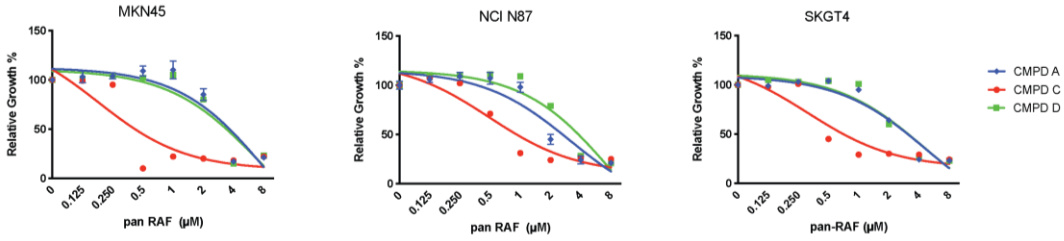

	IC$_{50}$ (μM)		
Cell Line	**CMPD A**	**CMPD C**	**CMPD D**
MKN45	8.6	0.2	6.6
NCI N87	3.2	0.5	7.9
SKGT4	4.6	0.3	4.5

Figure 3.5 Testing of three pan-RAF inhibitor compounds in GOA cell lines.

5 day growth assay of GOA cell lines treated with pan-RAF compounds (CMPDs) A, B and C Cell viability was measured by CellTitre-Blue. Signal at Day 0 was subtracted and data were normalised such that 100%= untreated growth and 0%=seeding density. Non-linear regression log response v three parameters curves were fitted by Graphpad Prism. Graphs indicate one representative repeat. Error bars indicate SD of six technical replicates.. (B) Table detailing IC_{50} values. IC_{50}s were calculated by Graphpad Prism.

Subsequent testing of pan-RAF inhibitor compound A / CCT196969 was performed in all six GOA cell lines from Table 3.1, including FLO-1 which has no known aberration in any RTK or the MAPK pathway. Treatment for 5 days with pan-RAF inhibitors showed effective growth suppression at high doses (4-8 µm) across all lines (**Figure 3.6** A and B). Strikingly, the *FGFR2* amplified cell line KATOIII was substantially more sensitive (IC_{50} ≈5 pM) compared to all other cell lines which all showed similar IC_{50}s (range; 1.60 µM – 2.72 µM) and residual growth did not exceed 25%. The cell numbers at 4-8 µm were similar to the seeding cell number (indicated by 0 on the graph), indicating that pan-RAF inhibition leads to a cytostatic rather than cytotoxic response. Importantly, as was observed with ERK and MEK inhibition, no upstream aberration conferred resistance to the pan-RAF inhibitor and it was interesting to see that even the wild type cell line FLO-1 responded.

A

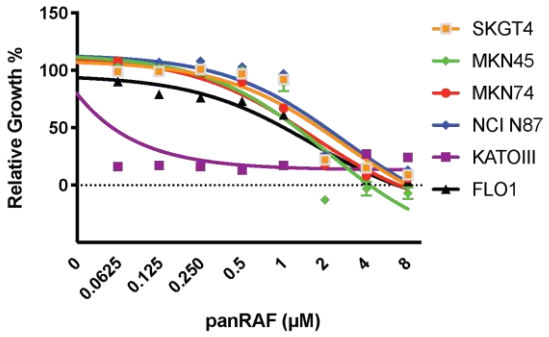

B

Cell Line	IC50 μM	Residual Growth %
SKGT4	2.68	9
KATOIII	$4.4x10^{-6}$	24
MKN45	2.05	-7
MKN74	1.60	6
NCI N87	2.72	13
FLO1	1.61	3

C

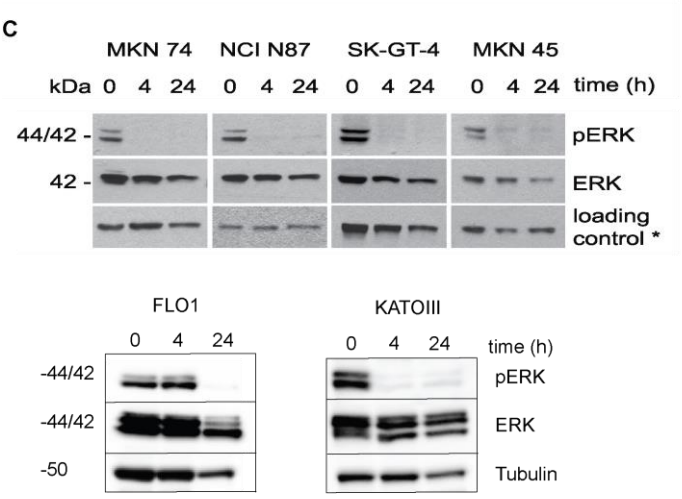

Figure 3.6 Cell line panel response to CCT196969.

(A) 5 day growth assay of GOA cell lines treated with panRAF inhibitior CCT196969 Cell viability was measured by CellTitre-Blue. Signal at Day 0 was subtracted and data were normalised such that 100%= untreated growth and 0%=seeding density. Non-linear regression log response v three parameters curves were fitted by Graphpad Prism.. Graphs indicate one representative repeat. Error bars indicate SD of six technical replicates. (B) Table detailing IC_{50} values. IC_{50}s were calculated by Graphpad Prism, and residual growth was calculated manually. (C) Western blot analysis of pERK (phosphorylated ERK) and ERK in cell lines treated with 10 μM CCT196969 for 4 and 24 hr. Either GAPDH or tubulin were used as loading controls. Western blots in the top panel were performed by Dr Marta Gomez-Martinez and used a different ERK antibody to the CST ERK antibody used throughout the thesis.

To determine if growth inhibition observed in the drug sensitivity assay was accompanied by downregulation of downstream MAPK pathway signalling, phosphorylation of ERK (pERK) was investigated by Western blotting (experiments were partially carried by Dr Gomez-Martinez in Prof Springer's Lab) (**Figure 3.6**C). Pathway deactivation was observed through loss of phospho-ERK signalling at 24 hr for all lines. Importantly, strong ERK phosphorylation was observed in the untreated FLO-1 cell line which is not known to harbour aberrations of RTKs or in the MAPK pathway, suggesting that the MAPK pathway can be activated through alternative mechanisms in GOA cells. Despite somewhat lower loading in the FLO1 Western blot, it can still be deduced that suppression of phosphorylated ERK occurred at 24 hr treatment. Together with the growth suppression observed, this suggests that GOA cells without RTK/MAPK pathway may nevertheless depend on signalling through the MAPK pathway. Interestingly, this cell line showed no loss of pERK signal at 4 hr, showing that it takes longer to suppress the MAPK pathway in the wildtype cell line compared to cells with activating genetic aberrations.

Taken together, it can be concluded that inhibitors of RAF, MEK and ERK can all achieve some growth inhibition in GOA cell lines. However, treatment with the pan-RAF inhibitor showed the lowest residual growth at doses that are conventionally used in drug sensitivity assays (usually up to ~ 10 μM). I hence chose this inhibitor for further analysis of efficacy *in vivo*.

3.5.2. Efficacy of pan-RAF inhibitors *in vivo*

In vivo modelling is the gold standard for any preclinical testing of novel compounds. Furthermore, I have demonstrated the efficacy of CCT196969 *in vitro* but relatively high doses (~8 μM) were required to achieve satisfactory growth inhibition with minimal residual growth. I thus wanted to assess if efficacy can also be achieved in xenografts in mice or if toxicities would essentially prevent reaching an effective dose. Three cell lines (MKN45, MKN74

and NCI N87) representing clinically relevant aberrations (*MET*, *NRAS* and *ERBB2* amplifications respectively) and that have previously been reported to grow in mice (Nukatsuka et al., 2015; Takaishi et al., 2009; Tsunemitsu et al., 2004) were injected subcutaneously into nude mice (**Figure 3.7**). Once the tumour reached ~100 mm^3 in volume, Mice were randomised into control and treatment groups (n= 8 in each group), and treated daily by oral gavage vehicle or 20 mg/kg CCT196969 (experiments performed by Dr Filipa Lopez, ICR). Treatment with CCT196969 significantly inhibited tumour growth in comparison to the vehicle control group in these xenograft models from all three cell lines. No significant toxicity was reported for any of the mice from the technicians in the animal facility and this is confirmed with the body weight measurements. This confirms *in vivo* that the pan-RAF inhibitor CCT196969 is a promising novel drug for the treatment of GOAs with activated MAPK signalling.

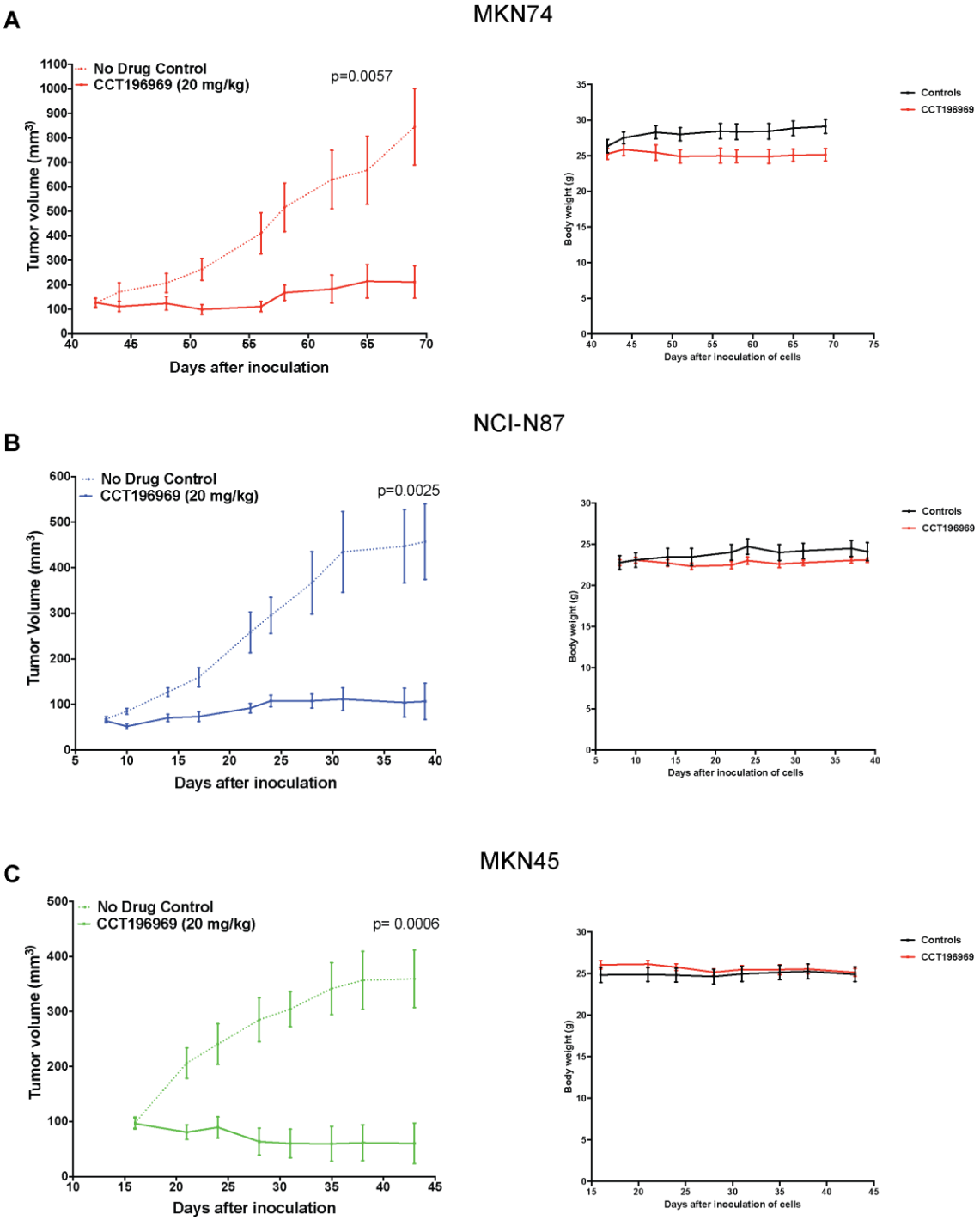

Figure 3.7 Pan-RAF inhibition is effective in preventing tumour growth *in vivo*.

Tumour volumes and body weights of xenografts (A) MKN74, (B) NCI-N87 and (C) MKN45 grown in nude mice and treated by oral gavage with the 20mg/kg CCT196969 inhibitor or vehicle alone. Statistical significance was determined by t-test.

3.5.3. Hypersensitivity of *FGFR2* amplified gastric cancer cell lines to pan-RAF inhibition

KATOIII is an *FGFR2*-amplified gastric cell and it had shown a substantially higher sensitivity to pan-RAF inhibitor compared to all other tested cell lines (**Figure 3.8**). Amplification of *FGFR2* has been observed in 5-8% of GOAs and such patients may hence particularly benefit from this pan-RAF inhibitor agent (Turner and Grose, 2010). In order to determine if *FGFR2* amplified GOA cells broadly show hypersensitivity to this inhibitor I next tested this in an additional *FGFR2*-amplified GOA cell line (OCUM-2M) and an *FGFR2* amplified spheroid line established form a GOA patient (FG51, obtained from Prof Turner's Lab, ICR) (**Figure 3.8** A). Hypersensitivity to pan-RAF blockade was observed in all three *FGFR2* amplified lines. Drug responses occurred at the lowest initially tested dose and thus, IC_{50}s could not accurately be calculated. The pan-RAF inhibitor was then further titrated down in KATOIII and this revealed an IC_{50} of 1.98 nM, 1075-fold more sensitive than all other non-FGFR2 amplified lines I had investigated (**Figure 3.8** B). I next questioned whether treatment with a much lower dose of 10 nM of the pan-RAF inhibitor would suppress ERK phosphorylation. Western blotting showed no decrease of pERK signalling (**Figure 3.8** C) despite the strong growth inhibitory effect of this dose. This indicates that hypersensitivity to the pan-RAF inhibitor is not exclusively dependent on suppression of the classical MAPK signalling.

.

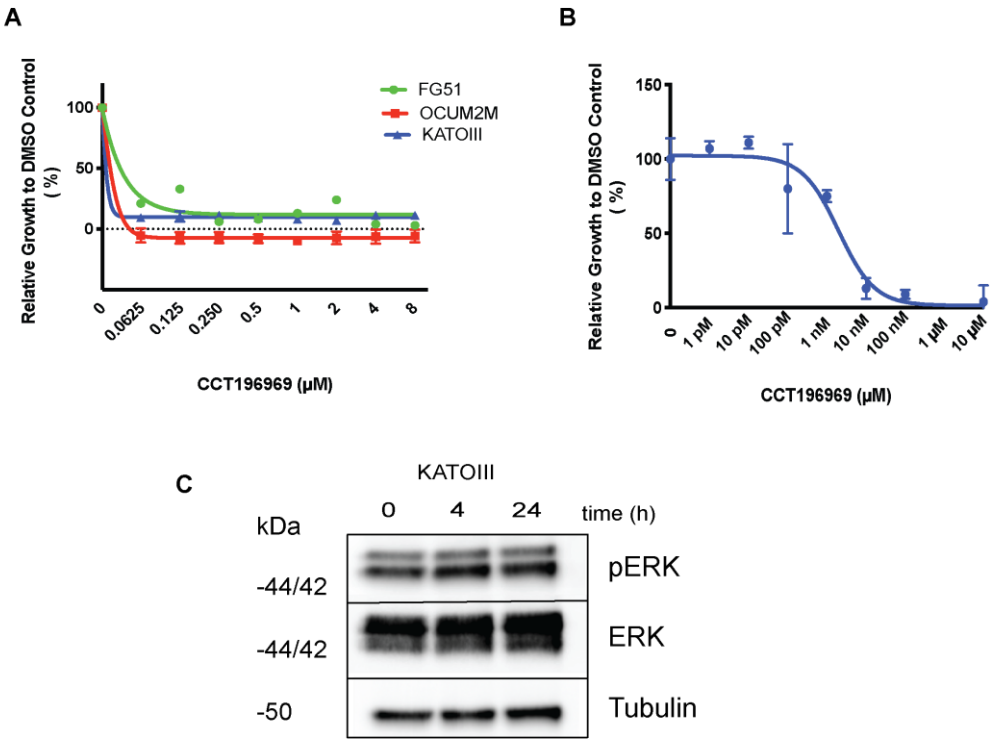

Figure 3.8 Hypersensitivity of FGFR2-amplified cell lines.

5 day growth assay of GOA cell lines treated with (A) 0.0625-8 µM and (B) 1 pM- 10 µM CCT196969 Cell viability was measured by CellTitre-Blue. Signal at Day 0 was subtracted and data were normalised such that 100%= untreated growth and 0%=seeding density. Non-linear regression log response v three parameters curves were fitted by Graphpad Prism. Graphs indicate one representative repeat. Error bars indicate SD of six replicates. (C) Western blot analysis of pERK and ERK in KATOIII treated with 10 nM CCT196969 for 4 and 24 hr. Tubulin was used as a loading control

3.6. Discussion

The development of precision medicine approaches targeting specific genetic aberrations such as *FGFR*-, *EGFR*- and *MET*-amplifications has largely been unsuccessful in GOA. This is likely explained by the observation that subclones with distinct activating aberrations of the MAPK pathway often co-exist within individual tumours and specific targeting of only one of the aberrations will likely prove futile and resistance will rapidly develop.

Thus, I hypothesised that targeting the MAPK pathway downstream of the majority of these aberrations where signalling converges, may prove a more effective strategy. Using a panel of GOA cell lines that harboured different RTK or RAS amplifications, the efficacy of the ERK inhibitor SCH772984, the MEK inhibitor trametinib and the pan-RAF inhibitor CCT196969 was shown. Based on the higher residual growth observed with both ERK and MEK inhibition, my data suggests that pan-RAF inhibitors may the most active in these tumours and this compound was further studies. It has been reported that at least 80% suppression of ERK phosphorylation is required for MAPK pathway inhibition to be clinically effective (Bollag et al., 2010). Almost complete loss of pERK signalling, observed in all GOA cell lines treated with the pan-RAF inhibitor, thus indicates that this could be a potentially useful clinical agent. Furthermore, suppression of pERK was not transient, with no pERK reactivation seen at 24 hr as has previously been reported in primary resistance to BRAF inhibitors. Similarly, sustained pathway suppression with RAF inhibitors has also been observed in melanoma cell lines where the drug is considered effective (Bollag et al., 2010).

The MAPK pathway is tightly regulated through multiple positive and negative feedback loops, indeed it is known as the prototypical biological example of negative feedback amplifier topology The existence of these feedback loops lend themselves heavily to the development of drug resistance when a protein in the MAPK pathway is inhibited (Corcoran et al., 2012; Prahallad et al., 2012;

Sturm et al., 2010). Indeed ERK-mediated AKT signalling has been shown as a resistance mechanism to MEK inhibitors in gastric cancer (Chen et al., 2017a). Pan-RAF inhibitors were thus designed to break the paradoxical pathway activation that can ensue following targeting of the pathway. The improved growth suppression with the Pan-RAF inhibitor compared to MEK or ERK inhibitors across my panel of cell lines may be the results of combating such feedback loop activation. This was not directly tested as I prioritised investigating the use of pan-RAF inhibitors in *in vivo* GOA models.

My data furthermore showed that pan-RAF inhibition with CCT196969 was even effective in a GOA cell line without any known RTK and MAPK pathway aberrations. ERK phosphorylation (pERK) at baseline was similar in this cell line compared to cells with RTK or *KRAS* amplifications. This suggests that alternative mechanisms activate this key growth and survival pathway. For example, MAPK wild type colorectal cancer cells frequently secrete growth factors that activated the EGF-receptor in an autocrine fashion, leading to MAPK pathway activation. Similar mechanisms of non-genetic pathway activation may play a role in some GOAs. This furthermore indicates that even GOAs without amplifications of RTK or MAPK pathway members such as *KRAS* can depend on MAPK pathway signalling and that pan-RAF inhibitors may therefore be active across an even larger fraction of these tumours. Although efficacy against a MAPK wild type GOA cell line is an important result, it should be further validated in a larger number of similar 'wildtype' GOA cell lines.

In vivo studies were carried out to confirm that the growth inhibition that was seen *in vitro* with high doses could be achieved in animal models without toxicity. This was confirmed and further strengthens the putative use of pan-RAF inhibitors as an effective strategy to treat GOAs with aberrant MAPK signalling. Whilst the *in vivo* data presented here shows promise, clinical trials will now be required to validate the use of pan-RAF inhibitor.

I furthermore found that cell lines harbouring *FGFR2* amplifications were hypersensitive to pan-RAF inhibition. Two GOA cell lines and a patient derived spheroid line with high-level *FGFR2* amplifications all showed similar results, suggesting that this is a general phenomenon in GOA. As aforementioned, 8% of gastric cancer patients harbour a *FGFR2* amplification (Turner and Grose, 2010), thus further work to elucidate the mechanism of the observed hypersensitivity to pan-RAF inhibitors would be warranted to provide insights into feedback loops and the cross-talks of specific genetic aberrations with different signalling pathways. High level *FGFR2* amplification has previously been shown to result in sensitisation to *FGFR* inhibition in gastric cancers, with the degree of amplification correlating with sensitivity (Pearson et al., 2016; Xie et al., 2013). Addiction to *FGFR2* signalling can be mediated by dependency on the PI3K pathway (Pearson et al., 2016). High-level expression of FGFR2 co-activates PI3K and mTOR signalling. In multiple myeloma it has been shown that inhibition with a pan-RAF inhibitor resulted in a profound downregulation of PI3K/mTOR signalling, evidencing that RAF can signal in a MEK-independent manner (Müller et al., 2017). This possible crosstalk between signalling pathways may provide some mechanistic explanation for the observed hypersensitivity and should be further investigated in response to pan-RAF inhibition in *FGFR2*-amplified GOAs. Unfortunately at the time I was performing the pan-RAF inhibitor work, the UK Home Office reclassified the *FGFR* inhibitor AZD4547 as a controlled drug which made the compound inaccessible for research purposes and I could not investigate further whether *FGFR* amplified GOA cell lines that acquired resistant to AZD4547 inhibitor would respond to pan-RAF inhibitor. This may prove an interesting line of research to pursue further and may potentially yield novel therapeutic options as it could mirror the suggested use of pan-RAF inhibitors in melanomas that are BRAF/MEK inhibitor targeted therapy resistant (Girotti et al., 2015).

Overall the therapeutic strategy of targeting the downstream MAPK pathway with pan-RAF inhibitor may present a novel therapeutic opportunity that diverges from the paradigm of personalised therapy. This may be

particularly beneficial in tumours where the exact subclonal composition is undefined, in particular in metastatic disease that is difficult to access for genetic analyses.

Chapter 4: Functional analysis of novel putative cetuximab resistance driver mutations

4.1. Introduction

The PROSPECT-C trial was a prospective clinical trial to investigate biomarkers of drug resistance to the anti-EGFR monoclonal antibody cetuximab in patients with RAS wildtype metastatic colon or rectal cancer who had failed prior standard chemotherapy (Chief Investigator: Prof Cunningham, Royal Marsden Hospital, (Khan et al., 2018b; Woolston et al., 2019)). Previous research in identifying markers to EGFR-therapy resistance had predominantly been studied in retrospective analyses of ctDNA (Bettegowda et al., 2014; Diaz et al., 2012; Misale et al., 2012). In PROSPECT-C patients were screened for *KRAS* and *NRAS* mutation status and only those that were wildtype for *KRAS* and *NRAS* at codons 12, 13, 59, 61, 117, and 146 were included in the study as mutations at these loci are well-characterised as genetic biomarkers of primary cetuximab resistance (Allegra et al., 2016; Bokemeyer et al., 2012; Tejpar et al., 2016) (Amado et al., 2008; Douillard et al., 2013). 46 patients had been registered on the trial and survival was similar to published data for cetuximab in the third line setting (**Figure 4.1** A-B).

Despite the use of patient stratification, only 43% of patients achieved clinical benefit with cetuximab (**Figure 4.2**) (Woolston et al., 2019). Furthermore, even in those patients that achieved prolonged benefit from cetuximab therapy (defined as those patients who remained progression free at the time the first per-protocol CT scan was performed at ~12 weeks), resistance invariably developed.

The aim of the trial was to identify novel biomarkers of both primary and acquired resistance to cetuximab therapy, which was enabled by the collection

of tissue biopsies from these patients before treatment initiation and again at progression. DNA extracted from these biopsies had been whole exome sequenced by my host lab with additional circulating tumour DNA (ctDNA) and RNA samples sequenced in a subset of cases. My aim was to identify potential novel mechanisms of primary or required resistance based on these genetic data. I then aimed to functionally validate any putative novel drivers to cetuximab resistance that were subsequently revealed by these analyses.

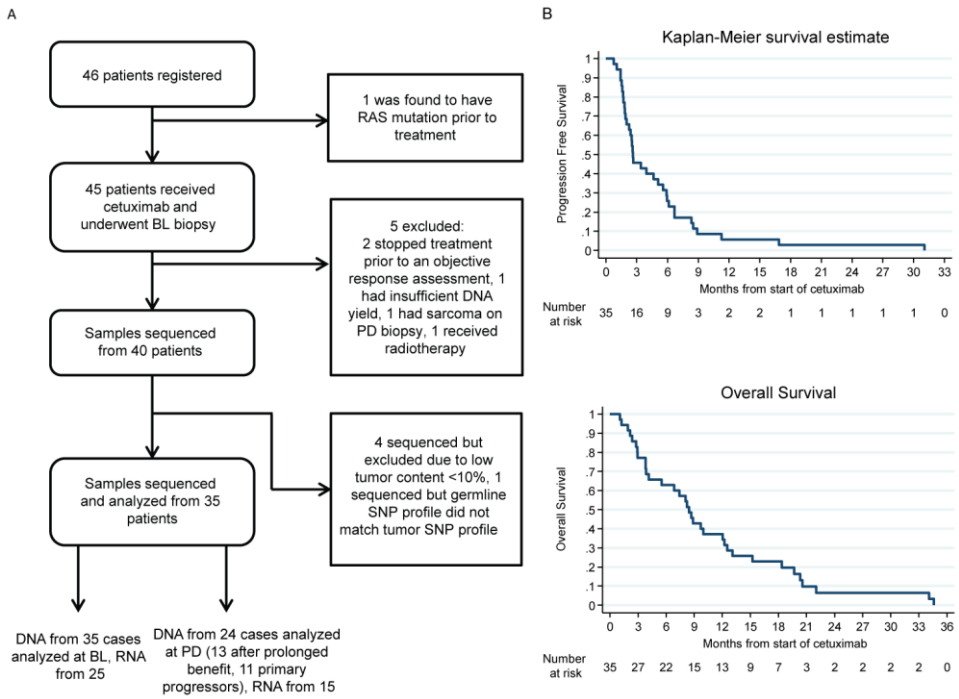

Figure 4.1 Flowchart of PROSPECT-C trial samples.

(A) CONSORT diagram of 46 patients (pts) included and biopsy samples analyzed. BL, baseline; PD, progressive disease. (B) Kaplan-Meier survival analysis of 35 pts whose samples were subjected to molecular analysis. Dr Woolston performed all bioinformatics analysis.

4.2. Identification of putative novel drivers of resistance from exome sequencing data

Whole exome sequencing data of biopsies from 35 cases taken at baseline (BL) and from biopsies of 24 cases taken at progressive disease (PD) were available for study. Based on published data that shows re-activation of the pathway as the only known mechanism of resistance to these drugs, I focused on alterations in the MAPK pathway members *RAS, RAF, MEK, ERK* and its regulators (e.g. *NF1*, upstream RTKs) and also on PIK3CA which has previously been suggested to confer anti-EGFR resistance (Sartore-Bianchi et al., 2009). Screening the exome sequencing data identified somatic aberrations in these genes in 22 of the 35 tumours (**Figure 4.2**). The same gene set was then analysed in the matched BL and PD samples. Mutations in *KRAS* and *EGFR* were acquired in two patients, with a *KRAS* amplification found in one additional patient. No other *RAS, RAF, MEK, ERK* or RTK aberrations were identified as being acquired.

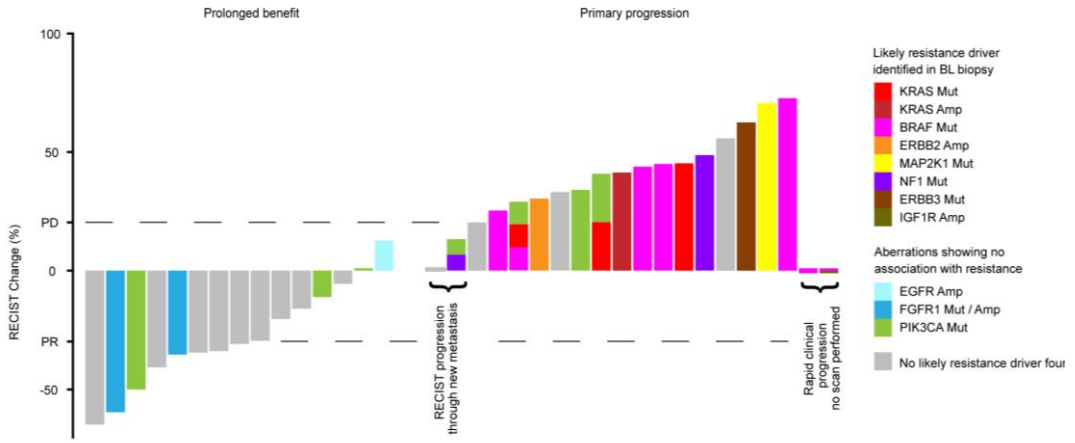

Figure 4.2 Molecular profiles of 35 BL biopsies categorized into cases with prolonged Cetuximab benefit and primary progressors.

Waterfall plot of best radiological response. Bar colours indicate the presence of genetic aberrations of MAPK pathway members or regulators and PIK3CA. Amp, amplification; Mut, mutation; PR, partial response; PD, progressive disease as per RECIST criteria. Dr Woolston performed all bioinformatics analysis.

MAPK pathway aberrations identified were then analysed to exclude those with a previously characterised role in resistance. Six out of seven patients with *BRAF* mutations were identified as having a V600E mutation thus supporting evidence that V600E is a driver of cetuximab resistance (Pietrantonio et al., 2015). A canonical resistance inducing KRAS G12D mutation was identified in one patient deemed *KRAS* wildtype on entry to the study. Thus this result is either due to a false negative in the clinical assay or intratumour heterogeneity. *KRAS* and *ERBB2* amplifications were identified in one patient each and have previously been associated with resistance (Bertotti et al., 2015; Valtorta et al., 2013). A canonical activating MAP2K1 K57N mutation in addition to MAP2K1 S228A previously described to not impact kinase activity were found in the same patient. Furthermore a P590L mutation in ERBB3 had already been reported to not impact cell growth and thus is a likely passenger mutation (Liang et al.,

2012). *PIK3CA* mutations have previously been reported as having a role in resistance (Bertotti et al., 2015; Sartore-Bianchi et al., 2009), yet no clear association with either primary progression or prolonged clinical benefit was found in this study.

Thus from the exome sequencing results of the PROSPECT-C trial and based on the exclusions detailed above, acquired *EGFR* mutations, non-canonical *BRAF* and *KRAS* mutations and *NF1* mutations were further investigated to determine their putative role as drivers of cetuximab resistance.

4.2.1. *EGFR* mutations

In a recent retrospective study ~25% of patients treated with cetuximab acquired *EGFR* mutations in the ectodomain (Van Emburgh et al., 2016). Ectodomain (ECD) mutations are known to abrogate antibody binding and are the most common EGFR variants seen in cetuximab-resistant CRCs (Arena et al., 2015; Misale et al., 2015; Misale et al., 2014; Montagut et al., 2012; Van Emburgh et al., 2016). Two different mutations in *EGFR* were acquired in two patients in the PROSPECT-C trial. One encoded for EGFR D278N, which has not previously been described and located to a Furin-like extracellular domain of EGFR. This mutation in the extracellular EGFR region did not affect any of the amino acids known to constitute the cetuximab binding epitope (Voigt et al., 2012). The other EGFR alteration, G322S, also did not seem to alter known cetuximab binding epitopes, neither did it coincide with any known EGFR activating oncogenic mutations. This mutation has been previously reported in the literature, although there is no functional information available (Fu et al., 2016). EGFR mutations that affect epitope binding have previously been described to result in acquired resistance (Montagut et al., 2012), however other mutations in the EGFR receptor are rare in CRC. EGFR D278N and G322S mutations were further investigated as they were located very close to each other and I wanted to investigate if they represented a novel yet rare mechanisms of EGFR activation. Furthermore no other driver mutations were

found to co-exist with EGFR D278N. EGFR G322s however co-existed with a KRAS G12D mutation.

4.2.2. *BRAF* mutations

Tumour C1011BL showed primary progression and exome sequencing identified a non-canonical BRAF D594F mutation, which co-existed concomitantly with a non-canonical KRAS L19F mutation. In addition, a BRAF D594N mutation was identified in the ctDNA in Patient C1030 who achieved prolonged benefit from cetuximab. The mutation was present in 6.8% of the ctDNA fraction before cetuximab treatment and increased 5.5-fold to 37.4% of the ctDNA fraction at the time the tumour progressed. Thus, somatic mutations altering the BRAF D594 amino acid were observed in one primary progressor and with an increasing frequency from BL to progression in a patient who initially benefitted, suggesting a role in resistance.

A search of known BRAF mutations in COSMIC (catalogue of somatic mutations in cancer) revealed a mutational hotspot at the D594 amino acid which locates within the BRAF kinase domain (**Figure 4.3**). D594 mutations have previously been reported in both colorectal cancer and melanomas (Heidorn et al., 2010). While the majority of BRAF mutations (Class I or II) are activating through their constitutive activation of the downstream signalling pathway, D594 mutations are Class III mutations, which despite reduced kinase activity, paradoxically still activate signals downstream (Wan et al., 2004; Yao et al., 2015; Yao et al., 2017). The kinase-impaired mutations have been reported to also have oncogenic function as they can still trans phosphorylate CRAF, which subsequently stimulates MEK signalling. The aspartic acid (D) at position 594 is a highly conserved amino acid residue that is part of the so-called DFG motif (D594, F595, G596). The role of this residue involves stabilising ATP binding in the catalytic site (Hanks and Hunter, 1995; Johnson et al., 1998). D594N has been reported in 13 cases of colorectal cancer (12 in large intestine and 1 in

small intestine) in the COSMIC database. D594F however has not previously been detected in any cancer type, possibly because it requires a dinucleotide mutation to result in this amino acid change as opposed to a single nucleotide mutation. As D594 mutations have been shown to activate downstream ERK signalling and the exome sequencing data from the PROSPECT-C trial associated them with both acquired and primary resistance, we hence decided to assess their functional relevance in cetuximab resistance.

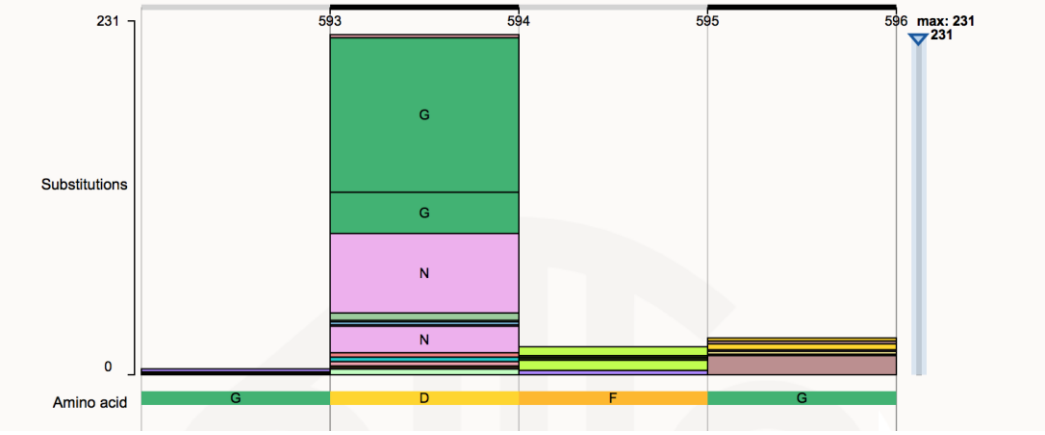

Figure 4.3 Somatic mutations reported for the BRAF D594 amino acid position in the COSMIC cancer mutation database (accessed on 13/09/2019).

231 mutations have been recorded in COSMIC for this locus but no D594F mutations have been described.

4.2.3. *KRAS* mutations

In the primary progressors group, two non-canonical KRAS mutations were detected that are not tested for in the clinical assay applied to each tumour to check trial eligibility: these were KRAS A18D and L19F. Both KRAS amino acid changes are rarely observed in cancer (**Figure 4.4**) but have previously been reported in colorectal adenocarcinomas and are implicated in tumourigenesis. KRAS A18D is a gain-of-function mutation with transforming capability (Scholl et al., 2009) and is reported in 14 cancers on COSMIC. In Tumour C1033BL the mutation was found on all seven copies of the polysomic chr12p. KRAS L19F,

seen in 37 cancers in COSMIC, has an attenuated phenotype (Smith et al., 2010) compared to classical KRAS hotspot mutations. Consequently both were modelled *in vitro* to determine their role in cetuximab resistance.

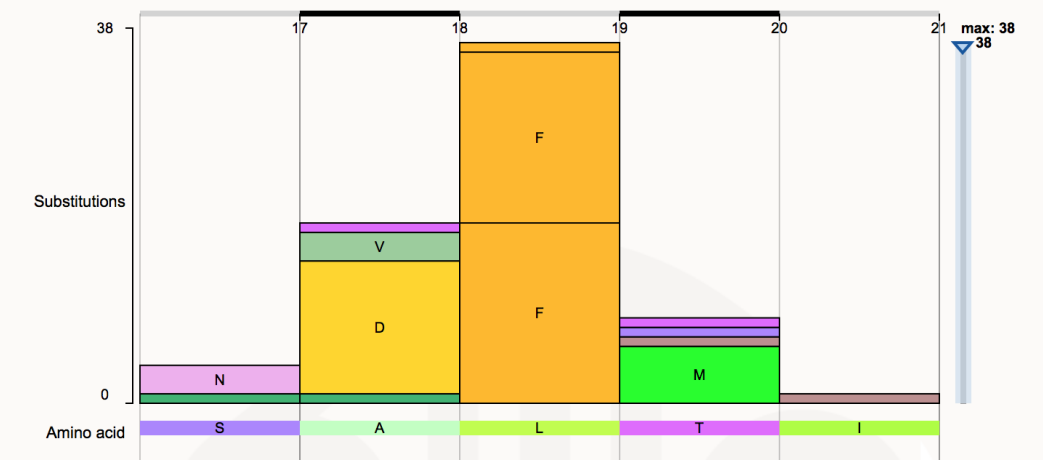

Figure 4.4 Somatic mutations reported for the KRAS A18 and L19 amino acid positions in the COSMIC cancer mutation database (accessed on 13/09/2019).

14 A18D and 37 L19F mutations have been recorded in COSMIC.

.

4.2.4. *NF1* mutations

Furthermore, two tumours (C1021BL and C1045BL) harboured disrupting mutations (one frameshift and one nonsense mutation respectively) of the *NF1* gene. Both tumours showed loss of heterozygosity of the *NF1* locus on chromosome 17. Thus, both copies of *NF1* had been inactivated through genetic aberrations. *NF1* is a known tumour suppressor gene that negatively regulates RAS activation through accelerating the hydrolysis of RAS-GTP into RAS-GDP (Basu et al., 1992). Importantly, low *NF1* expression has furthermore been shown to confer resistance to the small molecule EGFR kinase-inhibitor erlotinib in lung cancer through re-activation of the MAPK pathway (de Bruin et al., 2014). Biallelic *NF1* inactivation therefore appeared to be a strong candidate as a novel genetic mechanism of cetuximab resistance in CRC.

4.3. Cell line selection

In order to model and functionally validate newly identified candidate drivers of cetuximab resistance we selected a panel of colorectal cancer cell lines known to be *KRAS* and *BRAF* wildtype and therefore sensitive to cetuximab (Arena et al., 2015; Bardelli et al., 2013; Misale et al., 2012). One *KRAS* mutant cell line was also included as a control in the drug sensitivity assay for a resistant phenotype (Table 4.1). DiFi, LIM1215 and HCA-46 cell lines were sensitive to cetuximab over 5-days of treatment (**Figure 4.5**). However, HCA46 grew slowly and was more difficult to culture than DiFi and LIM1215. The KRAS G12V mutant control cell line SKCO-1 was resistant to cetuximab treatment and the NCI-H508 line showed an intermediate sensitivity. Based on the response data, I selected DiFi and LIM1215 as the model cell lines for the investigation of novel genetic cetuximab resistance drivers. (Arena et al., 2015; Misale et al., 2012).

Cell Line	KRAS mutation status	BRAF mutation status	Other genetic aberrations with relevance to MAPK signalling
DiFi	**WT**	**WT**	**EGFR amplified x20**
LIM1215	**WT**	**WT**	
NCI-H508	**WT**	**p.G596R**	
HCA-46	**WT**	**WT**	
SK-CO-1	**p.G12V**	**WT**	

Table 4.1 CRC Cell Line Panel

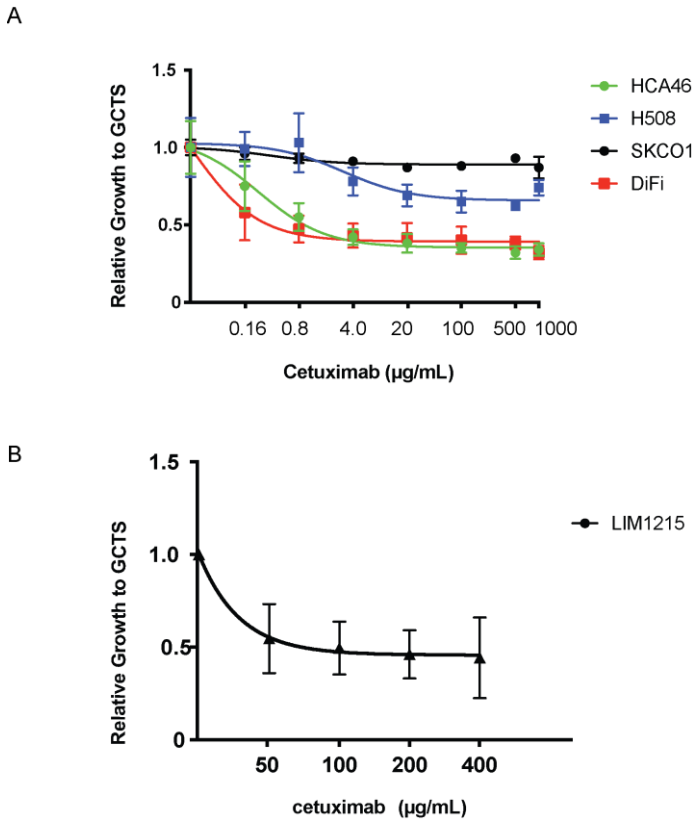

Figure 4.5 Cetuximab sensitivity testing of CRC cell lines.

(A) Panel of four CRC cell lines treated with cetuximab (0.16-1000 mg/mL) for 5 days. (B) LIM1215 cells treated with cetuximab (50-400 µg/mL) for 5 days. Cell viability was assessed by Cell-Titre blue (CTB). Background determined by CTB at Day 0 of treatment was subtracted from the raw values and data were then normalised such that 1 indicates growth in the presence of vehicle alone (GCTS) and 0 indicates no growth from seeding density. One representative experiment is shown. Error bars represent SD of 6 technical replicates.

4.4. Introduction of mutations into CRC cell lines

Mutations selected for functional analysis were introduced into cDNA expression vectors encoding the respective gene of interest. Accurate mutagenesis and absence of unintended mutations was confirmed by Sanger sequencing following which the mutated cDNA was subcloned into a lentiviral expression vector and transduced into both DiFi and LIM1215 cell lines (**Figure 4.6**). Successfully transduced cells were selected with antibiotics according to

the resistance gene encoded by the lentiviral construct. Wildtype *EGFR*, *KRAS* and *BRAF* were also transduced into cell lines as negative controls.

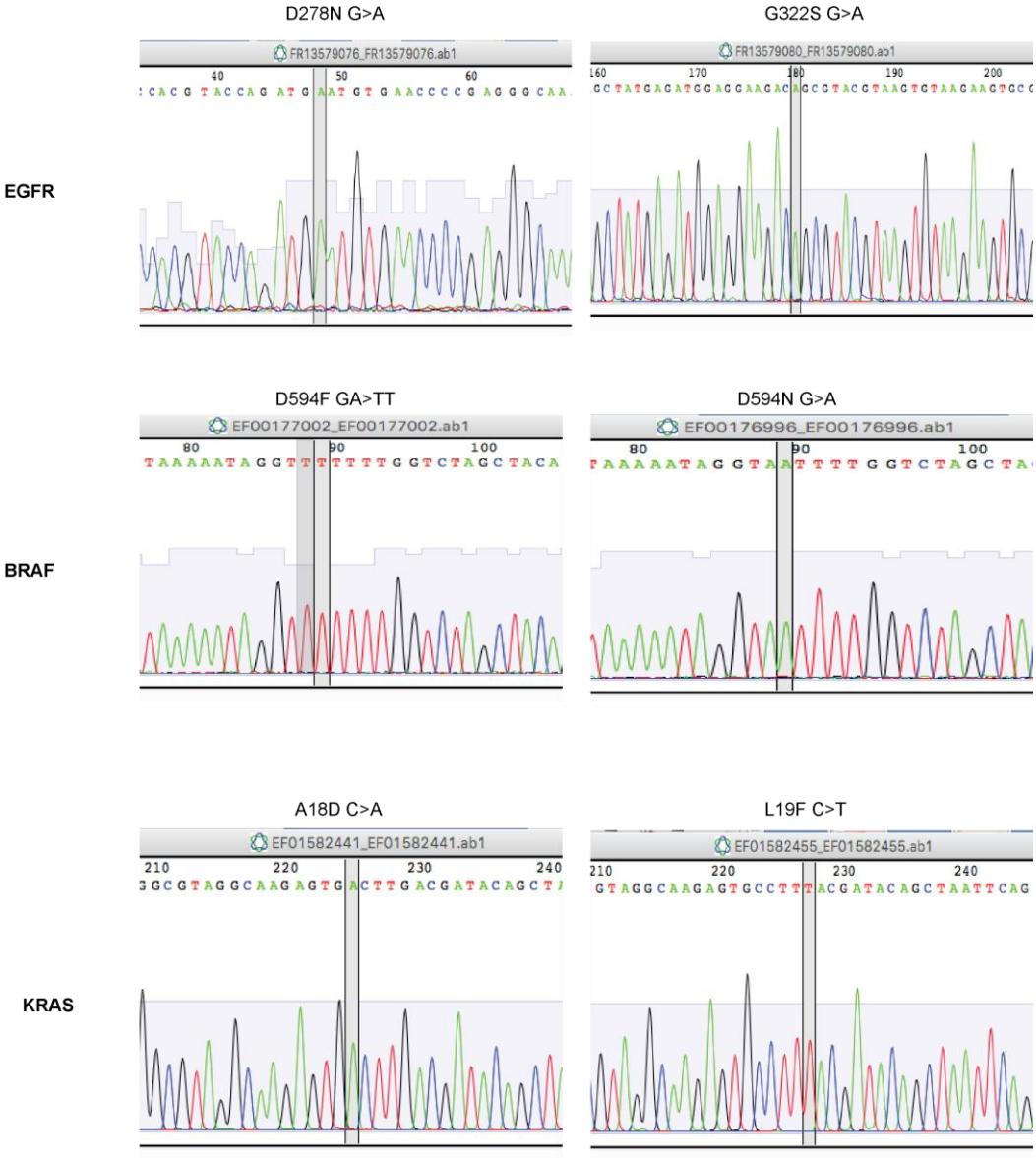

Figure 4.6 Sanger sequencing confirms mutagenesis.

Screenshots of Sanger sequencing traces of EGFR D278N, EGFR G322S, BRAF D594F, BRAF D594N, KRAS A18D and KRAS L19F. The base substitution that results in the desired amino acid change is indicated in each trace.

4.5. Analysis of novel EGFR mutations as putative drivers of resistance

4.5.1. EGFR D278N and EGFR G322S mutations do not confer resistance to cetuximab in a CRC cell line.

Both EGFR D278N and G322S mutations were introduced into the CRC cell line LIM1215 to investigate whether these are activating mutations that lead to cetuximab resistance. In a 5-day treatment drug sensitivity assay in LIM1215 mutant cell lines neither EGFR mutation rescued growth compared to an introduced EGFR wildtype construct (**Figure 4.7** A). To assess if these mutations increase intracellular EGFR signalling activity, I measured EGFR auto-phosphorylation and MAPK pathway signalling by Western blot analysis of ERK phosphorylation. EGFR phosphorylation was downregulated through cetuximab treatment in LIM1215 cells transduced with an EGFR wildtype construct and also in both EGFR mutant constructs (**Figure 4.7** B). It is interesting to note that EGFR G322S appeared to downregulate total EGFR protein when compared to all other used cell lines and constructs.

ERK phosphorylation was almost completely suppressed after 2 hr of cetuximab treatment in all mutant and control lines, however, a small amount of rebound signalling with an increase in ERK phosphorylation became apparent after 24 hr of cetuximab treatment. Some signal rescue can be detected after 2 hr of cetuximab treatment in the D278N mutant cells indicating there may be a small but not significant upregulation in the signalling pathway as a result of the mutation. No rescue in pERK signalling could be detected in the G322S mutant cells, in keeping with the pEGFR and EGFR results.

Thus, my results do not support either EGFR D278N or G322S to notably reactivate the MAPK pathway and they showed no rescue of LIM1215 proliferation when treated with cetuximab. Furthermore, as EGFR G322S was found to co-exist with a clonally dominant KRAS G12D mutation, a known

resistance driver, we concluded that a G322S mutation in EGFR was likely to be a passenger mutation.

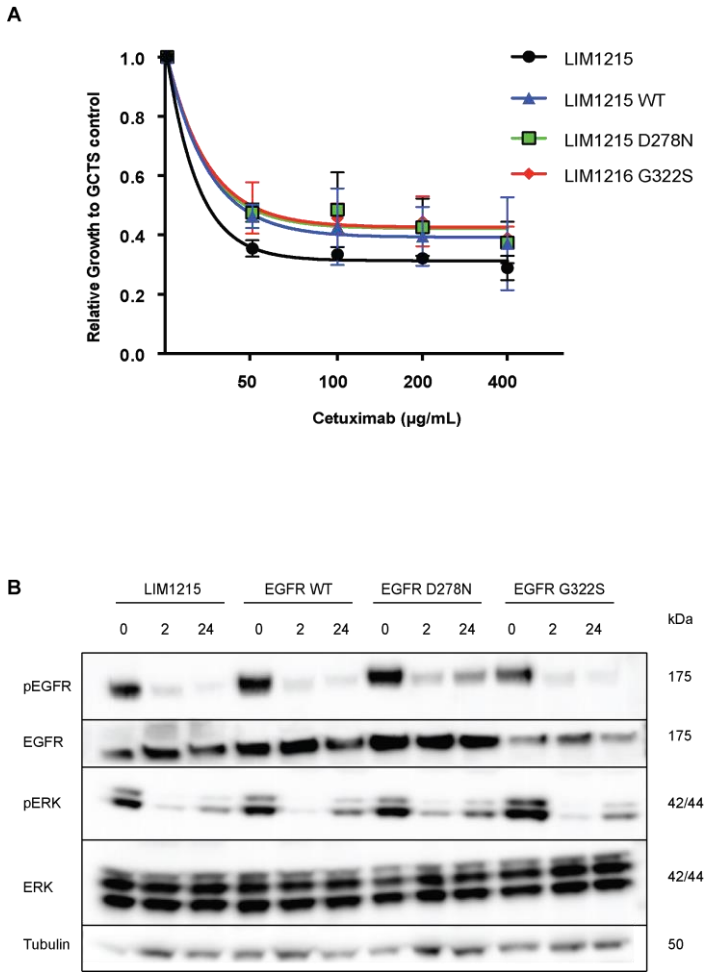

Figure 4.7 EGFR D278N and G322S mutations do not induce cetuximab resistance.

(A) Growth analysis of EGFR mutant LIM1215 cell lines treated with cetuximab (50-400 µg/mL) for 5 days. Cell viability was assessed by Cell-Titre blue (CTB). Signal determined by CTB at Day 0 of treatment was subtracted from the raw values and data were then normalised such that 1.0 indicates growth in the presence of GCTS and 0 indicates no growth from seeding density. One representative repeats is shown. Error bars represent SD of 6 replicates. (B) Western blot analysis of pEGFR, EGFR, pERK and ERK in EGFR mutant cell lines treated with cetuximab (200 µg/mL) for 2 and 24 hr. Tubulin was used as a loading control.

4.5.2. EGFR D278N does not induce cetuximab resistance in an EGFR-null cell line.

To elucidate whether EGFR D278N could reactivate ERK signalling in the absence of endogenous EGFR, I decided to introduce D278N into the EGFR-null murine fibroblast cell line NIH-3T3, where any EGFR signalling activity would exclusively result from the introduced transgene. EGFR signalling in NIH-3T3 that has been transduced with the EGFR receptor must be induced by stimulation with recombinant EGF. EGF stimulation (5 ng/mL) for 5 minutes resulted in phosphorylation of EGFR in both the EGFR WT and EGFR D278N transduced cells (**Figure 4.8** A). EGFR phosphorylation was not maintained after 2 hr cetuximab treatment in either the WT or mutant cell line thus demonstrating that no constitutive pEGFR signalling was induced by D278N.

As the EGFR D278N mutation was found subclonally in the tumour, we hypothesised that EGFR D278N mutants may only show a phenotypic effect when it can dimerise with EGFR WT as this is likely to occur *in vivo*. Therefore the EGFR WT construct was transduced into EGFR D278N cell lines. As they both contain the same antibiotic resistance marker, it was not possible to select for the double transfected population. However, Sanger sequencing was performed on an aliquot of transiently transfected EGFR D278N cell line 48 hr after transduction with EGFR-WT and this showed a ratio of approximately 2/3 mutant DNA and 1/3 wildtype DNA in the population, and hence confirmed that a fraction of the population now contained both constructs (**Figure 4.8** B). However, double transfection did not show an increase in EGFR or ERK phosphorylation in the presence of ligand stimulation and cetuximab treatment. I hence concluded that the D278N mutation in EGFR is highly likely to be a passenger mutation without an effect on EGFR signalling, ERK signalling or cetuximab resistance.

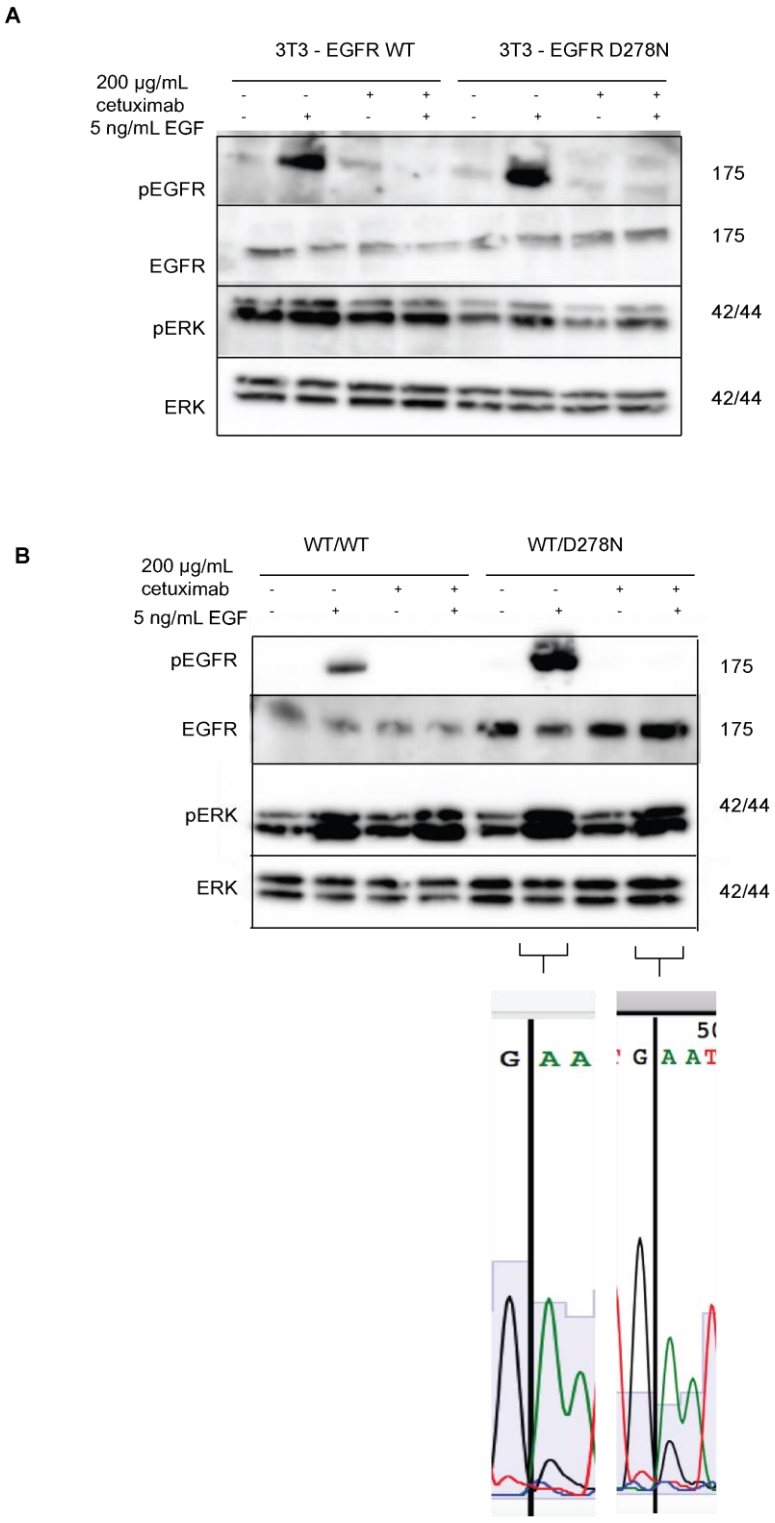

Figure 4.8 EGFR D278N mutations do not induce cetuximab resistance in an EGFR-null cell line.

(A) Western blot analysis of pEGFR, EGFR, pERK and ERK in NIH-3T3 EGFR wildtype and mutant cell lines treated with cetuximab (200 µg/mL) for 2 hr. ERK was used as a loading control. (B) Western blot analysis of pEGFR, EGFR, pERK and ERK in double transfection cells lines WT/WT and WT/D278N with cetuximab (200 µg/mL) for 2 hr ERK was used as a loading control. Sections of Sanger traces to show ratio of wildtype (G, middle black peak) to D278N encoding mutation (A, middle green peak) in the cell lines indicated.

4.6. Analysis of kinase-impaired BRAF mutations as putative drivers of resistance

The BRAF D594F and D594N mutations, identified in the patient cohort, as well as the known BRAF kinase-dead D594H mutation, used as a positive control, were lentivirally transduced into the DiFi cell line and stably selected with puromycin.

ERK phosphorylation was investigated by Western blotting in wildtype and mutant cell lines that were either treated with 200 µg/mL cetuximab or with vehicle GCTS, for 2 hr (**Figure 4.9**). DiFi cells transduced with wildtype or mutant BRAF all showed increased ERK phosphorylation compared to the DiFi cells that had been transduced with a lentivirus encoding luciferase as a control, suggesting that an increase in the dosage of BRAF augments MAPK pathway signalling. Following treatment with cetuximab, the control cell line showed almost complete loss of pERK signal as expected for a cetuximab sensitive cell line. Although cetuximab treatment reduced ERK phosphorylation in the DiFi cell lines transduced with the putative resistance drivers BRAF D594F and BRAF D594N as well as in those expressing the known kinase-dead and oncogenic BRAF D594H, the residual ERK phosphorylation remained higher than in DiFi cells expressing either luciferase or wildtype BRAF. This shows that BRAF mutations that impair the kinase function can maintain a low level of MAPK pathway signalling during cetuximab treatment in CRC. Together with the clinical observation of BRAF D594F and D594N in tumours with primary and acquired resistance, respectively, these results support a role as novel drivers of resistance to anti-EGFR antibodies in CRC. Furthermore, Western blot data shows quantitative difference in ERK phosphorylation during cetuximab exposure. However, in the absence of further controls to assess the protein abundance of each BRAF mutant, this does not allow us to draw definitive conclusions about differences in the activity of the three mutated BRAF proteins.

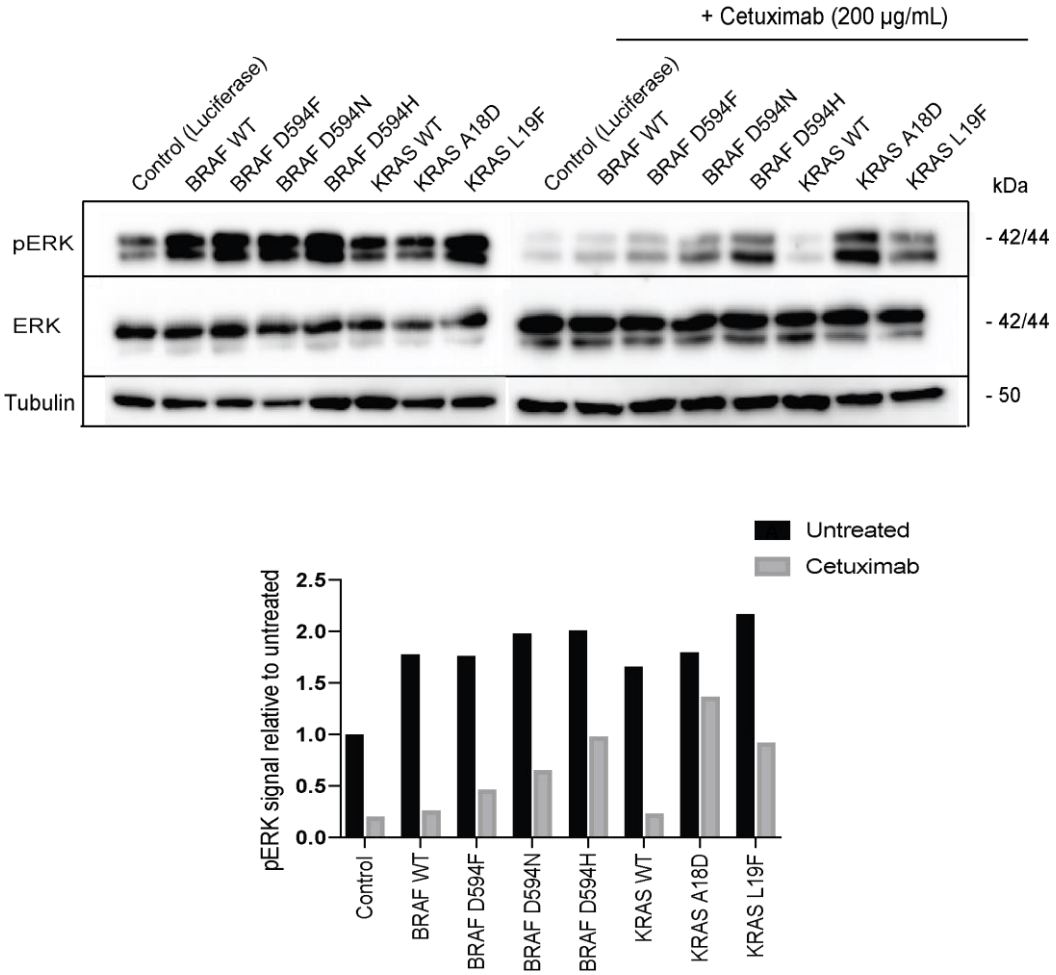

Figure 4.9 Novel BRAF and KRAS mutations induce pERK signalling in the presence of cetuximab.

Western blot analysis of pERK and ERK in BRAF and KRAS mutant cell lines treated with cetuximab (200 µg/mL) for 2 hr. Tubulin was used as a loading control. Quantification of blots was performed using ImageJ. Signal density was normalised to total ERK signal.

4.7. Analysis of novel KRAS mutations as putative drivers of resistance

The non-canonical KRAS A18D and L19F mutations were transduced into DiFi cell lines and selected with puromycin treatment. Following selection they were treated with cetuximab or vehicle as described for the BRAF mutations. The KRAS A18D mutation conferred a strong rescue of ERK phosphorylation when treated with cetuximab, with a signal that was comparable to the untreated KRAS A18D mutant line (**Figure 4.9**). The KRAS L19F mutation achieved a much more modest rescue of ERK phosphorylation during cetuximab exposure. This supports data from previous publications that described this KRAS mutation as hypomorphic compared to canonical KRAS codon 12 and 13 mutations. Taken together with the identification of KRAS A18D and L19F mutations in CRCs that showed primary resistance in the PROSPECT-C trial, this supports a purported functional role for both mutations as novel drivers of cetuximab resistance.

4.8. Analysis of inactivating NF1 as putative drivers of resistance

4.8.1. siRNA-mediated knockdown of *NF1*

Two tumours that showed primary progression during cetuximab treatment both harboured loss-of-function mutations in *NF1* combined with a DNA copy number loss of the second *NF1* allele. To investigate whether loss of expression of the *NF1* tumour suppressor gene leads to persistent MAPK pathway activity and enables the cells to continue growth despite cetuximab treatment, I first used siRNA technology to repress *NF1* expression.

The cetuximab sensitive LIM1215 cell line was transfected with two distinct *NF1* siRNA oligonucleotides (*NF1-3*, *NF1-4*) and also with a commercially available

pool of four *NF1*-targeting oligonucleotides and grown for 48 hr. *GAPDH* siRNA was used as a further control. Repression of *GAPDH* and *NF1* mRNA were then assessed by RTqPCR. A 93% knockdown of *GAPDH* (p=0.0005) confirmed effective siRNA transfection into the LIM1215 cells (**Figure 4.10** A). Out of the two individual *NF1*-targeting siRNAs and the pool of four siRNAs, the best knockdown, with a significant 75% reduction of *NF1* mRNA, was achieved by the siRNA pool (p=0.002). In contrast, individual siRNAs reduced expression by only 52% and 64% (p<0.001) (**Figure 4.10** B). NF1 knockdown was repeated and after 48 hr, cells analysed by Western blot. This showed a good reduction of NF1 protein levels with the *NF1-3* and *NF1-4* siRNAs and with the pool of *NF1* siRNAs. This correlates with the degree of NF1 knockdown observed at the mRNA level (**Figure 4.10** C).

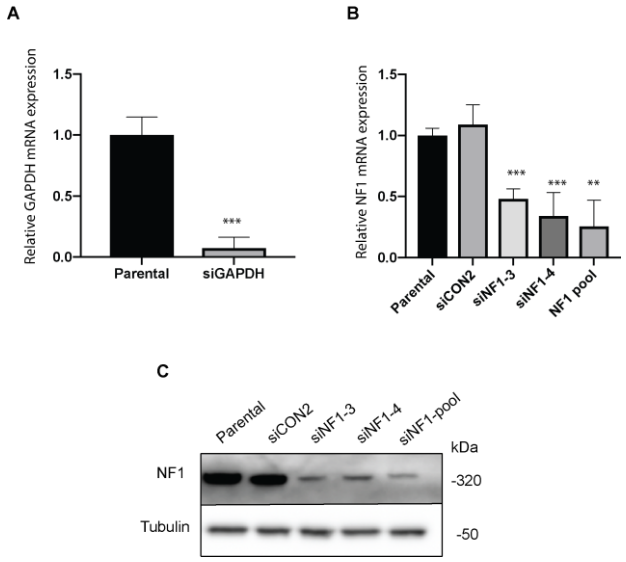

Figure 4.10 Efficacy of *NF1* knockdown by siRNA in LIM1215 cell lines.

(A) Expression of *GAPDH* mRNA following siRNA repression in LIM1215 cell lines by qPCR. Expression values were normalized to 1 in the parental cell lines (B) Expression of *NF1* mRNA in the LIM1215 cell line transfected with the indicated siRNAs targeting *NF1* (*siNF1-3*, *siNF1-4* and *NF1* pool) or with scrambled control siRNA (siCON2). Expression values were normalized to 1 in the parental control. One representative repeat is shown. Error bars indicate the standard deviation of triplicate measurements. Data were normalised using the delta-delta CT method. (C) Western blot analysis of LIM1215 cells 48 hr after transfection with the indicated NF1 or control siRNAs.

4.8.2. *NF1* repression rescues ERK phosphorylation but not growth of CRC cells during low-dose cetuximab treatment

Due to good knockdown achieved with the pool of four *NF1* siRNAs at mRNA and protein level pool, I chose this approach for subsequent experiments. The effect of *NF1* knockdown on pERK signalling during treatment with a range of cetuximab doses (6.25-100 μg/mL) was next investigated. *NF1* repression partially rescued ERK phosphorylation at relatively low cetuximab doses (6.25 μg/mL and 25 μg/mL) but 100 μg/mL cetuximab repressed pERK suppression similarly in the LIM1215 cells transfected with control siRNA and those with *NF1* siRNA (**Figure 4.11**). Thus, although NF1 loss can partially rescue MAPK pathway signalling at low cetuximab doses, high dose remains effective.

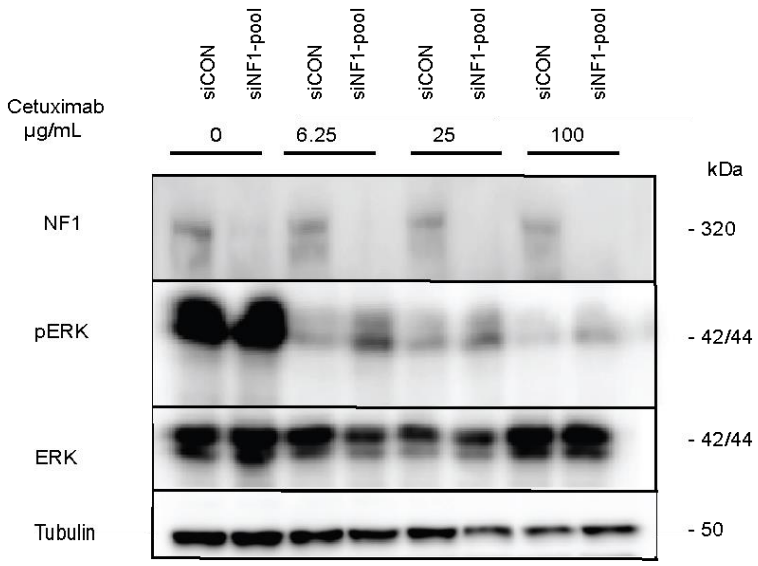

Figure 4.11 pERK signal is rescued at lower doses of cetuximab in siNF1 cells.

(A) Western blot analysis of NF1 knockdown in cells treated with 6.25-100 µg/mL cetuximab for 2 hr post 48 hr knockdown. Tubulin was used as a loading control.

I next investigated whether this reactivation of pERK and thus MAPK signalling would result in a growth rescue phenotype. *NF1* was knocked-down in LIM1215 cells and 24 hr later cetuximab treatment was commenced for 5 days. Despite the biochemical results showing maintained ERK phosphorylation, following *NF1* knockdown and treatment with 6.25 µg/mL and 25 µg/mL cetuximab, no rescue of growth was observed at these drug concentrations. *siNF1*-pool cells showed no growth rescue with any dose of cetuximab investigated compared to parental or the control transfection line (siCON2) (**Figure 4.12**) . For the drug sensitivity assay the cells are exposed to cetuximab for a longer timeframe post knockdown than they are in the Western blot (5 days vs. 2 hr). I hypothesized that siRNA knockdown of *NF1* may not be maintained over this prolonged time period and that this may preclude the observation of growth rescue.

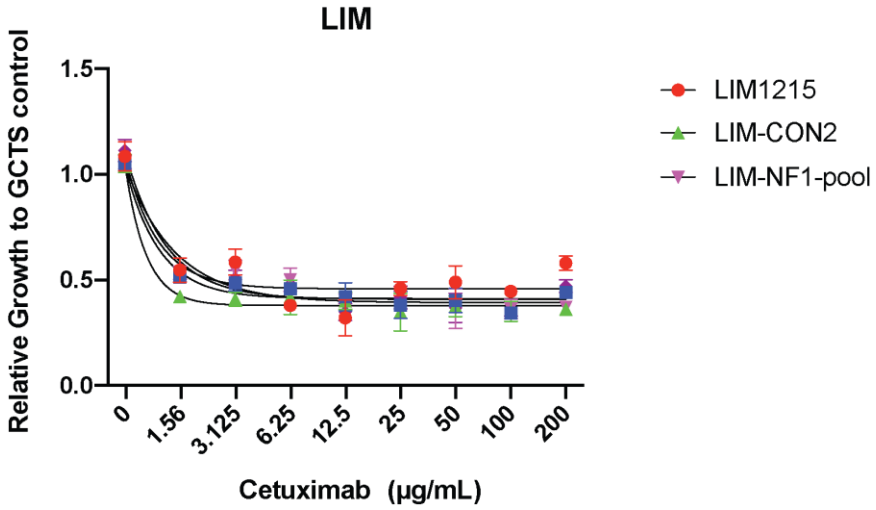

Figure 4.12 siRNA repression of *NF1* does not rescue the growth of LIM1215 cells during cetuximab treatment.

Drug sensitivity assay of LIM1215 parental cells vs those transfected with *NF1*-pool or scrambled control (CON2) and treated with a range of cetuximab doses (1.56-200 µg/mL) for 5 days. Cell viability was assessed by Cell-Titre blue (CTB). Signal determined by CTB at Day 0 of treatment was subtracted from the raw values and data were then normalised such that 1.0 indicates growth in the presence of GCTS and 0 indicates no growth from seeding density. One representative repeat is shown. Error bars represent the standard deviation of 6 replicates.

4.8.3. CRISPR-mediated knockout of *NF1*

Silencing mRNA expression through siRNA may only result in transient knockdown. I therefore investigated using CRISPR (Clustered regularly interspaced palindromic repeats) to genetically modify the *NF1* gene and thus create a stable loss-of-function model. CRISPR technology comprises of two key components; a guide RNA which is a short synthetic RNA comprising of a scaffold sequence and a 20 nucleotide sequence specific to the target gene, and a CRISPR-associated endonuclease (Cas9) (**Figure 4.13**). The scaffold in the guide RNA contains the binding site for the Cas9 protein, allowing it to bind to the DNA and to cleave it through its endonuclease activity. This results in a double

strand break. Double strand breaks (DSB) can be repaired in a cell through one of two mechanisms; either through the fast but error-prone non-homologous end joining (NHEJ) or through the high fidelity but less efficient homologous directed repair (HDR) pathway. In the absence of a repair template the double strand break induced by Cas9 is usually re-ligated by NHEJ resulting in random insertions and deletions (indels) in the DNA sequence as a consequence of the repair. These indels in the target DNA cause frameshifts, amino acid substitutions and introduction of premature stop codons, which ultimately results in a loss-of-function phenotype in the gene in question. Importantly, the CRISPR CAS9 system is sufficiently efficient to inactivate multiple copies of an individual gene, which is important as the genome is diploid and cancer cells frequently have even higher ploidy levels.

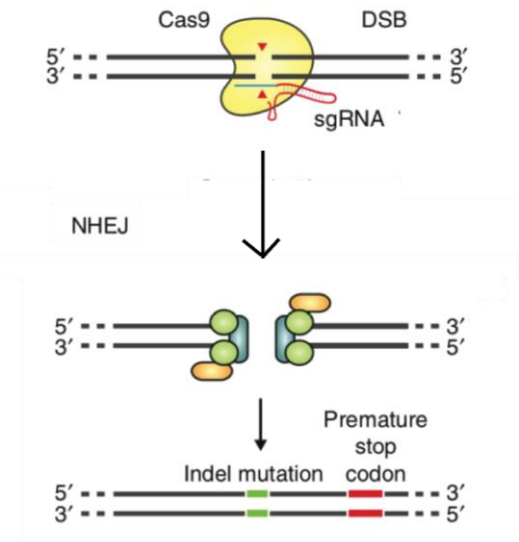

Figure 4.13 Schematic of CRISPR technology.

The Cas9 endonuclease is guided to the DNA target site by a 20nt scaffold guide RNA sequence (sgRNA) and cleaves the DNA with a double strand break (DSB). Cas9 double strand breaks are predominantly repaired by non-homologous end joining (NHEJ) which is inherently error-prone, resulting in random insertions and deletions (indels) in the base sequence. This ultimately results in frameshifts, nonsense or missense mutations and subsequently a loss-of-function phenotype. Image adapted from (Ran et al., 2013)

There are multiple methods of delivering the CRISPR Cas9 system. The ribonucleoprotein (RNP) complex method was initially selected as it allows for transient expression of CRISPR components in the cell (**Figure 4.14** A). This is thought to reduce potential off-target effects in the cells. Purified Cas9 protein and the guide RNAs (gRNAs) form a RNP complex that is then incubated with transfection reagent to deliver to the cell through lipid delivery. The knock out phenotype can then be achieved within 48-72 hr. U20S cells were used in a first attempt to optimise the transfection condition. U20S cell lines were first transduced with GFP in order for the positive control eGFP guide-RNA provided with the kit to be used. However, despite following the manufacturer's protocol provided for U20S cells, knockout of GFP could not be achieved. The percentage of GFP cells was analysed by flow cytometry, and this showed no reduction in the GFP population following incubation with the Cas9 and eGFP gRNA (**Figure 4.14** B). Furthermore, correspondence with the manufacturer revealed that 15-20% efficiency was considered to be a positive result. The CRC cetuximab sensitive cell lines were known to have poor transfection efficiency and therefore only 15-20% efficiency in cells that do not transfect well was deemed too low. Thus the decision was made at this time to try an alternative delivery system for CRISPR.

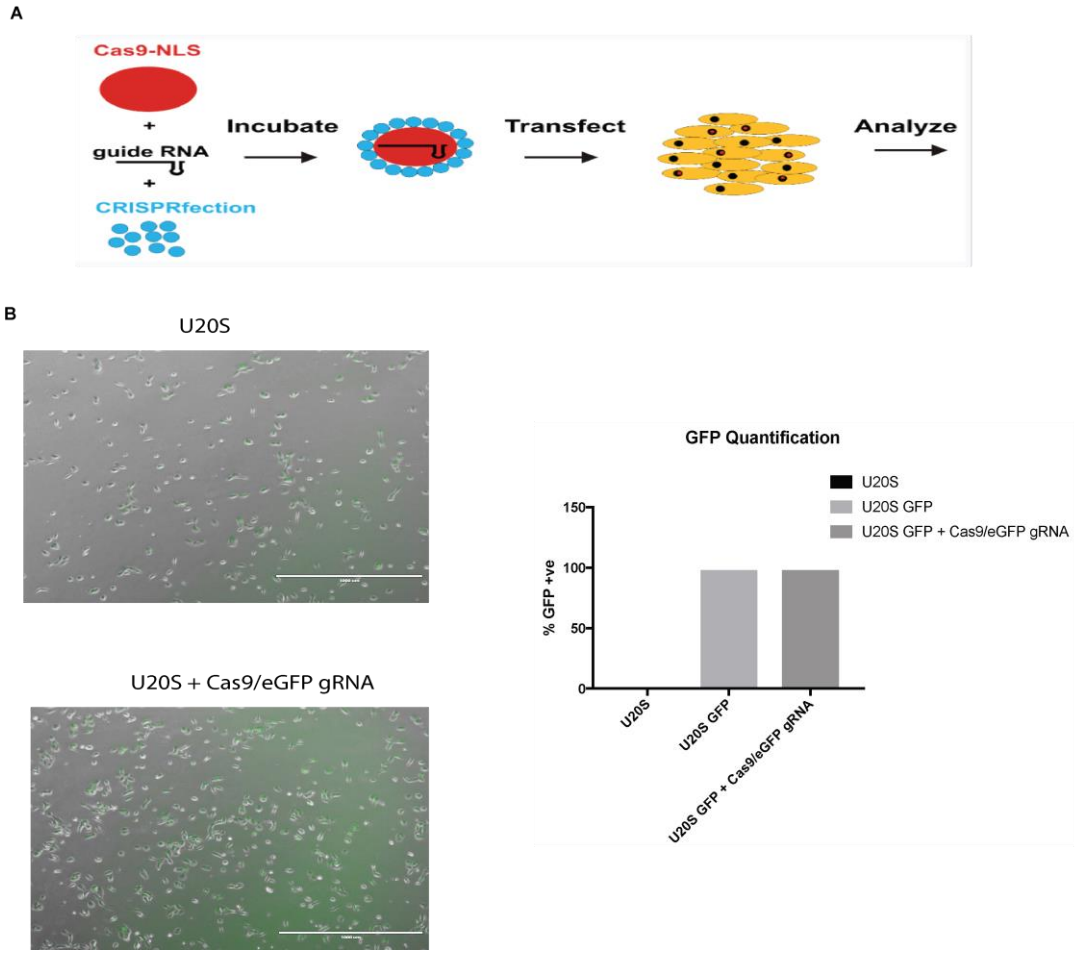

Figure 4.14 Optimising RNP-delivery of CRISPR.

(A) Schematic of RNP delivery of Cas9 and sgRNA. Image taken from Eupheria Biotechnology (Eupheria Biotechnology). (B) Representative images of GFP-tagged U20S cells treated with Cas9/eGFP RNP complex. Quantification of percentage of GFP+ve cells determined by flow cytometry.

4.8.4. Lentiviral CRISPR inactivation of *NF1.*

Lentiviral delivery of the Cas9 protein to produce a stably expressing cell line, followed by lentiviral delivery of the guide RNAs is often recommended for more difficult to transfect cell lines. The transfection efficiency in both DiFi and LIM1215 cell lines was observed to be low in previous experiments (data not shown) and the lentiviral CRISPR Cas9 approach appeared promising. LIM1215 cells were first transduced with a lentivirus encoding for a constitutively active Cas9 enzyme, kindly provided by Prof. Lord's laboratory at the ICR. Cells that

were successfully transduced were positively selected by treatment with Blasticidin (5 µg/mL).

Following successful selection and expansion of the LIM1215 cell line, expression of Cas9 was confirmed by Western blot. These Cas9 expressing cell lines are henceforth referred to as LIM-Cas9. Analysis of pERK in LIM-Cas9 revealed a slight increase in ERK phosphorylation relative to the LIM1215 parental cells. Thus analysis of pERK in subsequent experiments was relative to the LIM-Cas9 cell line as a control.

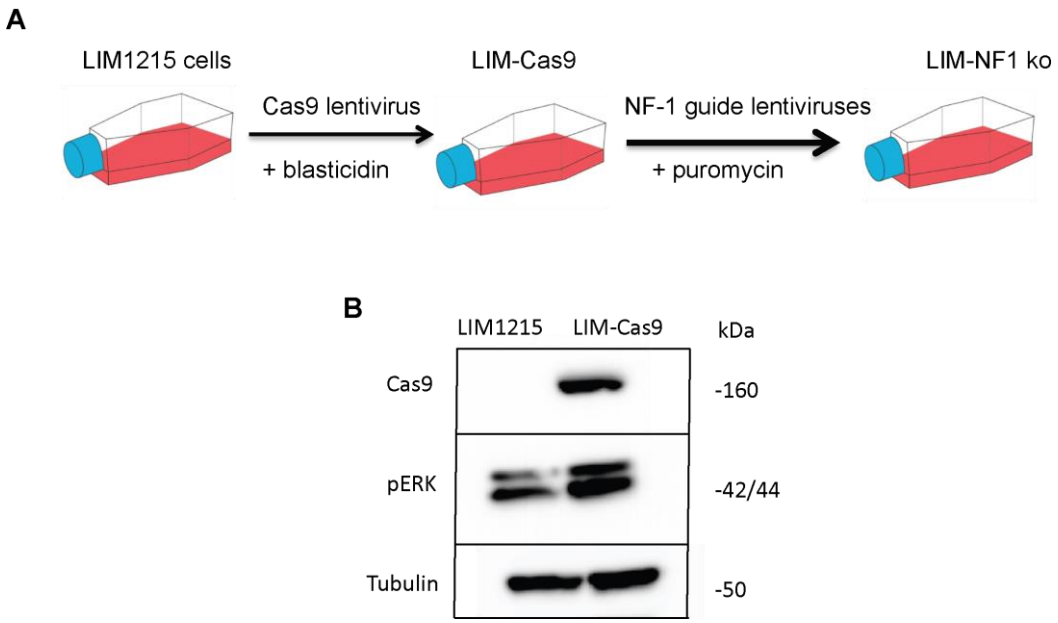

Figure 4.15 Lentiviral mediated CRISPR.

(A) Schematic of experimental plan for generating NF1 knockout (ko) LIM1215 cells. (B) Western blot analysis of Cas9 expression in LIM1215-Cas9 cells. Tubulin is used as a loading control.

NF1 guide constructs were taken from a genome-wide library available from the Lord lab. The screen contained 9 individual guides, however these guides had not been subsequently used in validation studies. Using IGV software, we located the cut sites of all 9 guides and mapped these relative to the two known mutations that were seen in the patients. In Patient C1021 a frameshift mutation led to premature termination of the 2,818 amino acid long NF1 protein, relatively close to the N terminus (L252fs). In contrast, the tumour from Patient C1045 had a stop-gain mutation terminating the protein sequence closer to the C terminus (E2448X). I chose four guides, two that cut relatively early in the NF1 coding sequence and two that cut at later codons, to best model the changes seen in the patients (Table 4.2, **Figure 4.16**)

Guide Name	Target	20 nt sequence	Exon	Codon
C08	NF1	GGTGGAATGGGTCCAGGCCG	1	6
C09	NF1	GGCTTGTCGGCAAATCGGGG	18	676
D08	NF1	GCACACACTTCGAAGTTGAG	30	1358
D09	NF1	GTCCTCTTCTAAAGCCAAGG	36	1709

Table 4.2 NF1 guide sequences

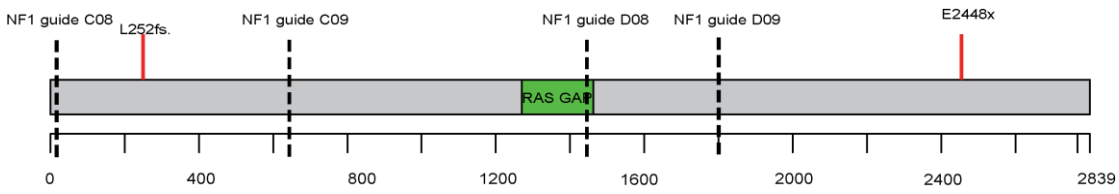

Figure 4.16 Location of cut sites of lentiviral guides in *NF1*.

(A) Schematic of *NF1* gene (scale=codons) indicating the cut sites of the 4 lentiviral guides (dashed lines) and the locations of the mutations (red lines) hypothesised to encode primary driver resistance mutations found in 2 patients in the PROSPECT-C trial. The catalytic RAS-GAP domain is indicated in green.

Plasmids encoding lentiviral DNA constructs for each of the guide sequences were sub-scultured and purified. Once virus was produced, the LIM-Cas9 cells lines were then transduced with the 4 different *NF1* guides and selected for successful integration using puromycin (5 μg/mL). Once the cells had expanded sufficiently, DNA was extracted and Sanger sequencing was used to investigate if the *NF1* gene had been edited by Cas9-induced NHEJ. Primers were designed to sequence around the intended cut site of each guide. Sanger traces show the base sequence and relative abundance of each nucleotide in the cellular population. Clear disruption of the sequence following each cut site can be seen relative to LIM-Cas9 cells sequenced with the same primer pair (**Figure 4.17**). This suggests successful genome editing as no sequence dominates in the population. The degree to which the gene was disrupted was then quantified using the TIDE (Tracking of Indels by Decomposition) web tool (**Figure 4.18**). TIDE decomposes the sequence trace in order to quantify genome editing (Brinkman et al., 2014) by aligning the target sequence to the sequence in the Cas9 expressing parental cell line. Using the 20-nucleotide guide sequence, the web tool marks the expected cut site on the Sanger sequencing trace. The editing efficiency in C08 and D08 was 66.4% and 39.9% respectively. The cut sites for C09 and D09 were too close to the start of the trace and therefore TIDE was unable to analyse editing efficiency in these guides.

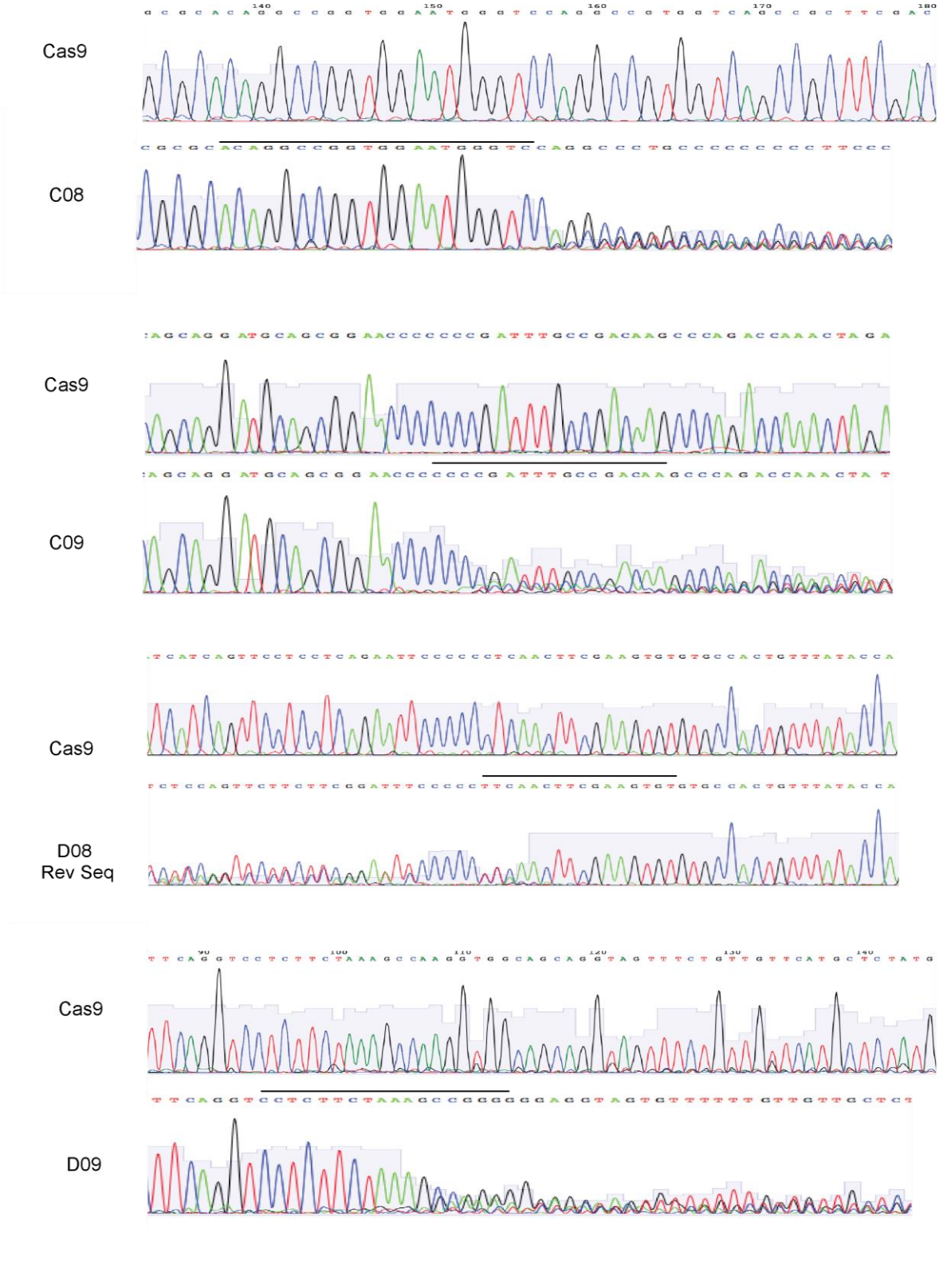

Figure 4.17 CRISPR-mediated disruption of *NF1* sequence.

Sanger traces of positively selected LIM1215 cells transduced with 4 different *NF1* guide RNAs. A black line above the trace identifies each cut site. Traces for LIM-Cas9 cells with each primer are shown for reference. Note that the reverse sequence trace is shown for D08.

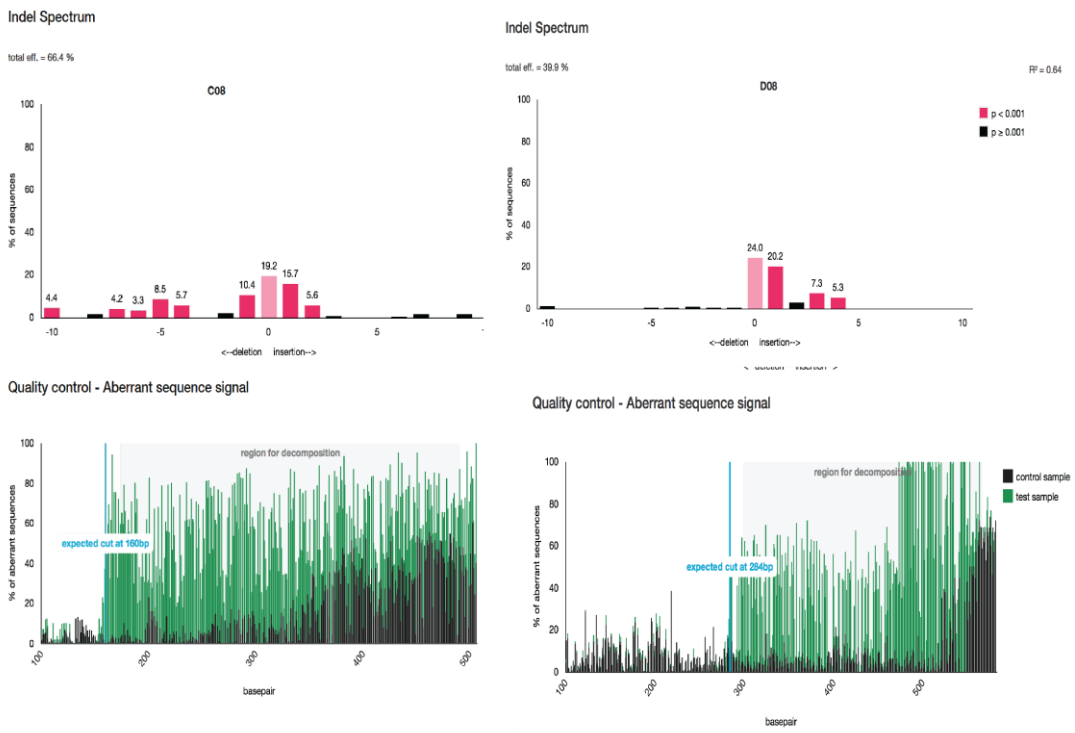

Figure 4.18 TIDE analysis.

Graphs produced by TIDE analysis web tool. Indel spectrum and total gene editing efficiency are indicated in the top panel. Aberrant signal after the predicted cut site is indicated in green with wildtype signal indicated in black in the bottom panel. Only C08 and D08 are shown as C09 and D09 could not be analysed by TIDE.

Once the 4 guides had been confirmed to result in genetic disruption following the cut site, Western blots were performed to establish the resultant effect on NF1 protein levels. All 4 guides had caused some degree of NF1 protein loss, however C08 and D09 showed the greatest effect (**Figure 4.19**). Cells disrupted by guides C08 and D09 were therefore chosen for further study as they would be more representative of the complete genetic *NF1* loss-of-function aberration which we had observed in two tumours. Herein C08 is referred to as *NF1* guide #1 and D09 as *NF1* guide #2.

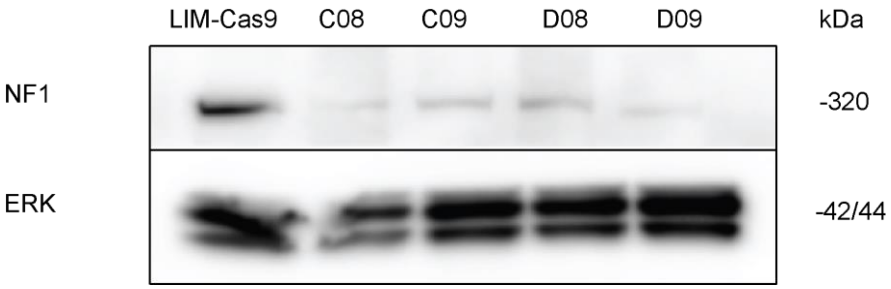

Figure 4.19 All lentiviral NF1 guides results in loss of protein.

Western blot analysis of NF1 protein expression in CRISPR-mediated NF1 knockout. ERK was used as a loading control. Quantification of blots was performed using ImageJ. Signal density was normalised to total ERK signal.

As siRNA knockdown of *NF1* had resulted in rescue of pERK signalling at lower doses of (6.25-25 µg/mL) cetuximab, 6.25 µg/mL was initially selected to treat the CRISPR knockdown lines for 24 hr (**Figure 4.20**). Following CRISPR inactivation of *NF1*, pERK signalling was rescued in the presence of cetuximab, thus confirming our siRNA data.

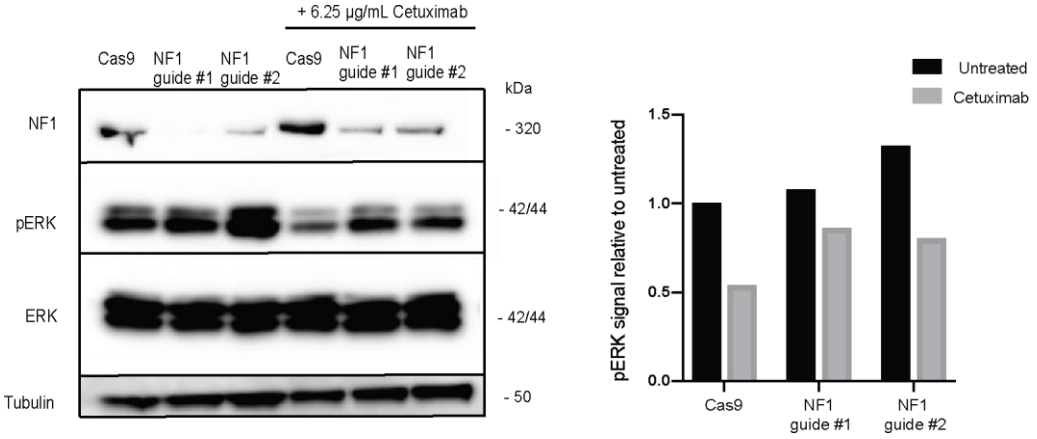

Figure 4.20 CRISPR-mediated inactivation of NF1 results in pERK signalling rescue.

Western blot analysis of CRISPR-mediated NF1 knockout in cells treated with 6.25 µg/mL cetuximab for 24 hr. Tubulin was used as a loading control. Quantification of blots was performed using ImageJ. Signal density was normalised to total ERK signal.

Importantly, CRISPR inactivation resulted in highly significant rescue of growth in a 5-day drug sensitivity assay in both *NF1* inactivated LIM-Cas9 cell lines ($p=0.0023$ and $p=0.4x10^{-8}$ respectively) compared to the unmodified LIM-Cas9 cell line (**Figure 4.21**). This supports my hypothesis that siRNA mediated knockdown of *NF1* was not maintained throughout the length of the drug sensitivity assay. Furthermore, the drug sensitivity assay shows that this increased cell growth in the presence of cetuximab is maintained even at high doses of drug, disproving my original hypothesis that the phenotype mediated by loss of *NF1* may be overcome by high level cetuximab inhibition. Even at the highest dose tested (200 µg/mL) the *NF1* guide #1 and guide #2 knockdown lines had a 2.7-fold and 3.9 fold increase in growth relative to LIM-Cas9 respectively. I also performed a clonogenic assay to confirm that cell growth could be maintained at high doses for an extended period of time (8 days). Once again, it was evident that loss of *NF1* results in significant growth rescue in comparison to untreated LIM-Cas9 cells.

These data provide the first indication, supported by functional data, of *NF1* as a novel driver of primary resistance to the anti-EGFR antibody cetuximab in the context of metastatic colorectal cancer.

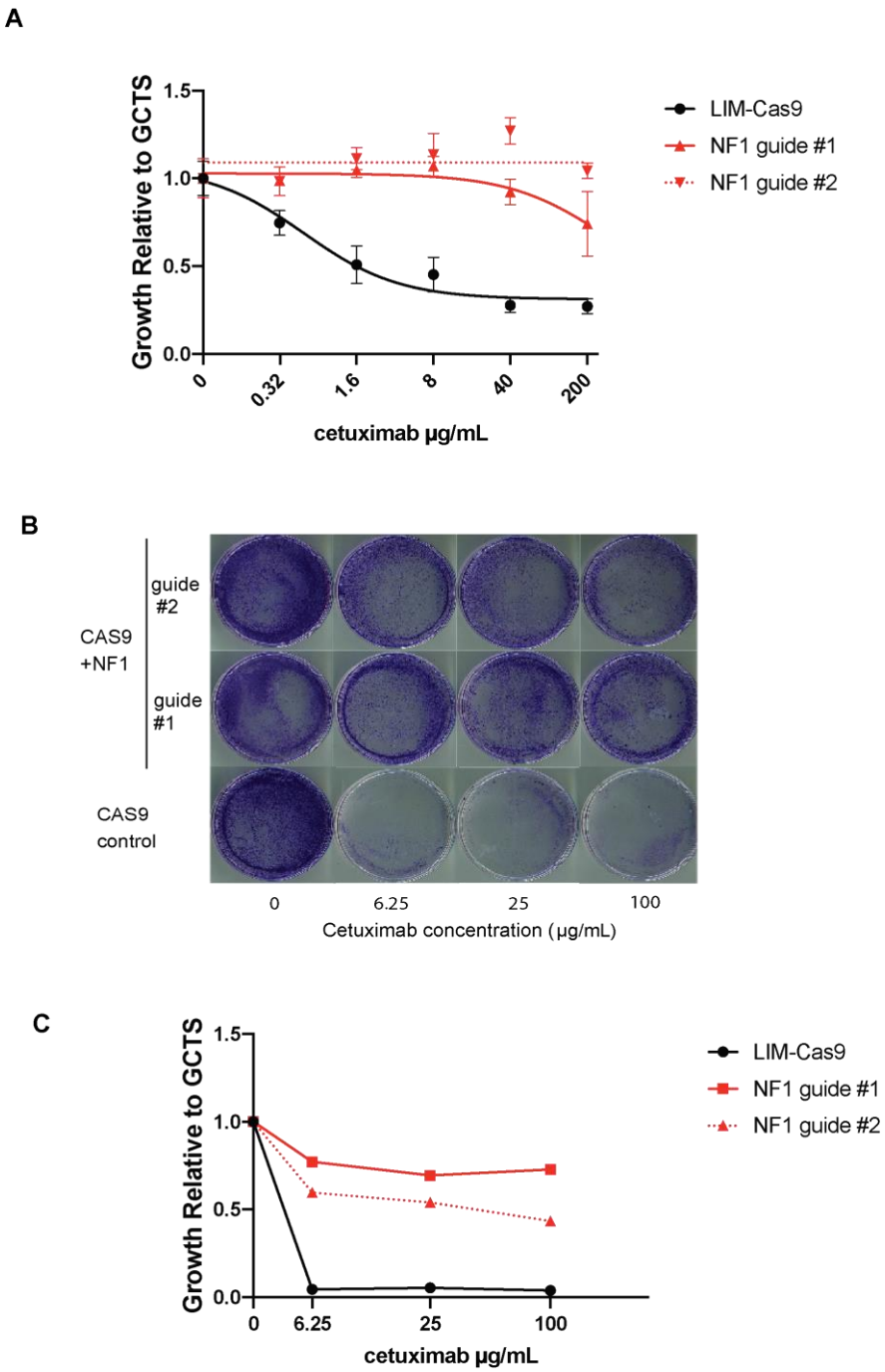

Figure 4.21 CRISPR-mediated inactivation of *NF1* results in growth rescue in an 8 day clonogenic growth assay.

(A) Growth analysis of *NF1* knockout LIM1215 cell lines treated with cetuximab (0.32-200 µg/mL) for 5 days. Cell viability was assessed by Cell-Titre blue (CTB). Background determined by CTB at Day 0 of treatment was subtracted from the raw values and data were then normalised such that 1.0 indicates growth in the presence of GCTS and 0 indicates no growth from seeding density. One representative repeat is shown. Error bars represent SD of 6 replicates. (B) Crystal violet staining of *NF1* knockout cell lines treated for 8 days with indicated doses of cetuximab. Treatment was replenished every 2 days. (C) Quantification of crystal violet. Absorbance readings were normalised according to the untreated control in each cell line.

4.9. Discussion

Despite patient stratification to enhance the efficacy of the monoclonal antibody cetuximab, primary resistance is a common occurrence. In this chapter, I have validated the role in MAPK pathway reactivation of novel mutations in *BRAF*, *KRAS* and *NF1* that had been found in a prospective clinical trial to be associated with both primary and acquired cetuximab resistance.

EGFR D278N and G322S were investigated as potential drivers of acquired resistance. As both mutations are found close to each other, I was interested to see if either led to a new mechanism of EGFR signalling activation. However, validation experiments did not reveal any increase in pERK signalling or growth potential thus both were eventually classified as likely passenger mutations. EGFR G322S had been acquired in the progression biopsy from case C1005PD. However, this same biopsy also had acquired a clonal KRAS G12C mutation. In the presence of this canonical oncogenic KRAS mutation with strong evidence for its role in cetuximab resistance, it is logical that the addition of a mutation that locates further upstream, within EGFR, confers no additional benefit for the tumour.

Kinase impaired or kinase dead-variants of BRAF have been shown to paradoxically increase ERK signalling, and collectively are referred to as inactivating BRAF mutations (Yao et al., 2017). D594H mutations, previously described by Wan *et al* and thus used as a control for kinase-dead variants in our analyses, did show increased ERK signalling in the presence of cetuximab. Our two novel variants D594F and D594N only showed moderately increased pERK signalling. D594F was a mutation found in a pre-treatment biopsy in our cohort, and thus our data showing moderate pERK reactivation in the presence of cetuximab suggests a mechanistic role in resistance. Upregulation of pERK signalling in kinase-impaired BRAF mutant cell lines is still dependent on sufficient upstream RAS signalling (Yao et al., 2017). Therefore it could be suggested that in our mutant cell lines, there is insufficient upstream RAS

signalling in the presence of cetuximab to induce a rescued ERK signalling phenotype.

However it is critical to note that BRAF D594F was present concurrently with a KRAS L19F mutation in the tumour. Thus, it is likely that the combination of the two mutations contributes to cetuximab resistance. In fact, inactivating BRAF mutations are often found to co-exist with RAS mutations or NF1 inactivation (Heidorn et al., 2010; Kordes et al., 2015; Yao et al., 2017). KRAS L19F mutation induced moderate pERK signalling. Further modelling of the BRAF D594F and KRAS L19F mutations in combination is therefore required to reveal if both mutations are necessary for a driver phenotypic effect.

BRAF D594N was only detected by ctDNA analysis. It increased 5.5 fold as a percentage of tumour cells between baseline and progression biopsies thus suggesting that it is an advantageous mutation for survival in the presence of cetuximab. Our data suggests that it may contribute to an overall resistance phenotype as elevated pERK signalling was observed in the presence of cetuximab. Furthermore the strong pERK reactivation observed with KRAS A18D mutation convincingly suggests that KRAS A18D is driver of primary cetuximab resistance.

Thus, I have validated that non-canonical BRAF and KRAS mutations found in the clinical setting are able to reactivate MAPK pathway signalling in the presence of cetuximab. However these mutations are rare in large CRC cohorts: all are present at <1% (Giannakis et al., 2016; TCGA, 2012). Furthermore whilst they are all non-canonical mutations they nonetheless are mutations in well-characterised anti-EGFR-therapy resistance-causing genes. Thus I decided to not further pursue these mutations as putative novel biomarkers. Growth assays are required to confirm if the pERK signal reactivation observed here correlates with an increased growth potential. In particular, combinatorial studies of BRAF D594F and KRAS L19F may provide interesting insights into the combinatorial role of MAPK pathway mutations in CRC. Whilst further validation is required to

confirm if these non-canonical mutations can be classed as drivers of resistance, their existence in the PROSPECT-C trial combined with the observed MAPK reactivation contributes to increasing evidence that the MAPK pathway is repeatedly involved in treatment failure to cetuximab. Thus following successful validation, inclusion in future molecular testing that more broadly encompasses primary RTK and MAPK pathway aberrations for anti-EGFR-therapy may be beneficial.

My results validated genetic *NF1* inactivation as a driver of resistance to cetuximab in mCRC, which occurs through strong pERK reactivation. This is exemplified by sustained proliferative capacity in the presence of drug. It is interesting that *NF1* inactivation by CRISPR induced significant growth rescue in the presence of cetuximab, yet no proliferative advantage was observed with siRNA-mediated knockdown. This may be due to the fact that knockdown of *NF1* was incomplete with siRNA, and also transient. This suggests that complete loss of *NF1* activity may be required to fully reactivate and maintain ERK signalling under EGFR inhibition.

NF1 mutations are found in ~5% of metastatic CRCs (Giannakis et al., 2016; Seshagiri et al., 2012; TCGA, 2012) and loss of heterozygosity is reported in 14-57% (Ahlquist et al., 2008; Cawkwell et al., 1994; Philpott et al., 2017). The prevalence of mutations in mCRC in combination with the data presented here, justifies *NF1* as a candidate for further validation as a predictive marker in clinical trials. This is further supported by the reported association of *NF1* mutations with poor progression free survival in colorectal cancer patients treated with cetuximab in combination with chemotherapy, although there was no testing for loss of heterozygosity in this study and 3/4 mutations were missense (Mei et al., 2018). In lung cancer, melanoma and colorectal cancer, *NF1* loss of function mutations are mutually exclusive to *KRAS* mutations thus establishing a molecular subgroup independent of *KRAS*-mutant patients that would not benefit from cetuximab (Post et al., 2019). Additionally it has been observed that *NF1* mutant cancers are amenable to combination MAPK

pathway targeting, unlike *KRAS*-mutant CRCs. This adds an additional need to stratify patients for loss-of-function *NF1* as not only have I shown that they will not respond to cetuximab therapy, but there is potential for alternative novel therapeutic strategies to which they may respond (Post et al., 2019). A role of *NF1* in EGFR-inhibitor resistance has previously been found in lung cancers (de Bruin et al., 2014) where reduced *NF1* expression conferred resistance to the small molecule EGFR inhibitor, erlotinib. I have therefore demonstrated a similar mechanism of resistance is present in CRCs using both reduced *NF1* expression by siRNA and genetic inactivation by CRISPR. Furthermore, whilst *NF1* mutations have been reported previously in CRC, the effect on cetuximab response had not been validated prior to the work in this thesis (Post et al., 2019).

Whilst my data strongly supports the identification of a novel subgroup of patients that are resistant to cetuximab there are clinical challenges in implementing stratification based on this. Firstly, we have shown loss of *NF1* as a result of CRISPR inactivation to model the mutations and concomitant LOH that was observed in patients, however identification of LOH or low copy number of the *NF1* gene is technically difficult to detect clinically. Secondly, data is currently lacking for individual mutations in the *NF1* gene that induce resistance. NF1 mutations are inactivating, often frameshifts, and can be found largely throughout the gene as opposed to occurring in mutational hotspots and thus screening approaches as are employed for *KRAS* and *NRAS* would not be yet be suitable. Nevertheless there is a need to validate *NF1* as either a prognostic or predictive biomarker for cetuximab resistance in randomised clinical trials.

Chapter 5: Investigating transcriptomic changes as drivers of cetuximab acquired resistance in colorectal cancer

5.1. Introduction

My host lab had shown by exome and deep sequencing that no genetic mechanisms of cetuximab resistance could be identified in 9 out of 14 progression biopsies (64%) from RAS wildtype CRCs that had first achieved clinical benefit from cetuximab and then progressed (Woolston et al., 2019). We hence hypothesized that non-genetic mechanisms of resistance may play a role in acquired cetuximab resistance. The lab had furthermore validated the colorectal cancer consensus molecular subtypes (CMS) (Guinney et al., 2015) as transcriptomic predictors of primary cetuximab sensitivity or resistance (**Figure 5.1** A). The CMS2 subtype was 3.4-fold enriched (p=0.017) in tumours from patients that achieved prolonged cetuximab benefit compared to the remaining subtypes (CMS1, CMS3, CMS4) that predominantly associated with primary resistance. An 84% correlation was observed between both the CMS subtypes and a preceding classification systems, CRCassigner (Sadanandam et al., 2013), confirming robustness of subtype assignments. As parallels are often seen between the mechanisms for primary and acquired resistance, we hypothesised that CMS subtypes may play a role in acquired resistance. We found that transcriptomic analysis of paired pre-treatment and post-progression biopsies from 7 tumours in which no genetic mechanisms of cetuximab resistance could be identified at the time of progression indeed showed that 5 of these (71%) had switched from the CMS2 subtype to the CMS4 subtype. In contrast CMS2 to CMS4 (CMS2>CMS4) switches were not observed in paired pre-treatment and post-progression biopsies from patients with primary progression. The CMS4 subtype is characterised by enrichment in high level EMT and TGFβ signalling gene signatures. Expression of TGFβ1 and TGFβ2 were significantly increased (3.1-fold, p=0.038 and 2.9-fold, p=0.028 respectively) in the progression

samples of patients that had undergone the CMS2>4 subtype switch (**Figure 5.1** B). Furthermore TGFβ and EMT signalling signatures were significantly increased in progression biopsies (p=0.004 and P=0.01 respectively) (**Figure 5.1** C). TGFβ is a master regulator of CMS4, a subtype which been shown to be fibroblast rich (Guinney et al., 2015) and the increase in TGFβ signalling was accompanied by an increase in fibroblast abundance at progression (p=0.01) (**Figure 5.1** D). Normal fibroblasts are not activated unless they are involved in wound healing (Attieh and Vignjevic, 2016). CAFs are activated fibroblasts that are found in the tumour microenvironment (Kalluri and Zeisberg, 2006). They become activated through interactions with the tumour cells and promote invasion and metastases of cancers. Consequently, it was hypothesised that a CAF-rich environment may contribute to the transcriptomic switch and thus provided the rationale for investigating if CAFs induce cetuximab resistance.

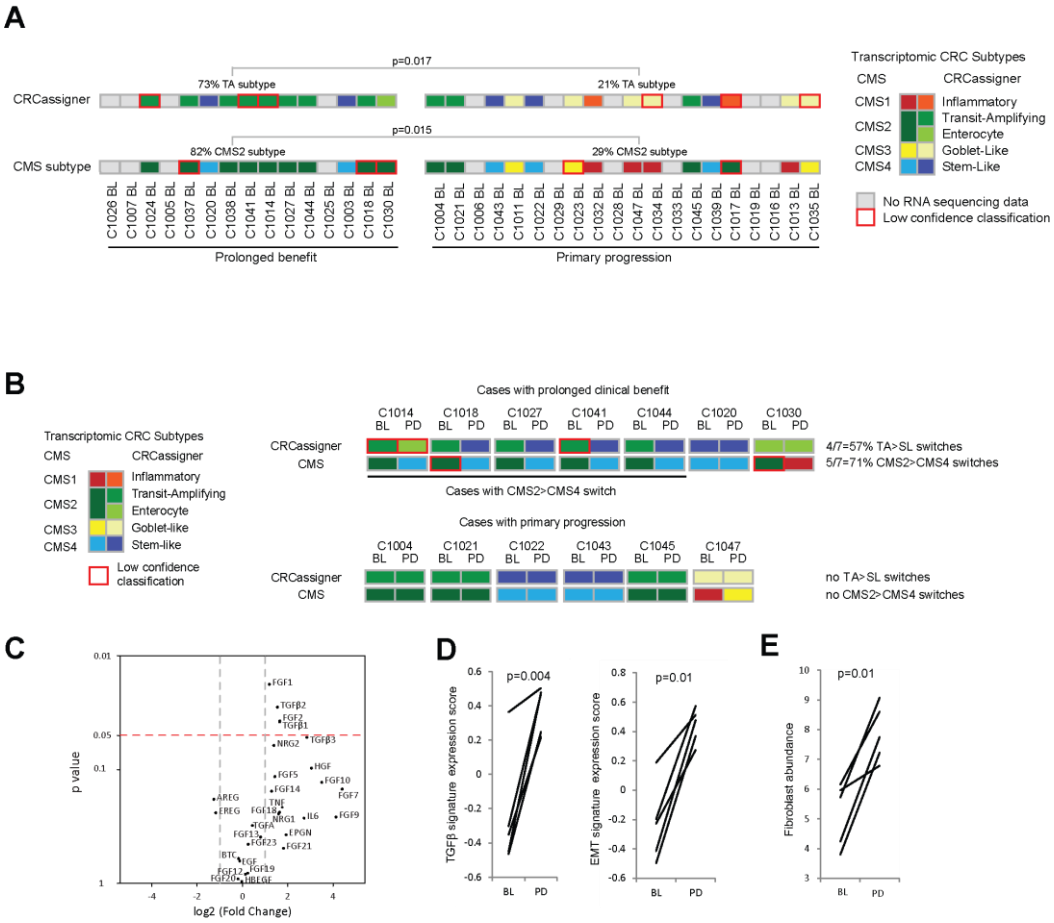

Figure 5.1 CMS2>CMS4 subtype switched observed in PROSPECT-C cohort.

(A) Transcriptomic subtype assignment of pre-treatment biopsies categorized into cases with prolonged clinical benefit and primary progression. The figure legend for the transcriptomic subtypes is arranged to show the most similar CMS and CRCassigner subtypes next to each other. Significance was assessed by the Fisher's exact test. (B) Transcriptomic subtypes in 13 BL and PD biopsy pairs. TA, transit amplifying; SL, stem-like. (C) Volcano plot showing differential expression of growth factors in 5 cases from (A) undergoing CMS2>4 switches. Significance was assessed by paired t test. (D) Changes in TGFβ and EMT transcriptomic signatures through CMS2>4 switches. (E) Changes in fibroblast abundance through CMS2>4 switches based on MCP-counter analysis. Dr Woolston performed all bioinformatics analysis. BL= baseline, PD= Progressive disease.

5.2. CAF-conditioned medium rescues cetuximab induced growth suppression

Immortalised human fibroblasts from a rectal carcinoma, herein referred to as CAFs, were received as a gift from Fernando Calvo (ICR, London) (initially provided by Danijela Vignjevic, Institut Curie, Paris). Cetuximab sensitive colorectal cancer cell lines were treated with cetuximab with and without addition of conditioned medium from these CAFs (CAF CM). Conditioned medium alone induced a moderate increase in proliferation in these cell lines (1.3-fold increase, p=0.0009) (**Figure 5.2** A). Treatment with conditioned medium in addition to cetuximab induced a significant, strong growth rescue phenotype, a 4.12-fold and 3.33-fold increase in growth in DiFi and LIM respectively ($p<0.01$), thus supporting the role of CAFs in cetuximab resistance (**Figure 5.2** B). To assess whether the CAF conditioned medium was inducing cetuximab resistance through the MAPK pathway, pERK signalling was investigated by western blotting. Consistent with the strong growth response observed, pERK signalling was clearly rescued to the same level as in the absence cetuximab (**Figure 5.2** C). It can therefore be concluded that CAFs are capable of reversing the growth inhibitory effects and MAPK pathway suppression of cetuximab.

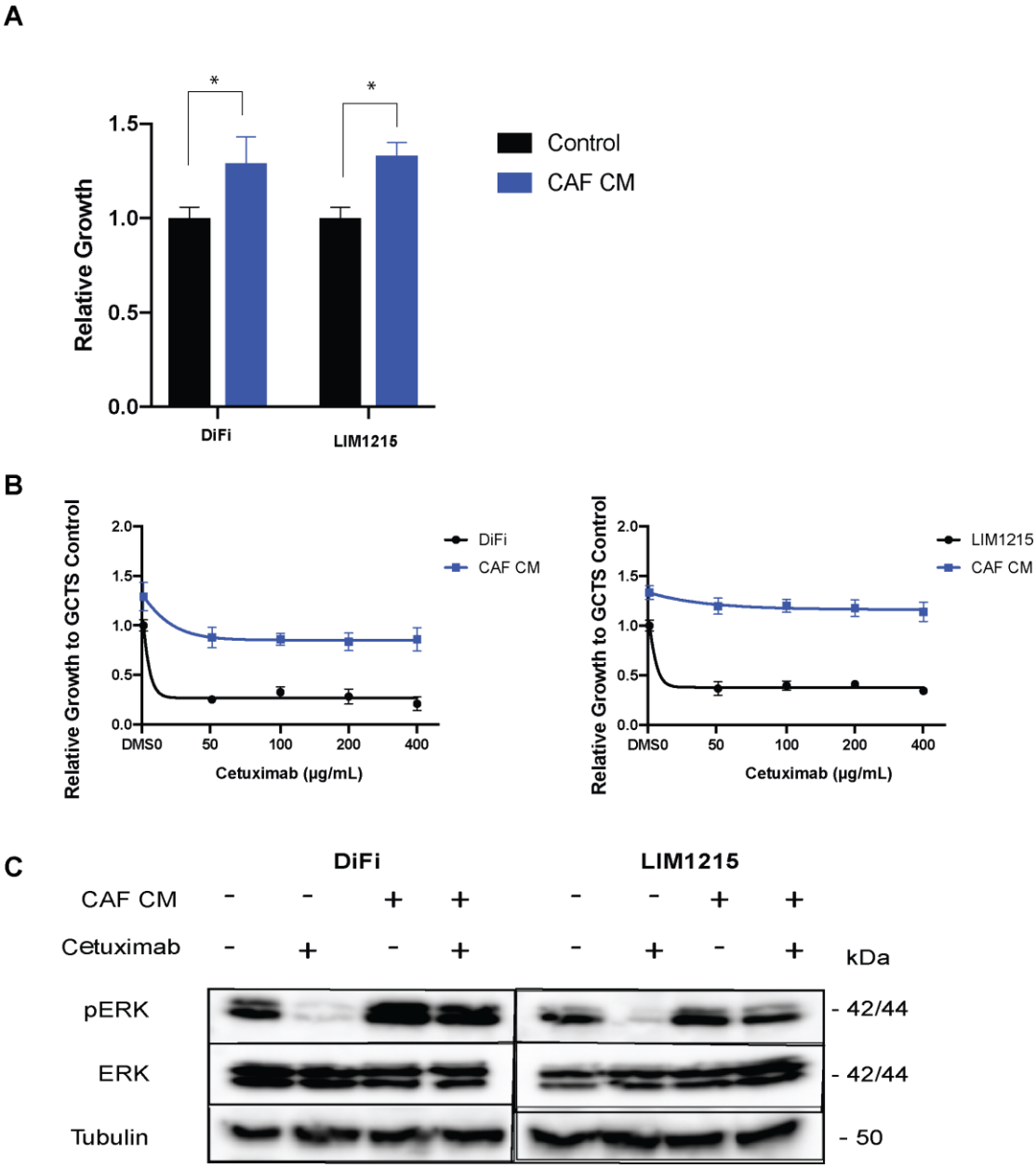

Figure 5.2 CAF conditioned medium rescues growth in cetuximab sensitive cell lines.

(A) Impact of CAF conditioned medium (CM) on the growth of DiFi and LIM1215 in the absence of cetuximab treatment. (B) Impact of cetuximab conditioned medium on the growth of cell lines treated with a range of cetuximab concentrations or vehicle (GCTS) for 5 days. (F) Western blot analysis of pERK expression in CRC cell lines treated with 200 µg/mL cetuximab for 2 h. Tubulin was used as a loading control. All experiments shown are one representative repeat and error bars represent SD of 6 technical replicates. Significance was assessed by student's t-test. *=p<0.05.

5.3. Co-culturing CAFs and CRC cell lines confirms cetuximab resistance

I next wished to investigate whether crosstalk between cancer cells and CAFS that may occur during co-culturing would enhance this phenotype. First I modelled co-culturing in CAFs and CRC cell lines *in vitro*. Two ratios of cell densities were investigated; 2:1 and 5:1 CAF: CRC respectively. CRC cell lines were stably transduced with a GFP construct driving nuclear expression to enable growth monitoring by an ImageXpress confocal microscopy imaging system. CAFs showed a high level of auto-fluorescence in the GFP channel. Due to the size difference between the CAFs and CRC cell lines, stringent filtering to exclude CAFS on the basis of cell diameter and area was built into the image analysis to eliminate CAFs from the cell count readout (**Figure 5.3** A-C). Co-culture of CAFS and CRC cell lines *in vitro* again led to an increase in proliferation of CRC cell lines (**Figure 5.3** D). The greater fold increase (average fold change = 3.17) in growth observed in the direct co-culture compared to conditioned medium, potentially suggests that there is cross talk between the two different cell types and that this induces a stronger growth response than just the presence of the secreted factors. Additionally elevated proliferation may be the consequence of either the high CAF to cancer cell ratios or non-secreted factors such as cell-cell contact. The 2:1 CAF to tumour cell ratio induced greater proliferation than the 5:1 ratio, however this result is most likely confounded by the fact the CAFs are too confluent in the 5:1 ratio and thus there isn't sufficient room for growth for the CRC cell lines. In the presence of cetuximab the normalised growth rescue increases proportionally with an increased ratio of CAFS (**Figure 5.3** E). As it would be expected that the more CAFs are present in the well, the higher the concentration of the growth factors, the data suggests a growth factor concentration-dependent rescue response. From this co-culture experiment I confirmed the CAF conditioned medium data.

In both co-culture and conditioned medium experiments cell growth was restored to similar levels as untreated cells. Growth of untreated cell lines in co-culture with CAFS is at least 2.3 fold greater than normal cancer cell growth, and as treatment with cetuximab is capable of maintaining cell growth relative to untreated controls in co-culture with CAFS we can conclude that CAFS are able to induce an increased proliferative effect even in the presence of cetuximab.

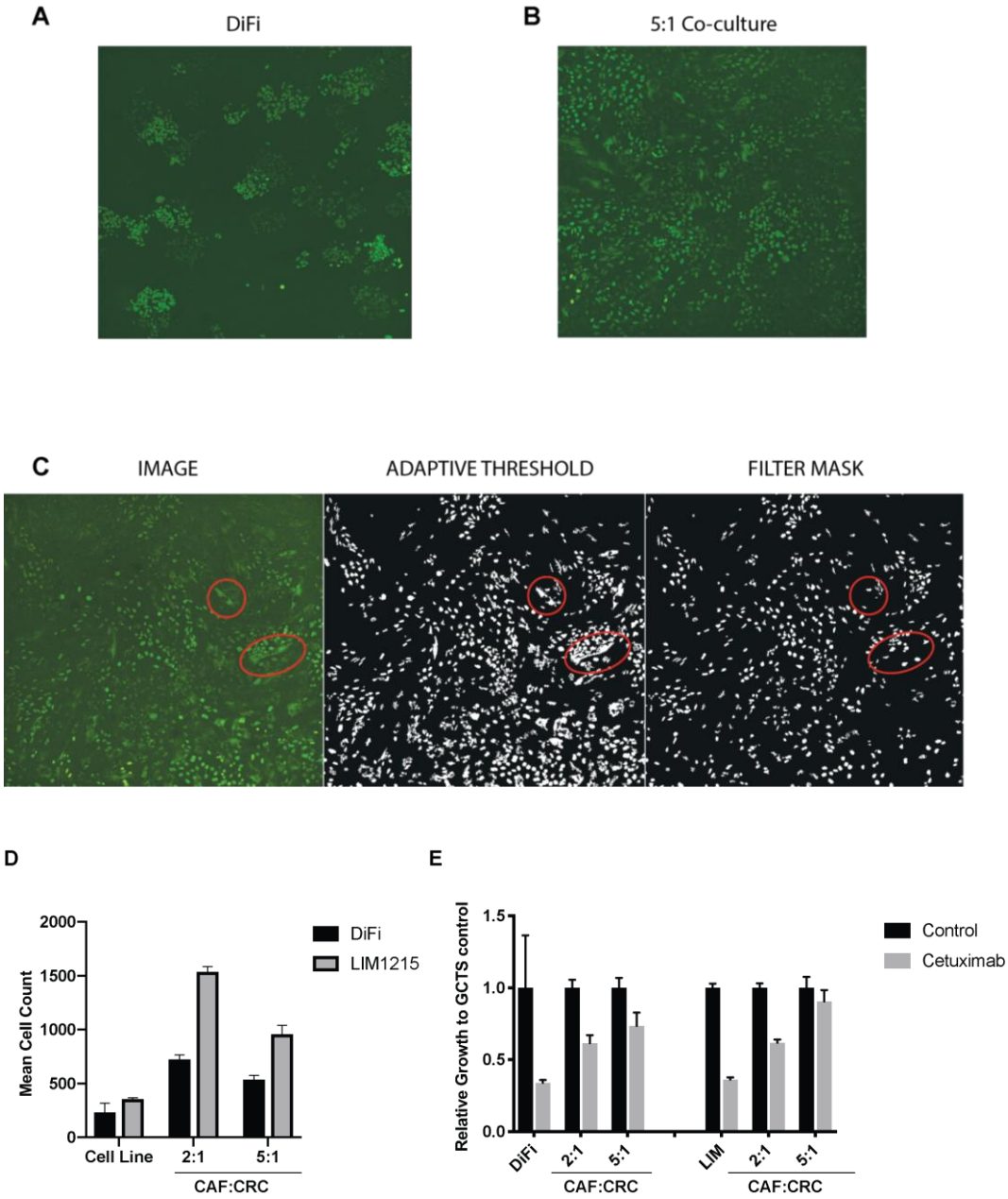

Figure 5.3 Co-culturing of CAFs and CRC cell lines induces growth rescue during cetuximab treatment.

(A) Representative image of DiFi cells plated without CAFs after 5 days growth. (B) Representative image of co-culture in 5:1 ratio of CAF and DiFi cells. (C) Representative images to show the application of the filters to remove fibroblast from cell counts. 5:1 DiFi and CAF co-culture with some examples of autofluroescent CAFS highlighted in red circles (right panel), cells counted after adaptive threshold filtering to select based on size (middle panel), cells counted after filtering mask applied (left panel). (D) Mean cell counts of GFP tagged DiFi and LIM1215 in a 2:1 and 5:1 CAF:CRC ratio. (E) Mean cell counts of CAF:CRC co-culture in DiFi and LIM1215 treated with 200 µg/mL cetuximab for 5 days. Mean cell counts for (D) and (E) were generated by imaging with ImageXpress and analysed with MetaXpress software. One representative repeats is shown and error bars represent SD of triplicate wells. Data were normalised to mean growth in untreated conditions.

5.4. Investigating the secretome of CAFs

As I now had shown evidence that the presence of CAFs or the growth factors that they produce in conditioned medium can rescue CRC cell lines from cetuximab-induced growth suppression, we next wished to identify the growth factors that could be driving this phenotype. Thus we interrogated the secretome of CAFs through cytokine arrays and RNA sequencing.

5.4.1. Growth factors present in CAF conditioned medium

Conditioned medium contains a cocktail of different growth factors, metabolites and extracellular matrix proteins, the exact composition of which is unknown. As it was known that expression of TGFβ1 and TGFβ2 were significantly increased in CMS4 subtype samples, we wanted to determine if this was a key growth factor being secreted by the CAFS, as well as elucidating the secreted profile of the conditioned medium. A semi-quantitative antibody cytokine array to detect 80 human cytokines was used as it tests a wide range of factors simultaneously (**Figure 5.4** A). Cytokine arrays showed that the concentration of 15 growth factors and cytokines was at least 3-fold higher in CAF conditioned medium than in the non-conditioned CAF growth medium (**Figure 5.4** B and C). With a 426-fold increase in signal, IL-6 was most strongly upregulated (**Figure 5.4** D). HGF, IL-6, IL-8 and GRO-alpha, previously identified CAF produced cytokines (Luraghi et al., 2014), were all expressed highly. Interestingly, TGFβ1 and TGFβ2, both of which were present in the array, were not > 3 fold upregulated. Given that TGFβ was not identified in this array, yet was significantly upregulated in CMS2>4 patients and has previously been shown to be made by CAFS I theorised that the concentration of some growth factors may be too low to be detected in this cytokine array.

A

	A	B	C	D	E	F	G	H	I	J	K
1	POS	POS	POS	POS	NEG	NEG	ENA-78 (CXCL5)	G-CSF	GM-CSF	GRO a/b/g	GRO alpha (CXCL1)
2	I-309 (CCL1)	IL-1 alpha (IL-1 F1)	IL-1 beta (IL-1 F2)	IL-2	IL-3	IL-4	IL-5	IL-6	IL-7	IL-8 (CXCL8)	IL-10
3	IL-12 p40/p70	IL-13	IL-15	IFN-gamma	MCP-1 (CCL2)	MCP-2 (CCL8)	MCP-3 (CCL7)	M-CSF	MDC (CCL22)	MIG (CXCL9)	MIP-1 beta (CCL4)
4	MIP-1 delta	RANTES (CCL5)	SCF	SDF-1 alpha	TARC (CCL17)	TGF beta 1	TNF alpha	TNF beta (TNFSF1B)	EGF	IGF-1	Angiogenin
5	OSM	TPO	VEGF-A	PDGF-BB	Leptin	BDNF	BLC (CXCL13)	Ck beta 8-1 (CCL23)	Eotaxin-1 (CCL11)	Eotaxin-2 (CCL24)	Eotaxin-3 (CCL26)
6	FGF-4	FGF-6	FGF-7 (KGF)	FGF-9	FLT-3 Ligand	Fractalkine (CX3CL1)	GCP-2 (CXCL6)	GDNF	HGF	IGFBP-1	IGFBP-2
7	IGFBP-3	IGFBP-4	IL-16	IP-10 (CXCL10)	LIF	LIGHT (TNFSF14)	MCP-4 (CCL13)	MIF	MIP-3 alpha	NAP-2 (CXCL7)	NT-3
8	NT-4	OPN (SPP1)	OPG (TNFRSF11	PARC	PLGF	TGF beta 2	TGF beta 3	TIMP-1	TIMP-2	POS	POS

B

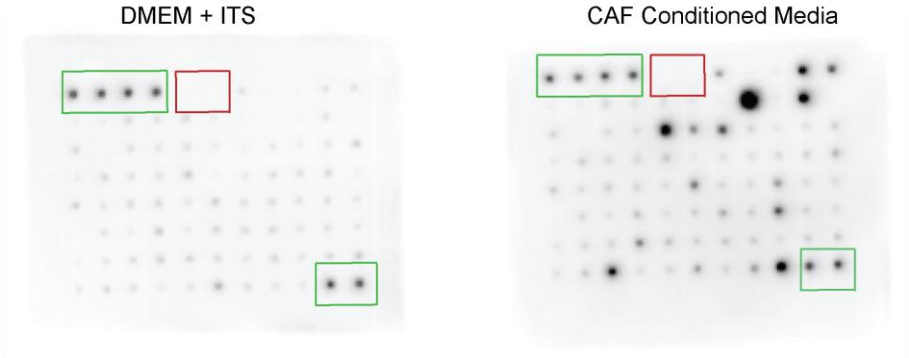

C

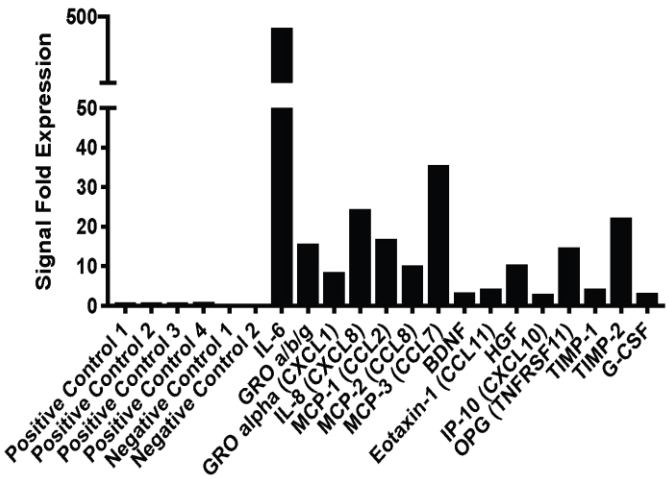

Cytokine	Fold Change
IL-6	426.7
GRO a/b/g	15.8
GRO alpha (CXCL1)	8.5
IL-8 (CXCL8)	24.5
MCP-1 (CCL2)	17.0
MCP-2 (CCL8)	10.3
MCP-3 (CCL7)	35.6
BDNF	3.5
Eotaxin-1 (CCL11)	4.4
HGF	10.6
IP-10 (CXCL10)	3.1
OPG (TNFRSF11)	14.8
TIMP-1	4.4
TIMP-2	22.3
G-CSF	3.3

Figure 5.4 Cytokines present in CAF conditioned medium.

(A) Map from RayBioTech of the cytokines present in the array. (B) Cytokine array incubated with CAF culture medium, 10% FCS DMEM medium containing ITS (left) and 72 hr CAF conditioned medium (right). (C) Quantification of cytokine array. Spots were quantified by measuring density using ImageJ. Data were normalised according to the RayBioTech protocol. Growth factors that were at least 3 times higher than positive control were graphed. Table details fold change.

5.4.2. Co-culturing CAFS and CRC cell lines does not result in an altered secretome.

I next wished to see if co-culturing the cells would impact the secretome. Thus the cytokine array was repeated to analyse factors present in the medium of the CAF conditioned medium, tumour cell conditioned medium and co-culture of CRC cell line and CAF conditioned medium (**Figure 5.5** A-C). Data from co-culture of both DiFi and LIM1215 cells respectively with CAFs showed little variation in cytokines present versus the CAF conditioned medium alone (**Figure 5.5** D-G). The only upregulated cytokine was RANTES in the LIM1215:CAF co-culture. RANTES is chemotactic cytokine for T cells, eosinophils and basophils. Repeated experiments would be required to confirm if the upregulation of RANTES observed in the medium of LIM1215 cell co-cultured with CAFs is reproducible. This is a semi-quantitative array and thus the results presented here should be interpreted with caution. Too much emphasis should not be placed on the results of the individual arrays, instead trends in increased fold change that can be seen consistently, such as IL-6, should be investigated. However, we can conclude co-culturing of CRC cell lines and CAFs does not appear to induce any notable changes to the secretome. Furthermore this analysis is limited by the pre-determined list of cytokines in the array.

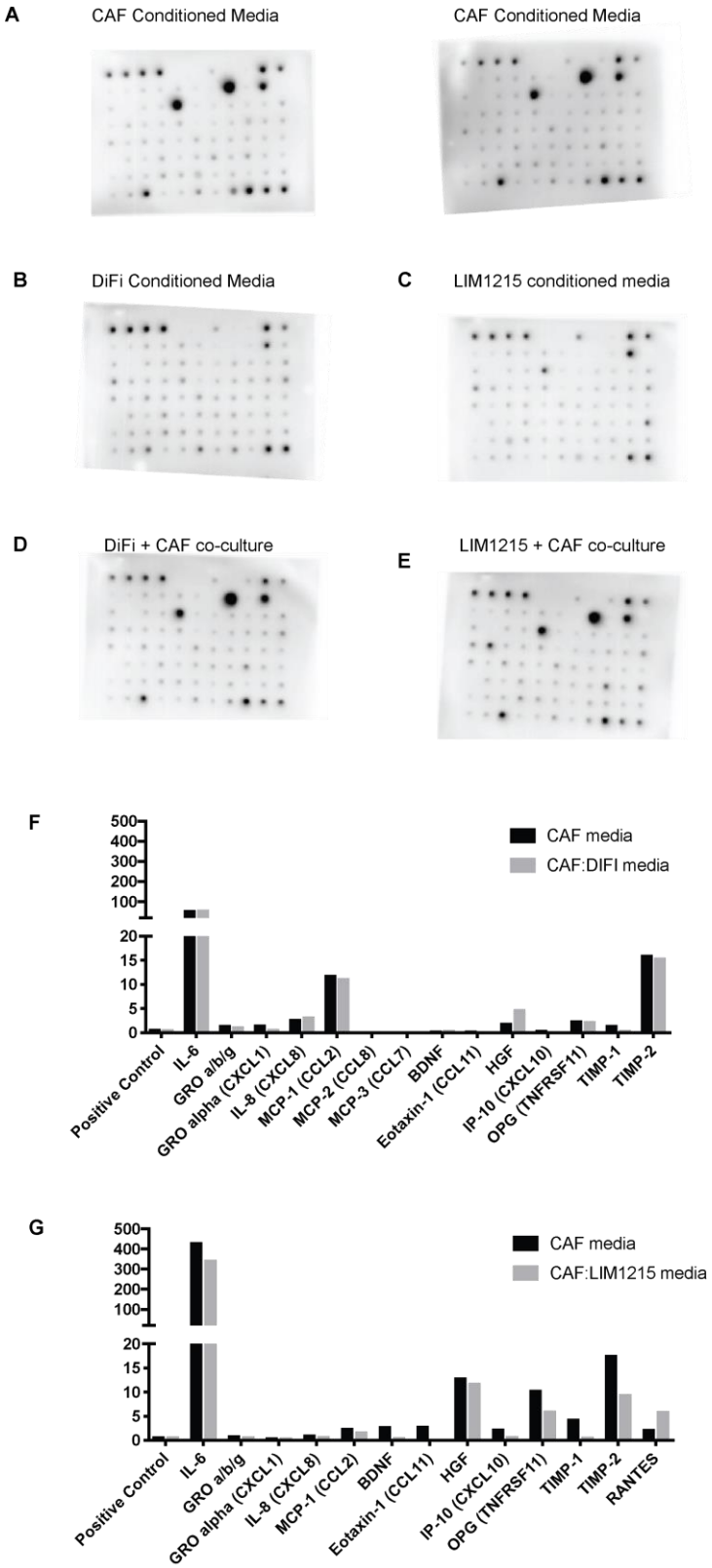

Figure 5.5 Cytokine array of co-culture medium.

(A), (B) and (C) Cytokine arrays of 72 hr conditioned medium from CAF, DiFi and LIM1215 cells respectively. (D) and (E) Cytokine arrays of medium from co-cultures of CAFs with DiFi and LIM1215 respectively. (F) and (G) Quantification of CAF conditioned medium array and DiFi and LIM1215 co-culture arrays respectively. Spots were quantified by measuring density using ImageJ. Data were normalised according to the RayBioTech protocol.

5.5. Expression of growth factors in CAFs

As aforementioned, differential expression analysis of cases that underwent the CMS2>4 switch revealed TGFβ1, TGFβ2, FGF1 and FGF2 as statistically significant upregulated. I have previously shown TGFβ1 and TGFβ2 were not upregulated in the cytokine array. However we could not evaluate the presence of the FGF1 and FGF2, as they were not included in the array. Thus I applied RNA-sequencing to CAFs to assess if any of the growth factors that were significantly upregulated in tumours that underwent a CMS2>CMS4 switch, were expressed in these cells lines (**Figure 5.6**). DiFi and LIM1215 cell lines were also RNA sequenced to determine the expression of the corresponding growth factors receptors. Cytokines that consistently showed increased fold change in conditioned medium in the cytokine array were also investigated; IL-6; a pro-inflammatory cytokine; GRO alpha, a cytokine involved in inflammation and neutrophil recruitment; IL-8, a chemokine and MCP1 or CCL2, also a chemokine. TNFRSF11B, a cytokine receptor in the Tumour Necrosis Factor superfamily and TIMP2, an inhibitor of matrix metalloproteases were excluded from analysis in RNAseq data as despite their inclusion in the pre-determined array, they are not cytokines. Growth factors FGF1, FGF2, TGFβ1 and TGFβ2 that were significantly expressed in CMS2>CMS4 patients were all expressed by CAFs in this RNAseq analysis. For all growth factors analysed there was a trend for higher expression in the CAF line versus the CRC lines. This is important as I am looking to identify growth factors that are secreted by the CAFs, and not by the cancer cell itself. As these are growth factors that are not abundantly expressed in the CRC cell lines, it would suggest that their presence in the CAF medium is consequential in the cetuximab resistance phenotype observed.

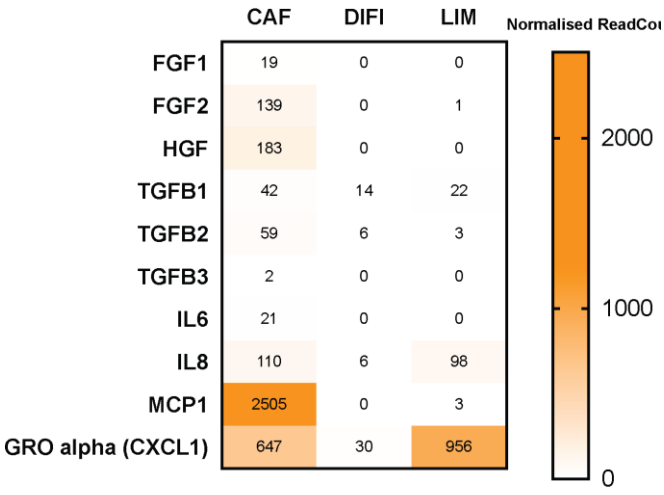

Figure 5.6 Growth factor RNA expression.

Heatmap of normalised RNA expression counts of growth factors in CAF, DiFi and LIM1215 cells. Read counts were normalised according the Lexogen DESeq algorithm.

Next, I assessed the gene expression levels of the corresponding receptors (**Figure 5.7**). MET receptor, for which HGF is the only ligand, was highly expressed by DiFi and LIM1215 cells. FGF receptors (FGFRs) and TGFβ receptors (TGFβR) were also expressed in both CRC cell lines. Therefore as HGF, FGF and TGFβ were all expressed by the CAFs and their concomitant receptors are expressed in the CRC cell lines, this suggests a potential communication pathway resulting in cetuximab resistance. Expression of the receptors for IL-6, IL-8, MCP-1 and GROa were very low, if non-existent, in both CRC cell lines, indicating that these growth factors are not driving the MAPK pathway reactivation and thus the resistance to cetuximab.

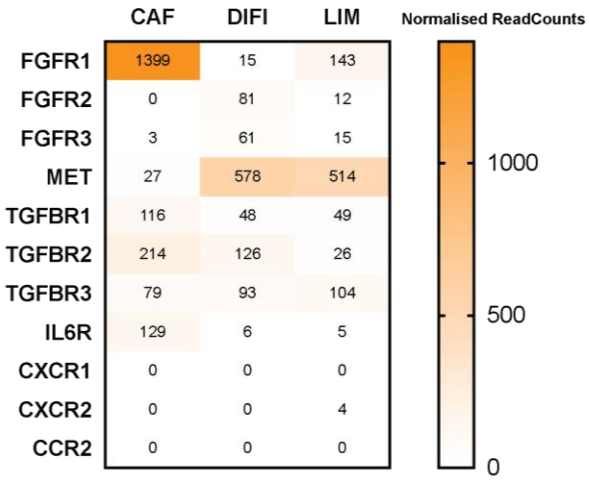

Figure 5.7 Receptor RNA expression.

Heatmap of normalised RNA expression counts of receptors in CAF, DiFi and LIM1215 cells. Read counts were normalised according the Lexogen DESeq algorithm.

Taking into consideration RNA expression of both growth factors and receptors in CAFs and CRC cell lines respectively, I chose key growth factors for functional analysis that indicate a signalling loop between CAFs and CRC cell lines. Growth factor expression must be high exclusively in the CAFs with high expression of the corresponding receptor seen in CRC cell lines. This criterion precludes the inclusion of any growth factors that the CRC cell lines may be producing themselves. Moreover, cytokines with a known association with MAPK signalling were chosen as cetuximab resistance is almost exclusively mediated by MAPK pathway reactivation. Thus due to these criteria, HGF, FGF1 and FGF2 were chosen for further analysis to determine their effect on cetuximab treated CRC cells *in vitro*. However since enrichment in CMS4 patients was observed significantly in TGFβ1 and TGFβ2 these were included also. TGFβ3 was additionally investigated as a control to see if any TGFβ cytokine played a role in resistance. Despite not reaching significance it was also highly upregulated in CMS2>CMS4 patients. Recombinant growth factors were added individually to DiFi and LIM1215 cells and these were treated with cetuximab (**Figure 5.8** A). Treatment with FGF1 (20 ng/mL), FGF2 (20 ng/mL) and HGF (50 ng/mL)

significantly rescued growth during cetuximab treatment in both cell lines ($p<0.0001$). In contrast, neither TGFβ 1,2 and 3 (all 10 ng/mL) were able to rescue growth during cetuximab treatment. Western blot analysis showed sustained ERK phosphorylation despite cetuximab treatment when cells were stimulated with FGF1, FGF2 and HGF (**Figure 5.8** B). Interestingly the level of pERK when stimulated with FGF1 and treated with cetuximab was similar to that of stimulation with either FGF2 or HGF, despite not having as significant an impact on growth as the latter two growth factors in the drug sensitivity assay. A potential explanation for this may be that FGF2 and HGF which bind to FGFR1-4 and MET respectively stimulate additional signalling pathways that allow stronger restoration of growth. These results show that FGF1, 2 and HGF can rescue growth of CRC cell lines during cetuximab treatment *in vitro*. This is likely mediated by the observed re-activation of the MAPK pathway, which is the key mechanism of resistance engaged by all previously described genetic resistance drivers.

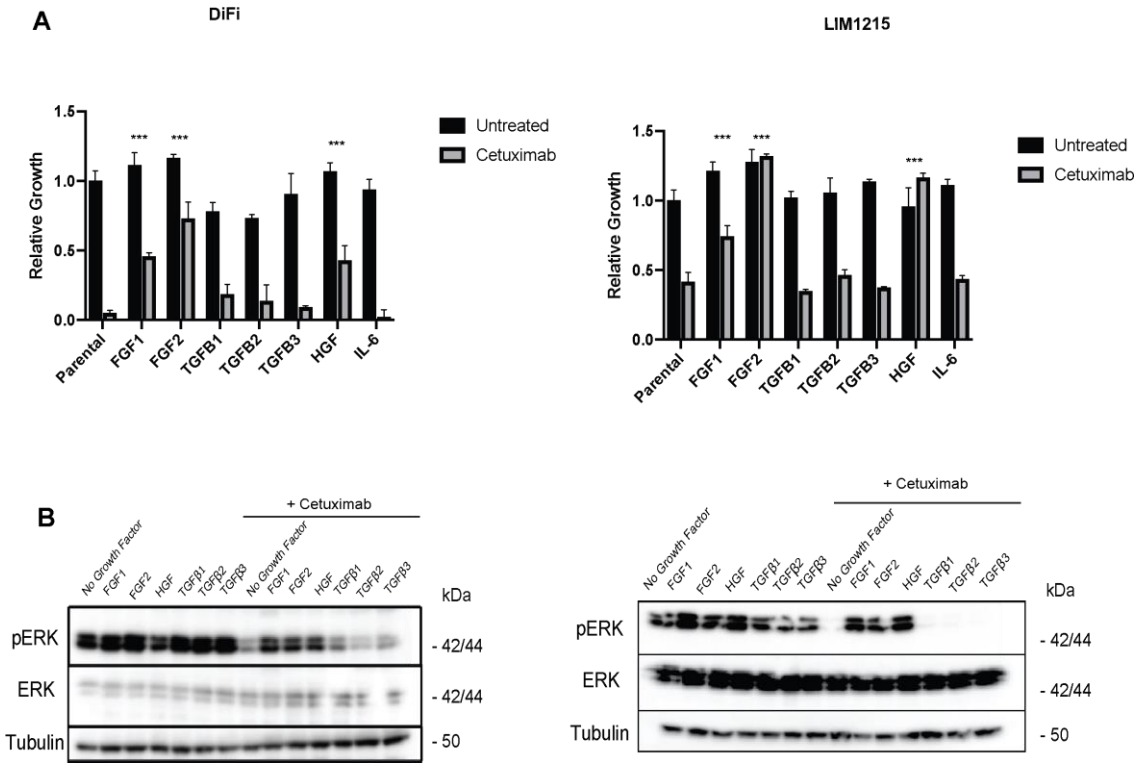

Figure 5.8. FGF1, FGF2 and HGF rescue CRC cell lines from cetuximab-mediated growth inhibition.

(A) and (B) Growth assay with 200 mg/mL cetuximab and recombinant GF at a concentration of 20 ng/mL (FGF1/2), 10 ng/mL (TGFβ 1-3) and 50 ng/mL (HGF) for 5 days in DiFi and LIM1215 cell lines. (C) And (D) Western blots analysis of pERK with and without recombinant GF treatment in the presence or absence of 200 µg/mL cetuximab in DiFi and LIM1215 respectively. Tubulin was used included as a loading control. ***=p<0.001. CAF CM = CAF conditioned medium.

Next we assessed whether inhibitors of pan-FGFR or MET could prevent CAF conditioned medium from inducing cetuximab resistance (**Figure 5.9** A). Treatment with the MET inhibitor (METi) AMG-337 alone had no impact on CRC cell growth in CAF conditioned medium. The MET inhibitor reduced growth rescue during cetuximab exposure, however the observed rescue was still significant ($p=0.0007$ and $p=0.0002$, DiFi and LIM1215 respectively), indicating that MET signalling is involved in driving growth rescue but inhibition of this pathway is not sufficient to abrogate the effects of conditioned medium rescue. Similarly in treatment with the pan-FGFR inhibitor (FGFRi) BGJ-398 the same trend was observed ($p=0.003$ and $p=0.00003$, DiFi and LIM1215 respectively). The combination of METi and FGFRi resulted in the greatest growth suppression in the presence of cetuximab despite CAF conditioned medium. Whilst some growth was still observed, the significance was reduced ($p=0.006$ and $p=0.02$, DiFi and LIM1215). Consistent with the stronger effect of MET inhibition compared to FGFR inhibition, treatment with cetuximab and BGJ-398, the FGFR inhibitor, showed no reduction in ERK phosphorylation whereas cetuximab in combination with the MET inhibitor decreased pERK (**Figure 5.9** B). This suggests that HGF is the more dominant factor in driving resistance mediated by CAF conditioned medium. Strikingly, the combination of METi and FGFRi suppressed pERK almost completely when combined with cetuximab. However the efficacy of one drug versus another within this assay cannot be concluded without taking into consideration the half-life of the drug, which was not tested for here. Overall the results would suggest that both the MET pathway and FGFR signalling pathways would need to be targeted together with cetuximab treatment to fully combat the emergence of CAF-mediated cetuximab resistance.

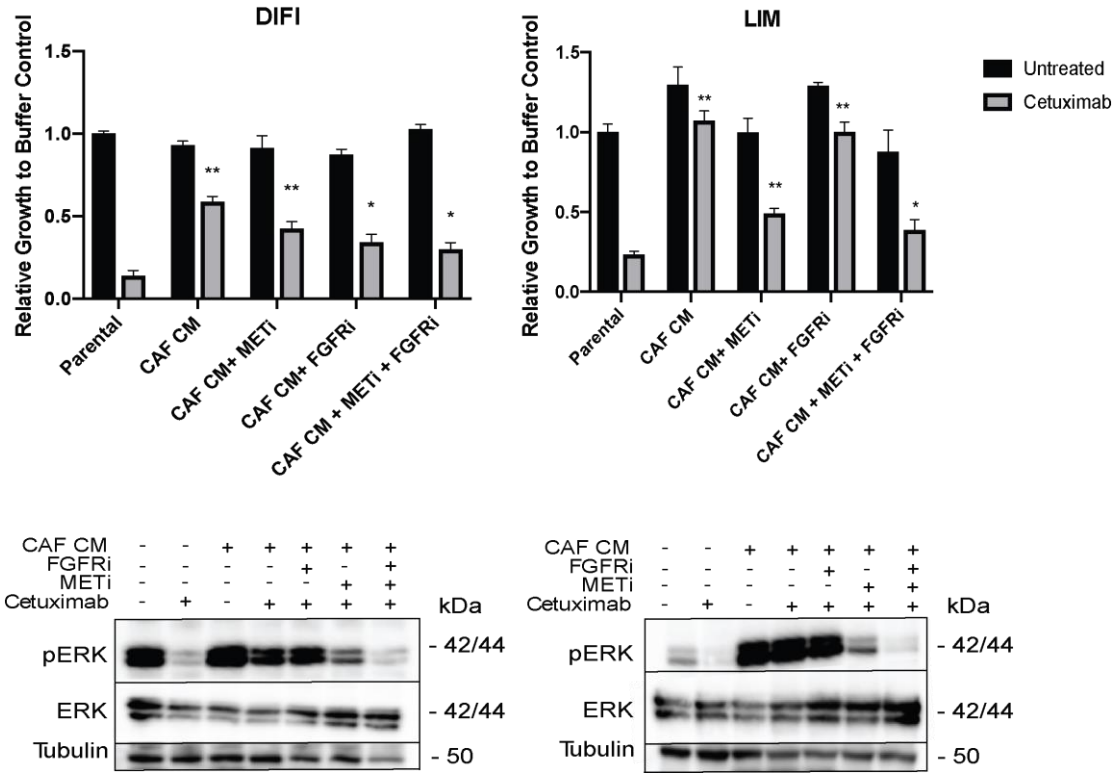

Figure 5.9. Combined MET and FGFR inhibition reverses cetuximab resistance by CAF conditioned medium.

(A) and (B) Growth assay with CAF conditioned medium, 200 mg/mL cetuximab, 100nM MET inhibitor AMG-337 and 1μM FGFR inhibitor BGJ-398) for 5 days in DiFi and LIM1215. (C) and (D) Western blot analysis of pERK with and without MET and FGFR inhibition in the presence or absence of 200 μg/mL cetuximab in DiFi and LIM1215 respectively. Tubulin was used included as a loading control. *=p<0.05, **=p<0.01.

5.6. Effect of cetuximab and conditioned medium treatment on RNA expression in LIM1215 cells.

RNA sequencing was then repeated on LIM1215 and DiFi treated with conditioned medium to confirm HGF and FGF signalling pathway expression. CRC cell lines were treated with 72 hr-conditioned medium for 24 hr before RNA extraction and sequencing. Unfortunately some of the DiFi samples failed quality control and thus could not be further analysed. Expression levels of growth factors and their receptors were examined in LIM1215 under the following conditions; untreated, 24 hr cetuximab treatment, 24 hr conditioned medium treatment and combination conditioned medium and 24 hr cetuximab treatment (**Figure 5.10**). Expression of the MET receptor notably increased in the conditioned medium treated LIM1215 cells. Cetuximab treatment of LIM1215 downregulates MET receptor expression (2.18-fold) and conversely CAF conditioned medium appears to upregulate expression (1.5-fold). Whilst combination of cetuximab and conditioned medium does reduce expression relative to conditioned medium treatment alone, it nevertheless maintains MET expression at the same level as the untreated sample (1.03-fold change). Therefore CAF conditioned medium is capable of reversing downregulation of MET receptor expression even in the presence of cetuximab. As HGF is the only known ligand for the MET receptor, this ratifies our previous finding that HGF/MET signalling induced by CAFs is driving cetuximab resistance. FGF1 and FGF2 are not expressed by LIM1215 cells and expression is not induced by CAF conditioned medium. There is no clear trend for the pattern of expression induced in the family of FGFR receptors by either conditioned medium or cetuximab and expression of all receptors was very low in all conditions analysed. Thus taken together with the previous data, this provides compelling evidence that in my model system HGF and FGF ligands are exclusively produced by CAFs and they signal through their concomitant receptors expressed in the cancer cells to produce the cetuximab resistance phenotype observed.

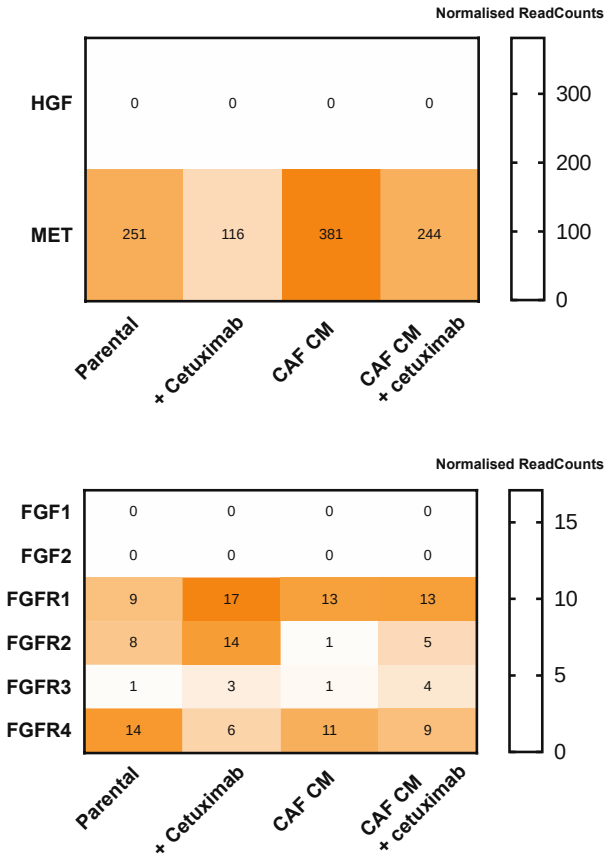

Figure 5.10 RNA expression of HGF and FGF signalling in LIM1215 cells.

Heatmaps of normalised read counts of growth factors and receptors involved in HGF signalling and FGF signalling. Read counts were normalised according the Lexogen DESeq algorithm.

5.7. In vivo modelling of co-cultures of CAFs and CRC cell lines

Finally I aimed to investigate whether CAF-mediated cetuximab resistance could be modelled and confirmed *in vivo* through mouse xenograft models. Firstly DiFi and LIM1215 cells were injected into immune-deficient CD1 (CD-1Foxn1nu) mice, and xenograft tumour growth was monitored to see both how well each line grew *in vivo* and to confirm their response to cetuximab (**Figure 5.11**). Groups of 5 mice were injected subcutaneously with 2x10^6 cells. Cetuximab treatment was started once the mean diameter of the tumours in the group exceeded 5 mm. All mice were treated with 1 mg cetuximab twice weekly by intraperitoneal injection. Body weight measurements confirmed mice were of a

healthy bodyweight throughout the experiment (**Figure 5.11** B). All five DiFi xenografts responded to treatment. Response was most evident in tumours that had consistently grown before treatment initiation. However, even tumours that had only grown for a limited period of time and had then remained static in size responded. Mice were culled once they had received 30 doses of drug. No tumour had acquired resistance at this time-point, confirming the efficacy of cetuximab in DiFi xenograft tumours. The LIM1215 cell line showed poor engraftment and growth in this xenograft model, with only one out of five injected mice developing a tumour. Cetuximab treatment was started after 10.5 weeks in all mice even though the mean tumour diameter in this group had not reached 5mm. In this one tumour that grew well, cetuximab effectively cause tumour shrinkage. Based on these data, the DiFi cell line was selected for further *in vivo* experiments.

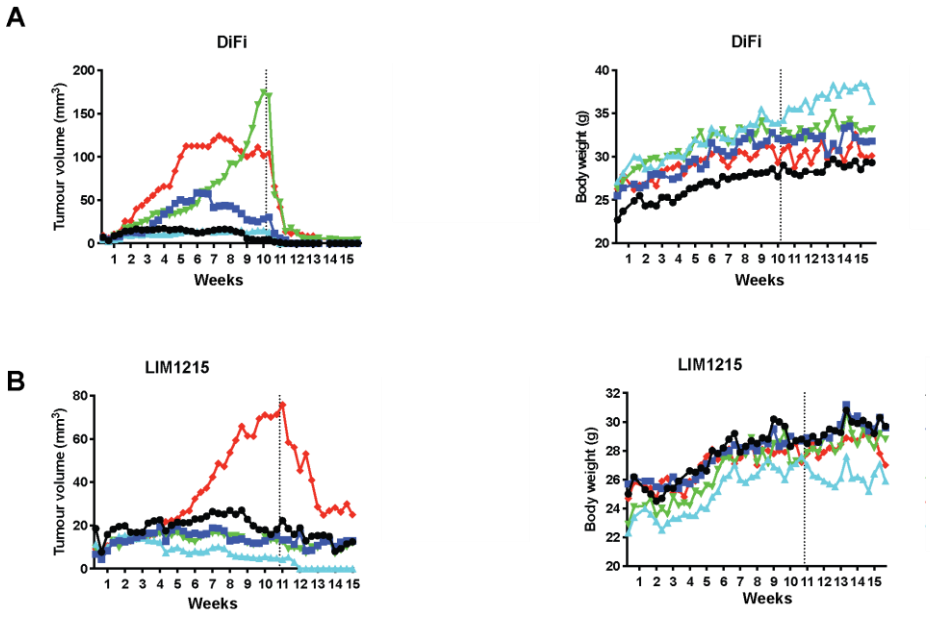

Figure 5.11 CRC cell line xenograft growth.

(A) Tumour volume and body weight of DiFi xenografts in CD1 nude mice. (B) Tumour volume and body weight of LIM1215 xenografts in CD1 nude mice. Tumour volume and body weight measurements were taken twice weekly. Mice were treated with 1 mg cetuximab intravenously twice weekly at least 10 weeks after engraftment (dotted line indicated on the graph).

I next investigated whether co-injection of CAFs with DiFi cells would allow me to model the impact on CAFs on cetuximab responses *in vivo* . The experimental setup should address two questions; whether increased CAF infiltrates could be reliably identified in tumours after engraftment of a mix of DiFi cells with CAFs compared to xenograft grown from DiFi cells alone, and whether tumours established from DiFi cells and CAFs would be more resistant to cetuximab therapy than tumours grown from DiFi cells alone.

For xenografting, DiFi cells and CAFs were mixed in matrigel in a 1:1 ratio or DiFi cells only were mixed into matrigel and injected into CD1 mice. 15 mice per group (DiFi or DiFi + CAFs) were injected subcutaneously at the start of the experiment. Cetuximab treatment was planned to start already at 3 weeks after xenografting, as I wanted to increase the probability that CAFs were still present. Bodyweight measurements were performed to monitor the health of the mice and this showed no decline throughout the experiment (**Figure 5.12** A). Nevertheless, 2 mice injected with DiFi cells had to be culled due to an acute illness. At 3 weeks the 15 mice in the DiFi + CAF group and the remaining 13 mice in the DiFi group were randomised into 3 groups, each; an untreated control group (n=5 for DiFi + CAF, n=4 for DiFi), a cetuximab treated (1 mg intraperitoneally, twice weekly) group (n=5 for each DiFi + CAF and for DiFi) and a group that would be culled at the time the other two groups started cetuximab treatment (n=5 for DiFi + CAF, n=4 for DiFi). One week after randomisation, one further mouse died due to illness unrelated to the xenograft leaving only three mice in the DiFi untreated group for the remainder of the experiment.

Between the untreated DiFi and CAF xenografts, 4/5 tumours grew to large sizes but only 1/3 DiFi xenograft showed similar growth (**Figure 5.12** B). The five DiFi xenografts and the five DiFi and CAF xenografts that were treated with cetuximab all showed similar tumour shrinkage (**Figure 5.11** C). Thus, although the experiment was hampered by the unexpected loss of several mice,

cetuximab treatment was effective *in vivo* in both groups and co-engraftment of CAFs did not lead to resistance. Due to low numbers in the untreated DiFi group, it is difficult make clear conclusions on the impact of CAFs on xenograft growth.

Tumours explanted from mice that had been culled at week 3 were subsequently formalin fixed and embedded in paraffin and stained for alpha smooth muscle actin (α-SMA), a marker that has been widely used for the identification of CAFs (Attieh and Vignjevic, 2016; Shiga et al., 2015). Only three and four of the DiFi and DiFi+CAF xenografts scored contained cancer cells with the remaining showing fibrotic material only. Stained slides were analysed by a senior histopathology speciality registrar in my host lab, Dr Challoner. Intratumoural blood vessels showed perivascular α-SMA staining consistent with the presence of pericytes as previously described for CRCs (**Figure 5.13**). However, no increase in intratumoural CAFs was apparent in the xenografts from the DiFi and CAF group compared to the DiFi group. There was hence no evidence that the CAFs that were injected as a co-culture with DiFi cells were still present in the xenograft excised after 3 weeks of growth and this impairs the ability to interpret the effect of CAFs on cetuximab resistance in this experiment.

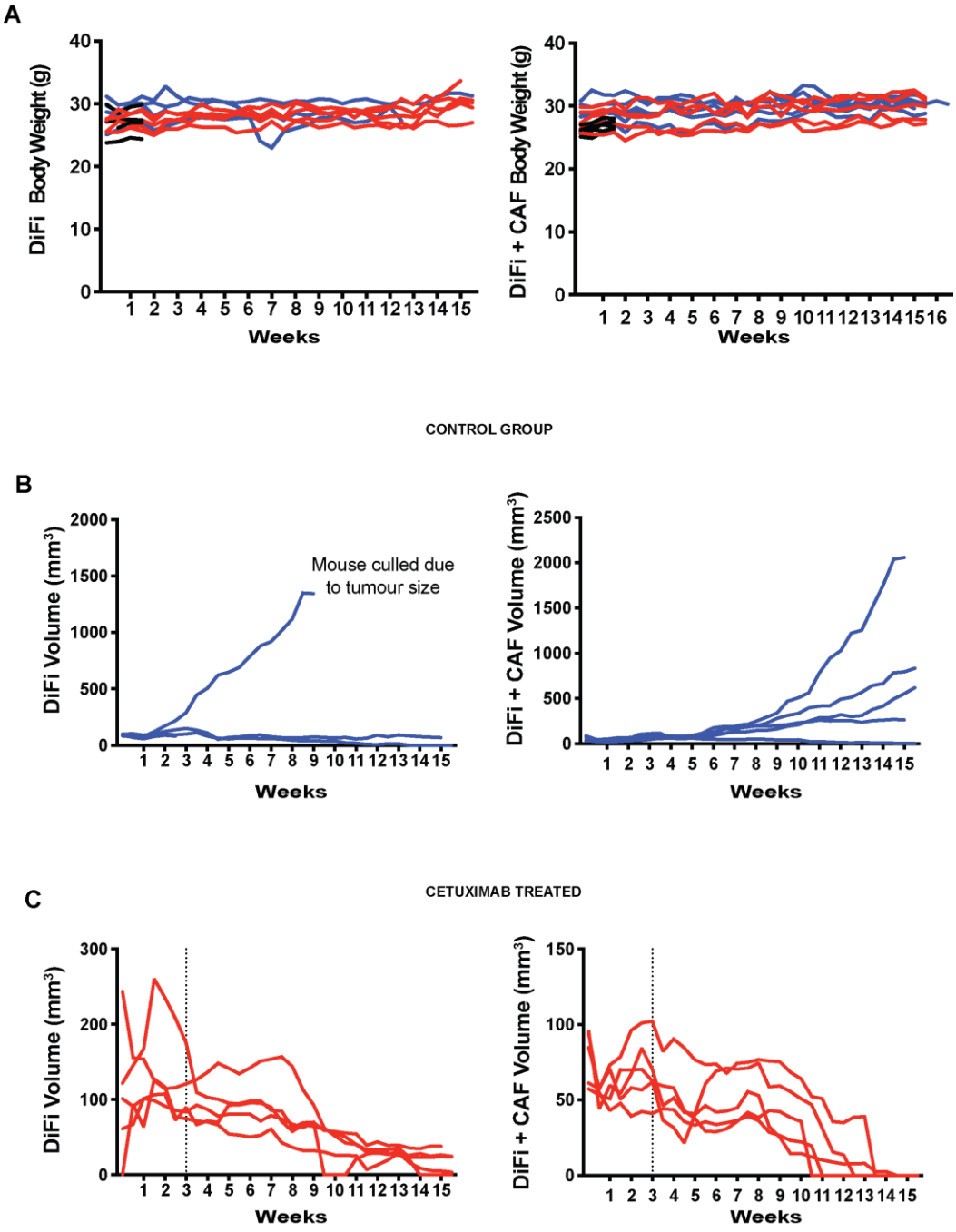

Figure 5.12 DiFi and CAF co culture xenograft growth.

(A) Body weights for DiFi and DiFi and CAF co-culture (control (blue) and treated (red) mice). Black lines represent mice culled for tumour sections. (B) Tumour volumes for control group engrafted with DiFi cells and DiFi and CAF Co-culture. (C) Tumour volumes for treated group engrafted with DiFi cells and DiFi and CAF Co-culture treated with 1mg cetuximab twice weekly by intravenous injection. Start of treatment at 3 weeks is indicated by the dotted line.

	DiFi	DiFi + CAF
Tumours scored (n=)	3	4
Pattern of tumour growth	Solid nodular = 0 Small nests and sheets = 3	Solid nodular = 3 Small nests and sheets = 1
Pattern of α-SMA	Intratumoural thin walled vessels (strong α-SMA)	Intratumoural thin walled vessels (strong α-SMA) peripheral fibrohistiocytic cells surrounding tumour nodules (patchy and weak α-SMA)

Table 5.1 Summary of α-SMA staining in xenograft tumours

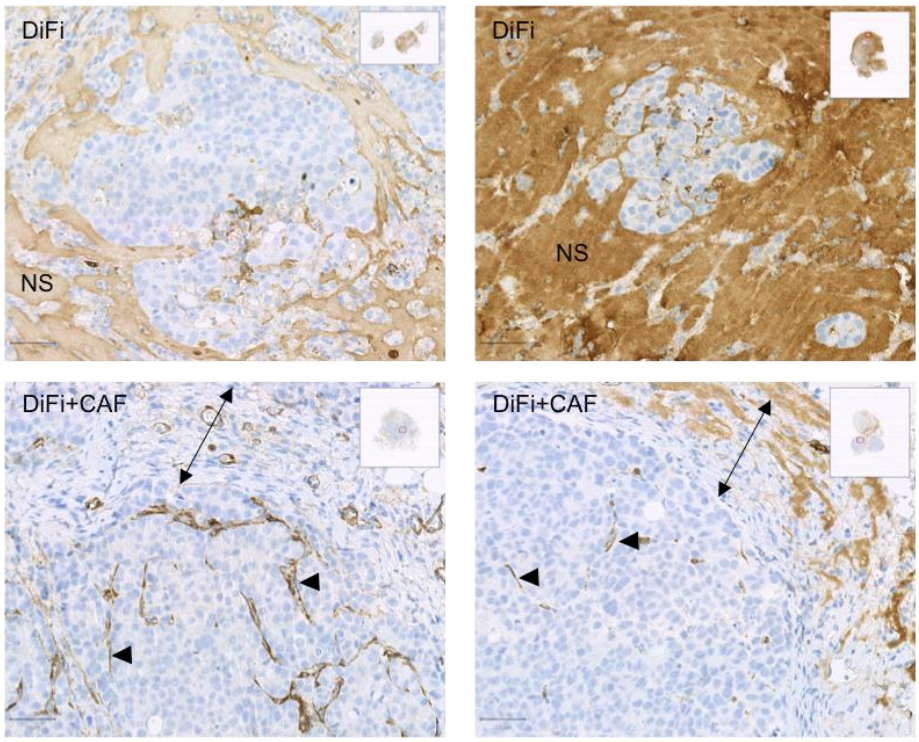

Figure 5.13 Example Images of α-SMA-stained xenografts.

Xenografts stained for α-SMA in DiFi xenografts (top) and DiFi+CAF xenografts (bottom). Tumour areas (T) are negative for α-SMA. α-SMA is strongly positive in pericytes of intratumoural vessels (single arrowheads). Fibrohistiocytic like cells (double arrowhead) are seen peripherally to DiFi+CAF xenograft tumour. Non-specific background staining (NS) is seen within acellular areas.

5.8. Discussion

64% of PD biopsies in patients who had prolonged clinical benefit to cetuximab before progression harboured no identifiable genetic resistance drivers. This lack of genetic mechanisms of acquired cetuximab resistance challenges the paradigm that genetic mechanisms dominate the resistance landscape. Subtype switching from the CMS2 transcriptomic subtype to the CMS4 subtype occurred in 71% cases with no known genetic driver. This is indeed consistent with other, albeit more limited, genetic studies in CRCs that acquired resistance to anti-EGFR antibodies that also identified no genetic drivers of acquired resistance in 41-46% of biopsies (Arena et al 2015, Pietrantonio et al 2017). The CMS4 subtype has been described as a 'mesenchymal subtype' that is associated with poor prognosis to both chemotherapy and anti-EGFR therapy in colorectal cancer (Felipe De Sousa et al., 2013; Song et al., 2016; Trinh et al., 2017). The transcriptome of primary CMS4 CRCs has been described to be influenced by tumour microenvironment (TME) signalling (Calon et al., 2015; Isella et al., 2015). A major role of the tumour microenvironment as a determinant of cancer drug resistance has been described for several other tumour types (Straussman et al., 2012; Wilson et al., 2012; Östman, 2012). A key component of the TME is CAFs. In CRC, CAFS have been described as a major contributor to poor prognosis (Calon et al., 2012). Furthermore, CAFs have been shown *in vitro* to confer resistance to small molecule EGFR inhibitors in lung cancer (Wang et al., 2009) and to BRAF inhibitors in melanomas (Hirata et al., 2015; Straussman et al., 2012). My data, based on analyses from a prospective clinical trial, strongly suggests that CAFs are also responsible for non-genetic mechanisms of resistance to cetuximab in CRC through the secretion of FGF and HGF growth factors.

I have shown that both, CAF conditioned medium and direct co-culture of CAFs are capable of reversing the growth inhibition induced by cetuximab exposure in CRC cell lines. I furthermore confirmed that CAF conditioned medium re-

activated ERK phosphorylation and hence MAPK pathway signalling. Contrary to one of my initial hypotheses, TGFβ1-2, which were both significantly upregulated and TGFβ3 (not significant, but highly upregulated) in CRCs that switched from the CMS2 to the CMS4 subtype did not confer resistance *in vitro*. Further investigation showed that this was instead driven by FGF1, FGF2 and HGF. TGFβ is known to be a master regulator of the tumour microenvironment and of the CMS4 subtype through the induction of a TGFβ-activated microenvironment (Tauriello and Batlle, 2016). In fact, TGFβ is the most commonly associated growth factor with fibroblast activation (Attieh and Vignjevic, 2016). TGFβ promotes the differentiation of fibroblasts into activated fibroblasts, and can maintain them in an activated state by autocrine signalling (Evans et al., 2003; Kojima et al., 2010). Taken together, this supports a model where TGFβ may stimulate fibroblast to acquire a CAF phenotype that produce HGF, FGF1 and FGF2 (**Figure 5.14**). I showed that cetuximab sensitive DiFi and LIM1215 cell lines express the cognate receptors for these ligands and that the growth factors together reactivate the MAPK pathway and maintain growth the presence of cetuximab. This reinforces the existing concept that resistance to cetuximab treatment requires the re-activation of this key growth pathway in CRC which has been based on the discovery that mutations upstream or in the MAPK pathway lead to cetuximab resistant. (Misale et al., 2014)

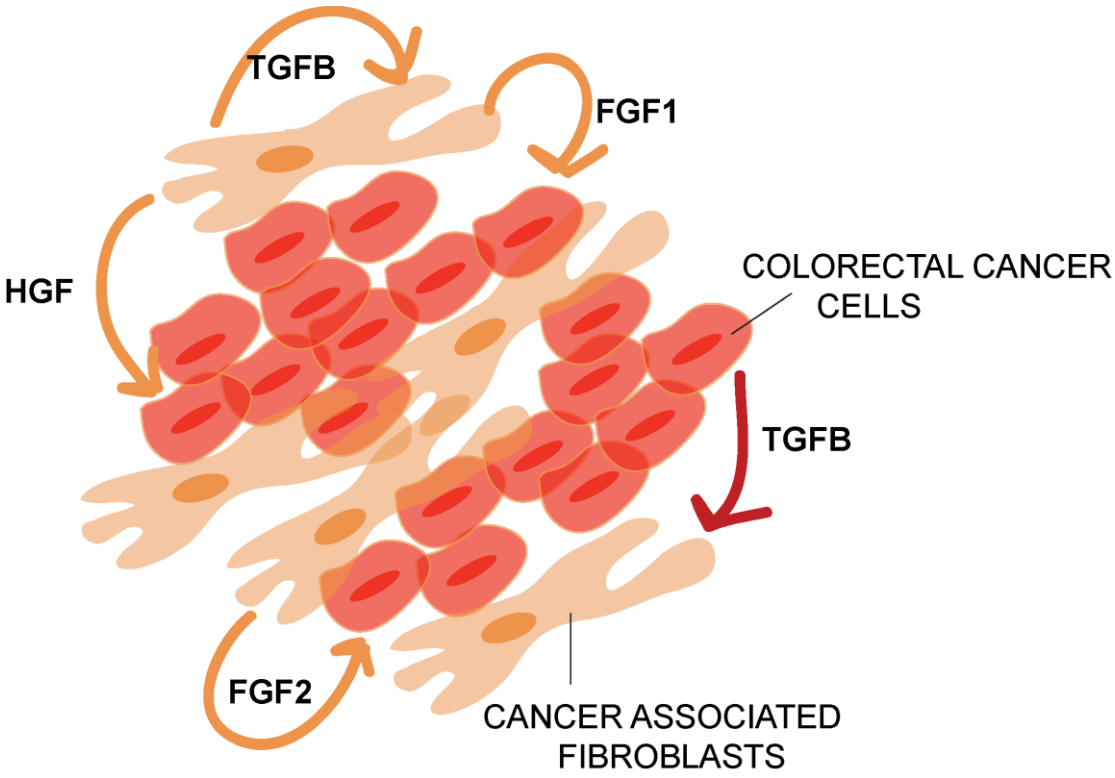

Figure 5.14 Proposed model of CAF-mediated resistance.

CAFs and CRC cells are intermixed populations of cells that have both autocrine and paracrine signalling occurring. The proposed model shows that CAFs are maintained in a TGFβ -activated environment by autocrine TGFβ signalling and paracrine TGFβ signalling from CRC cells. CAFS then produce HGF, FGF1 and FGF2 that bind CRC receptors and induce increased MAPK signalling in CRC cells and thus induce cetuximab resistance.

The model that I have proposed above is further strengthened by the histologies seen in the *in vivo* experiments performed in this thesis and those observed in patients (**Figure 5.15**). In the PROSPECT-C trial it was seen that patients who were CMS2 subtype at baseline, the cancer cells and surrounding stroma were separate entities. However following CMS2>4 switching at progression in these tumours, the cancer cells and surrounding stroma became more intermixed, and there is a pattern of stromal infiltration (Woolston et al., 2019). Unfortuantely, there was no material left over from this analysis to stain for α-SMA and thus identification of CAFs in these samples is not possible. The histology results from the *in vivo* co-culture experiment interestingly also show spatial segregation of fibroblasts, identified by weak α-SMA staining and cancer cell populations. Thus similarities can be seen in the histologies we observed in xenografts and in CMS2 subtype patients, correlating with cetuximab sensitivity in both. It is possible that human CAFs have an insufficient lifetime in xenograft tumours or that they revert back to quiescent fibroblasts that no longer show the typical characteristics of the CAF such as SMA expression. They fail to proliferate and are outnumbered by cancer cells even after the short period. RNAseq data does however at least confirm that CAFs were highly expressing α-SMA *in vitro*.

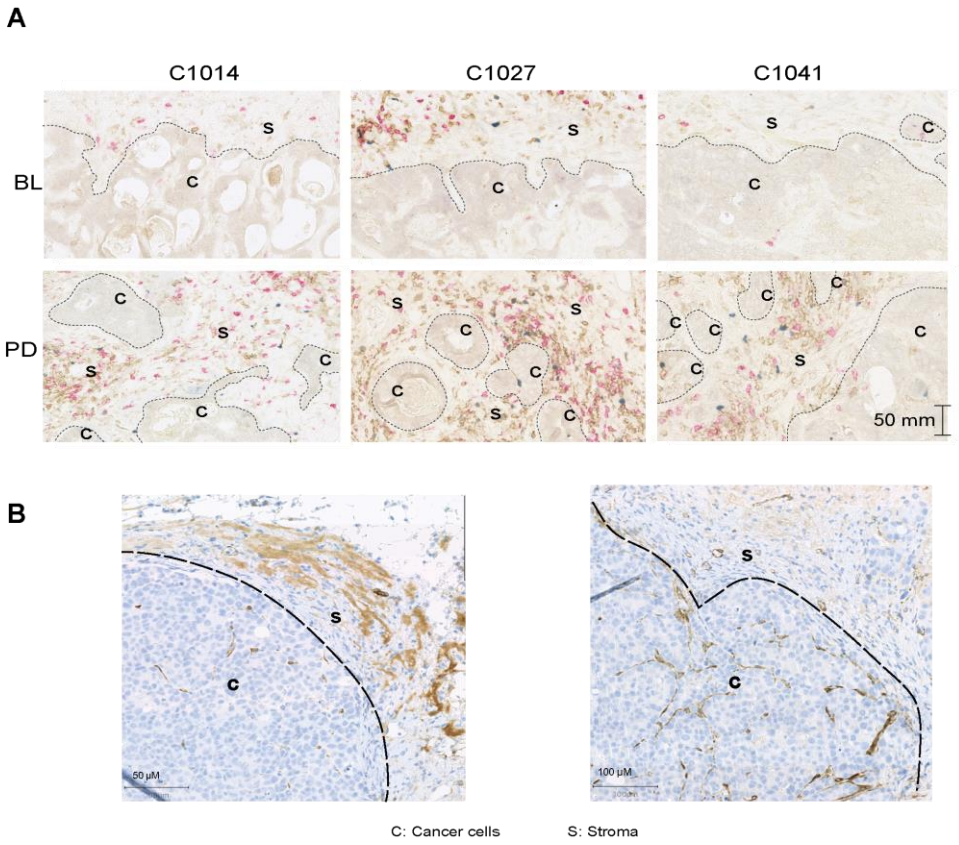

Figure 5.15 Examples images of cancer and stroma populations.

(A) Images C1014, C1027 and C1041 are examples from the PROSPECT-C trial of cancer cell (c) and stromal populations (s) in BL and PD, before and after subtype switches. (B) Images from DIFI + CAF xenografts stained for α-SMA. Cancer cell (c) and stromal cell (s) areas are indicated.

The secretome of the single immortalized rectal carcinoma CAF line which was available for my experiments was highly similar to the secretome of CAFs previously published (Luraghi et al., 2014), suggesting that this model system is representative of typical CAFs. This was also supported by the high expression of IL-6 and IL-8, both EMT-promoting pro-inflammatory cytokines (Fuxe and Karlsson, 2012) in the CAF conditioned medium from this line.

HGF has previously been associated with driving CAF-mediated resistance in stem-like CRC cells (Luraghi et al., 2014). Recombinant HGF has furthermore been described to drive cetuximab resistance through MET signalling *in vitro* (Liska et al., 2011). My results further substantiate this association. MET is the only known receptor for HGF and therefore key to its downstream effect (Birchmeier et al., 2003). My data further demonstrated that MET expression is in fact upregulated (2.18-fold) at the mRNA level in the CRC cell line following CAF conditioned medium treatment. This may further support the activation of the MAPK pathway downstream of MET through CAF conditioned medium, however, future studies of the impact of CAF conditioned medium on MET protein expression are warranted to confirm this.

In normal physiology, FGF2, also known as basic FGF (bFGF) maintains pluripotency in colorectal cancer stem cells (Danopoulos et al., 2017). FGF2 has been shown in prostate cancer to induce mesenchymal properties in epithelial cells and thus facilitates EMT in a MAPK-driven manner (Chen et al., 2017b; Liu et al., 2015). My results show a role for FGF2 in inducing growth driven by MAPK reactivation in cetuximab resistance. MET signalling also contributes to an EMT phenotype through promoting invasion (Bradley et al., 2016) and promoting cancer stem cell features in CRCs (Vermeulen et al., 2010). It is interesting in this context that despite similar pERK reactivation induced by HGF, FGF1 and FGF2, a much more modest rescue of growth during cetuximab treatment was observed with FGF1 stimulation. Hence, additional pathways such as EMT or the activation of other growth promoting signalling pathways

may play a role downstream of FGF2 and HGF and this could be further investigated in order to dissect the detailed mechanism of how CAFs can induce resistance.

I showed that in order to counter resistance induced by CAF conditioned medium and to effectively suppress pERK signalling, a triple combination of cetuximab, MET and FGFR inhibitors was required. In a recent Phase II study assessing the use of MET inhibitor tivantinib and cetuximab in Met overexpressing KRAS-wildtype metastatic CRC that had previously been treated with anti-EGFR inhibitor, fewer than 10% of patients achieved objective responses (Rimassa et al., 2019). My data would suggest that this is due to the lack of an FGFR inhibitor in combination. Applying a triple combination of cetuximab, FGFR and MET inhibitor to patients who acquired cetuximab resistance through CMS2>4 switches, where high levels of HGF are expressed by fibroblasts, may hence be a novel indication for these agents. However, in the PROSPECT-C cohort several tumours that underwent CMS2 to CMS4 subtype switched concurrently acquired genetic resistance mechanism including RAS mutations in distinct subclones. The triple therapy described above would not be able to control these subclones, and hence may not be clinically successful. However, it may be worthwhile to investigate the triple combination of EGFR, MET and FGFR inhibitors in *RAS* wildtype CRCs that have not previously been treated with cetuximab. Furthermore the triple combination should also be investigated *in vitro* in co-culture assays. This would reveal whether forestalling the CAF-induced resistance that appears relatively common based on my data could prolong time to progression. In addition to inhibiting the effect of the mitogenic growth factors produced by CAFs, novel therapeutic options may also look to prevent subtype switching by targeting the CAFs themselves (Kalluri, 2016) or TGFβ (Hawinkels and ten Dijke, 2011; Lonning et al., 2011) as the likely master regulator of the CMS4 CRC subtype.

Chapter 6: Investigating chemotherapy resistance using patient-derived organoid (PDO) models

6.1. Introduction

Fluoropyrimidines (5FU) or the oral 5FU derivative capecitabine are together referred to as 5FU here, as the drugs have the same mechanism of action. Both drugs can be used interchangeably in metastatic CRCs, in combination with either the platinum drug oxaliplatin or with the topoisomerase-I inhibitor irinotecan and are among the most effective and most widely used systemic treatment regimens for metastatic CRC. The median progression-free survival for chemotherapies (18-20 months (Grothey et al., 2004; Tournigand et al., 2004) is greater than for subsequently given lines of targeted therapies (Grothey et al., 2013; Hewish and Cunningham, 2011). Despite good initial activity of chemotherapy in the majority of patients with metastatic CRC, resistance eventually develops in all patients, leading to progression and death. Currently, the drivers of acquired resistance to 5FU and irinotecan are very poorly understood. Resistance is often attributed to a host of different mechanisms acting at the level of the tumour, such as altered drug efflux (Thomas and Coley, 2003), impaired apoptosis (Longley et al., 2003; Miyashita and Reed, 1992), or the activation of pro-survival pathways. Genetic mechanisms of resistance such as thymidylate-synthase gene amplifications were identified in 7 of 32 CRC metastases after exposure to single agent fluoropyrimidines (Wang et al., 2004). Non-genetic resistance mechanisms have also been proposed, including the selection of intrinsically chemotherapy resistant cancer stem cells (Kemper et al., 2010) and microenvironmental influences (Straussman et al., 2012). Due to the difficulties of obtaining biopsies from patients with end-stage chemotherapy refractory CRCs, chemotherapy resistance has mainly been investigated in vitro and in xenografts (Dylla et al., 2008; Kreso et al., 2013; Zhang et al., 2008). However, cancer population sizes

in model systems are much smaller than in patients and chemotherapy is often administered for short periods and as single agent. As a consequence, it remains unknown which of the proposed resistance mechanisms contribute to acquired combination chemotherapy resistance in patients or whether additional ones evolve. Furthermore, it is not understood whether these mechanisms are intrinsic to the cancer cells or if tumour microenvironmental factors play a role.

Recent patient derived organoid culture technologies (Sato et al., 2011) enable the long term *in vitro* propagation of cancer cells from CRC biopsies, providing new opportunities to directly study and compare PDOs derived from patient tumours that have acquired chemotherapy resistance to PDOs from untreated CRCs in order to understand molecular mechanisms that contribute to resistance. 3D PDO cultures from biopsies are also thought to better represent the biology of CRCs than traditional cell lines that may have changed their cellular and molecular characteristics long-term culture in 2D conditions on plastic.

Biopsy material from patients enrolled in the PROSPECT-C and PROSPECT-R clinical trials (Khan et al., 2018a; Khan et al., 2018b; Woolston et al., 2019) had all been exposed to and failed to effectively respond to standard combination chemotherapy with 5FU, irinotecan and oxaliplatin. Biopsies from the FORMAT clinical trial were from metastatic CRCs with variable prior chemotherapy exposure (Moorcraft et al., 2017). An ongoing project in my host lab applied exome or genome sequencing to biopsies from these trials in order to define the genetic landscape of chemotherapy refractory CRC and to identify potential genetic drivers of resistance. However, this has not identified any genetic drivers of drug resistance to date, indicating that the genetics of chemotherapy resistance is either very complex or that non-genetic or epigenetic mechanisms play a major role.

Together with Beatrice Griffiths, the technician in the lab, I used biopsies from a subgroup of these tumours (those where sufficient biopsy cores were obtained to first satisfy the tissue requirements for genetic analysis and where surplus fresh material was left over) to establish PDO cultures from chemotherapy resistant and chemotherapy naïve CRCs in order to establish a living CRC biobank. My aim was to establish methods to culture and to characterize the chemotherapy sensitivity of these innovative model systems and to start investigating the molecular characteristics of chemotherapy resistance in these cellular models.

6.2. Establishing PDOs from metastatic CRC patients

We used two methods to establish PDOs; larger percutaneous biopsies from metastatic CRC chemotherapy resistant patients and one endoscopic biopsy from a metastatic treatment naïve CRC patient were directly cultured in matrigel and the specially formulated medium described by Prof Clevers group that prevents differentiation of CRC cells and maintains long term viability (Sato et al., 2011). Successful direct cultures were usually heralded by the emergence of budding cells within a few weeks (**Figure 6.1** A and B). Very small core biopsies were implanted subcutaneously into immunodeficient nude mice and once a tumour had developed, mice were culled, tumour explanted and dissociated and cells were then seeded in matrigel. PDOs that continued to proliferation for at least 10 passages were subsequently used for experiments. My host lab established 10 PDO cultures from chemotherapy resistant CRC and I was actively involved in 5 of these (CRCCR-01, -02, -08, -09, -10). We only obtained 2 biopsies from treatment naïve CRCs in total, one of which successfully grew (CCRCR-08). Importantly, a second biopsy was performed on this patient after the tumour had developed resistance to 5FU and oxaliplatin and we also successfully established a PDO culture (CRCCR-10). This could be an important model system to assess whether chemotherapy sensitivity of the PDOs differed in line with the development of resistance in the clinic. I also obtained 5 additional PDOs established from treatment naïve CRCs from Prof

Clevers (Hubrecht Institute, Netherlands) to generate a similar sized cohort of organoids that would likely be drug sensitive (T37, T39, T42, T44 and T45). Overall, 5 of these PDOs derived in the lab (CRCCR-01, -02, -05, -07, -09) were derived from CRCs resistant to 5FU, oxaliplatin and irinotecan, 1 (CRCCR-10) from a CRC resistant to 5FU and irinotecan and 6 (CRCCR-08, T37, T39, T42, T44 and T45) from treatment naïve CRCs (**Figure 6.2**).

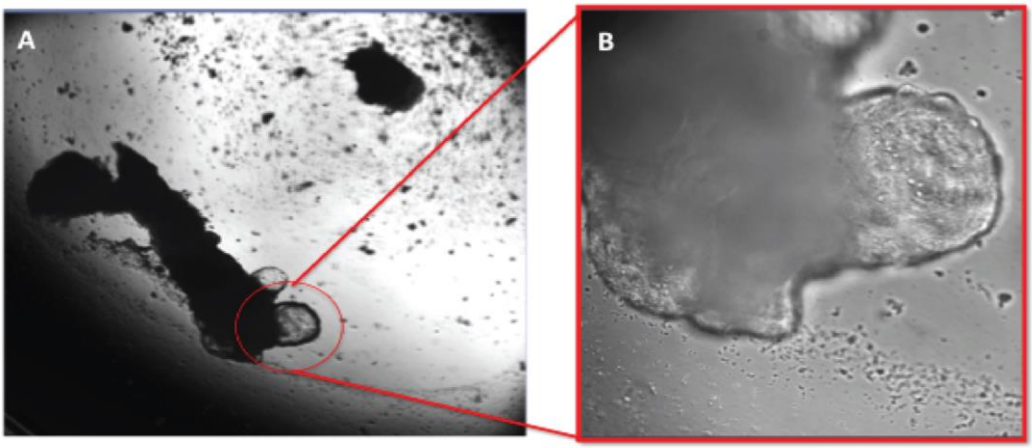

Figure 6.1 Representative images of organoid cultures.

(A) and (B) Representative images at 2.5X and 10X respectively of a core biopsy implanted into matrigel that shows budding. Images taken on a Zeiss Observer Microscope.

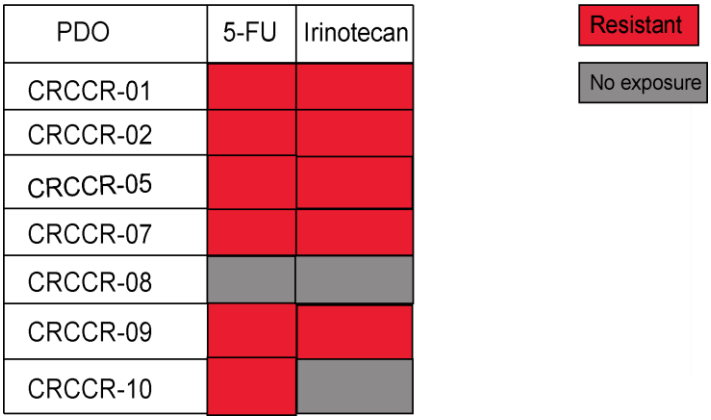

Figure 6.2 Prior exposure and resistance status of PDO derived in my host lab.

6.3. Drug sensitivity of metastatic chemotherapy refractory PDOs

My next aim was to characterise the sensitivity of these PDOs from 6 chemotherapy naïve and 4 resistant CRCs ($PDO_{naïve}$ and PDO_{res} respectively) to 5FU and to the active metabolite of irinotecan, SN38, through *in vitro* testing. Oxaliplatin was not investigated as it is not used as a single-agent in the clinic and has been described to be ineffective against CRC cell lines *in vitro* ((Schütte et al., 2017; Vlachogiannis et al., 2018).

In order to perform *in vitro* drug sensitivity testing with PDOs that grow as 3D structures in matrigel, I established the technique developed by Dr Garnett at the Sanger Institute for 3D drug screening and adapted it to suit manual pipetting as opposed to the high-throughput robotics design they had used for their large scale screens (Francies et al., 2016) (**Figure 6.3**). This drug sensitivity assay keeps the spheroids intact rather than plating them as a single cell suspension where cell-cell contacts are lost, aiming to maintain the physiological structure as this may influence the biology of the cancer cells (Francies et al., 2016). In this assay, data is normalised to the CellTiter Glo (CTG) values generated by staurosporine-induced killing and by growth in untreated PDOs where only the drug vehicle (DMSO) is added. Thus values of 0 and 1 represent complete cell death and unperturbed growth, respectively.

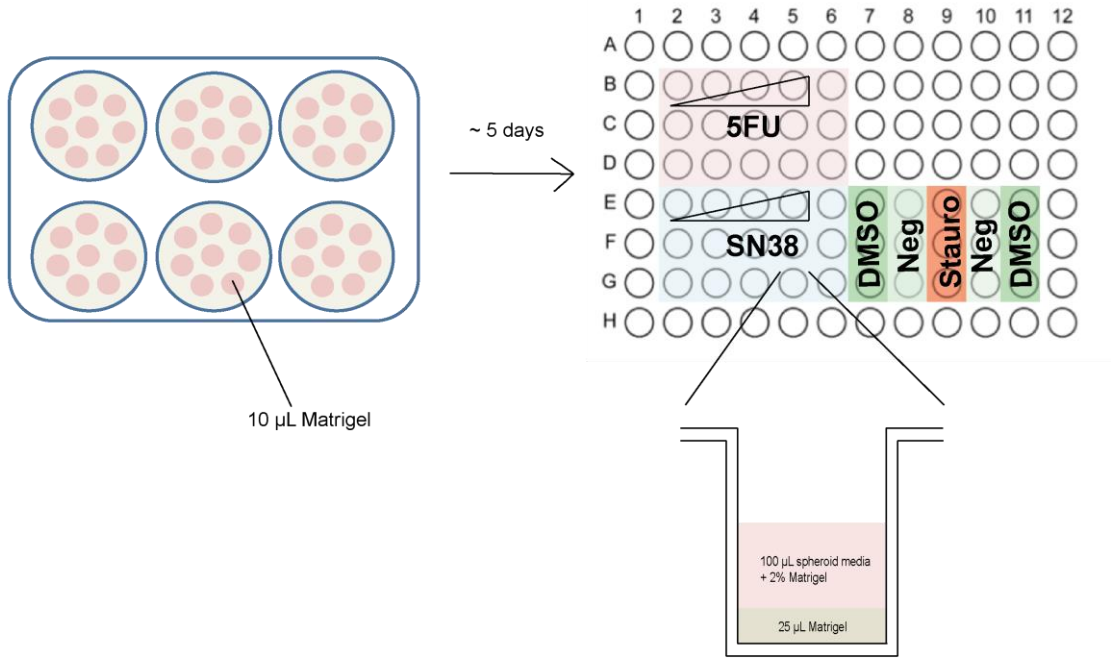

Figure 6.3 Schematic of 3D organoid drug screen.

Patient derived organoids were first plated in 10 µL matrigel dots and covered with medium in 6-well plates and grown for ~ 5 days. The matrigel in PDO cultures was then carefully disrupted and the spheroids were re-plated in 96-well plates pre-loaded with 25 µL of matrigel and growth medium containing 2% matrigel was added. Plates were treated with a drug (SN38 and 5FU) concentration gradient as shown in the layout, with both positive and negative control wells (figure based on (Francies et al., 2016).

Four PDO_{res} and six $PDO_{naïve}$ cultures were screened for their sensitivity to 5-FU (**Figure 6.4** A and B), and good responses were only observed at the highest used dose (100 µM). This is a dose commonly used in colorectal cancer cell lines (Bracht et al., 2010; Flis and SPŁAWIŃSKI, 2009). Due to the lack of a sigmoidal drug response curve in the 5FU drug titration assay, IC_{50}s could be not calculated and I instead used the relative viability at the maximum dose to assess growth in the presence of drug (**Figure 6.4** C and D). In response to treatment with 100 µM 5FU, differential sensitivities in PDO_{res} emerged. CRCCR-10 and CRCCR-09 showed only moderate inhibition (relative viabilities 0.78 and 0.53 respectively), even at a high dose of drug. CRCCR-01 and CRCCR-02 were sensitive to 5FU treatment at 100 µM (relative viabilities 0.15 and 0.20) but 5FU showed minimal growth effect at 10 µM in all PDO_{res}. Importantly, CCRCR-08 and CCRCR-10 that had been established from the same patient, the former before 5FU and oxaliplatin treatment and the latter after the tumour had acquired resistance to this combination, showed sensitivity of the former and resistance of the latter (3.8 fold increase in relative viability to 100 µM 5FU, light blue bars in **Figure 6.4** C and D). Furthermore, the maximum inhibition (E_{max}) at the highest dose was analysed as a measure of drug efficacy (Schütte et al., 2017) (**Figure 6.4** E). Maximal growth inhibition with 5FU treatment was significantly higher in PDO_{res} than in $PDO_{naïve}$ ($p=0.04$). Analysis at 10 µM and 100 µM 5FU revealed that residual growth was significantly higher in the $PDO_{naïve}$ lines compared to PDO_{res} ($p=0.0033$ and $p=0.0034$) (**Figure 6.4** F and G).

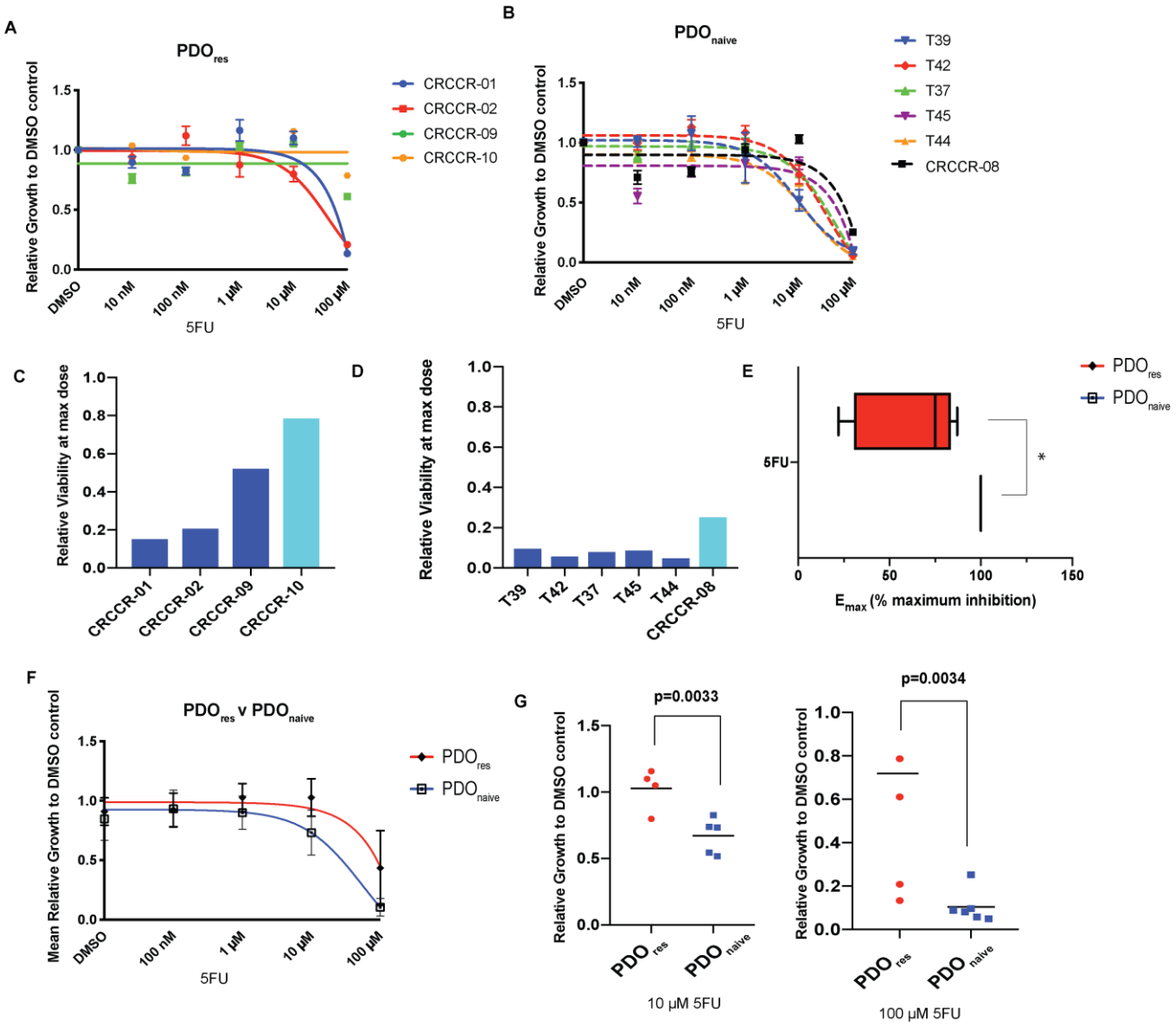

Figure 6.4 PDO responses to 5FU treatment.

One representative repeat of (A) $PDO_{res\ and}$ (B) $PDO_{naïve}$ lines treated with 5FU for 6 days. Relative viability of (C) $PDO_{res\ and}$ (D) $PDO_{naïve}$ at the maximum dose (100 µM) was calculated. Samples coloured light blue in (C) and (D) represent a matched $PDO_{naïve}$ and PDO_{res} pair. (E) Box and Whisker plots showing maximum inhibition of growth (E_{max}) achieved at the highest dose (100 µM 5FU) for $PDO_{naïve}$ (blue) and PDO_{res} (red) . Whiskers indicate maximum and minimal values, boxes the interquartile range and the line in the box indicates the median. (F) Mean response of $PDO_{naïve}$ and PDO_{res} lines. Cell-Titre Glo determined cell viability. Data were normalised such that 1= DMSO-treated growth and 0= cell death, as measured by the staurosporine control in each assay. Each experiment was performed in technical triplicate and mean relative growth calculated. Error bars indicate standard deviation. (G) Scatter plot of relative growth across PDO_{res} and $PDO_{naïve}$ treated with 10 and 100 µM 5FU respectively. Mean is indicated by the line. Significance was determined by unpaired t test. *=p<0.05.

The active irinotecan metabolite SN38 was effective at suppressing cancer cell growth of both $PDO_{naïve}$ and PDO_{res} at the highest dose (**Figure 6.5** A and B). However, a clear shift in the drug sensitivity curves was observed between PDO_{res} and $PDO_{naïve}$ (**Figure 6.5** C) and the mean IC_{50} value for PDO_{res} (IC_{50} = 163 nM) was 219-fold higher than for $PDO_{naïve}$ (IC_{50} = 0.73 nM, p=0.049). CRCCR-08 despite being derived from a treatment naïve tumour (**Figure 6.2**) had a much higher IC_{50} to SN38 than the rest of the $PDO_{naïve}$ cohort (**Figure 6.5** B) and this was similar to that of CCRCR-10 that had been established to the same tumour after it acquired chemotherapy resistance. This may suggest that this tumour may have shown primary resistance to irinotecan. However, this could not be formally assessed as the patient was treated clinically with 5FU and oxaliplatin. These data demonstrate that PDOs from chemotherapy resistant CRCs are significantly more resistant to chemotherapy when tested *in vitro* compared to those from treatment naïve CRCs. Thus, the drug sensitivity or resistance of the patient tumour is well represented in these models and this furthermore suggests that cell intrinsic factors, rather than microenvironmental factors, determine chemotherapy sensitivity.

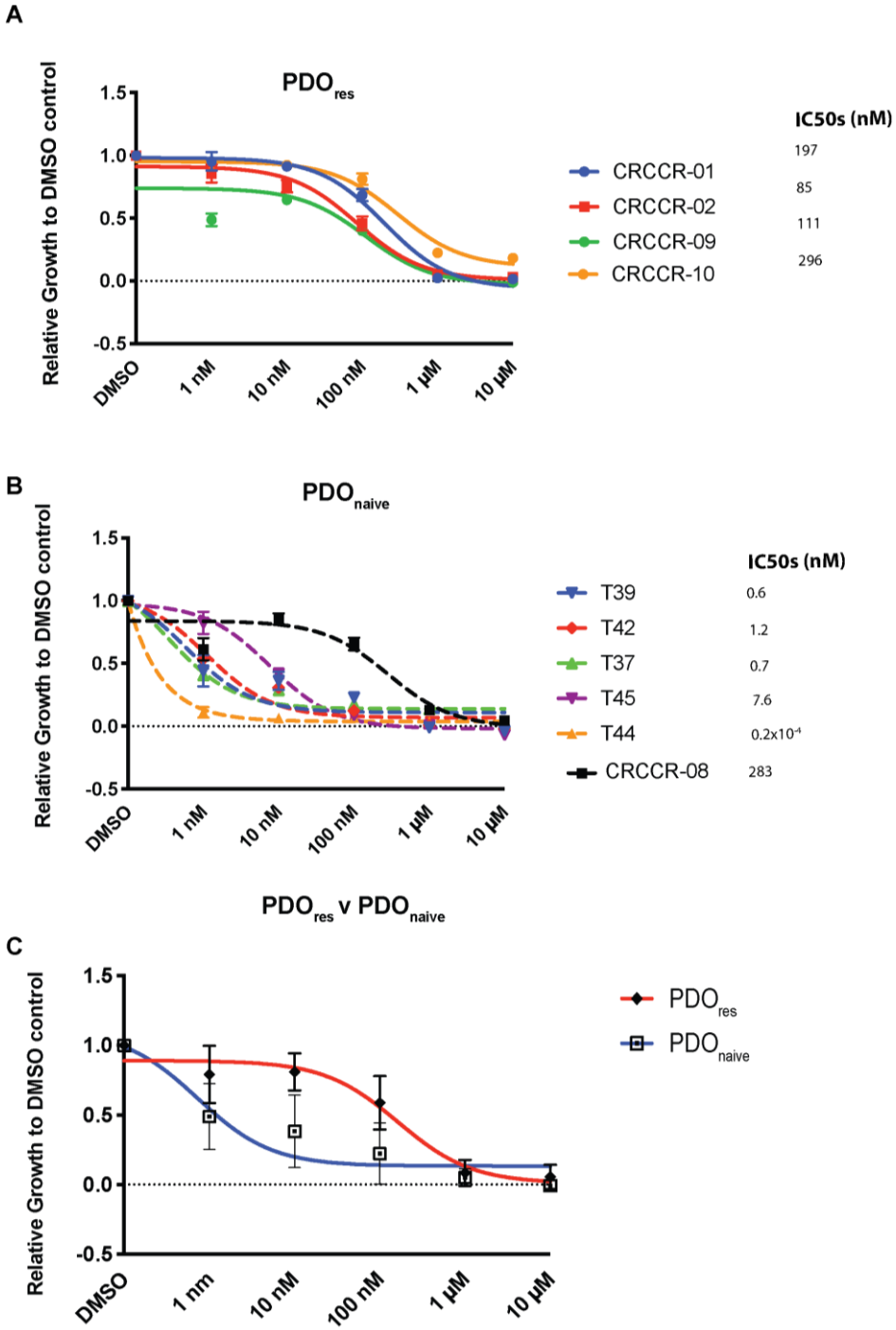

Figure 6.5 PDO responses to SN38.

(A) One representative repeat of PDO_{res} treated with SN38 for 6 days. (B) One representative repeat of $PDO_{naïve}$ lines treated with SN38 for 6 days. IC_{50} values were calculated using non-linear regression log response v three parameters by Graphpad Prism. (C) Mean response of the $PDO_{naïve}$ and the PDO_{res} lines tested in (A) and (B). Cell viability was determined by Cell-Titre Glo. Data were normalised such that 1= DMSO-treated growth and 0= complete cell death, as measured by the staurosporine control in each assay. Each experiment was performed in technical triplicate and mean relative growth calculated. Error bars indicate standard deviation.

6.3.1. Chemotherapy response of CRC cell lines

To furthermore compare the drug sensitivity of the PDO lines to established CRC cell lines, I also screened 5FU and SN38 in a panel of cell lines. The panel was assembled from CRC cell lines for which there was no mention in the literature of prior treatment with chemotherapeutics. Four cell lines that were KRAS wildtype and one mutant (KRAS G12V) line were selected. Mean E_{max} to 5FU was greater (99.9% in both) in CRC cell lines and $PDO_{naïve}$ compared to a mean E_{max} (60.6%) in PDO_{res}. Furthermore, mean IC_{50} to SN38 was much closer to that in $PDO_{naïve}$ (2.97 nM v 0.7 nM respectively) than to the mean IC_{50} (163 nM) observed in PDO_{res}. This shows that $PDO_{naïve}$ and cell lines which are unlikely to be from drug resistant tumours show similar sensitivity *in vitro*, suggesting that these models are relatively similar and that PDO_{res} indeed have much higher resistance than seen in $PDO_{naïve}$ and in cell lines.

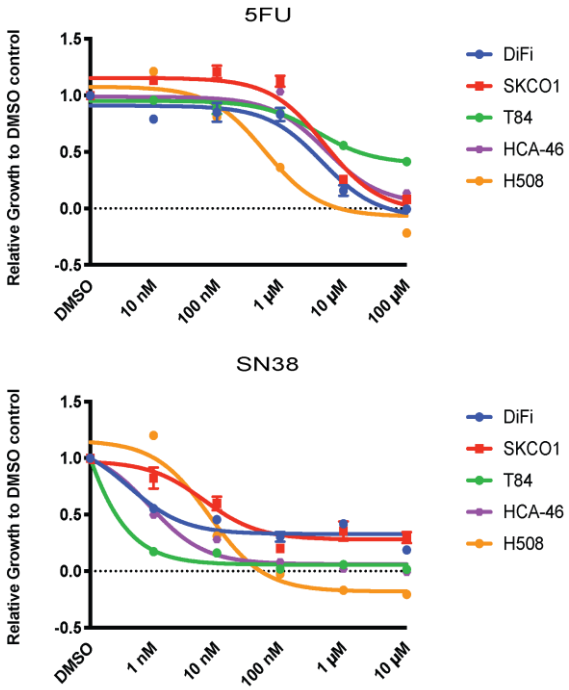

Figure 6.6 CRC cell line response to chemotherapeutics.

One representative repeat of 5 PDO lines treated with (A) 5FU, (B) SN38 for 6 days. Cell viability was determined by Cell-Titre Glo. Data were normalised such that 1= DMSO-treated growth and 0= cell death, as measured by the staurosporine control in each assay. Each experiment was performed in technical triplicate and mean relative growth calculated. Error bars indicate standard deviation.

6.4. Phenotypic analysis of PDOnaïve and PDOres by RNA sequencing

After confirming that PDOs derived from chemotherapy refractory tumours were more resistant to treatment with chemotherapy agents *in vitro,* my next aim was to apply RNA-sequencing to identify whether these groups of PDOs differed in gene expression levels and potentially in the expression of entire pathway signatures.

Using 3'-RNA sequencing and Bluebee cloud software for data analysis, RNA sequencing was performed on 6 $PDO_{naïve}$ and 4 PDO_{res} lines. Normalised read

counts were then put through the Gene Set Enrichment Analysis tool (GSEA) (Subramanian et al., 2005) to determine key expression signatures that are enriched in resistant samples. The expression data were interrogated against the GSEA Hallmarks, chemical and genetics perturbations and transcription factor targets databases. GSEA results were filtered to select gene sets with a false discovery rate (FDR) <0.25 and ranked by Normalised Enrichment Score (NES). Gene sets related to the MYC pathway, NFκB and TNFα signalling were repeatedly observed as being enriched in PDO_{res} samples (Table 6.1). All three signatures were enriched in all of the databases analysed.

Gene Set Database	Gene set	NES	FDR q-value
Hallmarks	HALLMARK_MYC_TARGETS_V2	-2.1	0
	HALLMARK_EPITHELIAL_MESENCHYMAL_TRANSITION	-1.96	0.001
	HALLMARK_TNFA_SIGNALING_VIA_NFKB	-1.8	0.006
	HALLMARK_APICAL_JUNCTION	-1.73	0.006
	HALLMARK_KRAS_SIGNALING_UP	-1.65	0.013
	HALLMARK_WNT_BETA_CATENIN_SIGNALING	-1.65	0.011
	HALLMARK_MYC_TARGETS_V1	-1.33	0.15
	HALLMARK_P53_PATHWAY	-1.29	0.188
	HALLMARK_IL6_JAK_STAT3_SIGNALING	-1.28	0.189
tft curated	RGTTAMWNATT_HNF1_01	-1.94	0.017
	GGGNNTTTCC_NFKB_Q6_01	-1.89	0.03
	NFKAPPAB65_01	-1.79	0.092
	NFKB_Q6_01	-1.77	0.114
	E2F_01	-1.74	0.159
	USF_02	-1.73	0.175
	NFKAPPAB_01	-1.72	0.194
	MYCMAX_01	-1.7	0.243
cpg curated	TIAN_TNF_SIGNALING_VIA_NFKB	-2.34	0.001
	RASHI_NFKB1_TARGETS	-2.21	0.015
	PHONG_TNF_TARGETS_UP	-2.2	0.016
	MATTIOLI_MGUS_VS_PCL	-2.1	0.081
	DAUER_STAT3_TARGETS_UP	-2.06	0.129
	SCHLOSSER_MYC_TARGETS_AND_SERUM_RESPONSE_DN	-2.04	0.165
	RICKMAN_TUMOR_DIFFERENTIATED_MODERATELY_VS_POORLY_DN	-2.03	0.174

Table 6.1 Gene expression signatures that were enriched in PDO_{res} vs $PDO_{naïve}$ based on Gene Set Enrichment Analysis (GSEA).

The table shows all significantly enriched (FDR p<0.25) pathways in PDOres (CRCCR-01, -02, -09, -10) vs $PDO_{naïve}$ (CRCCR-08, T37, T39, T42, T44 and T45). GSEA signature collections that were included were: Hallmarks collection, tft= transcription factor targets, cgp=chemical and genetic perturbations. NES= GSEA Normalised Enrichment Score, FDR=False Discovery rate.

MYC is a well-characterised family of transcription factors persistently expressed in cancer that encourage cell growth and survival. Overexpression of c-MYC has been described to contribute to both resistance and sensitisation to chemotherapeutics, thus its role is currently not well understood (Arango et al., 2003; Kugimiya et al., 2015). NFκB is a transcription factor that can regulate up to 200 genes involved in inflammation, innate immunity and cell growth and survival (Pereira and Oakley, 2008). NFκB is constitutively active in up to 40% of CRCs, where it plays a role in chemoresistance through promoting cell survival (Sakamoto et al., 2009; Voboril et al., 2004). TNF (Tumour necrosis factor) signalling has context-dependent effects which can either be tumour suppressive or support tumour growth roles (Balkwill, 2006). When TNFα induces NFκB signalling, it promotes cell survival and proliferation. The gene set TNFA_SIGNALLING_VIA_NFκB was observed to be enriched in PDO_{res} indicating that it may be the tumour promoting signalling of TNF that is active in resistance cells. My approach to comparing gene expression profiles of PDO_{res} vs $PDO_{naïve}$ hence identified multiple transcriptional signatures that are significantly upregulated in the resistant PDOs, demonstrating that these models differ in their gene expression profiles. Application of such high content molecular tests such as RNA sequencing that measure expression of thousands of genes to small sample sizes usually leads to false positive results, even when multiple testing correction is used as was done here. Thus, whether these pathways and the genes within them are mechanistically involved in chemotherapy resistance will require further validation studies. The identification of several pathways that can be targeted with existing inhibitors, for example the MYC pathway with bromodomain inhibitors or NFκB with RELB inhibitors, can be used for future validation.

6.4.1. Pathways enriched in PDO_{res} following 5FU treatment

Encouraged by the different gene expression profiles identified in untreated PDO_{res} vs $PDO_{naïve}$ my final aim was to assess whether there are gene expression programs that are enriched during 5FU chemotherapy treatment in PDO_{res} compared to $PDO_{naïve}$ but not in untreated PDO_{res} compared to $PDO_{naïve}$. 5FU treatment was chosen for this experiment, as it is the most effective and important chemotherapy drug in the clinic and as this allowed inclusion of the CRCCR-08/CRCCR-10 pair of PDOs from the same patient, which were sensitive and resistant respectively. 3' RNA sequencing was for this purpose repeated on 5 $PDO_{naïve}$ lines (T37 failed quality control and was not sequenced) and 6 PDO_{res} lines treated with either DMSO control or a sub-lethal dose of 5 µM 5FU for 48 hr.

Gene expression data showed 1127 genes differentially expressed in untreated vs 5FU treated $PDO_{naïve}$. In contrast, only 53 genes showed significant differential expression in untreated vs 5FU treated PDO_{res} (**Figure 6.7**). This appears to be consistent with PDO_{res} lines being much less responsive to 5FU treatment. Although 5FU had such a minimal impact on gene expression in PDO_{res}, most of the genes (43/53=81%) that were significantly deregulated in PDO_{res} during therapy were also significantly deregulated in the same direction in $PDO_{naïve}$ lines. Thus, resistant PDOs can still sense 5FU treatment to some degree and this triggers a small gene expression program that can also be observed in $PDO_{naïve}$ after 5FU exposure (**Figure 6.7**).

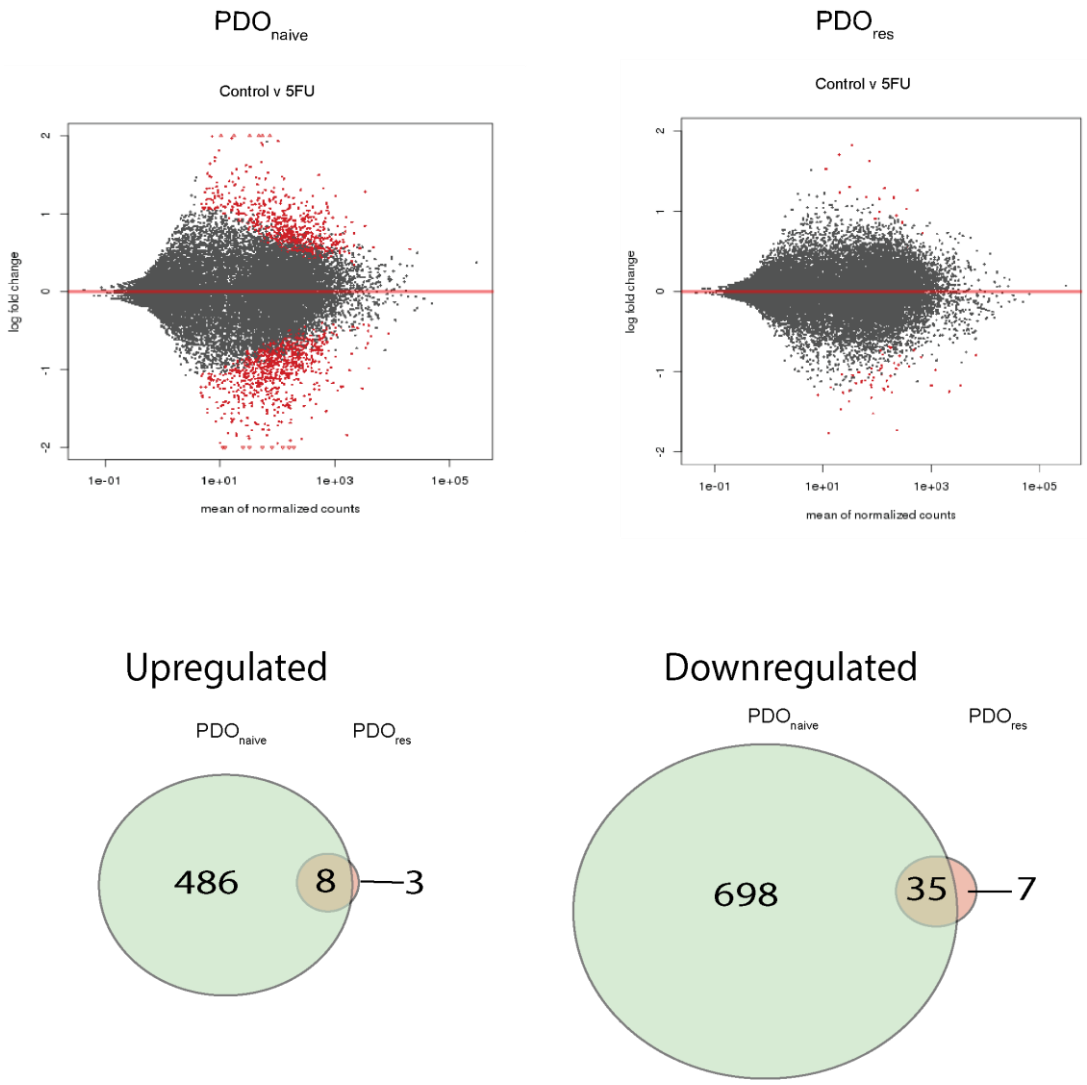

Figure 6.7 Differentially Expressed Genes in PDO_{res} and PDO_{naive} treated with 5FU.

PDO_{res} and $PDO_{naïve}$ lines treated with 5 µM 5FU for 48 hr before 3' RNA sequencing. MA plots generated by Bluebee platform of DEseq results. Red dots indicate differentially expressed genes. Venn diagrams show numbers of genes up- and downregulated in $PDO_{naïve}$ and PDO_{res} samples.

The small number of deregulated genes in 5FU treated PDO_{res} was too limited to apply pathway enrichment analysis for the identification of biological mechanisms that may contribute to resistance during 5FU treatment. I therefore applied a different approach that first identified pathways that were significantly deregulated in untreated $PDO_{naïve}$ vs PDO_{res} and pathways significantly deregulated in 5FU treated $PDO_{naïve}$ vs PDO_{res} (**Figure 6.8**). I then removed pathways that were deregulated in the same direction in the absence and presence of 5FU treatment in each PDO group. The remaining pathways were those that were only significantly deregulated in PDO_{res} compared to

$PDO_{naïve}$ when treated with 5FU but not when these cells were untreated. Importantly, this approach is more stringent than the GSEA enrichment approach used for the initial comparison of PDO_{res} vs $PDO_{naïve}$ as it is not based on the changes in the expression rank of all genes in the RNA-Seq data, but is restricted to those genes showing significant and large expression changes of at least 2-fold.

Application of the GSEA Hallmarks pathway collection identified 9 pathways that were significantly upregulated in PDO_{res} during 5FU treatment but not in $PDO_{naïve}$ during treatment, with one significantly downregulated pathway (**Figure 6.8**). Hallmark signatures upregulated by TNFα, by p53, by low level hypoxia and genes implicated in apoptosis were the most interesting pathways that were significantly enriched in PDO_{res} during 5FU treatment. The TNFα signature had already been identified to be significantly enriched in PDO_{res} in comparison to $PDO_{naïve}$ in the absence of treatment and this indicates that there is further increase in TNFα signalling in PDO_{res} vs $PDO_{naïve}$ during 5FU treatment. These data, generated through a second independent expression analysis of the biobank of chemotherapy naïve and resistant PDOs in the presence or absence of 5FU therefore further highlight a potential contribution of increased TNFα to 5FU resistance in PDO_{res}.

I finally investigated whether genes that have been described to associate with chemotherapy resistance, predominantly based on the study of CRC cell lines, were deregulated in our PDO_{res}. No upregulation of TYMS expression was observed; neither were multi-drug efflux pumps (so called ABC transporters) overexpressed in PDO_{res} in the absence of treatment or following 5FU. Thus, based on RNA-sequencing analysis of our living CRC biobank, we would not support a role of these genes as mediators of chemoresistance in these models.

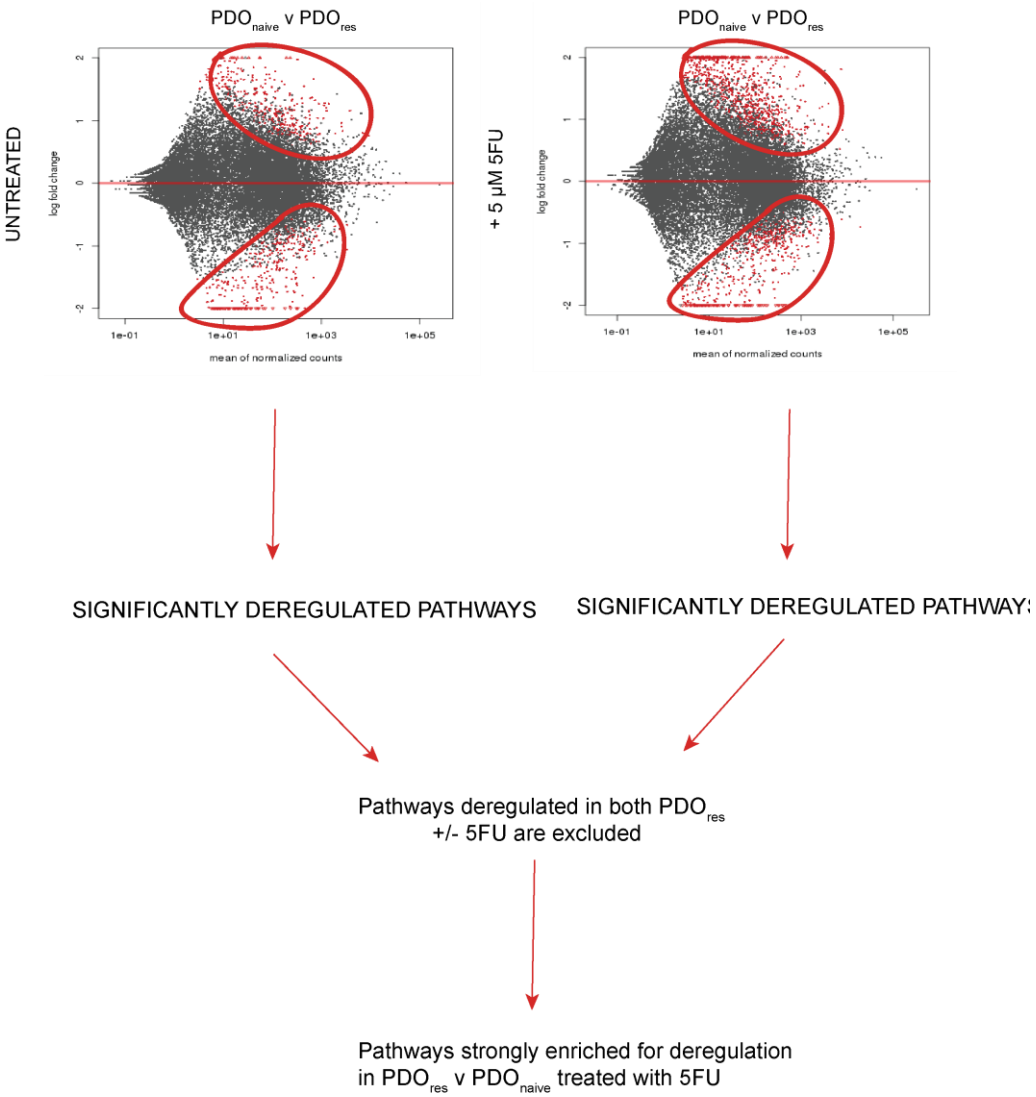

Gene Set Database	Gene Set Name	# Genes in Overlap	FDR q-value
Hallmark pathways	HALLMARK_TNFA_SIGNALING_VIA_NFKB	16	8.39 e-8
	HALLMARK_P53_PATHWA	15	3.6 e-7
	HALLMARK_HYPOXIA	14	1.33 e-6
	HALLMARK_BILE_ACID_METABOLISM	10	6.73 e-6
	HALLMARK_GLYCOLYSIS	13	6.73 e-6
	HALLMARK_MYOGENESIS	12	3.02 e-5
	HALLMARK_COMPLEMENT	11	1.39 e-4
	HALLMARK_APOPTOSIS	9	4.84 e-4
	HALLMARK_ADIPOGENESIS	10	4.84 e-4
	HALLMARK_HEME_METABOLISM	8	6.85 e-4

Figure 6.8 Workflow of pathway analysis.

MA plots show genes differentially expressed in $PDO_{naïve}$ and PDO_{res} in both untreated and 5FU treated conditions. Upregulated and downregulated gene lists were then run through GSEA pathway analysis to give significantly deregulated pathways in both untreated and 5FU conditions. Any pathways that were significantly deregulated in both PDO_{res} untreated and 5FU treated were excluded. This left pathways that are significantly deregulated in $PDO_{naïve}$ v PDO res after 5FU treatment. Top pathways from the Hallmarks database and Oncogenic Signature database (FDR<0.25) are shown. Red shading indicates upregulation, and blue shading indicates downregulation.

6.5. Discussion

Gaining a better understanding of the mechanisms behind chemotherapy resistance is essential to be able to improve patient outcomes in the future. In this chapter, I have established and characterised a clinically relevant collection of PDO models that will enable future interrogation of CRC chemoresistance mechanisms. Over the past few years, increasing numbers of studies have been published detailing biobanks of PDOs from patient specimens with multiomics analysis approaches in many different cancer types (Li et al., 2018; Tiriac et al., 2018; Vlachogiannis et al., 2018). The accumulation of these data exemplifies that PDOs are considered key models to facilitate clinical translation problems.

Characterisation of the drug sensitivities of two cohorts of PDO; PDO_{res} and $PDO_{naïve}$, validated that PDOs derived from patients that have failed to respond to chemotherapy are resistant to 5FU and SN38 *in vitro.* Importantly, this indicates that chemoresistance is a cell intrinsic property. Furthermore, the cohort includes a matched pair of chemotherapy naïve and resistant PDOs from the same patient who had acquired resistance to 5FU. This is reflected in the drug sensitivity data of the PDO pair. The following data are important for our understanding of chemoresistance as new *in vitro* model systems with long term viability for the study of drug resistance mechanisms can be interrogated by various molecular technologies and can also be perturbed for example using CRISPR. They can furthermore be used for preclinical analysis and validation of novel drugs that are thought to overcome chemoresistance in CRC. As the drug sensitivity assay that I used adapted was from a high-throughput screening protocol, it is therefore possible to perform large-scale drug screens in this PDO model in the future. A previous study which derived PDOs from the same patient cohort as those described in this chapter, concluded that PDOs have the capability to be used for functional genomics and could be used to inform treatment decisions in patients (Vlachogiannis et al., 2018). Studies that have derived PDOs from patient specimens (Tiriac et al., 2018; Vlachogiannis et al., 2018) have used them to determine potential targeted therapies that can be

used once a patient is deemed chemo-refractory, thus highlighting the future application of the model derived here.

RNA sequencing data of PDO_{res} vs $PDO_{naïve}$ showed that these two groups significantly differed with respect to the expression of pathway signatures including MYC expression, NFκB signalling and TNFα signalling. Furthermore, genes involved in TNFα signalling were further upregulated in PDO_{res} during 5FU treatment suggesting this is an important signalling pathway for 5FU resistance. TNFα has two forms, as a soluble cytokine and a transmembrane receptor. The receptor is cleaved by metalloproteases to give the soluble form (Balkwill, 2006). The soluble pleiotropic cytokine TNFα has been shown to induce drug resistance through constitutive activation of NFκB signalling (Acharyya et al., 2012; Wang et al., 2005). Furthermore, transmembrane TNFα has also been implicated in doxorubicin resistance in breast cancer via constitutive activation of NFκB (Zhang et al., 2018). Conversely, in CRC cell lines, TNFα-dependent necroptosis, a newly described form of programmed cell death was seen in response to 5FU treatment (Metzig et al., 2016). Thus the role that pleotropic TNFα signalling plays in 5FU resistance, and moreover if this is mediated through constitutive NFκB, requires further research. Analysis of the genes in the TNFα signature that are significantly deregulated in 5FU-treated resistant PDOs may start to identify genes of interest.

I found that over 1000 genes were significantly deregulated through a sub-lethal dose of 5FU in $PDO_{naïve}$ but only 53 in PDO_{res}, consistent with the minimal effect of 5FU observed *in vitro* in some PDO_{res} lines. As mentioned, an overlap of 43 differentially expressed genes indicates similarity in responses do occur, however limited they may be. The reduced response observed in resistance lines could potentially be the result of chemotherapy not triggering effector mechanisms such as apoptosis and cell arrest in the resistant cells. The enrichment of genes regulated by p53 or with a role in apoptosis in PDO_{res} during 5FU treatment was most surprising as these pathways are considered to

promote cell death and chemotherapy sensitivity. However, p53 and apoptosis signatures both contain large numbers of genes and it will be important to assess through future functional studies whether these relatively small subsets involve predominantly negative regulators of apoptotic response. Many hypoxia-induced genes, another upregulated signature, mediate resilience to the harsh conditions encountered by cells within the tumour and future functional analyses here may also be promising.

This is a rich dataset which will be further analysed in my host lab however these results have already begun to define specific pathways and lists of deregulated genes that are likely to include the mechanisms that are responsible for drug resistance in these PDOs. My host lab is currently developing plans for CRISPR knockout and overexpression screens and to test whether targeting these pathways with relevant drugs can reverse resistance and hence validate the specific molecular changes that drive resistance. This may indicate novel targeted therapies or combination therapies that are effective against chemo-refractory CRCs.

Chapter 7: Final Conclusions and Future Implications.

The aim of my thesis was to better understand the mechanisms that underlie drug resistance in gastro-intestinal (GI) cancers and to investigate new therapeutic approaches to overcome resistance. I assessed mechanisms of primary resistance that are a major hindrance for more effective oncogene targeting therapies in gastro-oesophageal adenocarcinomas (GOAs) and for anti-EGFR therapies in colorectal cancer (CRC). In addition, despite good responses achieved with anti-EGFR agents in a proportion of CRCs, the acquisition of resistance is inevitable in most of these patients and I also investigated the mechanism behind this.

The work presented here addresses multiple aspects that have all been suggested or shown to contribute to drug resistance and therapy failure in cancer, such as intratumour heterogeneity, the need for improved stratification strategies, the contribution of cell intrinsic characteristics versus the tumour microenvironment and finally starts to address the complex and poorly understood field of chemotherapy resistance. Crucially, as my work is informed by clinical data, genetic and transcriptomic analyses of tumour samples and by PDOs established from clinical trial patients, the drivers and mechanisms of drug resistance that were interrogated and validated here are clinically relevant.

In Chapter 3, I have shown that GOA cell lines that harboured a diverse RTK (*ERBB2, MET*) and *NRAS* amplifications and *KRAS* mutations can be targeted with equal efficacy with a novel class of paradox-breaking pan-RAF inhibitors developed at the ICR. I furthermore showed hypersensitivity of *FGFR2*-amplified GOA cells to this new agent and found that even a GOA cell line without any known aberrations of RTKs or the MAPK pathway responded. Although efficacy required high doses *in vitro*, tumour control was also achieved in three GOA

different xenograft models *in vivo*, providing pre-clinical proof of concept that this agent is effective against GOAs. These results detail the first use of pan-RAF inhibitors in GOA. Furthermore, these data suggest that pan-RAF inhibitors may be able to successfully combat GOA tumours that often harbour subclones with multiple distinct RTK or MAPK pathway aberrations by inhibiting the downstream signalling pathway where the functional effect converges. The pan-RAF inhibitor used in this study was effective as a single-agent drug whereas other inhibitors of the MAPK pathway such as ERK and MEK inhibitors were only able to partially suppress growth. This may start to move the paradigm away from the idea of ever increasing patient stratification to an approach that instead targets the common downstream pathway. This may not only be beneficial as it potentially reduces the need for accurate molecular testing which is challenging in metastatic tumours with high intratumour heterogeneity of driver aberrations, but the pan-RAF inhibitor may not need to be administered as a combinatorial drug regimen, as has been shown to be necessary for example for MEK inhibitors in many tumour types, and thus this may reduce toxicities (Long et al., 2014; Long et al., 2015). Due to the breadth of the aberrations that may be targeted using this drug, it has the benefits of a combinatorial drug regimen yet the side effects associated with combination therapies may also be alleviated. Furthermore the hypersensitivity against *FGFR2*-amplified GOAs warrants testing against other cancer types with these amplifications, such as breast cancer. Additionally further analysis of the signalling pathway inhibition induced in *FGFR2*-amplified GOAs versus other RTK amplifications will gather insights into the mechanistic bias of this hypersensitivity. Overall, the work presented here provides evidence to justify of pan-RAF inhibitor testing in early clinical trials in GOA.

Patient stratification is reliant on the identification of predictive biomarkers for response. As stated in the introduction, despite treatment stratification to exclude patients with activating *KRAS* and *NRAS* mutations, primary resistance to the anti-EGFR antibody cetuximab is still commonly observed in the clinic. My results in Chapter 4 detail a new driver of primary resistance, *NF1,* that was fully

validated in both biochemical assays showing reactivation of ERK phosphorylation and drug sensitivity assays in cell lines expressing the mutated gene. Additionally BRAF D594 mutations and hypomorphic KRAS were validated by biochemical assays. Several of the latter putative drivers were observed clinically, either together (BRAF D594F and KRAS L19F) or in combination with low level gain of the mutant allele (KRAS A18D) which may suggest that these aberrations cooperate and thus this should be further interrogated. It is however more difficult to validate the predictive role of hypomorphic *KRAS* mutations and BRAF D594 mutations as these are rare in large cohorts, <1%, hence requiring very clinical large trials. Their low prevalence would also limit their clinical impact. Collectively though these results indicate that that pre-screening stratification for known drivers of resistance in cetuximab should potentially be extended beyond the current inclusions of *KRAS* and *NRAS* codons. My group has provided further evidence that BRAF V600E mutations were invariably associated with primary resistance to cetuximab (Loupakis et al., 2009; Woolston et al., 2019) and thus further supports the use of this as a predictive biomarker.

NF1 inactivation as a primary driver of cetuximab resistance now requires validation in randomized trials with cetuximab therapy. This should hopefully confirm its role in resistance as either a predictive or prognostic biomarker and use in stratification, which would save up to 5% of CRC patients that show *NF1* mutations unnecessary treatment. However *NF1* inactivation will be more difficult to detect by genetic assays than other biomarkers such as *KRAS* as it will require testing for biallelic inactivation that often occurs through a combination of mutation and copy number loss.

When my host lab started analysing samples from the PROSPECT-C trial, acquired cetuximab resistance was thought to be driven almost exclusively by genetic aberrations that re-activate the MAPK pathway (Misale et al., 2014). However, we found that 64% of biopsies from CRC that had acquired resistance to single agent cetuximab in this trial did not harbour any known or novel

genetic resistance driver. This could either indicate that there are genetic events that are too infrequent to be identifiable in this small cohort to contribute to resistance or indeed that non-genetic factors play a role. Based on transcriptomic analyses of pre-treatment and progression biopsies from the trial, my host lab showed that such tumours frequently changed their transcriptomic subtype from the cetuximab sensitive CMS2 subtype to the fibroblast rich mesenchymal subtype CMS4. In Chapter 5, I demonstrated that CAF conditioned medium alone was sufficient to reverse growth inhibition and suppression of ERK phosphorylation caused by cetuximab treatment in CRC cell lines. I subsequently showed that this was mediated by HGF, FGF1 and FGF2, growth factors that were produced by fibroblasts. Combined blockade of the receptors for these growth factors with MET and pan-FGFR inhibitors together with cetuximab was furthermore able to reverse resistance induced by CAF-conditioned medium. However treatment-related toxicities often limit the impact of combination therapies, and furthermore can require dose-reduction relative to singe-agent maximum doses (Al-Lazikani et al., 2012). Thus although inhibiting MET, FGFR and EGFR signalling in combination is able to combat the effect of conditioned medium *in vitro*, it is unlikely that this presents a viable therapeutic option. Whilst I have successfully validated a role of CAFs as a mediator of acquired cetuximab resistance *in vitro,* I was unable to model this interaction *in vivo*. α-SMA staining of tumours 3 weeks post injection revealed that fibroblasts could not be detected in excess in comparison to tumours with tumour cells only. Thus better mouse modelling systems for the *in vivo* co-culture of CAFs and tumour cells are required. Better modelling will allow for the elucidation of answers to questions such as; how cancer cells can recruit and activate fibroblasts and also how these interactions result in poor survival and resistance to treatment, concepts that are currently still not well understood. Recently CMS subtypes have been faithfully recapitulated in PDX models from primary CRCs, liver metastases and CRC cell lines and these could be utilised in the future to model CAF-mediated resistance (Linnekamp et al., 2018; Sveen et al., 2018). Effective modelling of the TME in mice is difficult for two reasons; firstly there is a discord between signalling molecules produced by

mice and humans and secondly these studies are often carried out in mice lacking an immune system, a key part of the TME. Targeting or reprogramming factors in the TME to prevent cancer progression feeds into a paradigm of understanding cancer as a "*complex ecosystem"* rather than a *"tenacious weed"* (Tauriello and Batlle, 2016). Reprogramming the TME therapeutically requires a translational research effort, whereby scientific research must be informed by relevant clinical data. My data furthermore reinforces the need to integrate the analysis of tumour stromal composition and its interactions with cancer cells into translational clinical studies and cancer models as this can have profound and clinically important effects.

Finally, in Chapter 6 I have developed and characterized a living biobank of chemotherapy naïve and resistant CRC patient derived PDOs. Chemotherapy is still the most effective treatment modality in metastatic CRCs and this PDO collection now allows us to investigate mechanisms of therapy resistance that should eventually lead to approaches to reverse or target resistance. Furthermore, this PDO collection can also be used to preclinically test novel drugs for their activity against treatment refractory CRCs in PDO model systems which are thought to better represent patient tumours than existing cell lines (Vlachogiannis et al., 2018). The RNAseq data generated in this thesis was a first attempt to reveal some of the molecular pathways associated with resistance. Several interesting pathways were identified, such as TNF signalling, and testing is now required to dissect their impact on chemoresistance. Furthermore I found no evidence of often suggested resistance mechanism such as TYMS or ABR multidrug efflux pump upregulation. Thus the model PDO system is already proving useful in identifying that previous concepts of chemotherapy resistance may need to be revised. More PDOs are under development in my host lab, and thus this model system will be further added to in the future. Taken together, this living CRC biobank is a novel tool that may eventually provide a game-changing understanding of why CRCs fail to respond to chemotherapy.

To conclude, in my thesis I have tackled the multifaceted yet recurrent issue of drug resistance in two of the most common cancers to result in death (World Health Organisation). In GOA, and in particular *FGFR2*-amplified GOA, I have provided evidence and rational basis for a clinical trial of a novel indication of the targeted therapy, CCT196969, a pan-RAF inhibitor. The use of such drug highlights how carefully designed targeted therapies may interrogate intratumour heterogeneity. In colorectal cancer, I have validated a novel driver of primary resistance, NF1, which following successful validation in clinical trials would prevent ~5% of colorectal cancer patients receiving unnecessary treatment. I have elucidated a mechanism through which CAFs are able to induce acquired cetuximab resistance, therefore providing an explanation for the CMS2>4 subtype switch observed in patients. Lastly I have established and characterised a translational model system for chemotherapy resistance that can be used in further research. Thus I have shown data to further the understanding of many key themes of the complexity of drug resistance; intratumour heterogeneity, patient stratification and the role of the tumour microenvironment. The clinical basis of the data that I have shown highlights its importance in furthering our understanding of drug resistance. Further validation of these results will hopefully inform novel biomarker and treatment strategies that can ultimately lead to better cancer patient outcomes through increased survival and sparing them toxicities from ineffective treatments.

Chapter 8: References

Abolhoda, A., Wilson, A. E., Ross, H., Danenberg, P. V., Burt, M., and Scotto, K. W. (1999). Rapid activation of MDR1 gene expression in human metastatic sarcoma after in vivo exposure to doxorubicin. Clinical Cancer Research *5*, 3352-3356.

Acharyya, S., Oskarsson, T., Vanharanta, S., Malladi, S., Kim, J., Morris, P. G., Manova-Todorova, K., Leversha, M., Hogg, N., and Seshan, V. E. (2012). A CXCL1 paracrine network links cancer chemoresistance and metastasis. Cell *150*, 165-178.

Agarwal, R., and Kaye, S. B. (2003). Ovarian cancer: strategies for overcoming resistance to chemotherapy. Nature Reviews Cancer *3*, 502-516.

Ahlquist, T., Bottillo, I., Danielsen, S. A., Meling, G. I., Rognum, T. O., Lind, G. E., Dallapiccola, B., and Lothe, R. A. (2008). RAS signaling in colorectal carcinomas through alteration of RAS, RAF, NF1, and/or RASSF1A. Neoplasia (New York, NY) *10*, 680.

Al-Hajj, M., Wicha, M. S., Benito-Hernandez, A., Morrison, S. J., and Clarke, M. F. (2003). Prospective identification of tumorigenic breast cancer cells. Proceedings of the National Academy of Sciences *100*, 3983-3988.

Al-Lazikani, B., Banerji, U., and Workman, P. (2012). Combinatorial drug therapy for cancer in the post-genomic era. Nature biotechnology *30*, 679.

Allegra, C. J., Rumble, R. B., Hamilton, S. R., Mangu, P. B., Roach, N., Hantel, A., and Schilsky, R. L. (2016). Extended RAS Gene Mutation Testing in Metastatic Colorectal Carcinoma to Predict Response to Anti-Epidermal Growth Factor Receptor Monoclonal Antibody Therapy: American Society of Clinical Oncology Provisional Clinical Opinion Update 2015. J Clin Oncol *34*, 179-185.

Amado, R. G., Wolf, M., Peeters, M., Van Cutsem, E., Siena, S., Freeman, D. J., Juan, T., Sikorski, R., Suggs, S., Radinsky, R.*, et al.* (2008). Wild-type KRAS is required for panitumumab efficacy in patients with metastatic colorectal cancer. J Clin Oncol *26*, 1626-1634.

Arango, D., Mariadason, J., Wilson, A., Yang, W., Corner, G., Nicholas, C., Aranes, M., and Augenlicht, L. H. (2003). c-Myc overexpression sensitises colon cancer cells to camptothecin-induced apoptosis. British journal of cancer *89*, 1757.

Arena, S., Bellosillo, B., Siravegna, G., Martinez, A., Canadas, I., Lazzari, L., Ferruz, N., Russo, M., Misale, S., Gonzalez, I.*, et al.* (2015). Emergence of Multiple EGFR Extracellular Mutations during Cetuximab Treatment in Colorectal Cancer. Clin Cancer Res *21*, 2157-2166.

Attieh, Y., and Vignjevic, D. M. (2016). The hallmarks of CAFs in cancer invasion. European journal of cell biology *95*, 493-502.

Balkwill, F. (2006). TNF-α in promotion and progression of cancer. Cancer and Metastasis Reviews *25*, 409.

Banck, M. S., and Grothey, A. (2009). Biomarkers of resistance to epidermal growth factor receptor monoclonal antibodies in patients with metastatic colorectal cancer. Clinical Cancer Research *15*, 7492-7501.

Bang, Y.-J., Van Cutsem, E., Feyereislova, A., Chung, H. C., Shen, L., Sawaki, A., Lordick, F., Ohtsu, A., Omuro, Y., and Satoh, T. (2010). Trastuzumab in combination with chemotherapy versus

chemotherapy alone for treatment of HER2-positive advanced gastric or gastro-oesophageal junction cancer (ToGA): a phase 3, open-label, randomised controlled trial. The Lancet *376*, 687-697.

Bardelli, A., Corso, S., Bertotti, A., Hobor, S., Valtorta, E., Siravegna, G., Sartore-Bianchi, A., Scala, E., Cassingena, A., Zecchin, D*., et al.* (2013). Amplification of the MET receptor drives resistance to anti-EGFR therapies in colorectal cancer. Cancer Discov *3*, 658-673.

Basu, T. N., Gutmann, D. H., Fletcher, J. A., Glover, T. W., Collins, F. S., and Downward, J. (1992). Aberrant regulation of ras proteins in malignant tumour cells from type 1 neurofibromatosis patients. Nature *356*, 713.

Bertotti, A., Papp, E., Jones, S., Adleff, V., Anagnostou, V., Lupo, B., Sausen, M., Phallen, J., Hruban, C. A., Tokheim, C*., et al.* (2015). The genomic landscape of response to EGFR blockade in colorectal cancer. Nature *526*, 263-267.

Bettegowda, C., Sausen, M., Leary, R. J., Kinde, I., Wang, Y., Agrawal, N., Bartlett, B. R., Wang, H., Luber, B., Alani, R. M*., et al.* (2014). Detection of circulating tumor DNA in early- and late-stage human malignancies. Sci Transl Med *6*, 224ra224.

Birchmeier, C., Birchmeier, W., Gherardi, E., and Woude, G. F. V. (2003). Met, metastasis, motility and more. Nature reviews Molecular cell biology *4*, 915.

Bokemeyer, C., Bondarenko, I., Hartmann, J., De Braud, F., Schuch, G., Zubel, A., Celik, I., Schlichting, M., and Koralewski, P. (2011). Efficacy according to biomarker status of cetuximab plus FOLFOX-4 as first-line treatment for metastatic colorectal cancer: the OPUS study. Annals of Oncology *22*, 1535-1546.

Bokemeyer, C., Van Cutsem, E., Rougier, P., Ciardiello, F., Heeger, S., Schlichting, M., Celik, I., and Kohne, C. H. (2012). Addition of cetuximab to chemotherapy as first-line treatment for KRAS wild-type metastatic colorectal cancer: pooled analysis of the CRYSTAL and OPUS randomised clinical trials. Eur J Cancer *48*, 1466-1475.

Boland, C. R., Thibodeau, S. N., Hamilton, S. R., Sidransky, D., Eshleman, J. R., Burt, R. W., Meltzer, S. J., Rodriguez-Bigas, M. A., Fodde, R., and Ranzani, G. N. (1998). A National Cancer Institute Workshop on Microsatellite Instability for cancer detection and familial predisposition: development of international criteria for the determination of microsatellite instability in colorectal cancer. In, (AACR).

Bollag, G., Hirth, P., Tsai, J., Zhang, J., Ibrahim, P. N., Cho, H., Spevak, W., Zhang, C., Zhang, Y., Habets, G*., et al.* (2010). Clinical efficacy of a RAF inhibitor needs broad target blockade in BRAF-mutant melanoma. Nature *467*, 596-599.

Bracht, K., Nicholls, A., Liu, Y., and Bodmer, W. (2010). 5-Fluorouracil response in a large panel of colorectal cancer cell lines is associated with mismatch repair deficiency. British journal of cancer *103*, 340.

Bradley, C. A., Dunne, P. D., Bingham, V., McQuaid, S., Khawaja, H., Craig, S., James, J., Moore, W. L., McArt, D. G., and Lawler, M. (2016). Transcriptional upregulation of c-MET is associated with invasion and tumor budding in colorectal cancer. Oncotarget *7*, 78932.

Brinkman, E. K., Chen, T., Amendola, M., and van Steensel, B. (2014). Easy quantitative assessment of genome editing by sequence trace decomposition. Nucleic acids research *42*, e168-e168.

Calon, A., Espinet, E., Palomo-Ponce, S., Tauriello, D. V., Iglesias, M., Céspedes, M. V., Sevillano, M., Nadal, C., Jung, P., Zhang, X. H., *et al.* (2012). Dependency of colorectal cancer on a TGF-β-driven program in stromal cells for metastasis initiation. Cancer Cell *22*, 571-584.

Calon, A., Lonardo, E., Berenguer-Llergo, A., Espinet, E., Hernando-Momblona, X., Iglesias, M., Sevillano, M., Palomo-Ponce, S., Tauriello, D. V., Byrom, D., *et al.* (2015). Stromal gene expression defines poor-prognosis subtypes in colorectal cancer. Nat Genet *47*, 320-329.

Campbell, P. J., Stephens, P. J., Pleasance, E. D., O'Meara, S., Li, H., Santarius, T., Stebbings, L. A., Leroy, C., Edkins, S., Hardy, C., *et al.* (2008). Identification of somatically acquired rearrangements in cancer using genome-wide massively parallel paired-end sequencing. Nat Genet *40*, 722-729.

Cancer Research UK. In.

Carcas, L. P. (2014). Gastric cancer review. Journal of carcinogenesis *13*.

Cawkwell, L., Lewis, F., and Quirke, P. (1994). Frequency of allele loss of DCC, p53, RBI, WT1, NF1, NM23 and APC/MCC in colorectal cancer assayed by fluorescent multiplex polymerase chain reaction. British journal of cancer *70*, 813.

Chapman, P. B. (2013). Mechanisms of resistance to RAF inhibition in melanomas harboring a BRAF mutation. Am Soc Clin Oncol Educ Book.

Chapman, P. B., Hauschild, A., Robert, C., Haanen, J. B., Ascierto, P., Larkin, J., Dummer, R., Garbe, C., Testori, A., and Maio, M. (2011). Improved survival with vemurafenib in melanoma with BRAF V600E mutation. New England Journal of Medicine *364*, 2507-2516.

Chen, C. H., Hsia, T. C., Yeh, M. H., Chen, T. W., Chen, Y. J., Chen, J. T., Wei, Y. L., Tu, C. Y., and Huang, W. C. (2017a). MEK inhibitors induce Akt activation and drug resistance by suppressing negative feedback ERK‐mediated HER 2 phosphorylation at Thr701. Molecular oncology *11*, 1273-1287.

Chen, T., You, Y., Jiang, H., and Wang, Z. Z. (2017b). Epithelial–mesenchymal transition (EMT): a biological process in the development, stem cell differentiation, and tumorigenesis. Journal of cellular physiology *232*, 3261-3272.

Chuang, C.-F., and Ng, S.-Y. (1994). Functional divergence of the MAP kinase pathway ERK1 and ERK2 activate specific transcription factors. FEBS letters *346*, 229-234.

Ciardiello, F., Arnold, D., Casali, P. G., Cervantes, A., Douillard, J.-Y., Eggermont, A., Eniu, A., McGregor, K., Peters, S., and Piccart, M. (2014). Delivering precision medicine in oncology today and in future—the promise and challenges of personalised cancer medicine: a position paper by the European Society for Medical Oncology (ESMO). In, (Oxford University Press).

Ciardiello, F., and Tortora, G. (2008). EGFR antagonists in cancer treatment. New England Journal of Medicine *358*, 1160-1174.

Clevers, H. (2006). Wnt/β-catenin signaling in development and disease. Cell *127*, 469-480.

Clevers, H. (2011). The cancer stem cell: premises, promises and challenges. Nature medicine *17*, 313.

Corcoran, R. B., Ebi, H., Turke, A. B., Coffee, E. M., Nishino, M., Cogdill, A. P., Brown, R. D., Della Pelle, P., Dias-Santagata, D., Hung, K. E., *et al.* (2012). EGFR-mediated re-activation of MAPK signaling contributes to insensitivity of BRAF mutant colorectal cancers to RAF inhibition with vemurafenib. Cancer Discov *2*, 227-235.

Cox, A. D., Fesik, S. W., Kimmelman, A. C., Luo, J., and Der, C. J. (2014). Drugging the undruggable RAS: Mission possible? Nat Rev Drug Discov *13*, 828-851.

Cunningham, D., Allum, W. H., Stenning, S. P., Thompson, J. N., Van de Velde, C. J., Nicolson, M., Scarffe, J. H., Lofts, F. J., Falk, S. J., and Iveson, T. J. (2006). Perioperative chemotherapy versus surgery alone for resectable gastroesophageal cancer. New England Journal of Medicine *355*, 11-20.

Cunningham, D., Humblet, Y., Siena, S., Khayat, D., Bleiberg, H., Santoro, A., Bets, D., Mueser, M., Harstrick, A., Verslype, C*., et al.* (2004). Cetuximab monotherapy and cetuximab plus irinotecan in irinotecan-refractory metastatic colorectal cancer. N Engl J Med *351*, 337-345.

Cunningham, D., Pyrhönen, S., James, R. D., Punt, C. J., Hickish, T. F., Heikkila, R., Johannesen, T. B., Starkhammar, H., Topham, C. A., and Awad, L. (1998). Randomised trial of irinotecan plus supportive care versus supportive care alone after fluorouracil failure for patients with metastatic colorectal cancer. The Lancet *352*, 1413-1418.

Cunningham, D., Starling, N., Rao, S., Iveson, T., Nicolson, M., Coxon, F., Middleton, G., Daniel, F., Oates, J., and Norman, A. R. (2008). Capecitabine and oxaliplatin for advanced esophagogastric cancer. New England Journal of Medicine *358*, 36-46.

Cunningham, D., Tebbutt, N. C., Davidenko, I., Murad, A. M., Al-Batran, S.-E., Ilson, D. H., Tjulandin, S., Gotovkin, E., Karaszewska, B., and Bondarenko, I. (2015). Phase III, randomized, double-blind, multicenter, placebo (P)-controlled trial of rilotumumab (R) plus epirubicin, cisplatin and capecitabine (ECX) as first-line therapy in patients (pts) with advanced MET-positive (pos) gastric or gastroesophageal junction (G/GEJ) cancer: RILOMET-1 study. In, (American Society of Clinical Oncology).

Davies, H., Bignell, G. R., Cox, C., Stephens, P., Edkins, S., Clegg, S., Teague, J., Woffendin, H., Garnett, M. J., and Bottomley, W. (2002). Mutations of the BRAF gene in human cancer. Nature *417*, 949.

de Bruin, E. C., Cowell, C., Warne, P. H., Jiang, M., Saunders, R. E., Melnick, M. A., Gettinger, S., Walther, Z., Wurtz, A., Heynen, G. J*., et al.* (2014). Reduced NF1 expression confers resistance to EGFR inhibition in lung cancer. Cancer Discov *4*, 606-619.

Deak, M., Clifton, A. D., Lucocq, J. M., and Alessi, D. R. (1998). Mitogen‐and stress‐activated protein kinase‐1 (MSK1) is directly activated by MAPK and SAPK2/p38, and may mediate activation of CREB. The EMBO journal *17*, 4426-4441.

Dhillon, A. S., Hagan, S., Rath, O., and Kolch, W. (2007). MAP kinase signalling pathways in cancer. Oncogene *26*, 3279-3290.

Diaz, L. A., Jr., Williams, R. T., Wu, J., Kinde, I., Hecht, J. R., Berlin, J., Allen, B., Bozic, I., Reiter, J. G., Nowak, M. A*., et al.* (2012). The molecular evolution of acquired resistance to targeted EGFR blockade in colorectal cancers. Nature *486*, 537-540.

Douillard, J., Cunningham, D., Roth, A., Navarro, M., James, R., Karasek, P., Jandik, P., Iveson, T., Carmichael, J., and Alakl, M. (2000). Irinotecan combined with fluorouracil compared with fluorouracil alone as first-line treatment for metastatic colorectal cancer: a multicentre randomised trial. The Lancet *355*, 1041-1047.

Douillard, J. Y., Oliner, K. S., Siena, S., Tabernero, J., Burkes, R., Barugel, M., Humblet, Y., Bodoky, G., Cunningham, D., Jassem, J*., et al.* (2013). Panitumumab-FOLFOX4 treatment and RAS mutations in colorectal cancer. N Engl J Med *369*, 1023-1034.

Downward, J. (2009). Cancer: A tumour gene's fatal flaws. Nature *462*, 44.

Downward, J., Parker, P., and Waterfield, M. (1984). Autophosphorylation sites on the epidermal growth factor receptor. Nature *311*, 483.

Dutton, S. J., Ferry, D. R., Blazeby, J. M., Abbas, H., Dahle-Smith, A., Mansoor, W., Thompson, J., Harrison, M., Chatterjee, A., Falk, S.*, et al.* (2014). Gefitinib for oesophageal cancer progressing after chemotherapy (COG): a phase 3, multicentre, double-blind, placebo-controlled randomised trial. Lancet Oncol *15*, 894-904.

Dylla, S. J., Beviglia, L., Park, I.-K., Chartier, C., Raval, J., Ngan, L., Pickell, K., Aguilar, J., Lazetic, S., and Smith-Berdan, S. (2008). Colorectal cancer stem cells are enriched in xenogeneic tumors following chemotherapy. PloS one *3*, e2428.

Eupheria Biotechnology. In, p. esiCRISPR kits.

Evans, R. A., Tian, Y. C., Steadman, R., and Phillips, A. O. (2003). TGF-β1-mediated fibroblast–myofibroblast terminal differentiation—the role of smad proteins. Experimental cell research *282*, 90-100.

Fearon, E. R., and Vogelstein, B. (1990). A genetic model for colorectal tumorigenesis. cell *61*, 759-767.

Felipe De Sousa, E. M., Wang, X., Jansen, M., Fessler, E., Trinh, A., De Rooij, L. P., De Jong, J. H., De Boer, O. J., Van Leersum, R., and Bijlsma, M. F. (2013). Poor-prognosis colon cancer is defined by a molecularly distinct subtype and develops from serrated precursor lesions. Nature medicine *19*, 614.

Ferrell, J. E., and Bhatt, R. R. (1997). Mechanistic studies of the dual phosphorylation of mitogen-activated protein kinase. Journal of Biological Chemistry *272*, 19008-19016.

Ferro, A., Peleteiro, B., Malvezzi, M., Bosetti, C., Bertuccio, P., Levi, F., Negri, E., La Vecchia, C., and Lunet, N. (2014). Worldwide trends in gastric cancer mortality (1980–2011), with predictions to 2015, and incidence by subtype. European journal of cancer *50*, 1330-1344.

Flaherty, K. T., Robert, C., Hersey, P., Nathan, P., Garbe, C., Milhem, M., Demidov, L. V., Hassel, J. C., Rutkowski, P., Mohr, P.*, et al.* (2012). Improved survival with MEK inhibition in BRAF-mutated melanoma. N Engl J Med *367*, 107-114.

Flis, S., and SPŁAWIŃSKI, J. (2009). Inhibitory effects of 5-fluorouracil and oxaliplatin on human colorectal cancer cell survival are synergistically enhanced by sulindac sulfide. Anticancer research *29*, 435-441.

Francies, H. E., Barthorpe, A., McLaren-Douglas, A., Barendt, W. J., and Garnett, M. J. (2016). Drug Sensitivity Assays of Human Cancer Organoid Cultures. Methods Mol Biol.

Fu, Y., Jovelet, C., Filleron, T., Pedrero, M., Motté, N., Boursin, Y., Luo, Y., Massard, C., Campone, M., and Levy, C. (2016). Improving the performance of somatic mutation identification by recovering circulating tumor DNA mutations. Cancer research *76*, 5954-5961.

Fuchs, C. S., Tomasek, J., Yong, C. J., Dumitru, F., Passalacqua, R., Goswami, C., Safran, H., Dos Santos, L. V., Aprile, G., and Ferry, D. R. (2014). Ramucirumab monotherapy for previously treated advanced gastric or gastro-oesophageal junction adenocarcinoma (REGARD): an international, randomised, multicentre, placebo-controlled, phase 3 trial. The Lancet *383*, 31-39.

Fuxe, J., and Karlsson, M. C. (2012). TGF-β-induced epithelial-mesenchymal transition: a link between cancer and inflammation. Paper presented at: Seminars in cancer biology (Elsevier).

Gerlinger, M., Horswell, S., Larkin, J., Rowan, A. J., Salm, M. P., Varela, I., Fisher, R., McGranahan, N., Matthews, N., and Santos, C. R. (2014). Genomic architecture and evolution of clear cell renal cell carcinomas defined by multiregion sequencing. Nature genetics *46*, 225.

Gerlinger, M., Rowan, A. J., Horswell, S., Larkin, J., Endesfelder, D., Gronroos, E., Martinez, P., Matthews, N., Stewart, A., and Tarpey, P. (2012). Intratumor heterogeneity and branched evolution revealed by multiregion sequencing. New England journal of medicine *366*, 883-892.

Gerlinger, M., and Swanton, C. (2010). How Darwinian models inform therapeutic failure initiated by clonal heterogeneity in cancer medicine. British journal of cancer *103*, 1139.

Giacchetti, S., Perpoint, B., Zidani, R., Le Bail, N., Faggiuolo, R., Focan, C., Chollet, P., Llory, J., Letourneau, Y., and Coudert, B. (2000). Phase III multicenter randomized trial of oxaliplatin added to chronomodulated fluorouracil–leucovorin as first-line treatment of metastatic colorectal cancer. Journal of clinical oncology *18*, 136-136.

Giannakis, M., Mu, X. J., Shukla, S. A., Qian, Z. R., Cohen, O., Nishihara, R., Bahl, S., Cao, Y., Amin-Mansour, A., Yamauchi, M.*, et al.* (2016). Genomic Correlates of Immune-Cell Infiltrates in Colorectal Carcinoma. Cell Rep *15*, 857-865.

Girotti, M. R., Lopes, F., Preece, N., Niculescu-Duvaz, D., Zambon, A., Davies, L., Whittaker, S., Saturno, G., Viros, A., Pedersen, M.*, et al.* (2015). Paradox-breaking RAF inhibitors that also target SRC are effective in drug-resistant BRAF mutant melanoma. Cancer Cell *27*, 85-96.

Gottesman, M. M., Fojo, T., and Bates, S. E. (2002). Multidrug resistance in cancer: role of ATP–dependent transporters. Nature Reviews Cancer *2*, 48-58.

Gottesman, M. M., Ludwig, J., Xia, D., and Szakacs, G. (2009). Defeating drug resistance in cancer. Discovery medicine *6*, 18-23.

Grothey, A., Sargent, D., Goldberg, R. M., and Schmoll, H.-J. (2004). Survival of patients with advanced colorectal cancer improves with the availability of fluorouracil-leucovorin, irinotecan, and oxaliplatin in the course of treatment. Journal of Clinical Oncology *22*, 1209-1214.

Grothey, A., Van Cutsem, E., Sobrero, A., Siena, S., Falcone, A., Ychou, M., Humblet, Y., Bouche, O., Mineur, L., Barone, C.*, et al.* (2013). Regorafenib monotherapy for previously treated metastatic colorectal cancer (CORRECT): an international, multicentre, randomised, placebo-controlled, phase 3 trial. Lancet *381*, 303-312.

Guinney, J., Dienstmann, R., Wang, X., de Reyniès, A., Schlicker, A., Soneson, C., Marisa, L., Roepman, P., Nyamundanda, G., Angelino, P.*, et al.* (2015). The consensus molecular subtypes of colorectal cancer. Nat Med *21*, 1350-1356.

Hanahan, D., and Coussens, L. M. (2012). Accessories to the crime: functions of cells recruited to the tumor microenvironment. Cancer cell *21*, 309-322.

Hanahan, D., and Weinberg, R. A. (2000). The hallmarks of cancer. cell *100*, 57-70.

Hanahan, D., and Weinberg, R. A. (2011). Hallmarks of cancer: the next generation. cell *144*, 646-674.

Hanks, S. K., and Hunter, T. (1995). Protein kinases 6. The eukaryotic protein kinase superfamily: kinase (catalytic) domain structure and classification. The FASEB journal *9*, 576-596.

Hawinkels, L. J., and ten Dijke, P. (2011). Exploring anti-TGF-β therapies in cancer and fibrosis. Growth factors *29*, 140-152.

Hay, E. D., and Zuk, A. (1995). Transformations between epithelium and mesenchyme: normal, pathological, and experimentally induced. American Journal of Kidney Diseases *26*, 678-690.

Heidorn, S. J., Milagre, C., Whittaker, S., Nourry, A., Niculescu-Duvas, I., Dhomen, N., Hussain, J., Reis-Filho, J. S., Springer, C. J., Pritchard, C., and Marais, R. (2010). Kinase-dead BRAF and oncogenic RAS cooperate to drive tumor progression through CRAF. Cell *140*, 209-221.

Heinemann, V., von Weikersthal, L. F., Decker, T., Kiani, A., Vehling-Kaiser, U., Al-Batran, S.-E., Heintges, T., Lerchenmüller, C., Kahl, C., and Seipelt, G. (2014). FOLFIRI plus cetuximab versus FOLFIRI plus bevacizumab as first-line treatment for patients with metastatic colorectal cancer (FIRE-3): a randomised, open-label, phase 3 trial. The lancet oncology *15*, 1065-1075.
Hewish, M., and Cunningham, D. (2011). First-line treatment of advanced colorectal cancer. Lancet *377*, 2060-2062.

Hirata, E., Girotti, M. R., Viros, A., Hooper, S., Spencer-Dene, B., Matsuda, M., Larkin, J., Marais, R., and Sahai, E. (2015). Intravital imaging reveals how BRAF inhibition generates drug-tolerant microenvironments with high integrin beta1/FAK signaling. Cancer Cell *27*, 574-588.

Holohan, C., Van Schaeybroeck, S., Longley, D. B., and Johnston, P. G. (2013). Cancer drug resistance: an evolving paradigm. Nature Reviews Cancer *13*, 714-726.

Honkanen, T. J., Tikkanen, A., Karihtala, P., Mäkinen, M., Väyrynen, J. P., and Koivunen, J. P. (2019). Prognostic and predictive role of tumour-associated macrophages in HER2 positive breast cancer. Scientific reports *9*, 10961.

Isella, C., Terrasi, A., Bellomo, S. E., Petti, C., Galatola, G., Muratore, A., Mellano, A., Senetta, R., Cassenti, A., and Sonetto, C. (2015). Stromal contribution to the colorectal cancer transcriptome. Nature genetics *47*, 312.

Janjigian, Y. Y., Bendell, J., Calvo, E., Kim, J. W., Ascierto, P. A., Sharma, P., Ott, P. A., Peltola, K., Jaeger, D., and Evans, J. (2018). CheckMate-032 study: efficacy and safety of nivolumab and nivolumab plus ipilimumab in patients with metastatic esophagogastric cancer. Journal of Clinical Oncology *36*, 2836-2844.

Jemal, A., Bray, F., Center, M. M., Ferlay, J., Ward, E., and Forman, D. (2011). Global cancer statistics. CA: a cancer journal for clinicians *61*, 69-90.

Jha, S., Morris, E. J., Hruza, A., Mansueto, M. S., Schroeder, G. K., Arbanas, J., McMasters, D., Restaino, C. R., Dayananth, P., and Black, S. (2016). Dissecting therapeutic resistance to ERK inhibition. Molecular cancer therapeutics *15*, 548-559.

Johnson, L. N., Lowe, E. D., Noble, M. E., and Owen, D. J. (1998). The structural basis for substrate recognition and control by protein kinases 1. FEBS letters *430*, 1-11.

Jones, S., Chen, W.-d., Parmigiani, G., Diehl, F., Beerenwinkel, N., Antal, T., Traulsen, A., Nowak, M. A., Siegel, C., and Velculescu, V. E. (2008). Comparative lesion sequencing provides insights into tumor evolution. Proceedings of the National Academy of Sciences *105*, 4283-4288.

Jonker, D. J., O'Callaghan, C. J., Karapetis, C. S., Zalcberg, J. R., Tu, D., Au, H.-J., Berry, S. R., Krahn, M., Price, T., and Simes, R. J. (2007). Cetuximab for the treatment of colorectal cancer. New England Journal of Medicine *357*, 2040-2048.

Jänne, P. A., Gray, N., and Settleman, J. (2009). Factors underlying sensitivity of cancers to small-molecule kinase inhibitors. Nature reviews Drug discovery *8*, 709.

Kalluri, R. (2016). The biology and function of fibroblasts in cancer. Nat Rev Cancer *16*, 582-598.

Kalluri, R., and Zeisberg, M. (2006). Fibroblasts in cancer. Nature Reviews Cancer *6*, 392.

Kandoth, C., McLellan, M. D., Vandin, F., Ye, K., Niu, B., Lu, C., Xie, M., Zhang, Q., McMichael, J. F., and Wyczalkowski, M. A. (2013). Mutational landscape and significance across 12 major cancer types. Nature *502*, 333.

Karapetis, C. S., Khambata-Ford, S., Jonker, D. J., O'Callaghan, C. J., Tu, D., Tebbutt, N. C., Simes, R. J., Chalchal, H., Shapiro, J. D., and Robitaille, S. (2008). K-ras mutations and benefit from cetuximab in advanced colorectal cancer. New England Journal of Medicine *359*, 1757-1765.

Kemper, K., Grandela, C., and Medema, J. P. (2010). Molecular identification and targeting of colorectal cancer stem cells. Oncotarget *1*, 387.

Khan, K., Rata, M., Cunningham, D., Koh, D.-M., Tunariu, N., Hahne, J. C., Vlachogiannis, G., Hedayat, S., Marchetti, S., and Lampis, A. (2018a). Functional imaging and circulating biomarkers of response to regorafenib in treatment-refractory metastatic colorectal cancer patients in a prospective phase II study. Gut *67*, 1484-1492.

Khan, K. H., Cunningham, D., Werner, B., Vlachogiannis, G., Spiteri, I., Heide, T., Mateos, J. F., Vatsiou, A., Lampis, A., Darvish Damavandi, M.*, et al.* (2018b). Longitudinal Liquid Biopsy and Mathematical Modeling of Clonal Evolution Forecast Time to Treatment Failure in the PROSPECT-C Phase II Colorectal Cancer Clinical Trial. Cancer Discov.

Kojima, Y., Acar, A., Eaton, E. N., Mellody, K. T., Scheel, C., Ben-Porath, I., Onder, T. T., Wang, Z. C., Richardson, A. L., and Weinberg, R. A. (2010). Autocrine TGF-β and stromal cell-derived factor-1 (SDF-1) signaling drives the evolution of tumor-promoting mammary stromal myofibroblasts. Proceedings of the National Academy of Sciences *107*, 20009-20014.
Kolch, W. (2000). Meaningful relationships: the regulation of the Ras/Raf/MEK/ERK pathway by protein interactions. Biochemical Journal *351*, 289-305.

Kopetz, S., Desai, J., Chan, E., Hecht, J. R., O'Dwyer, P. J., Maru, D., Morris, V., Janku, F., Dasari, A., Chung, W.*, et al.* (2015). Phase II Pilot Study of Vemurafenib in Patients With Metastatic BRAF-Mutated Colorectal Cancer. J Clin Oncol *33*, 4032-4038.

Kordes, M., Röring, M., Heining, C., Braun, S., Hutter, B., Richter, D., Geörg, C., Scholl, C., Roth, W., and Rosenwald, A. (2015). Cooperative Activity of BRAF F595L and Mutant HRAS in Histiocytic Sarcoma Provides New Insights into Oncogenic BRAF Signaling. In, (Am Soc Hematology).

Kreso, A., O'Brien, C. A., Van Galen, P., Gan, O. I., Notta, F., Brown, A. M., Ng, K., Ma, J., Wienholds, E., and Dunant, C. (2013). Variable clonal repopulation dynamics influence chemotherapy response in colorectal cancer. Science *339*, 543-548.

Kugimiya, N., Nishimoto, A., Hosoyama, T., Ueno, K., Enoki, T., Li, T. S., and Hamano, K. (2015). The c‐MYC‐ABCB5 axis plays a pivotal role in 5‐fluorouracil resistance in human colon cancer cells. Journal of cellular and molecular medicine *19*, 1569-1581.

Lawrence, M. S., Stojanov, P., Mermel, C. H., Robinson, J. T., Garraway, L. A., Golub, T. R., Meyerson, M., Gabriel, S. B., Lander, E. S., and Getz, G. (2014). Discovery and saturation analysis of cancer genes across 21 tumour types. Nature *505*, 495.

Li, X., Francies, H. E., Secrier, M., Perner, J., Miremadi, A., Galeano-Dalmau, N., Barendt, W. J., Letchford, L., Leyden, G. M., and Goffin, E. K. (2018). Organoid cultures recapitulate esophageal adenocarcinoma heterogeneity providing a model for clonality studies and precision therapeutics. Nature communications *9*, 2983.

Liang, H., Cheung, L. W., Li, J., Ju, Z., Yu, S., Stemke-Hale, K., Dogruluk, T., Lu, Y., Liu, X., Gu, C.*, et al.* (2012). Whole-exome sequencing combined with functional genomics reveals novel candidate driver cancer genes in endometrial cancer. Genome Res *22*, 2120-2129.

Liegl, B., Kepten, I., Le, C., Zhu, M., Demetri, G., Heinrich, M., Fletcher, C., Corless, C., and Fletcher, J. (2008). Heterogeneity of kinase inhibitor resistance mechanisms in GIST. The Journal of Pathology: A Journal of the Pathological Society of Great Britain and Ireland *216*, 64-74.

Lievre, A., Bachet, J.-B., Le Corre, D., Boige, V., Landi, B., Emile, J.-F., Côté, J.-F., Tomasic, G., Penna, C., and Ducreux, M. (2006). KRAS mutation status is predictive of response to cetuximab therapy in colorectal cancer. Cancer research *66*, 3992-3995.

Linnekamp, J. F., van Hooff, S. R., Prasetyanti, P. R., Kandimalla, R., Buikhuisen, J. Y., Fessler, E., Ramesh, P., Lee, K. A., Bochove, G. G., and de Jong, J. H. (2018). Consensus molecular subtypes of colorectal cancer are recapitulated in in vitro and in vivo models. Cell Death & Differentiation *25*, 616.

Liska, D., Chen, C. T., Bachleitner-Hofmann, T., Christensen, J. G., and Weiser, M. R. (2011). HGF rescues colorectal cancer cells from EGFR inhibition via MET activation. Clin Cancer Res *17*, 472-482.

Liu, C., Guan, H., Wang, Y., Chen, M., Xu, B., Zhang, L., Lu, K., Tao, T., Zhang, X., and Huang, Y. (2015). miR-195 inhibits EMT by targeting FGF2 in prostate cancer cells. PloS one *10*, e0144073.
Liu, F., Yang, X., Geng, M., and Huang, M. (2018). Targeting ERK, an Achilles' Heel of the MAPK pathway, in cancer therapy. Acta pharmaceutica sinica B *8*, 552-562.

Liu, L. F., Desai, S. D., LI, T. K., Mao, Y., Sun, M., and SIM, S. P. (2000). Mechanism of action of camptothecin. Annals of the New York Academy of Sciences *922*, 1-10.

Long, G. V., Fung, C., Menzies, A. M., Pupo, G. M., Carlino, M. S., Hyman, J., Shahheydari, H., Tembe, V., Thompson, J. F., Saw, R. P.*, et al.* (2014). Increased MAPK reactivation in early resistance to dabrafenib/trametinib combination therapy of BRAF-mutant metastatic melanoma. Nat Commun *5*, 5694.

Long, G. V., Stroyakovskiy, D., Gogas, H., Levchenko, E., de Braud, F., Larkin, J., Garbe, C., Jouary, T., Hauschild, A., Grob, J. J.*, et al.* (2015). Dabrafenib and trametinib versus dabrafenib and placebo for Val600 BRAF-mutant melanoma: a multicentre, double-blind, phase 3 randomised controlled trial. Lancet *386*, 444-451.

Longley, D., and Johnston, P. (2005). Molecular mechanisms of drug resistance. The Journal of Pathology: A Journal of the Pathological Society of Great Britain and Ireland *205*, 275-292.
Longley, D. B., Harkin, D. P., and Johnston, P. G. (2003). 5-fluorouracil: mechanisms of action and clinical strategies. Nature reviews cancer *3*, 330.

Lonning, S., Mannick, J., and M McPherson, J. (2011). Antibody targeting of TGF-β in cancer patients. Current pharmaceutical biotechnology *12*, 2176-2189.

Lordick, F., Kang, Y. K., Chung, H. C., Salman, P., Oh, S. C., Bodoky, G., Kurteva, G., Volovat, C., Moiseyenko, V. M., Gorbunova, V.*, et al.* (2013). Capecitabine and cisplatin with or without cetuximab for patients with previously untreated advanced gastric cancer (EXPAND): a randomised, open-label phase 3 trial. Lancet Oncol *14*, 490-499.

Loupakis, F., Ruzzo, A., Cremolini, C., Vincenzi, B., Salvatore, L., Santini, D., Masi, G., Stasi, I., Canestrari, E., Rulli, E.*, et al.* (2009). KRAS codon 61, 146 and BRAF mutations predict resistance to cetuximab plus irinotecan in KRAS codon 12 and 13 wild-type metastatic colorectal cancer. Br J Cancer *101*, 715-721.

Luraghi, P., Reato, G., Cipriano, E., Sassi, F., Orzan, F., Bigatto, V., De Bacco, F., Menietti, E., Han, M., Rideout, W. M., 3rd*, et al.* (2014). MET signaling in colon cancer stem-like cells blunts the therapeutic response to EGFR inhibitors. Cancer Res *74*, 1857-1869.

Maemondo, M., Inoue, A., Kobayashi, K., Sugawara, S., Oizumi, S., Isobe, H., Gemma, A., Harada, M., Yoshizawa, H., and Kinoshita, I. (2010). Gefitinib or chemotherapy for non–small-cell lung cancer with mutated EGFR. New England Journal of Medicine *362*, 2380-2388.

Mao, C., Huang, Y. F., Yang, Z. Y., Zheng, D. Y., Chen, J. Z., and Tang, J. L. (2013). KRAS p. G13D mutation and codon 12 mutations are not created equal in predicting clinical outcomes of cetuximab in metastatic colorectal cancer: A systematic review and meta‐analysis. Cancer *119*, 714-721.

Marais, R., Light, Y., Paterson, H. F., Mason, C. S., and Marshall, C. J. (1997). Differential regulation of Raf-1, A-Raf, and B-Raf by oncogenic ras and tyrosine kinases. Journal of Biological Chemistry *272*, 4378-4383.

Mariathasan, S., Turley, S. J., Nickles, D., Castiglioni, A., Yuen, K., Wang, Y., Kadel III, E. E., Koeppen, H., Astarita, J. L., and Cubas, R. (2018). TGFβ attenuates tumour response to PD-L1 blockade by contributing to exclusion of T cells. Nature *554*, 544.

Martinez-Balibrea, E., Martínez-Cardús, A., Ginés, A., de Porras, V. R., Moutinho, C., Layos, L., Manzano, J. L., Bugés, C., Bystrup, S., and Esteller, M. (2015). Tumor-related molecular mechanisms of oxaliplatin resistance. Molecular cancer therapeutics *14*, 1767-1776.
Mayer, R. J., Van Cutsem, E., Falcone, A., Yoshino, T., Garcia-Carbonero, R., Mizunuma, N., Yamazaki, K., Shimada, Y., Tabernero, J., and Komatsu, Y. (2015). Randomized trial of TAS-102 for refractory metastatic colorectal cancer. New England Journal of Medicine *372*, 1909-1919.

Mei, Z., Shao, Y. W., Lin, P., Cai, X., Wang, B., Ding, Y., Ma, X., Wu, X., Xia, Y., Zhu, D.*, et al.* (2018). SMAD4 and NF1 mutations as potential biomarkers for poor prognosis to cetuximab-based therapy in Chinese metastatic colorectal cancer patients. BMC Cancer *18*, 479.

Mendelsohn, J., Prewett, M., Rockwell, P., and Goldstein, N. I. (2015). CCR 20th anniversary commentary: a chimeric antibody, C225, inhibits EGFR activation and tumor growth. In, (AACR).

Metzig, M. O., Fuchs, D., Tagscherer, K., Gröne, H.-J., Schirmacher, P., and Roth, W. (2016). Inhibition of caspases primes colon cancer cells for 5-fluorouracil-induced TNF-α-dependent necroptosis driven by RIP1 kinase and NF-κB. Oncogene *35*, 3399.

Misale, S., Bozic, I., Tong, J., Peraza-Penton, A., Lallo, A., Baldi, F., Lin, K. H., Truini, M., Trusolino, L., Bertotti, A.*, et al.* (2015). Vertical suppression of the EGFR pathway prevents onset of resistance in colorectal cancers. Nat Commun *6*, 8305.

Misale, S., Di Nicolantonio, F., Sartore-Bianchi, A., Siena, S., and Bardelli, A. (2014). Resistance to anti-EGFR therapy in colorectal cancer: from heterogeneity to convergent evolution. Cancer discovery *4*, 1269-1280.

Misale, S., Yaeger, R., Hobor, S., Scala, E., Janakiraman, M., Liska, D., Valtorta, E., Schiavo, R., Buscarino, M., Siravegna, G.*, et al.* (2012). Emergence of KRAS mutations and acquired resistance to anti-EGFR therapy in colorectal cancer. Nature *486*, 532-536.

Miyashita, T., and Reed, J. C. (1992). bcl-2 gene transfer increases relative resistance of S49. 1 and WEHI7. 2 lymphoid cells to cell death and DNA fragmentation induced by glucocorticoids and multiple chemotherapeutic drugs. Cancer research *52*, 5407-5411.

Montagut, C., Dalmases, A., Bellosillo, B., Crespo, M., Pairet, S., Iglesias, M., Salido, M., Gallen, M., Marsters, S., and Tsai, S. P. (2012). Identification of a mutation in the extracellular domain of

the Epidermal Growth Factor Receptor conferring cetuximab resistance in colorectal cancer. Nature medicine *18*, 221.

Moorcraft, S., Gonzalez de Castro, D., Cunningham, D., Jones, T., Walker, B., Peckitt, C., Yuan, L., Frampton, M., Begum, R., and Eltahir, Z. (2017). Investigating the feasibility of tumour molecular profiling in gastrointestinal malignancies in routine clinical practice. Annals of Oncology *29*, 230-236.

Morelli, M. P., Overman, M. J., Dasari, A., Kazmi, S. M. A., Vilar Sanchez, E., Eng, C., Kee, B. K., Deaton, L., Garrett, C. R., and Diehl, F. (2013). Heterogeneity of acquired KRAS and EGFR mutations in colorectal cancer patients treated with anti-EGFR monoclonal antibodies. In, (American Society of Clinical Oncology).

Moroni, M., Veronese, S., Benvenuti, S., Marrapese, G., Sartore-Bianchi, A., Di Nicolantonio, F., Gambacorta, M., Siena, S., and Bardelli, A. (2005). Gene copy number for epidermal growth factor receptor (EGFR) and clinical response to antiEGFR treatment in colorectal cancer: a cohort study. The lancet oncology *6*, 279-286.

Morrison, D. K., and Cutler Jr, R. E. (1997). The complexity of Raf-1 regulation. Current opinion in cell biology *9*, 174-179.

Müller, E., Bauer, S., Stühmer, T., Mottok, A., Scholz, C., Steinbrunn, T., Brünnert, D., Brandl, A., Schraud, H., and Kreßmann, S. (2017). Pan-Raf co-operates with PI3K-dependent signalling and critically contributes to myeloma cell survival independently of mutated RAS. Leukemia *31*, 922. Network, C. G. A. R. (2014). Comprehensive molecular characterization of gastric adenocarcinoma. Nature *513*, 202.

Nieto, M. A., Huang, R. Y.-J., Jackson, R. A., and Thiery, J. P. (2016). EMT: 2016. Cell *166*, 21-45. Nooter, K., De La Riviere, G. B., Look, M., Van Wingerden, K., Henzen-Logmans, S., Scheper, R., Flens, M., Klijn, J., Stoter, G., and Foekens, J. (1997). The prognostic significance of expression of the multidrug resistance-associated protein (MRP) in primary breast cancer. British journal of cancer *76*, 486-493.

Nowell, P. C. (1976). The clonal evolution of tumor cell populations. Science *194*, 23-28. Nukatsuka, M., Nakagawa, F., and Takechi, T. (2015). Efficacy of combination chemotherapy using a novel oral chemotherapeutic agent, TAS-102, with oxaliplatin on human colorectal and gastric cancer xenografts. Anticancer research *35*, 4605-4615.

Oliveira, C., Pinto, M., Duval, A., Brennetot, C., Domingo, E., Espín, E., Armengol, M., Yamamoto, H., Hamelin, R., and Seruca, R. (2003). BRAF mutations characterize colon but not gastric cancer with mismatch repair deficiency. Oncogene *22*, 9192.

O'Brien, C. A., Pollett, A., Gallinger, S., and Dick, J. E. (2007). A human colon cancer cell capable of initiating tumour growth in immunodeficient mice. Nature *445*, 106-110.

Paget, S. (1889). The distribution of secondary growths in cancer of the breast. The Lancet *133*, 571-573.

Paterson, A. L., Shannon, N. B., Lao-Sirieix, P., Ong, C. A., Peters, C. J., O'Donovan, M., and Fitzgerald, R. C. (2013). A systematic approach to therapeutic target selection in oesophago-gastric cancer. Gut *62*, 1415-1424.

Pearson, A., Smyth, E., Babina, I. S., Herrera-Abreu, M. T., Tarazona, N., Peckitt, C., Kilgour, E., Smith, N. R., Geh, C., Rooney, C*., et al.* (2016). High-Level Clonal FGFR Amplification and Response to FGFR Inhibition in a Translational Clinical Trial. Cancer Discov *6*, 838-851.

Pereira, S. G., and Oakley, F. (2008). Nuclear factor-κB1: regulation and function. The international journal of biochemistry & cell biology *40*, 1425-1430.

Philpott, C., Tovell, H., Frayling, I. M., Cooper, D. N., and Upadhyaya, M. (2017). The NF1 somatic mutational landscape in sporadic human cancers. Human genomics *11*, 13.

Piccart-Gebhart, M. (2005). for Trastuzumab Adjuvant (HERA) Trial Study Team. Trastuzumab after adjuvant chemotherapy in HER2-positive breast cancer NEJM *353*, 1659-1672.

Pietrantonio, F., Petrelli, F., Coinu, A., Di Bartolomeo, M., Borgonovo, K., Maggi, C., Cabiddu, M., Iacovelli, R., Bossi, I., Lonati, V.*, et al.* (2015). Predictive role of BRAF mutations in patients with advanced colorectal cancer receiving cetuximab and panitumumab: A meta-analysis. European Journal of Cancer *51*, 587-594.

Polyak, K., and Weinberg, R. A. (2009). Transitions between epithelial and mesenchymal states: acquisition of malignant and stem cell traits. Nature Reviews Cancer *9*, 265.

Post, J. B., Hami, N., Mertens, A. E., Elfrink, S., Bos, J. L., and Snippert, H. J. (2019). CRISPR-induced RASGAP deficiencies in colorectal cancer organoids reveal that only loss of NF1 promotes resistance to EGFR inhibition. Oncotarget *10*, 1440.

Prahallad, A., Sun, C., Huang, S., Di Nicolantonio, F., Salazar, R., Zecchin, D., Beijersbergen, R. L., Bardelli, A., and Bernards, R. (2012). Unresponsiveness of colon cancer to BRAF(V600E) inhibition through feedback activation of EGFR. Nature *483*, 100-103.

Ran, F. A., Hsu, P. D., Wright, J., Agarwala, V., Scott, D. A., and Zhang, F. (2013). Genome engineering using the CRISPR-Cas9 system. Nature protocols *8*, 2281.

Raymond, E., Faivre, S., Chaney, S., Woynarowski, J., and Cvitkovic, E. (2002). Cellular and molecular pharmacology of oxaliplatin1. Molecular cancer therapeutics *1*, 227-235.

Rimassa, L., Bozzarelli, S., Pietrantonio, F., Cordio, S., Lonardi, S., Toppo, L., Zaniboni, A., Bordonaro, R., Di Bartolomeo, M., and Tomasello, G. (2019). Phase II Study of Tivantinib and Cetuximab in Patients With KRAS Wild-type Metastatic Colorectal Cancer With Acquired Resistance to EGFR Inhibitors and Emergence of MET Overexpression: Lesson Learned for Future Trials With EGFR/MET Dual Inhibition. Clinical colorectal cancer *18*, 125-132. e122.

Robey, R. W., Pluchino, K. M., Hall, M. D., Fojo, A. T., Bates, S. E., and Gottesman, M. M. (2018). Revisiting the role of efflux pumps in multidrug-resistant cancer. Nature reviews Cancer *18*, 452.

Rutman, R. J., Cantarow, A., and Paschkis, K. E. (1954). The catabolism of uracil in vivo and in vitro. J biol Chem *210*, 321-329.

Sadanandam, A., Lyssiotis, C. A., Homicsko, K., Collisson, E. A., Gibb, W. J., Wullschleger, S., Ostos, L. C., Lannon, W. A., Grotzinger, C., Del Rio, M.*, et al.* (2013). A colorectal cancer classification system that associates cellular phenotype and responses to therapy. Nat Med *19*, 619-625.

Sakamoto, K., Maeda, S., Hikiba, Y., Nakagawa, H., Hayakawa, Y., Shibata, W., Yanai, A., Ogura, K., and Omata, M. (2009). Constitutive NF-κB activation in colorectal carcinoma plays a key role in angiogenesis, promoting tumor growth. Clinical Cancer Research *15*, 2248-2258.

Salomon, D. S., Brandt, R., Ciardiello, F., and Normanno, N. (1995). Epidermal growth factor-related peptides and their receptors in human malignancies. Critical reviews in oncology/hematology *19*, 183-232.

Samatar, A. A., and Poulikakos, P. I. (2014). Targeting RAS-ERK signalling in cancer: promises and challenges. Nat Rev Drug Discov *13*, 928-942.

Sartore-Bianchi, A., Martini, M., Molinari, F., Veronese, S., Nichelatti, M., Artale, S., Di Nicolantonio, F., Saletti, P., De Dosso, S., Mazzucchelli, L*., et al.* (2009). PIK3CA mutations in colorectal cancer are associated with clinical resistance to EGFR-targeted monoclonal antibodies. Cancer Res *69*, 1851-1857.

Sato, T., Stange, D. E., Ferrante, M., Vries, R. G., Van Es, J. H., Van Den Brink, S., Van Houdt, W. J., Pronk, A., Van Gorp, J., and Siersema, P. D. (2011). Long-term expansion of epithelial organoids from human colon, adenoma, adenocarcinoma, and Barrett's epithelium. Gastroenterology *141*, 1762-1772.

Schmoll, H., Van Cutsem, E., Stein, A., Valentini, V., Glimelius, B., Haustermans, K., Nordlinger, B., Van de Velde, C., Balmana, J., and Regula, J. (2012). ESMO Consensus Guidelines for management of patients with colon and rectal cancer. a personalized approach to clinical decision making. Annals of oncology *23*, 2479-2516.

Scholl, C., Frohling, S., Dunn, I. F., Schinzel, A. C., Barbie, D. A., Kim, S. Y., Silver, S. J., Tamayo, P., Wadlow, R. C., Ramaswamy, S*., et al.* (2009). Synthetic lethal interaction between oncogenic KRAS dependency and STK33 suppression in human cancer cells. Cell *137*, 821-834.

Schütte, M., Risch, T., Abdavi-Azar, N., Boehnke, K., Schumacher, D., Keil, M., Yildiriman, R., Jandrasits, C., Borodina, T., Amstislavskiy, V*., et al.* (2017). Molecular dissection of colorectal cancer in pre-clinical models identifies biomarkers predicting sensitivity to EGFR inhibitors. Nat Commun *8*, 14262.

Secrier, M., Li, X., de Silva, N., Eldridge, M. D., Contino, G., Bornschein, J., MacRae, S., Grehan, N., O'Donovan, M., Miremadi, A*., et al.* (2016). Mutational signatures in esophageal adenocarcinoma define etiologically distinct subgroups with therapeutic relevance. Nat Genet *48*, 1131-1141.

Seshagiri, S., Stawiski, E. W., Durinck, S., Modrusan, Z., Storm, E. E., Conboy, C. B., Chaudhuri, S., Guan, Y., Janakiraman, V., and Jaiswal, B. S. (2012). Recurrent R-spondin fusions in colon cancer. Nature *488*, 660.

Shah, N. P., Nicoll, J. M., Nagar, B., Gorre, M. E., Paquette, R. L., Kuriyan, J., and Sawyers, C. L. (2002). Multiple BCR-ABL kinase domain mutations confer polyclonal resistance to the tyrosine kinase inhibitor imatinib (STI571) in chronic phase and blast crisis chronic myeloid leukemia. Cancer cell *2*, 117-125.

Sharma, S. V., Lee, D. Y., Li, B., Quinlan, M. P., Takahashi, F., Maheswaran, S., McDermott, U., Azizian, N., Zou, L., and Fischbach, M. A. (2010). A chromatin-mediated reversible drug-tolerant state in cancer cell subpopulations. Cell *141*, 69-80.

Shi, H., Hugo, W., Kong, X., Hong, A., Koya, R. C., Moriceau, G., Chodon, T., Guo, R., Johnson, D. B., and Dahlman, K. B. (2014). Acquired resistance and clonal evolution in melanoma during BRAF inhibitor therapy. Cancer discovery *4*, 80-93.

Shiga, K., Hara, M., Nagasaki, T., Sato, T., Takahashi, H., and Takeyama, H. (2015). Cancer-associated fibroblasts: their characteristics and their roles in tumor growth. Cancers *7*, 2443-2458.

Silva, A. N., Coffa, J., Menon, V., Hewitt, L. C., Das, K., Miyagi, Y., Bottomley, D., Slaney, H., Aoyama, T., Mueller, W*., et al.* (2016). Frequent Coamplification of Receptor Tyrosine Kinase and Downstream Signaling Genes in Japanese Primary Gastric Cancer and Conversion in Matched Lymph Node Metastasis. Ann Surg.

Singh, A., and Settleman, J. (2010). EMT, cancer stem cells and drug resistance: an emerging axis of evil in the war on cancer. Oncogene *29*, 4741-4751.

Smith, G., Bounds, R., Wolf, H., Steele, R. J., Carey, F. A., and Wolf, C. R. (2010). Activating K-Ras mutations outwith 'hotspot' codons in sporadic colorectal tumours - implications for personalised cancer medicine. Br J Cancer *102*, 693-703.

Song, N., Pogue-Geile, K. L., Gavin, P. G., Yothers, G., Kim, S. R., Johnson, N. L., Lipchik, C., Allegra, C. J., Petrelli, N. J., and O'Connell, M. J. (2016). Clinical outcome from oxaliplatin treatment in stage II/III colon cancer according to intrinsic subtypes: secondary analysis of NSABP C-07/NRG oncology randomized clinical trial. JAMA oncology *2*, 1162-1169.

Straussman, R., Morikawa, T., Shee, K., Barzily-Rokni, M., Qian, Z. R., Du, J., Davis, A., Mongare, M. M., Gould, J., and Frederick, D. T. (2012). Tumour micro-environment elicits innate resistance to RAF inhibitors through HGF secretion. Nature *487*, 500.

Sturm, O. E., Orton, R., Grindlay, J., Birtwistle, M., Vyshemirsky, V., Gilbert, D., Calder, M., Pitt, A., Kholodenko, B., and Kolch, W. (2010). The mammalian MAPK/ERK pathway exhibits properties of a negative feedback amplifier. Sci Signal *3*, ra90.

Subramanian, A., Tamayo, P., Mootha, V. K., Mukherjee, S., Ebert, B. L., Gillette, M. A., Paulovich, A., Pomeroy, S. L., Golub, T. R., Lander, E. S., and Mesirov, J. P. (2005). Gene set enrichment analysis: a knowledge-based approach for interpreting genome-wide expression profiles. Proc Natl Acad Sci U S A *102*, 15545-15550.

Sullivan, R. J., Infante, J. R., Janku, F., Wong, D. J. L., Sosman, J. A., Keedy, V., Patel, M. R., Shapiro, G. I., Mier, J. W., and Tolcher, A. W. (2018). First-in-class ERK1/2 inhibitor ulixertinib (BVD-523) in patients with MAPK mutant advanced solid tumors: results of a phase I dose-escalation and expansion study. Cancer discovery *8*, 184-195.

Sveen, A., Bruun, J., Eide, P. W., Eilertsen, I. A., Ramirez, L., Murumägi, A., Arjama, M., Danielsen, S. A., Kryeziu, K., and Elez, E. (2018). Colorectal cancer consensus molecular subtypes translated to preclinical models uncover potentially targetable cancer cell dependencies. Clinical Cancer Research *24*, 794-806.

Swanton, C. (2012). Intratumor heterogeneity: evolution through space and time. Cancer research *72*, 4875-4882.

Takaishi, S., Okumura, T., Tu, S., Wang, S. S., Shibata, W., Vigneshwaran, R., Gordon, S. A., Shimada, Y., and Wang, T. C. (2009). Identification of gastric cancer stem cells using the cell surface marker CD44. Stem cells *27*, 1006-1020.

Tam, W. L., and Weinberg, R. A. (2013). The epigenetics of epithelial-mesenchymal plasticity in cancer. Nature medicine *19*, 1438.

Tauriello, D. V., and Batlle, E. (2016). Targeting the microenvironment in advanced colorectal cancer. Trends in cancer *2*, 495-504.

TCGA (2012). Comprehensive molecular characterization of human colon and rectal cancer. Nature *487*, 330-337.

Tejpar, S., Stintzing, S., Ciardiello, F., Tabernero, J., Van Cutsem, E., Beier, F., Esser, R., Lenz, H. J., and Heinemann, V. (2016). Prognostic and Predictive Relevance of Primary Tumor Location in Patients With RAS Wild-Type Metastatic Colorectal Cancer: Retrospective Analyses of the CRYSTAL and FIRE-3 Trials. JAMA Oncol.

Terai, H., Soejima, K., Yasuda, H., Nakayama, S., Hamamoto, J., Arai, D., Ishioka, K., Ohgino, K., Ikemura, S., and Sato, T. (2013). Activation of the FGF2-FGFR1 autocrine pathway: a novel mechanism of acquired resistance to gefitinib in NSCLC. Molecular Cancer Research *11*, 759-767.

Thomas, H., and Coley, H. M. (2003). Overcoming multidrug resistance in cancer: an update on the clinical strategy of inhibiting p-glycoprotein. Cancer control *10*, 159-165.

Tiriac, H., Belleau, P., Engle, D. D., Plenker, D., Deschênes, A., Somerville, T. D., Froeling, F. E., Burkhart, R. A., Denroche, R. E., and Jang, G.-H. (2018). Organoid profiling identifies common responders to chemotherapy in pancreatic cancer. Cancer discovery *8*, 1112-1129.

Todaro, M., Alea, M. P., Di Stefano, A. B., Cammareri, P., Vermeulen, L., Iovino, F., Tripodo, C., Russo, A., Gulotta, G., and Medema, J. P. (2007). Colon cancer stem cells dictate tumor growth and resist cell death by production of interleukin-4. Cell stem cell *1*, 389-402.

Tournigand, C., Andre, T., Achille, E., Lledo, G., Flesh, M., Mery-Mignard, D., Quinaux, E., Couteau, C., Buyse, M., Ganem, G*., et al.* (2004). FOLFIRI followed by FOLFOX6 or the reverse sequence in advanced colorectal cancer: a randomized GERCOR study. J Clin Oncol *22*, 229-237.

Triller, N., Korošec, P., Kern, I., Košnik, M., and Debeljak, A. (2006). Multidrug resistance in small cell lung cancer: expression of P-glycoprotein, multidrug resistance protein 1 and lung resistance protein in chemo-naive patients and in relapsed disease. Lung cancer *54*, 235-240.

Trinh, A., Trumpi, K., Felipe De Sousa, E. M., Wang, X., De Jong, J. H., Fessler, E., Kuppen, P. J., Reimers, M. S., Swets, M., and Koopman, M. (2017). Practical and robust identification of molecular subtypes in colorectal cancer by immunohistochemistry. Clinical Cancer Research *23*, 387-398.

Tsunemitsu, Y., Kagawa, S., Tokunaga, N., Otani, S., Umeoka, T., Roth, J. A., Fang, B., Tanaka, N., and Fujiwara, T. (2004). Molecular therapy for peritoneal dissemination of xenotransplanted human MKN-45 gastric cancer cells with adenovirus mediated Bax gene transfer. Gut *53*, 554-560.

Turner, N., and Grose, R. (2010). Fibroblast growth factor signalling: from development to cancer. Nature Reviews Cancer *10*, 116.

Valtorta, E., Misale, S., Sartore-Bianchi, A., Nagtegaal, I. D., Paraf, F., Lauricella, C., Dimartino, V., Hobor, S., Jacobs, B., Ercolani, C*., et al.* (2013). KRAS gene amplification in colorectal cancer and impact on response to EGFR-targeted therapy. Int J Cancer *133*, 1259-1265.

Van Cutsem, E., Cervantes, A., Adam, R., Sobrero, A., Van Krieken, J., Aderka, D., Aranda Aguilar, E., Bardelli, A., Benson, A., and Bodoky, G. (2016). ESMO consensus guidelines for the management of patients with metastatic colorectal cancer. Annals of Oncology *27*, 1386-1422.

Van Cutsem, E., Kang, Y., Chung, H., Shen, L., Sawaki, A., Lordick, F., Hill, J., Lehle, M., Feyereislova, A., and Bang, Y. (2009a). Efficacy results from the ToGA trial: a phase III study of trastuzumab added to standard chemotherapy in first-line HER2-positive advanced gastric cancer. J clin oncol *27*, LBA4509.

Van Cutsem, E., Kohne, C.-H., Láng, I., Folprecht, G., Nowacki, M. P., Cascinu, S., Shchepotin, I., Maurel, J., Cunningham, D., and Tejpar, S. (2011). Cetuximab plus irinotecan, fluorouracil, and leucovorin as first-line treatment for metastatic colorectal cancer: updated analysis of overall survival according to tumor KRAS and BRAF mutation status. J clin Oncol *29*, 2011-2019.

Van Cutsem, E., Köhne, C.-H., Hitre, E., Zaluski, J., Chang Chien, C.-R., Makhson, A., D'Haens, G., Pintér, T., Lim, R., and Bodoky, G. (2009b). Cetuximab and chemotherapy as initial treatment for metastatic colorectal cancer. New England Journal of Medicine *360*, 1408-1417.

Van Cutsem, E., Nowacki, M., Lang, I., Cascinu, S., Shchepotin, I., Maurel, J., Rougier, P., Cunningham, D., Nippgen, J., and Kohne, C. (2007). Randomized phase III study of irinotecan and 5-FU/FA with or without cetuximab in the first-line treatment of patients with metastatic colorectal cancer (mCRC): The CRYSTAL trial. Journal of Clinical Oncology *25*, 4000-4000.

Van Emburgh, B. O., Arena, S., Siravegna, G., Lazzari, L., Crisafulli, G., Corti, G., Mussolin, B., Baldi, F., Buscarino, M., Bartolini, A*., et al.* (2016). Acquired RAS or EGFR mutations and duration of response to EGFR blockade in colorectal cancer. Nat Commun *7*, 13665.

Vanharanta, S., and Massagué, J. (2013). Origins of metastatic traits. Cancer cell *24*, 410-421.

Vermeulen, L., Felipe De Sousa, E. M., Van Der Heijden, M., Cameron, K., De Jong, J. H., Borovski, T., Tuynman, J. B., Todaro, M., Merz, C., and Rodermond, H. (2010). Wnt activity defines colon cancer stem cells and is regulated by the microenvironment. Nature cell biology *12*, 468.

Vlachogiannis, G., Hedayat, S., Vatsiou, A., Jamin, Y., Fernández-Mateos, J., Khan, K., Lampis, A., Eason, K., Huntingford, I., Burke, R*., et al.* (2018). Patient-derived organoids model treatment response of metastatic gastrointestinal cancers. Science *359*, 920-926.

Voboril, R., Hochwald, S. N., Li, J., Brank, A., Weberova, J., Wessels, F., Moldawer, L. L., Camp, E. R., and MacKay, S. L. (2004). Inhibition of NF-Kappa B augments sensitivity to 5-Fluorouracil/Folinic acid in colon cancer1. Journal of Surgical Research *120*, 178-188.

Vogelstein, B., Papadopoulos, N., Velculescu, V. E., Zhou, S., Diaz, L. A., and Kinzler, K. W. (2013). Cancer genome landscapes. science *339*, 1546-1558.

Voigt, M., Braig, F., Göthel, M., Schulte, A., Lamszus, K., Bokemeyer, C., and Binder, M. (2012). Functional dissection of the epidermal growth factor receptor epitopes targeted by panitumumab and cetuximab. Neoplasia *14*, 1023-IN1023.

Von Loga, K., Woolston, A., Punta, M., Barber, L. J., Griffiths, B., Semiannikova, M., Spain, G. J., Challoner, B., Fenwick, K., and Schiffmann, H. (2019). Extreme intratumour heterogeneity and driver evolution in mismatch repair deficient gastro-oesophageal cancer. BioRxiv, 755199.

Waddell, T., Chau, I., Cunningham, D., Gonzalez, D., Okines, A. F., Frances, A., Okines, C., Wotherspoon, A., Saffery, C., Middleton, G*., et al.* (2013). Epirubicin, oxaliplatin, and capecitabine with or without panitumumab for patients with previously untreated advanced oesophagogastric cancer (REAL3): a randomised, open-label phase 3 trial. Lancet Oncol *14*, 481-489.

Walther, A., Johnstone, E., Swanton, C., Midgley, R., Tomlinson, I., and Kerr, D. (2009). Genetic prognostic and predictive markers in colorectal cancer. Nature Reviews Cancer *9*, 489.

Wan, P. T., Garnett, M. J., Roe, S. M., Lee, S., Niculescu-Duvaz, D., Good, V. M., Project, C. G., Jones, C. M., Marshall, C. J., and Springer, C. J. (2004). Mechanism of activation of the RAF-ERK signaling pathway by oncogenic mutations of B-RAF. Cell *116*, 855-867.

Wang, L.-C., Okitsu, C. Y., and Zandi, E. (2005). Tumor necrosis factor α-dependent drug resistance to purine and pyrimidine analogues in human colon tumor cells mediated through IKK. Journal of Biological Chemistry *280*, 7634-7644.

Wang, T.-L., Diaz, L. A., Romans, K., Bardelli, A., Saha, S., Galizia, G., Choti, M., Donehower, R., Parmigiani, G., and Shih, I.-M. (2004). Digital karyotyping identifies thymidylate synthase amplification as a mechanism of resistance to 5-fluorouracil in metastatic colorectal cancer patients. Proceedings of the National Academy of Sciences *101*, 3089-3094.

Wang, W., Li, Q., Yamada, T., Matsumoto, K., Matsumoto, I., Oda, M., Watanabe, G., Kayano, Y., Nishioka, Y., and Sone, S. (2009). Crosstalk to stromal fibroblasts induces resistance of lung cancer to epidermal growth factor receptor tyrosine kinase inhibitors. Clinical Cancer Research *15*, 6630-6638.

Ware, K., Hinz, T., Kleczko, E., and Singleton, K. (2013). L a M, B a H, Cummings CT, Graham DK, Astling D, Tan aC, Heasley LE. A mechanism of resistance to gefitinib mediated by cellular reprogramming and the acquisition of an FGF2-FGFR1 autocrine growth loop. Oncogene *2*, e39.

Weber, J. D., RABEN, D. M., Phillips, P. J., and Baldassare, J. J. (1997). Sustained activation of extracellular-signal-regulated kinase 1 (ERK1) is required for the continued expression of cyclin D1 in G1 phase. Biochemical Journal *326*, 61-68.

Whittaker, S. R., Cowley, G. S., Wagner, S., Luo, F., Root, D. E., and Garraway, L. A. (2015). Combined Pan-RAF and MEK Inhibition Overcomes Multiple Resistance Mechanisms to Selective RAF Inhibitors. Mol Cancer Ther *14*, 2700-2711.

Wilson, T. R., Fridlyand, J., Yan, Y., Penuel, E., Burton, L., Chan, E., Peng, J., Lin, E., Wang, Y., Sosman, J.*, et al.* (2012). Widespread potential for growth-factor-driven resistance to anticancer kinase inhibitors. Nature *487*, 505-509.

Woolston, A., Khan, K., Spain, G., Barber, L. J., Griffiths, B., Gonzalez-Exposito, R., Hornsteiner, L., Punta, M., Patil, Y., Newey, A.*, et al.* (2019). Genomic and Transcriptomic Determinants of Therapy Resistance and Immune Landscape Evolution during Anti-EGFR Treatment in Colorectal Cancer. Cancer Cell *36*, 35-50.e39.

World Health Organisation. In, p. Cancer Fact Sheet.
Xie, L., Su, X., Zhang, L., Yin, X., Tang, L., Zhang, X., Xu, Y., Gao, Z., Liu, K., and Zhou, M. (2013). FGFR2 gene amplification in gastric cancer predicts sensitivity to the selective FGFR inhibitor AZD4547. Clinical cancer research *19*, 2572-2583.

Yang, W., Soares, J., Greninger, P., Edelman, E. J., Lightfoot, H., Forbes, S., Bindal, N., Beare, D., Smith, J. A., and Thompson, I. R. (2012). Genomics of Drug Sensitivity in Cancer (GDSC): a resource for therapeutic biomarker discovery in cancer cells. Nucleic acids research *41*, D955-D961.

Yao, Z., Torres, N. M., Tao, A., Gao, Y., Luo, L., Li, Q., de Stanchina, E., Abdel-Wahab, O., Solit, D. B., and Poulikakos, P. I. (2015). BRAF mutants evade ERK-dependent feedback by different mechanisms that determine their sensitivity to pharmacologic inhibition. Cancer cell *28*, 370-383.

Yao, Z., Yaeger, R., Rodrik-Outmezguine, V. S., Tao, A., Torres, N. M., Chang, M. T., Drosten, M., Zhao, H., Cecchi, F., and Hembrough, T. (2017). Tumours with class 3 BRAF mutants are sensitive to the inhibition of activated RAS. Nature *548*, 234.

Yates, L. R., and Campbell, P. J. (2012). Evolution of the cancer genome. Nature Reviews Genetics *13*, 795.

Ychou, M., Boige, V., Pignon, J.-P., Conroy, T., Bouché, O., Lebreton, G., Ducourtieux, M., Bedenne, L., Fabre, J.-M., and Saint-Aubert, B. (2011). Perioperative chemotherapy compared with surgery alone for resectable gastroesophageal adenocarcinoma: an FNCLCC and FFCD multicenter phase III trial. J Clin Oncol *29*, 1715-1721.

Yonesaka, K., Zejnullahu, K., Okamoto, I., Satoh, T., Cappuzzo, F., Souglakos, J., Ercan, D., Rogers, A., Roncalli, M., and Takeda, M. (2011). Activation of ERBB2 signaling causes resistance to the EGFR-directed therapeutic antibody cetuximab. Science translational medicine *3*, 99ra86-99ra86.

Zalcberg, J., Hu, X., Slater, A., Parisot, J., El-Osta, S., Kantharidis, P., Chou, S., and Parkin, J. (2000). MRP1 not MDR1 gene expression is the predominant mechanism of acquired multidrug resistance in two prostate carcinoma cell lines. Prostate cancer and prostatic diseases *3*, 66-75.

Zhang, N., Yin, Y., Xu, S.-J., and Chen, W.-S. (2008). 5-Fluorouracil: mechanisms of resistance and reversal strategies. Molecules *13*, 1551-1569.

Zhang, W., and Liu, H. T. (2002). MAPK signal pathways in the regulation of cell proliferation in mammalian cells. Cell research *12*, 9.

Zhang, Z., Lin, G., Yan, Y., Li, X., Hu, Y., Wang, J., Yin, B., Wu, Y., Li, Z., and Yang, X.-P. (2018). Transmembrane TNF-alpha promotes chemoresistance in breast cancer cells. Oncogene *37*, 3456.

Zheng, C.-F., and Guan, K.-L. (1994). Activation of MEK family kinases requires phosphorylation of two conserved Ser/Thr residues. The EMBO journal *13*, 1123-1131.

Zhou, B.-B. S., Zhang, H., Damelin, M., Geles, K. G., Grindley, J. C., and Dirks, P. B. (2009). Tumour-initiating cells: challenges and opportunities for anticancer drug discovery. Nature reviews Drug discovery *8*, 806-823.

Östman, A. (2012). The tumor microenvironment controls drug sensitivity. Nature medicine *18*, 1332.